ABSTRACT

WU, JIAN. Characterization of Protein Body Related Ubiquitination in Maize Endosperm Mutants. (Under the direction of Dr. Rebecca S. Boston.)

The packing of zein storage proteins into protein bodies is a highly organized process. However, accumulation of defective α-zeins disturbs the protein packing and induces a series of unfolded protein responses (UPR) in the maize endosperm mutants *Defective endosperm B30* (*De*-B30*) and *floury-2* (*fl2*). Two related cellular responses, endoplasmic reticulum-associated degradation (ERAD) and ubiquitination, were investigated in these mutants. Increases in ubiquitin signals, and the membrane bound ERAD proteins ZmCDC48 and ZmHRD1, were specifically associated with *De*-B30* and *fl2* protein bodies, and positively correlated with expression of the mutant alleles throughout endosperm development. Ubiquitinated proteins were enriched from *De*-B30* protein bodies and identified with mass spectrometry. Starch synthesis-related enzymes were among the identified proteins. Their ubiquitination raises a new perspective to explain the low starch content in *De*-B30* endosperm. Protein-protein interactions between ZmCDC48 and ZmHRD1, and ZmCDC48 and ZmUFD1 were characterized in co-immunoprecipitation assays. A direct interaction between recombinant ZmCDC48 and ZmUFD1 was demonstrated *in vitro*. Together, increases in ubiquitination and membrane bound ZmCDC48 and ZmHRD1 are suggestive of an induced ERAD in response to misfolded proteins in *De*-B30* and *fl2* protein bodies. In addition, protein interactions between ZmCDC48 and ZmHRD1, and ZmCDC48 and ZmUFD1 indicate a likely conservation of function in ERAD.

Characterization of Protein Body Related Ubiquitination in Maize Endosperm Mutants

by
Jian Wu

A dissertation submitted to the Graduate Faculty of
North Carolina State University
in partial fulfillment of the
requirements for the degree of
Doctor of Philosophy

Plant Biology

Raleigh, North Carolina

2011

APPROVED BY:

_____	_____
Rebecca S. Boston Chair of Advisory Committee	Wendy F. Boss
_____	_____
Ralph E. Dewey	Heike Winter-Sederoff

DEDICATION

To my parents, my wife, and my daughter!

谨以此文献给我的家人。

BIOGRAPHY

Jian Wu was born in Jiaocheng, China. He is the first son of Aizhong Wu and Caixia Wei. In 1998, he was enrolled in Xiamen University and received his Bachelor of Science in Biology, and Master of Science in Plant Developmental Biology under the direction of Dr. Hui Qiao Tian. In 2005, he came to North Carolina State University and met his wife Xin Yang. He settled in Dr. Rebecca S. Boston's lab to work on maize storage protein degradation. During his Ph.D. study, his family was blessed with a wonderful daughter, Emily.

ACKNOWLEDGMENTS

I would like to express my deepest gratitude to my advisor Dr. Rebecca S. Boston for her guidance and support throughout my Ph.D. study. I want to especially thank her for going out to the corn field and spending every morning pollinating during the summer. I also want to thank my committee members, Dr. Wendy F. Boss, Dr. Ralph E. Dewey, and Dr. Heike Winter-Sederoff, for their invaluable suggestions on my project. Their doors were always open to me for questions and discussions.

I want to thank Dr. Jeffrey W. Gillikin for his lab training and helpful discussions, former members of the Boston lab (Mariana Kirst, Norma Houston, and Robert Holmes) for their help at the beginning of my Ph.D. study, and everyone in the Plant Metabolic Engineering family, Dr. Boss's and Dr. Dewey's lab members, Irena Brglez, Imara Perera, Yang Ju Im, Catherine Dieck, Brian Phillippy, Carol Griffin, Steven Bowen, Erin Parker, Jianli Lu, Harry Lopez, Matthew Keogh, and Rafaelo Galvão for being great friends and colleagues. Many thanks to the entire Plant Biology Department, and a special thanks to Sue Vitello for help throughout my course of study.

My sincere gratitude goes to members of Dr. Michael B. Goshe's lab. The mass spectrometry work would not have been possible without their expertise and generous help. Dr. Michael B. Goshe provided critical discussions and comments, and Kevin Blackburn, Flaubert Mbeunkui, and Mialy Ramaroson taught me sample preparation and data mining.

Many thanks to Dr. Candace H. Haigler and members of her lab, especially to Rami Alkhatib for all the valuable time and effort he spent teaching me the microwave fixation protocol and examining TEM samples. A big thanks to Valerie Knowlton at the Center for Electron Microscopy for sectioning and examining my sections, to Dr. Michael Dykstra and Jeanette Shipley-Phillips at the Laboratory for Advanced Electron and Light Optical Methods for their scientific discussions and generous help, and to Dr. Eva Johannes for helping with the confocal laser scanning microscopy at the Cellular and Molecular Imaging Facility. Many thanks also to Eric Fulkerson and Jyoti Kajla for kindly providing fluorescent secondary antibodies, to Dr. Anna Stepanova for teaching me Arabidopsis crossing techniques, to Daniel Wrenn for his great help with Arabidopsis genotyping and stress tests, to Wei Shen for sharing his Arabidopsis genome DNA extraction protocol.

Many thanks to Dr. Dominique Robertson for settling me in when I first came to the U.S., to Sang Yoon Lee for rides to grocery shops and many other places when I did not have a car. I also want to thank all of my best friends in Raleigh for giving me wonderful memories that will be cherished in the years to come.

I offer a special thank you to my parents-in-law, and my parents for traveling halfway around the world to babysit my daughter.

Finally, I want to thank my dear wife and daughter for their unconditional love. Without their support, it would not be possible for me to make this happen.

TABLE OF CONTENTS

LIST OF TABLES

LIST OF FIGURES

LIST OF ABBREVIATIONS

AAA - ATPases associated with diverse cellular activities
ATF6 - activating transcription factor 6
ALG12 - asparagine-linked glycosylation 12
ATP - adenosine triphosphate
A1PiZ - Z variant of α-1-protease inhibitor
BACE457 - beta-Secretase
β-ME - β-mercaptoethanol
BiP - immunoglobulin binding protein
bp - base pair
BSA - bovine serum albumin
BT - brittle
BR - brassinosteroids
bri1 - brassinosteroid-insensitive 1
CCT - choline-phosphate cytidylyltransferase
CDC48 - cell division cycle 48
CFTR - cystic fibrosis transmembrane conductance regulator
CLSM - confocal laser scanning microscopy
CNX - calnexin
CPY - carboxypeptidase Y
CRT - calreticulin
CTA1 - cholera toxin A1 subunit
Cue1 - factor for coupling of ubiquitin conjugation to ER degradation
De-B30* - defective endosperm B30
ΔGpαF - *N*-glycosylation site mutant alpha-factor precursor protein
DAP - days after pollination
DAG - days after germination
Der - degradation in the ER
Derlin - Der1-like
DTT - dithiothreitol
DU1 - DULL1
ebs - EMS-mutagenized bri1 suppressor
EDEM - ER degradation enhancing α -mannosidase-like protein
EDTA - ethylenediamine tetraacetic acid
EF-1α - elongation factor-1α
ER - endoplasmic reticulum
ERAD - endoplasmic reticulum associated degradation
ERMan I - ER mannosidase I
ERO1 - ER oxidation 1
ERp57 - ER-resided p57
ERQC - endoplasmic reticulum quality control
fl2 - floury-2

GFP - green fluorescence protein
$GlcNAc_2$-Man_9-Glc3 - *N*- acetylglucosamine$_2$-mannose$_9$-glucose$_3$
gp78 - glycoprotein precursor 78
GRP94 - glucose-regulated protein 94
GST - glutathione *S*-transferase
HCs - heavy chains
HMG-CoA - 3-hydroxy-3-methylglutaryl coenzyme A reductase
Hrd - HMG-CoA reductase degradation
Hsp - heat shock protein
Htm1 - homologoue to mannosidase 1
Ire1 - inositol requiring enzyme 1
Jem1 - DnaJ-like protein of the ER membrane 1
Kar2 - karyogamy gene 2
Kif - kifunensine
LC/MS^E - liquid chromatography-mass spectrometry with elevated collision energy
Mc - mucronate
MHC - major histocompatibility complex
MLO - mildew resistance O
MW - molecular weight
Mnl1 - mannosidase - like 1
Npl4 - nuclear protein localization 4
NZF - Npl4 zinc finger
o2 - opaque 2
OST - oligosaccaryl transferase
PB - protein body
PBS - phosphate-buffered saline
PDI - protein disulphide isomerase
PERK - protein kinase-like endoplasmic reticulum kinase
PMA1 - plasma membrane ATPase 1
PMSF- phenylmethylsulfonyl fluoride
Png1 - peptide:N-glycanase 1
PP1 - phosphoprotein phosphatase 1
PrA - proteinase yscA
RAMP4 - ribosome-associated membrane protein 4
RCA A - *Ricinus communis* agglutinin A chain
RIP - ribosome-inactivating protein
RPN10 - regulatory particle non-ATPase 10
RTA - ricin toxin A chain
RT-PCR - reverse transcription polymerase chain reaction
Scj1p - *Saccharomyces cerevisiae* DnaJ
SDS - sodium lauryl sulfate
SDS-PAGE - SDS polyacrylamide gel electrophoresis
SEL1L - sel-1 suppressor of lin-12-like

SH - shrunken
SPP - signal peptide peptidase
TEM - transmission electron microscopy
Tm - tunicamycin
UBA - ubiquitin-associated
Ubc - ubiquitin conjugating enzyme
Ube2g2 - ubiquitin-conjugating enzyme E2G 2
UBL - ubiquitin-like
UBX - ubiquitin regulatory X
Ufd1 - ubiquitin fusion degradation 1
UGGT - UDP-glucose: glycoprotein glucosyltransferase
UPL1 - ubiquitin-protein ligase 1
UPR - unfolded protein response
VIMP - VCP (another name for p97)-interacting membrane protein
XBP1 - X box binding protein 1
Yos9 - yeast homolog of the OS-9

Chapter 1: Introduction

General introduction

The endoplasmic reticulum (ER[1]) is the primary site for secretory protein synthesis and the entry point for the secretory pathway. Secretory proteins are typically synthesized by ER membrane bound ribosomes and simultaneously or subsequently translocated into the ER. Furthermore, secretory proteins need to be folded and modified to proper conformations for their biological functions before they are exported from ER to intracellular membranes or lumen, or secreted to the outside of the cell. The ER recruits ER resident molecular chaperones, folding and modification enzymes to ensure that newly synthesized polypeptides achieve their proper conformations. As a protein is translocated into the ER, ER resident molecular chaperones immediately recognize and bind to the nascent polypeptide of the secretory protein in order to promote its folding and prevent undesirable aggregations. In addition, folding and modification enzymes catalyze intra- or inter- molecule disulfide bond formation and *N*-linked glycosylation.

Despite the assistance from molecular chaperones and enzymes responsible for translational modifications, errors could emerge at any point in the process from the DNA template to protein maturation, and result in misfolded proteins within the ER. The presence of misfolded proteins disturbs the ER homeostasis, congests the secretory pathway and even leads to severe defects when misfolded protein aggregates accumulate within the ER. To correct these mistakes, a conserved and sophisticated ER quality control system including the ER molecular chaperone and modification enzymes has evolved to keep secretory proteins

[1]Standard abbreviations are used and full names are listed in the abbreviation table.

under tight surveillance. However, if the conformation fault can not be corrected, a disposal mechanism referred as ER-associated degradation (ERAD) will dislocate misfolded proteins to the cytoplasm for degradation.

Because of the broad regulatory roles of secretory proteins, the ERAD pathway has been extensively studied in yeast and mammals. Biochemical and genetic studies have been significantly advancing our understanding of the ERAD machinery and substrates, and a much more complete image has been pieced together. Accumulating evidence suggests that there is a conserved ERAD pathway in plants. However, ERAD research is much behind in plants by lacking both functional studies on putative ERAD components and identification of new ERAD substrates.

In this review chapter, I will first briefly summarize our current understanding about the ERAD components and substrates in yeast and mammals, and how ERAD cross talks with other stress responses. Finally, I will review the findings of ERAD in plants, and ERAD coordination with other stress responses in countering adverse conditions. Selected ERAD components in yeast, mammals, and plants discussed in this review chapter are listed in Table 1.

ERAD in yeast and mammals

As it emerges in the ER, a misfolded protein will be identified and retained by the ER molecular chaperones and folding enzymes for a prolonged period of time in order to achieve

its proper conformation. ERAD subsequently removes the misfolded protein and prevents meaningless energy consumption and folding attempts. A general ERAD pathway includes four critical steps: 1. substrate recognition in the ER lumen; 2. retrotranslocation through the ER membrane; 3. initial ubiquitination on the ER membrane; 4. ubiquitin-dependent protein degradation in the cytoplasm.

ER molecular chaperones and substrate recognition

ER molecular chaperones and folding enzymes, including immunoglobulin binding protein (BiP), protein disulfide isomerases (PDIs), calreticulin (CRT), and calnexin (CNX), act at the forefront to maintain the solubility of nascent polypeptides and assist them to achieve their proper conformations (Buck et al., 2007). Besides folding and modification, ER molecular chaperones and folding enzymes play vital roles in misfolded protein recognition and delivery to the ERAD transmembrane complexes (Gillece et al., 1999; Kabani et al., 2003; Ruddock and Molinari, 2006).

BiP, the ER member of the heat shock protein 70 (Hsp70) family, plays multiple pivotal roles in protein translocation, folding, and delivery to the ER membrane for degradation. In the protein translocation process, Kar2p, the yeast homolog of BiP is proposed to utilize the energy from ATP hydrolysis to bind the nascent polypeptide and engage its translocation process in one direction through a ratcheting mechanism (Rapoport, 2007). In the protein folding process, BiP promotes the newly synthesized protein to achieve its proper conformation by interacting with any exposed hydrophobic regions. This process is also ATP

dependent. When the ATPase domain of Kar2p is interrupted by mutation, the maturation of a native yeast glycoprotein carboxypeptidase yscY (CPY) is compromised, leading to its aggregation and retention within the ER (Simons et al., 1995). In the delivery for degradation, defective Kar2p with a mutation in the ATPase domain retards the degradation of soluble ERAD substrates, such as a mutated CPY (CPY*), an unglycosylated mutant form of the yeast mating pheromone pro-α factor (ΔGpαF), and the Z variant of the α 1-proteinase inhibitor (A1PiZ; Plemper et al., 1997; Brodsky et al., 1999).

The various functions of Kar2p in yeast depend in part on interactions with other molecular chaperones, such as DnaJ-domain containing heat shock protein 40 (Hsp40s), as well as direct binding to substrates. These interactions have been discovered through analysis of yeast mutants. Sec63p is a member of the DnaJ-domain containing Hsp40 family and a part of the translocon complex. Mutation in the J-domain interacting part of Kar2p disrupts its interaction with Sec63p, and compromises the translocation into the ER but not retrotranslocation out of the ER (Vembar et al., 2010). Two other DnaJ-domain containing Hsp40 proteins in yeast, including DnaJ-like protein of the ER membrane 1(Jem1p) and *Saccharomyces cerevisiae* DnaJ (Scj1p), show important roles in ERAD through interaction with Kar2p (Silberstein et al., 1998; Nishikawa et al., 2001). Scj1p and Jem1p interact with Kar2p to maintain ERAD substrate solubility within the ER lumen. When Scj1p and Jem1p were deleted, luminal protein CPY* but not membrane protein Sec61-2p started to aggregate.

PDIs are abundant thiol oxidoreductases within the ER lumen. PDIs play a crucial role in disulfide bond formation, which is indispensible for protein folding and protein subunit assembly for those proteins with intermolecular S-S bonds (Tu and Weissman, 2004). In the redox reaction, PDIs pass electrons from a thiol group through the ER oxidation 1 protein (ERO1) to molecular oxygen, which is the final receptor. PDIs have been shown to interact with substrates, including beta-secretase (BACE457) and ΔGpαF, during the ERAD process (Molinari et al., 2002; Wahlman et al., 2007). Cholera toxin is transported into the host ER through its binding with a plasma membrane receptor. Cholera toxin A1 subunit (CTA1) is subsequently unfolded in the ER and dislocated in the cytoplasm for its toxicity. A recent study demonstrated essential roles of PDI and ERO1 in the CTA1 unfolding and retrotranslocation processes (Moore et al., 2010). Both knockdown and overexpression of ERO1 disrupt the interaction between PDI and CTA1, and block the retrotranslocation process. Similar functions of ERO1 and PDI might be applied to other substrates during the ERAD process.

In addition to BiP and PDIs, the ER molecular chaperones CRT and CNX, specialize in recognizing and assisting the folding of glycoproteins in mammalian cells (Brodsky, 2007). Besides CRT and CNX, an elaborated glycan protein quality control mechanism is conserved from yeast to mammals. In yeast, when emerging into the ER, the nascent polypeptide of a glycoprotein is first modified by the translocon-associated oligosaccaryl transferase (OST). A glycan moiety, *N*- acetylglucosamine$_2$-mannose$_9$-glucose$_3$ (GlcNAc$_2$-Man$_9$-Glc$_3$) is added on to the Asn residue in the Asn-X-Ser/Thr motif (Parodi, 2000). Cne1p, the yeast homolog of

CNX, subsequently binds and promotes the folding of monoglucosylated glycoproteins after two glucoses are trimmed by glucosidases I and II (Williams, 2006). Once the glycoprotein achieves its proper conformation and the last glucose is further trimmed by glucosidase II, the glycoprotein departs from Cne1p and leaves the ER. In an extended retention in the ER, the glycan chain is further trimmed down by yeast α-1, 2-mannosidase (Mns1p), and homologue to mannosidase 1 (Htm1p; Burke et al., 1996; Clerc et al., 2009). Mns1p trims the outmost mannose in the B glycan chain, and then Htm1p subsequently or independently trims down the mannose at the end of the C glycan chain to expose the α-1, 6 linked mannose (Jakob et al., 1998; Hosomi et al., 2010). Mns1p and Htm1p were also shown to form functional complexes with Pdi1p, the yeast homolog of PDI, to recognize and deliver substrates to the ERAD transmembrane complex (Clerc et al., 2009; Sakoh-Nakatogawa et al., 2009). The exposed α-1,6 linked mannose after the trimming by Htm1p serves as the ERAD signal recognized by a lectin like protein Yos9p, the yeast homolog of mammalian OS-9 and XTP3-B (Quan et al., 2008; Clerc et al., 2009). Yos9p, in turn, delivers the bound ERAD substrate to the ERAD transmembrane complex Hrd3p-Hrd1p (Carvalho et al., 2006). Kar2p has been shown to assist Yos9p during the delivery (Denic et al., 2006).

The recognition of *N*-linked glycolproteins in mammalian cells shares some similarities to, but is more sophisticated than, the recognition process in yeast. CRT and CNX first recognize and bind to the monoglucosylated glycoproteins after two glucose residues are trimmed by glucosidases I and II (Hirsch et al., 2009). If a hydrophobic region is still exposed in the incompletely folded glycoprotein during the interaction, UDP-glucose:

glycoprotein glucosyltransferase (UGGT) will sense and add glucose back to extend the binding between CRT, CNX and the glycoprotein until the glycoprotein achieves its proper conformation (Parodi, 2000). CRT and CNX also interact with a non-canonical PDI, ER-resident p57 (ERp57) for disulfide bond formation and the folding of glycoproteins (Oliver et al., 1999). With prolonged interaction with CRT and CNX, the glycan chain of misfolded glycoprotein can be trimmed down to $GlcNAc_2$–Man_8 and even further down to $GlcNAc_2$–$Man_{5\text{-}6}$ by ER mannosidase I (ERManI; Cabral et al., 2001; Avezov et al., 2008). Subsequently, the ER degradation enhancing α-mannosidase-like proteins (EDEMs), mammalian homologs to yeast Htm1p, liberate the unfolded glycoprotein through physical binding to CNX (Molinari et al., 2003; Oda et al., 2003), and deliver them to the sel-1 suppressor of lin-12-like (SEL1L), the mammalian homolog to yeast 3-hydroxy-3-methylglutaryl coenzyme A (HMG-CoA) reductase degradation 3 (Hrd3p; Cormier et al., 2009). In addition, EDEMs have been shown to prevent the aggregation of ERAD substrates (Hosokawa et al., 2006; Kosmaoglou et al., 2009). Besides EDEMs, Os-9 and XTP3-B are two other misfolded glycoprotein sensors. Os-9 forms a complex with glucose-regulated protein 94 (GRP94) to recognize and deliver misfolded glycosylated protein substrates to SEL1L (Christianson et al., 2008; Bernasconi et al., 2010). XTP3-B has been shown to form a functional complex with BiP and SEL1L for glycosylated ERAD substrate recognition and degradation (Hosokawa et al., 2008).

Not only the ER molecular chaperones, but also the transmembrane E3 ligases contain the recognition capacity for ERAD substrate recognition. The multi-transmembrane domain of

HMG-CoA reductase degradation 1 (Hrd1p) has recently been shown to recognize misfolded membrane proteins (Sato et al., 2009).

Retrotranslocation

Once the ERAD substrates are targeted to the ERAD transmembrane complex, they are required to cross back from the ER lumen into the cytoplasm for the necessary ubiquitination. This process is designated as retrotranslocation or dislocation. Although details of this export process still remain obscure, putative candidate proteins have emerged from recent studies.

The translocon, composed of six Sec61p proteins, forms a transmembrane channel for the import of nascent peptides on the ER membrane (Osborne et al., 2005; Rapoport, 2007). It had long been speculated that the translocon might function as the export channel as well. First evidence from the interaction between Sec61p and ERAD substrates ΔGpαF, CPY* and CTA1 indicates that Sec61p may be a general requirement for protein retrotranslocation (Pilon et al., 1997; Plemper et al., 1997; Schmitz et al., 2000). Second, degradation of ERAD substrates was impaired in *sec61* mutants. The degradation of Deg1:Sec62^{ProtA} derivatives of CPY was compromised in *sec61* mutants that showed normal protein import into the ER (Scott and Schekman, 2008; Willer et al., 2008). The result suggests that Sec61p is indispensible for the degradation of Deg1:Sec62^{ProtA}. Furthermore, a recent study showing the physical interaction between Sec61p and the ERAD transmembrane E3 ligase Hrd1p through Hrd3p (discussed in transmembrane E3 ligase section) strengthened evidence of the crucial role that Sec61p plays in the retrotranslocation process (Schafer and Wolf, 2009).

Sec61p independent retrotranslocation may exist because not all degradation of ERAD substrates is compromised in *sec61* mutants. Studies on two human cytomegalovirus proteins, US2 and US11, provide insights on the alternative retrotranslocation complexes. Both US2 and US11 localize to the ER membrane, and take over the ERAD pathway to export and eliminate major histocompatibility complex (MHC) class I heavy chains (HCs). However, the composition of the retrotranslocation complex is different. US2 recruits signal peptide peptidase (SPP) for the export of the MHC class I HC, and a recent study has shown that the interaction between SPP and PDI is indispensible for the process (Loureiro et al., 2006). In the presence of US2, knockdown of SPP or PDI compromises the degradation of the MHC class I HC. SPP and PDI have also been shown to be essential for the degradation of CD3δ (Lee et al., 2010). Taken together, the SPP dependent retrotranslocation is required for certain ERAD substrates.

On the other hand, US11 utilizes a multi-transmembrane protein Derlin-1, the mammalian homolog of yeast Der1-like protein 1 (Der1p), in coordination with BiP and CNX for the retrotranslocation of the MHC class I HC (Lilley and Ploegh, 2004; Hegde et al., 2006). A dominant-negative version of Derlin-1 retards the process. Derlin-1 has been shown to be critical for soluble protein degradation, but also is indispensible for some membrane protein degradation, such as the cystic fibrosis transmembrane conductance regulator (CFTR) and its mutant form CFTRΔF508 (Sun et al., 2006; Younger et al., 2006). Derlin-1 recognizes the non-ubiquitinated CFTR and exports it from the ER for degradation. Knockdown of the Derlin-1 leads to an increased level of CFTR by blocking degradation. Despite the specificity

of Sec61 and Derlin-1, retrotranslocation of certain ERAD substrates such as CTA1 and ΔGpαF requires both Sec61 and Derlin-1 (Pilon et al., 1997; Schmitz et al., 2000; Wahlman et al., 2007; Bernardi et al., 2008). However, how Derlin-1 and Sec61 coordinate with each other during the retrotranslocation remains unknown and requires further investigation. There are two other Derlin proteins (Derlin-2, Derlin-3) present in mammalian cells. Both Derlin-2 and Derlin-3 are involved in ERAD through interaction with EDEM1 and p97 (Oda et al., 2006). Unlike its mammalian homolog, yeast Der1p is required only to degrade soluble luminal misfolded proteins, but not membrane-bound ones (Taxis et al., 2003; Vashist and Ng, 2004; Carvalho et al., 2006).

Other mechanisms of retrotranslocation may also exist within the cell. Lipid droplets, which are commonly present in all eukaryotic cells, were proposed to be involved in the degradation of MHC class I HC (Ploegh, 2007), HMG-CoA reductase (Hartman et al., 2010), EDEM1 and COPII assisted CFTR degradation (Zuber et al., 2007).

Transmembrane E3 complexes

Shortly after or in parallel with their retrotranslocation, ERAD substrates are ubiquitinated in the cytoplasm by ER transmembrane E3 ligases. Increasing evidence suggests that distinct E3 ligases are utilized for the ubiquitination of substrates with different locations of misfolded regions. ERAD in yeast can be divided into three categories depending on the misfolded lesion of substrates residing in the lumen (ERAD-L), transmembrane (ERAD-M), or cytoplasm (ERAD-C; Carvalho et al., 2006; Denic et al., 2006). Two transmembrane E3

ligases have been well studied in yeast, Hrd1p in ERAD-L and ERAD-M, and Doa10p in ERAD-C.

Hrd1p is an ER membrane anchored E3 ubiquitin ligase that has six transmembrane domains and a RING finger motif at the C-terminal domain facing the cytosol (Figure 1; Hampton et al., 1996; Bays et al., 2001). Hrd1p not only ubiquitinates ER luminal and membrane substrates, but also recruits various cofactors to connect the substrate recognition in the ER lumen to the ubiquitinated substrate extraction in the cytoplasm. One luminal cofactor is Hrd3p, which was co-identified with Hrd1p in a genetic screen of HMG-CoA reductase degradation mutants (Gardner et al., 2000). Hrd3p contains a large N-terminal domain in the ER lumen, a single transmembrane domain, and small cytosolic domain at the C-terminus. Hrd3p directly interacts with and stabilizes Hrd1p in a 1:1 stoichiometric ratio through its luminal domain (Gardner et al., 2000). The Hrd3p luminal domain can recruit cofactors Kar2p and Yos9p for substrate recognition (Carvalho et al., 2006; Denic et al., 2006; Gauss et al., 2006). Yos9p specifically recognizes misfolded glycoproteins and Kar2p recognizes misfolded proteins by interacting with their exposed hydrophobic patches. On the ER membrane, Hrd1p interacts with the putative retrotranslocon, Der1p, through Usa1p (Carvalho et al., 2006; Carroll and Hampton, 2009; Horn et al., 2009). Usa1p is an integral membrane protein with two transmembrane domains and localization of its N and C termini in the cytoplasm. While the C terminus recruits Der1p, the N terminus of Usa1 binds to Hrd1p and promotes Hrd1p oligomerization, which is critical for membrane substrate degradation (Horn et al., 2009; Kim et al., 2009). When a part of the N terminus of Usa1 was

replaced by a 6xHA-tag, the Hrd1p oligomerization was abolished. The degradation of two soluble ERAD substrates, CPY* and a mutant proteinase yscA (PrA*), was slightly inhibited. However, the degradation of a membrane ERAD substrate, 6xmyc-Hmg2, was almost completely inhibited. Nevertheless, when only the N-terminus of Usa1was expressed, Hrd1 oligomerization and the degradation of 6xmyc-Hmg2 were both restored. In the cytoplasm, the E3 ligase activity of Hrd1p exclusively requires a cytosolic E2 ubiquitin-conjugating enzyme, either Ubc7p or Ubc1p (Bays et al., 2001). Ubc7p needs to be recruited to the membrane by its membrane anchor Cue1p in order to transfer ubiquitin to Hrd1p (Biederer et al., 1997; Bazirgan and Hampton, 2008). In a Δ*cue1* strain, the degradation of luminal and membrane ERAD substrates CPY* and Sec61-2p are inhibited despite the presence of Ubc7p in the cytosol. Another important cofactor of Hrd1p in the cytoplasm is Ubx2p, which contains an N-terminal ubiquitin-associated (UBA) domain and a C-terminal ubiquitin regulatory X (UBX) domain (Neuber et al., 2005; Schuberth and Buchberger, 2005). Ubx2p targets the cytoplasmic complex Cdc48p-Ufd1p-Npl4p to the transmembrane complex Hrd1p-Hrd3p through its UBX domain. In a Δ*Ubx2* strain, degradation of both luminal and membrane ERAD substrates, CPY* and Sec61-2p, were diminished. In mammalian cells, VIMP has been shown to recruit p97 to Derlin-1 on the ER membrane, however, no Ubx2p homolog has been identified yet (Ye et al., 2004).

The other important transmembrane E3 ligase in yeast is Doa10p (Swanson et al., 2001). Doa10p contains a RING finger domain at the N-terminus for its E3 ligase activity and 14 transmembrane domains at the C-terminus. The Doa10p complex is relatively simple and

shares several common cofactors with the Hrd1 complex. Doa10p utilizes Cue1p recruited Ubc7p or Ubc6p as its E2 for substrate ubiquitination. Subsequently, ubiquitinated transmembrane substrates are degraded in a Cdc48p-Ufd1p-Npl4p dependent process (Carvalho et al., 2006; Ravid et al., 2006). Even though yeast has only two E3 ligases that function in the three types of ERAD, growing evidence suggests that these two (Hrd1p and Doa10p) can compensate or function synergistically (Nakatsukasa et al., 2008).

Compared with yeast ERAD, mammalian ERAD is complicated with more E3 ligases and cofactors. Two mammalian homologs to Hrd1p are HRD1 and gp78 (Chen et al., 2006). The HRD1 complex includes OS-9 and XTP3-B, SEL1L, HERP, Derlin 1, 2, 3, and UBC7 (Figure 1; Hirsch et al., 2009). Similar to HRD1, gp78 encompasses an N-terminal transmembrane domain and a C-terminal RING finger domain (Chen et al., 2006). In addition, gp78 contains a Cue domain, which is dispensable for its binding with its E2 ligase, Ube2g2. A possible mammalian homolog of Doa10p is TEB4, which also contains a conserved RING finger at its N-terminus and 13 transmembrane domains (Hassink et al., 2005). Although TEB4 recruits UBC7 to degrade itself through ERAD, whether or not it has other substrates is still unclear.

Substrate extraction and 26S proteasome-dependent protein degradation

The ERAD substrate is initially ubiquitinated by transmembrane E3 ligase complexes. Once it emerges from the ER membrane, it still requires energy to be fully extracted for delivery to its final destination, the 26S proteasome. Although the 26S proteasome is able to bind to the

retrotranslocon and degrade substrates at the membrane by itself (Kalies et al., 2005; Ng et al., 2007), numerous studies have suggested that the Cdc48p-Ufd1p -Npl4p complex plays the critical role in the extraction processes of a broad range substrates (Meyer et al., 2000; Ye et al., 2001). In mammalian cells, p97 forms a similarly conserved complex with UFD1 and NPL4. Knockdown of any of these three proteins leads to the ERAD process being compromised (Ye et al., 2001). These results suggest that each protein of the complex plays an independent role in the ERAD process. As a member of the AAA family of ATPases, p97 forms a hexamer ring to hydrolyze ATP and provide energy for substrate extraction. Mutation in the ATP hydrolysis domain of p97 significantly inhibits the extraction of the MHC class I heavy chain from the ER into the cytoplasm. Besides two ATPase domains, p97 encompasses an N-terminal domain that binds to the heterodimer of UFD1 and NPL4 which recognize mono- or poly-ubiquitin chains (Pye et al., 2007). UFD1 contains the p97 and NPL4 binding domain at its C-terminus, and ubiquitin binding domain at its N-terminus (Park et al., 2005). The NPL4 zinc finger (NZF) domain, lacking in yeast Npl4p, has also been identified as a binding site for mono- and poly-ubiquitin chains (Wang et al., 2003). Even though the structure of the p97-UFD1-NPL4 complex has been resolved, details of the initial recognition of substrates at the ER membrane are still poorly understood. One possibility is that p97 functions like a molecular chaperone that directly recognizes the unfolded substrate once it emerges from the ER membrane (Thoms, 2002; Ye et al., 2003). For example, p97 was shown to interact directly with MHC class I HC without ubiquitination. The other possibility is that the p97-UFD1-NPL4 complex recognizes a polyubiquitin chain attached to a substrate (Jarosch et al., 2002). The blocked degradation of CPY* in a *Δhrd1*

mutant with normal function of Cdc48p-Ufd1p-Npl4p suggested that ubiquitination is required before the binding of the Cdc48p complex. Furthermore, the accumulation of monoubiquitinated CPY* in a *Δubc7* mutant suggested that the recognition requires a certain length of the polyubiquitin chain.

Cdc48p not only is able to directly deposit ubiquitinated species at the 26S proteasome (Dai et al., 1998; Verma et al., 2000), but also can recruit various ubiquitin binding or ubiquitin-like domain containing proteins to help with this process (Hartmann-Petersen et al., 2003). Ufd2p, a ubiquitin chain assembly factor, recognizes short ubiquitinated species on the Cdc48p complex and extends the poly-ubiquitin chain (Koegl et al., 1999). Rad23 and Dsk2, containing both ubiquitin-like (UBL) and ubiquitin-associated (UBA) domains, have been identified to function downstream of Ufd2p by recognizing and escorting polyubiquitined substrates from the Cdc48p complex to 26S proteasomes (Medicherla et al., 2004; Richly et al., 2005; Hanzelmann et al., 2010). Ubx4p is another identified Cdc48p complex cofactor functioning downstream of Ufd2p and upstream of 26S proteasomes (Alberts et al., 2009). In the absence of Ubx4p, an increased amount of ubiquitinated CPY* binds to the Cdc48p complex and the delivery of CPY* to 26S proteasomes is impaired.

ERAD substrates

Studies on diverse ERAD substrates in yeast and mammals have greatly improved our understanding of the ERAD machinery and its function (Hirsch et al., 2009). Taking advantage of technology advancements in recent years, researchers have developed various

methods to identify ubiquitinated species on a much broader scale, and even at the proteome level. Some methods that have been used successfully are tagged-ubiquitin, ubiquitin binding proteins, and ubiquitin antibody-based immunoprecipitation coupled with mass spectrometry. The same set of methods can be utilized for ERAD substrate searches. However, how to distinguish ERAD substrates from general ubiquitinated species is still a big challenge. The first attempt by Silver's group was developing a novel methodology by combining quantitative mass spectrometry with wild type yeast and ERAD deficient mutants, including an *npl4-1* mutant that is impaired in degradation but not ubiquitination, and an *npl4-1* Δ*ubc7* mutant that is lacking both ubiquitination and degradation (Hitchcock et al., 2003). As a result, the ubiquitinated peptides of ERAD substrates represent a low-high-low abundance profile in wild type, *npl4-1*, and *npl4-1* Δ*ubc7* respectively. The quantitative proteomics provided an accurate means to measure the abundance of ubiquitinated peptides. At the end, 211 ERAD substrates and more than 30 ubiquitination sites were identified in the experiment. Besides the substrate identification, ERAD and even entire secretory pathway components can be screened at a genome wide level (Copic et al., 2009; Jonikas et al., 2009). In addition, an *in vitro* system was developed to provide an alternative approach for investigating the required components for various ERAD substrates (Wahlman et al., 2007). In the system, fluorescence-labeled ERAD substrates along with selected luminal proteins were encapsulated into isolated ER microsomes, which were resuspended in solutions containing quenching reagent and chosen cytosolic proteins. The retrotranslocation process can be monitored by a fluorescence spectrometer, because the fluorescence will decrease when labeled substrates are exported out of microsomes and bind quenchers. The degradation

process can be determined by immunoblot analysis. For example, the retrotranslocation and degradation of Δgpαf-BOF is ATP and 26S proteasome but not ubiquitin and p97, dependent. In addition, PDI, but not BiP, and Derlin-1, but not Sec61α, are involved in its retrotranslocation. Although this *in vitro* system may not completely replicate the scenario *in vivo*, it can definitely provide a new way to understand various ERAD substrates and their required ERAD machinery in the future.

Cross-talk of ERAD with other ER quality control mechanisms

There are other ER quality control mechanisms functioning independently or jointly with ERAD to maintain ER homeostasis. The unfolded protein response (UPR) is a cellular stress response against massive unfolded protein loading in the ER. It has been shown that UPR tightly coordinates with ERAD in guarding ER homeostasis (Friedlander et al., 2000; Travers et al., 2000). When the degradation of CPY* was repressed in ERAD mutants, the UPR was constitutively induced. Likewise, dithiothreitol (DTT), compromising disulfide bond formation, triggered a strong UPR response and induced various ERAD components, such as Kar2p, Hrd1p, and Ubc7p. Furthermore, the induction of ERAD was completely abolished along with the induction of UPR in a mutant of the sole UPR sensor *Δire1*. The effect on yeast is lethality when both ERAD and UPR were blocked. IRE1 and ATF6, two of three known UPR sensors in mammalian cells, regulate various ERAD components including Derlins, HRD1, and SEL1L (Oda et al., 2006; Kaneko et al., 2007; Yamamoto et al., 2008). Besides its cross-talking with UPR to maintain ER integrity, ERAD is involved in regulating

cholesterol biosynthesis, cold adaptation, and oxidative stress (Hampton and Rine, 1994; Haynes et al., 2004; Loertscher et al., 2006).

In addition to ERAD, there are post-ER protein quality control mechanisms that can break down misfolded proteins. One mechanism is autophagy dependent protein degradation (Fujita et al., 2007; Ishida et al., 2009; Le Fourn et al., 2009). Autophagy is a conserved catabolic process that degrades a part of the cytoplasm or organelles through lysosomes. By using the autophagosome formation inhibitor wortmannin, Ishida et. al (2009) blocked the degradation of misfolded procollagen. In addition, they showed that knocking down an autophagy-related gene ATG5 stabilized the misfolded procollagen in the ER. The findings suggest that autophagy plays an essential role for misfolded procollagen degradation. Another mechanism is Golgi dependent protein degradation in the vacuole (Coughlan et al., 2004; Wang and Ng, 2010). Wsc1p is a single span transmembrane sensor of cell wall integrity. By using Wsc1p variants, Wang and Ng (2010) have shown that these proteins were stabilized in the *Sec12-4* mutant in which the vesicle trafficking from the ER to the Golgi apparatus was blocked. In a vacuolar proteolysis defective mutant *Δpep4*, degradation of these variants was also inhibited. Taken together, the evidence suggested that Wsc1p variants were degraded in the vacuole through the Golgi apparatus. Furthermore, there are cases that require both ERAD and autophagy, or both ERAD and Golgi functioning in concert (Brodsky and Scott, 2007; Kincaid and Cooper, 2007; Kroeger et al., 2009).

ERAD in plants

Most of our knowledge on ERAD is based on yeast and mammalian studies. However, accumulating evidence suggests that a conserved ER quality control mechanism including ERAD exists in plants to maintain ER homeostasis.

ER molecular chaperones

Like in yeast and mammalian cells, conserved ER molecular chaperones and folding enzymes, including BiP, PDI, CRT and CNX, regulate newly synthesized polypeptides in plants (Boston et al., 1996; Kawagoe et al., 2005; Pattison and Amtmann, 2009). In addition, they recognize and bind to misfolded proteins in plants (Kim et al., 2006; Hong et al., 2008; Jin et al., 2009).

BiP has been shown to be critical for rice protein body (PB) formation (Li et al., 1993). Rice endosperm contains two types of PBs. The type I PB contains polymeric prolamines that are a group of storage proteins with high proline, glutamine and solubility in alcohol solution. Prolamins are synthesized and directly stored within the ER. The type II PB is composed of monomeric glutelins that are soluble in acidic and alkaline solution and accounting for 80% of the total protein content in rice endosperm (Yamagata et al., 1982). Gutelins are synthesized from the ER, and deposited through the Golgi apparatus into storage protein vacuoles. BiP has been shown to interact with the prolamin nascent peptide and assist its folding during type I PB formation (Li et al., 1993; Saito et al., 2009). BiP may also play an important role for type II PB formation. When BiP was over-expressed under a glutelin

promoter, glutelin was retained by interacting with BiP in the ER rather than being secreted into storage protein vacuoles. In addition, the accumulation of glutelin is much less in the BiP overexpressing line when compared to wild type (Yasuda et al., 2009). Similarly, less ER protein accumulation was observed in the other BiP overexpression study (Park et al., 2010). XA21, one of the rice pathogen pattern recognition receptors (PRRs), is commonly synthesized in the ER and transported to the plasma membrane during plant innate immune response. In a BiP3 overexpression line, XA21 was shown to be constrained at the ER, and the protein level but not mRNA level is much less when compared with XA21 in wild type. Since BiP has been reported to deliver proteins to the membrane E3 ligase for degradation in yeast and mammals, the prolonged interaction between BiP and glutelin, or between BiP and XA21, not only disturbs their post-ER depositions to the storage protein vacuole or plasma membrane, but also possibly leads to ER associated degradation because of the extended interaction in the ER.

PDI is another important chaperone for rice and wheat PB formation (Shimoni et al., 1995; Kawagoe et al., 2005). In rice endosperm, PDI is indispensible for prolamin polymerization. A lack of PDI in the rice *esp2* mutant leads to a failure to separate pathways for localizing prolamin and glutelin precursors and leads to the diminishment of type I PBs (Takemoto et al., 2002). ERO1 functions in tandem with PDI in disulfide bond formation during PB formation in rice endosperm (Onda et al., 2009). After knocking out rice *ERO1*, Onda et al. (2009) showed a similar abnormal PB formation as in the *esp2* mutant. In addition to their function in seed protein body formation, PDIs have been shown to play a broad role in pollen

tube growth and embryo sac formation (Wang et al., 2008). In addition to their roles as chaperone and folding enzymes, BiP and PDI may recognize and assist misfolded protein degradation in plants. BiP and PDI are induced in the presence of mutant storage proteins in maize *Mucronate* (*Mc)*, *floury-2* (*fl2*), and *Defective endosperm* (*De*-B30*) mutants (Boston et al., 1991; Li and Larkins, 1996; Houston et al., 2005). In addition, BiP has been shown to recognize and bind to misfolded 16kDa γ-zein storage protein, which accumulates much less in the maize *Mc* mutant (Kim et al., 2006).

Besides BiP and PDI/ERO1, a set of conserved chaperones and enzymes is designated for the quality control of *N*-linked glycoproteins in plants as in yeast and mammals (Pattison and Amtmann, 2009). In a *gcs1* mutant and an *rsw3* mutant, α-glucosidase I and glucosidase II are knocked out, respectively (Boisson et al., 2001; Burn et al., 2002). The trimming of glucose is blocked in each heterozygous line. In addition, each Arabidopsis homozygous mutant is embryonic lethal and lacking cellulose synthesis. UGGT was reported in mammalian cells to add glucose back to glycol chains resulting in an extended folding of glycoprotein by CNX and CRT. Plant UGGT plays a similar function in the ER. An Arabidospsis UGGT has been reported to play an important role in the quality control of a functional mutant brassinosteroid (BR) cell membrane receptor bri1-9, which contains a defective structural conformation (S662F; Jin et al., 2007). In a wild type background, bri1-9 is detained in the ER at a low level by the ER quality control mechanism through interaction with CRTs. The detained bri1-9 leads to a BR insensitive phenotype. However, in the *ebs1* background lacking the Arabidopsis UGGT, bri1-9 can be exported out of the ER to the

plasma membrane and result in a partial restoration of the BR sensitive phenotype. A follow-up study has shown that CRT3 but no other CRTs and CNXs are involved in the retention of bri1-9 (Jin et al., 2009). A loss-of-function CRT3 mutant can recover the wild type phenotype of the *bri1-9* mutant, but mutation in either of the other two CRTs or in CNXs do not suppress the mutant phenotype of the *bri1-9* mutant. Furthermore, the glycan of bri1-9 was indicated to be required for generating an ERAD signal (Hong et al., 2009). In yeast, an α-1,6 mannosyltransferase named ALG12 was involved in the formation of a glycan moiety, $GlcNAc_2$-Man_9-Glc_3 (Burda et al., 1999). When the formation of a glycan chain, $GlcNAc_2$-Man_9-Glc_3, was blocked in the Arabidopsis homolog of a yeast ALG12 mutant background, the degradation of bri1-9 was inhibited. Other than their individual roles, BiP, PDI and CNXs were shown in other studies to function synergistically in the ER quality control process. For example, the ER retention of another mutant BR receptor bri1-5, which contains proper functionality but defective structure (C69Y), is accomplished by BiP, CNXs and PDI (Hong et al., 2008). CNXs and BiP were shown to be coimmunoprecipitated with bri1-5. Suppressed BiP expression can partially restore the BR sensitive phenotype by releasing bri1-5 to the plasma membrane. PDI catalyzes thiol groups to form inter- or intra-molecule disulfide bonds, and provides an additional ER retention mechanism. By removing the free thiol residue by replacing Cystine-62 to Tyrosine, Hong et al. (2008) showed that the expression of bri1-5C62Y-GFP in transgenic plants led to a more complete rescue of the wild type phenotype than was seen with the bri1-5-GFP transgenic plants, probably because the bri1-5C62Y-GFP escapes from the thiol-retention mechanism.

ERAD components

In addition to the ER molecular chaperones, there are other conserved ERAD components in plants based on sequence similarity. However, relatively little is known about the functions of these putative components in plants. AtCDC48, the Arabidopsis homolog of yeast Cdc48p, has been shown to play an essential role in the degradation of mutant barley mildew resistance o (MLO) proteins (Muller et al., 2005), and the retrotranslocation of ricin toxin A chain (RTA) from *Ricinus communis* (Marshall et al., 2008). Similar to retrotranslocation in mammalian cells, the retrotranslocation requires ATP consumption. A mutant AtCDC48A with defective ATP hydrolysis (AtCDC48A QQ) leads to the inhibition of degradation of MLO-1 proteins in the Arabidopsis protoplast. The AtCDC48A QQ has also been shown to inhibit the export of RTA from the ER lumen into the cytoplasm. These results suggested that the ERAD of both substrates is driven by AtCDC48 generated energy. However, the interaction between AtCDC48 and RTA during the retrotranslocation appears to be ubiquitin independent, as shown in several cases of other eukaryotic systems (Thoms, 2002; Ye et al., 2003).

Other identified ERAD components in plants are Arabidopsis homologs of yeast Hrd1p and Hrd3p. Their genes were among the up-regulated ones in Arabidopsis seedlings under ER stress (Kamauchi et al., 2005). In addition, these two proteins were indicated to function in the ERAD of mutant brassinosteroid receptors bri1-5 and bri1-9 (Su et al., 2011). The lack of one Arabidopsis *HRD3* (At1g18260) or two *HRD1* (At1g65040 and At3g16090) genes slowed down the ERAD of mutant receptors bri1-5 or bri1-9. Arabidopsis HRD3 was also

shown to interact with bri1-5 and bri1-9 in immunoprecipitation assays. Furthermore, the coding region of Arabidopsis *HRD3* (At1g18260) was cloned into the vector pYEp352 containg the promoter and terminator of the yeast ALG12 gene. Transformation of Arabidopsis this *HRD3* gene (At1g1g65040) can functionally complement the degradation defect of carboxypeptidase Y (CPY*) in a *Δhrd3* yeast mutant.

The other defined plant ERAD components are Zm Derlins, maize homologs of yeast Der1p protein. Zm Derlin1 proteins are induced by misfolded storage proteins contained in maize endosperm mutants (Kirst et al., 2005). Although Zm Derlin2-1 is not dramatically induced, both Zm Derlins can partially complement the function of the yeast homolog. Transformations of Zm Derlin1-1 or Zm Derlin2-1 recover the growth of a *Δire1/Δder* temperature sensitive double mutant of yeast at the nonpermissive temperature of 37°C. In addition, Zm Derlins have been shown in cellular fractionation experiments to preferentially localize to the PB fraction where the misfolded zeins are deposited instead of the ER fraction. These findings further strengthen that Zm Derlins are ERAD components in maize.

Dissecting plant ERAD is complicated by the existence of unconventional retrotranslocation and 26S proteasome independent degradation. One example is that the ricin toxin A chain (RTA) does not need to be ubiquitinated for its retrotranslocation. Without ricin toxin B chain, RTA is recognized as a defective protein and dislocated into cytoplasm for degradation. In addition, the cytoplasmically localized RTA escaping from degradation can inhibit protein synthesis during its degradation. It has been shown that degradation but not

retrotranslocation of RTA requires ubiquitination in tobacco protoplasts (Di Cola et al., 2005). When two lysine residues are replaced by arginine residues in the RTA (RTA0K), the degradation is retarded. However, the presence of proteinase K sensitive RTA0K forms and stronger protein synthesis inhibition by RTA0K compared to the protein synthesis inhibition by RTA indicated an unaffected retrotranslocation process. On the other hand, adding four extra Lys residues led to an acceleration of the degradation and less functional RTA to block protein synthesis. The other example is the 26S proteasome independent degradation of mutant BR receptor bri1-5 (Hong et al., 2008). Kifunensine, an inhibitor of α1, 2-mannosidases, blocked glycan trimming and stabilized bri1-5 in the ER. However, MG132, a 26S proteasome inhibitor, did not affect the degradation of bri1-5. The findings suggested the degradation of bri1-5 requires proper glycan modification and is 26S proteasome independent. The various characteristics in different substrate degradation processes imply a sophisticated ERAD machinery is present in plants as in yeast and mammals.

Cross-talk of ERAD with other ER quality control mechanisms

ERAD has been related to various stress responses, including UPR. Tunicamycin is an *N*-linked glycosylation inhibitor, and DTT inhibits protein disulfide bond formation. Both chemicals are widely used to produce misfolded protein in the ER and induce UPR. Microarray analysis on tunicamycin and DTT stressed Arabidopsis seedlings indicated the broad synergistic correlation between UPR, ERAD and other cellular stress responses against overloaded misfolded protein within the plant ER (Martinez and Chrispeels, 2003; Kamauchi et al., 2005). The correlation between UPR and ERAD is well demonstrated in three maize

endosperm mutants, *Mc*, *fl2* and *DeB*-30*. The production of defective zeins in these three mutants triggers the induction of various ER molecular chaperones, folding catalysts (Boston et al., 1991; Houston et al., 2005), and ERAD related proteins (Kirst et al., 2005), leading to broad changes in PB morphology and lipid metabolism (Shank et al., 2001; Hunter et al., 2002).

In addition to ERAD, post ER compartments were shown to be important for protein quality control in yeast. Models have been proposed for ER exit including substrates lacking interaction with ER molecular chaperones or substrates containing ER exit signals (Coughlan et al., 2004; Kincaid and Cooper, 2007). In plants, two studies on BiP and PDI raised the possibility that there is a post ER compartment-involved protein quality control of normal ER chaperone proteins. BiP and PDI were reported with less accumulation in Arabidopsis suspension cell cultures at stationary phase (Tamura et al., 2004). The co-fractionation of BiP, PDI and two vacuolar proteases in the vacuoplast indicated a vacuole dependent degradation process. However, routes to the vacuole are different. The high mannose glycan of vacuolar localized PDI suggested the delivery of PDI to the vacuole is Golgi independent. A later study suggested that BiP is degraded in the vacuoles through the Golgi apparatus (Pimpl et al., 2006). When transport from the vacuole back to the Golgi was specifically inhibited by wortmannin, the secretion of BiP through the vacuole into the medium was increased in tobacco protoplasts. Furthermore, the secretion of BiP was inhibited by blocking COPII dependent ER to Golgi vesicle traffic. Pimpl et al. (2006) speculated that the ligands that BiP interacts with or BiP itself contain a vacuolar sorting signal that can be recognized by the

plant vacuolar sorting receptor BP80. When BiP-ligand complexes escape from the HDEL receptor, BP80 can interact and deliver BiP-ligand complexes from the Golgi apparatus to the vacuole for degradation. However, without the interaction data between BP80 and BiP-ligand complexes, it is still unknown whether this vacuole dependent protein degradation is a selective protein quality control or a passive general protein turnover.

Summary of plant ERAD

ERAD is involved in normal secretory protein turnover and misfolded secretory protein degradation. The importance of ERAD in regulating plant growth and development, and maintaining ER homeostasis under adverse stress conditions is far undervalued. Indeed, BiP and other ER molecular chaperones are induced to enhance the ER folding capacity for increased protein loading in the ER under various stress conditions, including the plant immune response (Wang et al., 2005), cold stress (Anderson et al., 1994), heat response (Gao et al., 2008), and osmotic stress (Irsigler et al., 2007). Considering the increased amount of misfolded protein in the ER because of either elevated loading for generating stress responsive proteins or a disturbed ER luminal environment, it is reasonable to hypothesize that ERAD is coordinated with other protein degradation processes to play essential roles to eliminate accumulated misfolded proteins and maintain ER integrity.

Thesis plan

My thesis is mainly focused on the investigation of ubiquitinated species and conserved ERAD components associated with protein body fractions in maize *De*-B30* endosperm.

In Chapter 2, I discovered increased ubiquitin signals primarily associated with *De*-B30* and *fl2* protein body fractions in which defective α-zeins are synthesized and deposited. I demonstrated that the accumulation of ubiquitinated species positively correlates with *De*-B30* and *fl2* gene dosages, and with defective zein production during endosperm development. In collaboration with Dr. Mialy F. Ramaroson and Dr. Michael B. Goshe, I identified these ubiquitinated proteins by using mass spectrometry. I was also able to map ubiquitination sites on these substrates with the identification of ubiquitinated peptides. I prepared in-gel trypsin digested samples, and Mialy ran the quadrupole time-of-flight spectrometer and performed database searches. I performed protein annotation and data mining.

In Chapter 3, I produced and purified full length recombinant proteins of ZmUFD1 and ZmCDC48 from *E. coli*, and demonstrated their direct interaction in pull-down assays *in vitro*. I also produced and purified truncated recombinant proteins of ZmCDC48, ZmHRD1 and ZmUFD1 in *E. coli* for antibody production. By using immunoblotting and mass spectrometry, I showed successful pull-downs of ZmUFD1, ZmCDC48, and ZmHRD1. Furthermore, I showed the interaction between ZmCDC48 and ZmUFD1 by using immunoprecipitation. In addition to protein-protein interaction studies, I characterized that increased amounts of ZmCDC48 were recruited to *De*-B30* and *fl2* protein body fractions

when compared to those of normal ones. The induction pattern of ZmHRD1 in *De*-B30* and *fl2* protein body fractions is similar to the increased recruitment of ZmCDC48.

In Appendix 1, I performed immunolocalization studies on endosperm and isolated protein body samples to understand the subcellular localization of ubiquitinated species, ZmCDC48 and ZmHRD1 associated with protein body fractions. My results demonstrated the immunolabeling of ZmCDC48 and ZmHRD1. I was not able to immunolocalize ubiquitinated species in spite of several attempts with three different ubiquitin antibodies. I did the fixation, embedding, and immunolabeling. Valerie Knowlton performed sectioning and assisted with transmission electron microscopy. Eva Johannes assisted with confocal laser scanning microscopy.

In Appendix 2, I reported a small group of maize ribosome associated membrane protein 4 (RAMP4), which are primarily localized to membrane fractions. Semi-quantitative studies suggested that one of five *ZmRAMP4* genes was slightly induced in *fl2* mutant endosperm. This study is based on TJV Sreenivasa Rao's work as a postdoc in the Boston lab.

In Appendix 3, I genotyped Arabidopsis *HRD1* and *RAMP4* T-DNA insertion lines. I attempted to characterize their root growth phenotypes under various stresses. However, there was no phenotypic difference between wild type and Arabidopsis *HRD1* and *RAMP4* T-DNA insertion lines. I performed genotyping and stress test experiments with help from

Daniel Wrenn, an undergraduate assistant. Dr. Anna Stepanova assisted with Arabidopsis crossing.

References

Alberts SM, Sonntag C, Schafer A, Wolf DH (2009) Ubx4 modulates cdc48 activity and influences degradation of misfolded proteins of the endoplasmic reticulum. J Biol Chem **284:** 16082-16089

Anderson JV, Li QB, Haskell DW, Guy CL (1994) Structural organization of the spinach endoplasmic reticulum-luminal 70-kilodalton heat-shock cognate gene and expression of 70-kilodalton heat-shock genes during cold acclimation. Plant Physiol **104:** 1359-1370

Avezov E, Frenkel Z, Ehrlich M, Herscovics A, Lederkremer GZ (2008) Endoplasmic reticulum (ER) mannosidase I is compartmentalized and required for *N*-glycan trimming to $Man_{5-6}GlcNAc_2$ in glycoprotein ER-associated degradation. Mol Biol Cell **19:** 216-225

Bays NW, Gardner RG, Seelig LP, Joazeiro CA, Hampton RY (2001) Hrd1p/Der3p is a membrane-anchored ubiquitin ligase required for ER-associated degradation. Nat Cell Biol **3:** 24-29

Bazirgan OA, Hampton RY (2008) Cue1p is an activator of Ubc7p E2 activity in vitro and in vivo. J Biol Chem **283:** 12797-12810

Bernardi KM, Forster ML, Lencer WI, Tsai B (2008) Derlin-1 facilitates the retro-translocation of cholera toxin. Mol Biol Cell **19:** 877-884

Bernasconi R, Galli C, Calanca V, Nakajima T, Molinari M (2010) Stringent requirement for HRD1, SEL1L, and OS-9/XTP3-B for disposal of ERAD-LS substrates. J Cell Biol **188:** 223-235

Biederer T, Volkwein C, Sommer T (1997) Role of Cue1p in ubiquitination and degradation at the ER surface. Science **278:** 1806-1809

Boisson M, Gomord V, Audran C, Berger N, Dubreucq B, Granier F, Lerouge P, Faye L, Caboche M, Lepiniec L (2001) *Arabidopsis glucosidase I* mutants reveal a critical role of *N*-glycan trimming in seed development. EMBO J **20:** 1010-1019

Boston RS, Fontes EB, Shank BB, Wrobel RL (1991) Increased expression of the maize immunoglobulin binding protein homolog b-70 in three zein regulatory mutants. Plant Cell **3:** 497-505

Boston RS, Viitanen PV, Vierling E (1996) Molecular chaperones and protein folding in plants. Plant Mol Biol **32:** 191-222

Brodsky JL (2007) The protective and destructive roles played by molecular chaperones during ERAD (endoplasmic-reticulum-associated degradation). Biochem J **404:** 353-363

Brodsky JL, Scott CM (2007) Tipping the delicate balance: defining how proteasome maturation affects the degradation of a substrate for autophagy and endoplasmic reticulum associated degradation (ERAD). Autophagy **3:** 623-625

Brodsky JL, Werner ED, Dubas ME, Goeckeler JL, Kruse KB, McCracken AA (1999) The requirement for molecular chaperones during endoplasmic reticulum-associated protein degradation demonstrates that protein export and import are mechanistically distinct. J Biol Chem **274:** 3453-3460

Buck TM, Wright CM, Brodsky JL (2007) The activities and function of molecular chaperones in the endoplasmic reticulum. Semin Cell Dev Biol **18:** 751-761

Burda P, Jakob CA, Beinhauer J, Hegemann JH, Aebi M (1999) Ordered assembly of the asymmetrically branched lipid-linked oligosaccharide in the endoplasmic reticulum is ensured by the substrate specificity of the individual glycosyltransferases. Glycobiology **9:** 617-625

Burke J, Lipari F, Igdoura S, Herscovics A (1996) The Saccharomyces cerevisiae processing alpha 1,2-mannosidase is localized in the endoplasmic reticulum, independently of known retrieval motifs. Eur J Cell Biol **70:** 298-305

Burn JE, Hurley UA, Birch RJ, Arioli T, Cork A, Williamson RE (2002) The cellulose-deficient *Arabidopsis* mutant *rsw3* is defective in a gene encoding a putative glucosidase II, an enzyme processing N-glycans during ER quality control. Plant J **32:** 949-960

Cabral CM, Liu Y, Sifers RN (2001) Dissecting glycoprotein quality control in the secretory pathway. Trends Biochem Sci **26:** 619-624

Carroll SM, Hampton RY (2009) Usa1p is required for optimal function and regulation of the Hrd1p endoplasmic reticulum-associated degradation ubiquitin ligase. J Biol Chem **285:** 5146-5156

Carvalho P, Goder V, Rapoport TA (2006) Distinct ubiquitin-ligase complexes define convergent pathways for the degradation of ER proteins. Cell **126:** 361-373

Chen B, Mariano J, Tsai YC, Chan AH, Cohen M, Weissman AM (2006) The activity of a human endoplasmic reticulum-associated degradation E3, gp78, requires its Cue domain, RING finger, and an E2-binding site. Proc Natl Acad Sci USA **103:** 341-346

Christianson JC, Shaler TA, Tyler RE, Kopito RR (2008) OS-9 and GRP94 deliver mutant alpha1-antitrypsin to the Hrd1-SEL1L ubiquitin ligase complex for ERAD. Nat Cell Biol **10:** 272-282

Clerc S, Hirsch C, Oggier DM, Deprez P, Jakob C, Sommer T, Aebi M (2009) Htm1 protein generates the N-glycan signal for glycoprotein degradation in the endoplasmic reticulum. J Cell Biol **184:** 159-172

Copic A, Dorrington M, Pagant S, Barry J, Lee MC, Singh I, Hartman JL 4th, Miller EA (2009) Genomewide analysis reveals novel pathways affecting endoplasmic reticulum homeostasis, protein modification and quality control. Genetics **182:** 757-769

Cormier JH, Tamura T, Sunryd JC, Hebert DN (2009) EDEM1 recognition and delivery of misfolded proteins to the SEL1L-containing ERAD complex. Mol Cell **34:** 627-633

Coughlan CM, Walker JL, Cochran JC, Wittrup KD, Brodsky JL (2004) Degradation of mutated bovine pancreatic trypsin inhibitor in the yeast vacuole suggests post-endoplasmic reticulum protein quality control. J Biol Chem **279**: 15289-15297

Dai RM, Chen E, Longo DL, Gorbea CM, Li CC (1998) Involvement of valosin-containing protein, an ATPase Co-purified with IkappaBalpha and 26 S proteasome, in ubiquitin-proteasome-mediated degradation of IkappaBalpha. J Biol Chem **273:** 3562-3573

Denic V, Quan EM, Weissman JS (2006) A luminal surveillance complex that selects misfolded glycoproteins for ER-associated degradation. Cell **126:** 349-359

Di Cola A, Frigerio L, Lord JM, Roberts LM, Ceriotti A (2005) Endoplasmic reticulum-associated degradation of ricin A chain has unique and plant-specific features. Plant Physiol **137:** 287-296

Friedlander R, Jarosch E, Urban J, Volkwein C, Sommer T (2000) A regulatory link between ER-associated protein degradation and the unfolded-protein response. Nat Cell Biol **2:** 379-384

Fujita E, Kouroku Y, Isoai A, Kumagai H, Misutani A, Matsuda C, Hayashi YK, Momoi T (2007) Two endoplasmic reticulum-associated degradation (ERAD) systems for the novel variant of the mutant dysferlin: ubiquitin/proteasome ERAD(I) and autophagy/lysosome ERAD(II). Hum Mol Genet **16:** 618-629

Gao H, Brandizzi F, Benning C, Larkin RM (2008) A membrane-tethered transcription factor defines a branch of the heat stress response in *Arabidopsis thaliana*. Proc Natl Acad Sci USA **105:** 16398-16403

Gardner RG, Swarbrick GM, Bays NW, Cronin SR, Wilhovsky S, Seelig L, Kim C, Hampton RY (2000) Endoplasmic reticulum degradation requires lumen to cytosol signaling. Transmembrane control of Hrd1p by Hrd3p. J Cell Biol **151:** 69-82

Gauss R, Jarosch E, Sommer T, Hirsch C (2006) A complex of Yos9p and the HRD ligase integrates endoplasmic reticulum quality control into the degradation machinery. Nat Cell Biol **8:** 849-854

Gillece P, Luz JM, Lennarz WJ, de La Cruz FJ, Romisch K (1999) Export of a cysteine-free misfolded secretory protein from the endoplasmic reticulum for degradation requires interaction with protein disulfide isomerase. J Cell Biol **147:** 1443-1456

Hampton RY, Gardner RG, Rine J (1996) Role of 26S proteasome and HRD genes in the degradation of 3-hydroxy-3-methylglutaryl-CoA reductase, an integral endoplasmic reticulum membrane protein. Mol Biol Cell **7:** 2029-2044

Hampton RY, Rine J (1994) Regulated degradation of HMG-CoA reductase, an integral membrane protein of the endoplasmic reticulum, in yeast. J Cell Biol **125:** 299-312

Hanzelmann P, Stingele J, Hofmann K, Schindelin H, Raasi S (2010) The yeast E4 ubiquitin ligase Ufd2 interacts with the ubiquitin-like domains of Rad23 and Dsk2 via a novel and distinct ubiquitin-like binding domain. J Biol Chem **285:** 20390-20398

Hartman IZ, Liu P, Zehmer JK, Luby-Phelps K, Jo Y, Anderson RG, DeBose-Boyd RA (2010) Sterol-induced retrotranslocation of 3-hydroxy-3-methylglutaryl coenzyme A reductase from endoplasmic reticulum membranes into the cytosol through a subcellular compartment resembling lipid droplets. J Biol Chem **285:** 19288-19298

Hartmann-Petersen R, Seeger M, Gordon C (2003) Transferring substrates to the 26S proteasome. Trends Biochem Sci **28:** 26-31

Hassink G, Kikkert M, van Voorden S, Lee SJ, Spaapen R, van Laar T, Coleman CS, Bartee E, Fruh K, Chau V, Wiertz E (2005) TEB4 is a C4HC3 RING finger-containing ubiquitin ligase of the endoplasmic reticulum. Biochem J **388:** 647-655

Haynes CM, Titus EA, Cooper AA (2004) Degradation of misfolded proteins prevents ER-derived oxidative stress and cell death. Mol Cell **15:** 767-776

Hegde NR, Chevalier MS, Wisner TW, Denton MC, Shire K, Frappier L, Johnson DC (2006) The role of BiP in endoplasmic reticulum-associated degradation of major

histocompatibility complex class I heavy chain induced by cytomegalovirus proteins. J Biol Chem **281:** 20910-20919

Hirsch C, Gauss R, Horn SC, Neuber O, Sommer T (2009) The ubiquitylation machinery of the endoplasmic reticulum. Nature **458:** 453-460

Hitchcock AL, Auld K, Gygi SP, Silver PA (2003) A subset of membrane-associated proteins is ubiquitinated in response to mutations in the endoplasmic reticulum degradation machinery. Proc Natl Acad Sci USA **100:** 12735-12740

Hong Z, Jin H, Fitchette AC, Xia Y, Monk AM, Faye L, Li J (2009) Mutations of an α1,6 mannosyltransferase inhibit endoplasmic reticulum-associated degradation of defective brassinosteroid receptors in *Arabidopsis*. Plant Cell **21:** 3792-3802

Hong Z, Jin H, Tzfira T, Li J (2008) Multiple mechanism-mediated retention of a defective brassinosteroid receptor in the endoplasmic reticulum of Arabidopsis. Plant Cell **20:** 3418-3429

Horn SC, Hanna J, Hirsch C, Volkwein C, Schutz A, Heinemann U, Sommer T, Jarosch E (2009) Usa1 functions as a scaffold of the HRD-ubiquitin ligase. Mol Cell **36:** 782-793

Hosokawa N, Wada I, Nagasawa K, Moriyama T, Okawa K, Nagata K (2008) Human XTP3-B forms an endoplasmic reticulum quality control scaffold with the HRD1-SEL1L ubiquitin ligase complex and BiP. J Biol Chem **283:** 20914-20924

Hosokawa N, Wada I, Natsuka Y, Nagata K (2006) EDEM accelerates ERAD by preventing aberrant dimer formation of misfolded alpha1-antitrypsin. Genes Cells **11:** 465-476

Hosomi A, Tanabe K, Hirayama H, Kim I, Rao H, Suzuki T (2010) Identification of an Htm1 (EDEM)-dependent, Mns1-independent endoplasmic reticulum-associated Degradation (ERAD) pathway in *Saccharomyces cerevisiae*: *Application of a novel assay for glycoprotein ERAD*. J Biol Chem **285:** 24324-24334

Houston NL, Fan C, Xiang JQ, Schulze JM, Jung R, Boston RS (2005) Phylogenetic analyses identify 10 classes of the protein disulfide isomerase family in plants, including single-domain protein disulfide isomerase-related proteins. Plant Physiol **137:** 762-778

Hunter BG, Beatty MK, Singletary GW, Hamaker BR, Dilkes BP, Larkins BA, Jung R (2002) Maize opaque endosperm mutations create extensive changes in patterns of gene expression. Plant Cell **14:** 2591-2612

Irsigler AS, Costa MD, Zhang P, Reis PA, Dewey RE, Boston RS, Fontes EP (2007) Expression profiling on soybean leaves reveals integration of ER- and osmotic-stress pathways. BMC Genomics **8:** 431

Ishida Y, Yamamoto A, Kitamura A, Lamande SR, Yoshimori T, Bateman JF, Kubota H, Nagata K (2009) Autophagic elimination of misfolded procollagen aggregates in the endoplasmic reticulum as a means of cell protection. Mol Biol Cell **20:** 2744-2754

Jakob CA, Burda P, Roth J, Aebi M (1998) Degradation of misfolded endoplasmic reticulum glycoproteins in Saccharomyces cerevisiae is determined by a specific oligosaccharide structure. J Cell Biol **142:** 1223-1233

Jarosch E, Taxis C, Volkwein C, Bordallo J, Finley D, Wolf DH, Sommer T (2002) Protein retrotranslocation from the ER requires polyubiquitination and the AAA-ATPase Cdc48. Nat Cell Biol **4:** 134-139

Jin H, Hong Z, Su W, Li J (2009) A plant-specific calreticulin is a key retention factor for a defective brassinosteroid receptor in the endoplasmic reticulum. Proc Natl Acad Sci USA **106:** 13612-13617

Jin H, Yan Z, Nam KH, Li J (2007) Allele-specific suppression of a defective brassinosteroid receptor reveals a physiological role of UGGT in ER quality control. Mol Cell **26:** 821-830

Jonikas MC, Collins SR, Denic V, Oh E, Quan EM, Schmid V, Weibezahn J, Schwappach B, Walter P, Weissman JS, Schuldiner M (2009) Comprehensive characterization of genes required for protein folding in the endoplasmic reticulum. Science **323:** 1693-1697

Kabani M, Kelley SS, Morrow MW, Montgomery DL, Sivendran R, Rose MD, Gierasch LM, Brodsky JL (2003) Dependence of endoplasmic reticulum-associated degradation on the peptide binding domain and concentration of BiP. Mol Biol Cell **14:** 3437-3448

Kalies KU, Allan S, Sergeyenko T, Kroger H, Romisch K (2005) The protein translocation channel binds proteasomes to the endoplasmic reticulum membrane. EMBO J **24:** 2284-2293

Kamauchi S, Nakatani H, Nakano C, Urade R (2005) Gene expression in response to endoplasmic reticulum stress in *Arabidopsis thaliana*. FEBS J **272:** 3461-3476

Kaneko M, Yasui S, Niinuma Y, Arai K, Omura T, Okuma Y, Nomura Y (2007) A different pathway in the endoplasmic reticulum stress-induced expression of human HRD1 and SEL1 genes. FEBS Lett **581:** 5355-5360

Kawagoe Y, Suzuki K, Tasaki M, Yasuda H, Akagi K, Katoh E, Nishizawa NK, Ogawa M, Takaiwa F (2005) The critical role of disulfide bond formation in protein sorting in the endosperm of rice. Plant Cell **17:** 1141-1153

Kim CS, Gibbon BC, Gillikin JW, Larkins BA, Boston RS, Jung R (2006) The maize *Mucronate* mutation is a deletion in the 16-kDa γ-zein gene that induces the unfolded protein response. Plant J **48:** 440-451

Kim I, Li Y, Muniz P, Rao H (2009) Usa1 protein facilitates substrate ubiquitylation through two separate domains. PLoS One **4**: e7604.

Kincaid MM, Cooper AA (2007) Misfolded proteins traffic from the endoplasmic reticulum (ER) due to ER export signals. Mol Biol Cell **18**: 455-463

Kirst ME, Meyer DJ, Gibbon BC, Jung R, Boston RS (2005) Identification and characterization of endoplasmic reticulum-associated degradation proteins differentially affected by endoplasmic reticulum stress. Plant Physiol **138:** 218-231

Koegl M, Hoppe T, Schlenker S, Ulrich HD, Mayer TU, Jentsch S (1999) A novel ubiquitination factor, E4, is involved in multiubiquitin chain assembly. Cell **96:** 635-644

Kosmaoglou M, Kanuga N, Aguila M, Garriga P, Cheetham ME (2009) A dual role for EDEM1 in the processing of rod opsin. J Cell Sci **122:** 4465-4472

Kroeger H, Miranda E, MacLeod I, Perez J, Crowther DC, Marciniak SJ, Lomas DA (2009) Endoplasmic reticulum-associated degradation (ERAD) and autophagy cooperate to degrade polymerogenic mutant serpins. J Biol Chem **284:** 22793-22802

Le Fourn V, Gaplovska-Kysela K, Guhl B, Santimaria R, Zuber C, Roth J (2009) Basal autophagy is involved in the degradation of the ERAD component EDEM1. Cell Mol Life Sci **66:** 1434-1445

Lee SO, Cho K, Cho S, Kim I, Oh C, Ahn K (2010) Protein disulphide isomerase is required for signal peptide peptidase-mediated protein degradation. EMBO J **29:** 363-375

Li CP, Larkins BA (1996) Expression of protein disulfide isomerase is elevated in the endosperm of the maize *floury-2* mutant. Plant Mol Biol **30:** 873-882

Li X, Wu Y, Zhang DZ, Gillikin JW, Boston RS, Franceschi VR, Okita TW (1993) Rice prolamine protein body biogenesis: a BiP-mediated process. Science **262:** 1054-1056

Lilley BN, Ploegh HL (2004) A membrane protein required for retrotranslocation of misfolded proteins from the ER. Nature **429:** 834-840

Loertscher J, Larson LL, Matson CK, Parrish ML, Felthauser A, Sturm A, Tachibana C, Bard M, Wright R (2006) Endoplasmic reticulum-associated degradation is required for cold adaptation and regulation of sterol biosynthesis in the yeast *Saccharomyces cerevisiae*. Eukaryot Cell **5:** 712-722

Loureiro J, Lilley BN, Spooner E, Noriega V, Tortorella D, Ploegh HL (2006) Signal peptide peptidase is required for retrotranslocation from the endoplasmic reticulum. Nature **441:** 894-897

Marshall RS, Jolliffe NA, Ceriotti A, Snowden CJ, Lord JM, Frigerio L, Roberts LM (2008) The role of CDC48 in the retro-translocation of non-ubiquitinated toxin substrates in plant cells. J Biol Chem **283:** 15869-15877

Martinez IM, Chrispeels MJ (2003) Genomic analysis of the unfolded protein response in Arabidopsis shows its connection to important cellular processes. Plant Cell **15:** 561-576

Medicherla B, Kostova Z, Schaefer A, Wolf DH (2004) A genomic screen identifies Dsk2p and Rad23p as essential components of ER-associated degradation. EMBO Rep **5:** 692-697

Meyer HH, Shorter JG, Seemann J, Pappin D, Warren G (2000) A complex of mammalian ufd1 and npl4 links the AAA-ATPase, p97, to ubiquitin and nuclear transport pathways. EMBO J **19:** 2181-2192

Molinari M, Calanca V, Galli C, Lucca P, Paganetti P (2003) Role of EDEM in the release of misfolded glycoproteins from the calnexin cycle. Science **299:** 1397-1400

Molinari M, Galli C, Piccaluga V, Pieren M, Paganetti P (2002) Sequential assistance of molecular chaperones and transient formation of covalent complexes during protein degradation from the ER. J Cell Biol **158:** 247-257

Moore P, Bernardi KM, Tsai B (2010) The Ero1alpha-PDI redox cycle regulates retro-translocation of cholera toxin. Mol Biol Cell **21:** 1305-1313

Muller J, Piffanelli P, Devoto A, Miklis M, Elliott C, Ortmann B, Schulze-Lefert P, Panstruga R (2005) Conserved ERAD-like quality control of a plant polytopic membrane protein. Plant Cell **17:** 149-163

Nakatsukasa K, Huyer G, Michaelis S, Brodsky JL (2008) Dissecting the ER-associated degradation of a misfolded polytopic membrane protein. Cell **132:** 101-112

Neuber O, Jarosch E, Volkwein C, Walter J, Sommer T (2005) Ubx2 links the Cdc48 complex to ER-associated protein degradation. Nat Cell Biol **7:** 993-998

Ng W, Sergeyenko T, Zeng N, Brown JD, Romisch K (2007) Characterization of the proteasome interaction with the Sec61 channel in the endoplasmic reticulum. J Cell Sci **120:** 682-691

Nishikawa SI, Fewell SW, Kato Y, Brodsky JL, Endo T (2001) Molecular chaperones in the yeast endoplasmic reticulum maintain the solubility of proteins for retrotranslocation and degradation. J Cell Biol **153:** 1061-1070

Oda Y, Hosokawa N, Wada I, Nagata K (2003) EDEM as an acceptor of terminally misfolded glycoproteins released from calnexin. Science **299:** 1394-1397

Oda Y, Okada T, Yoshida H, Kaufman RJ, Nagata K, Mori K (2006) Derlin-2 and Derlin-3 are regulated by the mammalian unfolded protein response and are required for ER-associated degradation. J Cell Biol **172:** 383-393

Oliver JD, Roderick HL, Llewellyn DH, High S (1999) ERp57 functions as a subunit of specific complexes formed with the ER lectins calreticulin and calnexin. Mol Biol Cell **10:** 2573-2582

Onda Y, Kumamaru T, Kawagoe Y (2009) ER membrane-localized oxidoreductase Ero1 is required for disulfide bond formation in the rice endosperm. Proc Natl Acad Sci USA **106:** 14156-14161

Osborne AR, Rapoport TA, van den Berg B (2005) Protein translocation by the Sec61/SecY channel. Annu Rev Cell Dev Biol **21:** 529-550

Park CJ, Bart R, Chern M, Canlas PE, Bai W, Ronald PC (2010) Overexpression of the endoplasmic reticulum chaperone BiP3 regulates XA21-mediated innate immunity in rice. PLoS One **5:** e9262

Park S, Isaacson R, Kim HT, Silver PA, Wagner G (2005) Ufd1 exhibits the AAA-ATPase fold with two distinct ubiquitin interaction sites. Structure **13:** 995-1005

Parodi AJ (2000) Protein glucosylation and its role in protein folding. Annu Rev Biochem **69:** 69-93

Pattison RJ, Amtmann A (2009) N-glycan production in the endoplasmic reticulum of plants. Trends Plant Sci **14:** 92-99

Pilon M, Schekman R, Romisch K (1997) Sec61p mediates export of a misfolded secretory protein from the endoplasmic reticulum to the cytosol for degradation. EMBO J **16:** 4540-4548

Pimpl P, Taylor JP, Snowden C, Hillmer S, Robinson DG, Denecke J (2006) Golgi-mediated vacuolar sorting of the endoplasmic reticulum chaperone BiP may play an active role in quality control within the secretory pathway. Plant Cell **18:** 198-211

Plemper RK, Bohmler S, Bordallo J, Sommer T, Wolf DH (1997) Mutant analysis links the translocon and BiP to retrograde protein transport for ER degradation. Nature **388:** 891-895

Ploegh HL (2007) A lipid-based model for the creation of an escape hatch from the endoplasmic reticulum. Nature **448:** 435-438

Pye VE, Beuron F, Keetch CA, McKeown C, Robinson CV, Meyer HH, Zhang X, Freemont PS (2007) Structural insights into the p97-Ufd1-Npl4 complex. Proc Natl Acad Sci USA **104:** 467-472

Quan EM, Kamiya Y, Kamiya D, Denic V, Weibezahn J, Kato K, Weissman JS (2008) Defining the glycan destruction signal for endoplasmic reticulum-associated degradation. Mol Cell **32:** 870-877

Rapoport TA (2007) Protein translocation across the eukaryotic endoplasmic reticulum and bacterial plasma membranes. Nature **450:** 663-669

Ravid T, Kreft SG, Hochstrasser M (2006) Membrane and soluble substrates of the Doa10 ubiquitin ligase are degraded by distinct pathways. EMBO J **25:** 533-543

Richly H, Rape M, Braun S, Rumpf S, Hoege C, Jentsch S (2005) A series of ubiquitin binding factors connects CDC48/p97 to substrate multiubiquitylation and proteasomal targeting. Cell **120:** 73-84

Ruddock LW, Molinari M (2006) N-glycan processing in ER quality control. J Cell Sci **119:** 4373-4380

Saito Y, Kishida K, Takata K, Takahashi H, Shimada T, Tanaka K, Morita S, Satoh S, Masumura T (2009) A green fluorescent protein fused to rice prolamin forms protein body-like structures in transgenic rice. J Exp Bot **60:** 615-627

Sakoh-Nakatogawa M, Nishikawa S, Endo T (2009) Roles of protein-disulfide isomerase-mediated disulfide bond formation of yeast Mnl1p in endoplasmic reticulum-associated degradation. J Biol Chem **284:** 11815-11825

Sato BK, Schulz D, Do PH, Hampton RY (2009) Misfolded membrane proteins are specifically recognized by the transmembrane domain of the Hrd1p ubiquitin ligase. Mol Cell **34:** 212-222

Schafer A, Wolf DH (2009) Sec61p is part of the endoplasmic reticulum-associated degradation machinery. EMBO J **28:** 2874-2884

Schmitz A, Herrgen H, Winkeler A, Herzog V (2000) Cholera toxin is exported from microsomes by the Sec61p complex. J Cell Biol **148:** 1203-1212

Schuberth C, Buchberger A (2005) Membrane-bound Ubx2 recruits Cdc48 to ubiquitin ligases and their substrates to ensure efficient ER-associated protein degradation. Nat Cell Biol **7:** 999-1006

Scott DC, Schekman R (2008) Role of Sec61p in the ER-associated degradation of short-lived transmembrane proteins. J Cell Biol **181:** 1095-1105

Shank KJ, Su P, Brglez I, Boss WF, Dewey RE, Boston RS (2001) Induction of lipid metabolic enzymes during the endoplasmic reticulum stress response in plants. Plant Physiol **126:** 267-277

Shimoni Y, Zhu XZ, Levanony H, Segal G, Galili G (1995) Purification, characterization, and intracellular localization of glycosylated protein disulfide isomerase from wheat grains. Plant Physiol **108:** 327-335

Silberstein S, Schlenstedt G, Silver PA, Gilmore R (1998) A role for the DnaJ homologue Scj1p in protein folding in the yeast endoplasmic reticulum. J Cell Biol **143:** 921-933

Simons JF, Ferro-Novick S, Rose MD, Helenius A (1995) BiP/Kar2p serves as a molecular chaperone during carboxypeptidase Y folding in yeast. J Cell Biol **130:** 41-49

Su W, Liu Y, Xia Y, Hong Z, Li J (2011) Conserved endoplasmic reticulum-associated degradation system to eliminate mutated receptor-like kinases in *Arabidopsis*. Proc Natl Acad Sci USA **108:** 870-875

Sun F, Zhang R, Gong X, Geng X, Drain PF, Frizzell RA (2006) Derlin-1 promotes the efficient degradation of the cystic fibrosis transmembrane conductance regulator (CFTR) and CFTR folding mutants. J Biol Chem **281:** 36856-36863

Swanson R, Locher M, Hochstrasser M (2001) A conserved ubiquitin ligase of the nuclear envelope/endoplasmic reticulum that functions in both ER-associated and Matalpha2 repressor degradation. Genes Dev **15:** 2660-2674

Takemoto Y, Coughlan SJ, Okita TW, Satoh H, Ogawa M, Kumamaru T (2002) The rice mutant *esp2* greatly accumulates the glutelin precursor and deletes the protein disulfide isomerase. Plant Physiol **128:** 1212-1222

Tamura K, Yamada K, Shimada T, Hara-Nishimura I (2004) Endoplasmic reticulum-resident proteins are constitutively transported to vacuoles for degradation. Plant J **39:** 393-402

Taxis C, Hitt R, Park SH, Deak PM, Kostova Z, Wolf DH (2003) Use of modular substrates demonstrates mechanistic diversity and reveals differences in chaperone requirement of ERAD. J Biol Chem **278:** 35903-35913

Taxis C, Vogel F, Wolf DH (2002) ER-Golgi traffic is a prerequisite for efficient ER degradation. Mol Biol Cell **13:** 1806-1818

Thoms S (2002) Cdc48 can distinguish between native and non-native proteins in the absence of cofactors. FEBS Lett **520:** 107-110

Travers KJ, Patil CK, Wodicka L, Lockhart DJ, Weissman JS, Walter P (2000) Functional and genomic analyses reveal an essential coordination between the unfolded protein response and ER-associated degradation. Cell **101:** 249-258

Tu BP, Weissman JS (2004) Oxidative protein folding in eukaryotes: mechanisms and consequences. J Cell Biol **164:** 341-346

Vashist S, Ng DT (2004) Misfolded proteins are sorted by a sequential checkpoint mechanism of ER quality control. J Cell Biol **165:** 41-52

Vembar SS, Jonikas MC, Hendershot LM, Weissman JS, Brodsky JL (2010) J domain co-chaperone specificity defines the role of BiP during protein translocation. J Biol Chem **285:** 22484-22494

Verma R, Chen S, Feldman R, Schieltz D, Yates J, Dohmen J, Deshaies RJ (2000) Proteasomal proteomics: identification of nucleotide-sensitive proteasome-interacting proteins by mass spectrometric analysis of affinity-purified proteasomes. Mol Biol Cell **11:** 3425-3439

Wahlman J, DeMartino GN, Skach WR, Bulleid NJ, Brodsky JL, Johnson AE (2007) Real-Time fluorescence detection of ERAD substrate retrotranslocation in a mammalian in vitro system. Cell **129:** 943-955

Wang B, Alam SL, Meyer HH, Payne M, Stemmler TL, Davis DR, Sundquist WI (2003) Structure and ubiquitin interactions of the conserved zinc finger domain of Npl4. J Biol Chem **278:** 20225-20234

Wang D, Weaver ND, Kesarwani M, Dong X (2005) Induction of protein secretory pathway is required for systemic acquired resistance. Science **308:** 1036-1040

Wang H, Boavida LC, Ron M, McCormick S (2008) Truncation of a protein disulfide isomerase, PDIL2-1, delays embryo sac maturation and disrupts pollen tube guidance in *Arabidopsis thaliana*. Plant Cell **20:** 3300-3311

Wang S, Ng DT (2010) Evasion of endoplasmic reticulum surveillance makes Wsc1p an obligate substrate of Golgi quality control. Mol Biol Cell **21:** 1153-1165

Willer M, Forte GM, Stirling CJ (2008) Sec61p is required for ERAD-L: genetic dissection of the translocation and ERAD-L functions of Sec61P using novel derivatives of CPY. J Biol Chem **283:** 33883-33888

Williams DB (2006) Beyond lectins: the calnexin/calreticulin chaperone system of the endoplasmic reticulum. J Cell Sci **119:** 615-623

Yamagata H, Sugimoto T, Tanaka K, Kasai Z (1982) Biosynthesis of storage proteins in developing rice seeds. Plant Physiol **70:** 1094-1100

Yamamoto K, Suzuki N, Wada T, Okada T, Yoshida H, Kaufman RJ, Mori K (2008) Human HRD1 promoter carries a functional unfolded protein response element to which XBP1 but not ATF6 directly binds. J Biochem **144:** 477-486

Yasuda H, Hirose S, Kawakatsu T, Wakasa Y, Takaiwa F (2009) Overexpression of BiP has inhibitory effects on the accumulation of seed storage proteins in endosperm cells of rice. Plant Cell Physiol **50:** 1532-1543

Ye Y, Meyer HH, Rapoport TA (2001) The AAA ATPase Cdc48/p97 and its partners transport proteins from the ER into the cytosol. Nature **414:** 652-656

Ye Y, Meyer HH, Rapoport TA (2003) Function of the p97-Ufd1-Npl4 complex in retrotranslocation from the ER to the cytosol: dual recognition of nonubiquitinated polypeptide segments and polyubiquitin chains. J Cell Biol **162:** 71-84

Ye Y, Shibata Y, Yun C, Ron D, Rapoport TA (2004) A membrane protein complex mediates retro-translocation from the ER lumen into the cytosol. Nature **429:** 841-847

Younger JM, Chen L, Ren HY, Rosser MF, Turnbull EL, Fan CY, Patterson C, Cyr DM (2006) Sequential quality-control checkpoints triage misfolded cystic fibrosis transmembrane conductance regulator. Cell **126:** 571-582

Zhang F, Boston RS (1992) Increases in binding protein (BiP) accompany changes in protein body morphology in three high-lysine mutants of maize. Protoplasma **171:** 142-152

Zuber C, Cormier JH, Guhl B, Santimaria R, Hebert DN, Roth J (2007) EDEM1 reveals a quality control vesicular transport pathway out of the endoplasmic reticulum not involving the COPII exit sites. Proc Natl Acad Sci USA **104:** 4407-4412

Table 1. Selected ERAD components in yeast, mammals, and plants (discussed in this review chapter)

Yeast	Mammals	Plants	Location	Function
Recognition and targeting				
Kar2p	BiP	BiP	ER lumen	Folding
Sec63p			ER lumen	Translocation
Jem1p, Scj1p			ER lumen	Folding
	GRP94		ER lumen	Folding
Pdi1p	PDIs	PDIs	ER lumen	Disulfide bond formation
Ero1p	ERO1	ERO1	ER lumen	Disulfide bond formation
Cne1p	Calnexin	Calnexin	ER membrane	Glycoprotein folding
	Calreticulin	Calreticulin	ER lumen	Glycoprotein folding
	UGGT	UGGT	ER lumen	Adding glucose
Htm1p	EDEMs			Exposing α-1,6 mannose
Yos9p	OS9 and XTP3-B		ER lumen	α-1,6 mannose recognition
Retrotranslocation				
Sec61p	Sec61		ER membrane	Dislocation
Der1p	Derlins	Derlins	ER membrane	Dislocation

Table 1. (continued)

Yeast	Mammals	Plants	Location	Function
E3 ligases and their cofactors				
Hrd1p-Hrd3p	HRD1-SEL1L	HRD1, HRD3	ER membrane	E3 ligase complex
	gp78		ER membrane	E3 ligase
Usa1p	HERP		ER membrane	recuiting Der1p to Hrd1p
Ubx2p			ER membrane	recruiting Cdc48p complex to Hrd1p
	VIMP		ER membrane	recruiting p97 complex to HRD1
Doa10p	TEB4		ER membrane	E3 ligase
Cue1p			ER membrane	recuiting Ubc7p to Hrd1p
Ubc7p	UBC7		Membrane associated	E2 ligase
	Ube2g2		Membrane associated	E2 ligase
Substrate extraction and Proteasomal degradation				
Cdc48p-Ufd1p-Npl4p	p97-UFD1-NPL4	CDC48	Membrane associated	Substrate extraction
Ufd2p			Cytoplasm	Polyubiquitin chain extension
Ubx4p			Cytoplasm	Delivery to 26S proteasomes

Figure 1. Schematic diagrams of selected components of the Hrd1 transmembrane complex in yeast (panel A), mammals (panel B), and plants (panel C). A. On the ER lumen side, yeast Hrd1p-Hrd3p recruits Yos9p and Kar2p for substrate recognition. In the membrane, Hrd1p interacts with Der1p through Usa1p. On the cytoplasm side, Hrd1p employs its E2 ligase Ubc7p through the membrane anchor Cue1p. In addition, the interaction between Hrd1p and Cdc48p is regulated by the membrane protein Ubx2p. B. Mammalian HRD1-SEL1L utilizes OS9, XTP3-B and BiP to recognize substrates. HRD1 interacts with Derlins through HERP. HRD1 also interacts with its E2 ligase UBC7. CDC48 directly or indirectly interacts with HRD1 through VIMP. C. The ER molecular chaperone BiP, transmembrane protein Derlins, and cytoplasmic protein CDC48 were identified in plants. HRD3, HRD1 were identified in genetic studies, and their localizations are predicted here. Their interactions are not clear in plants.

A

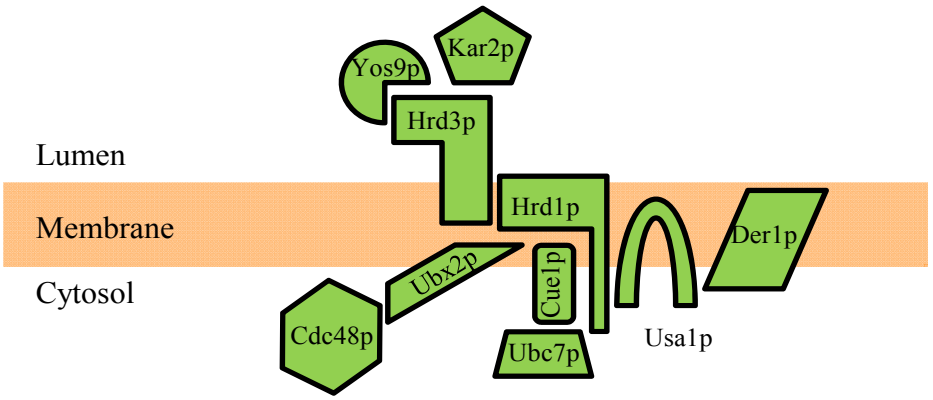
Kar2p
Yos9p
Hrd3p
Lumen
Membrane
Cytosol
Hrd1p
Der1p
Ubx2p
Cue1p
Cdc48p
Ubc7p
Usa1p

B

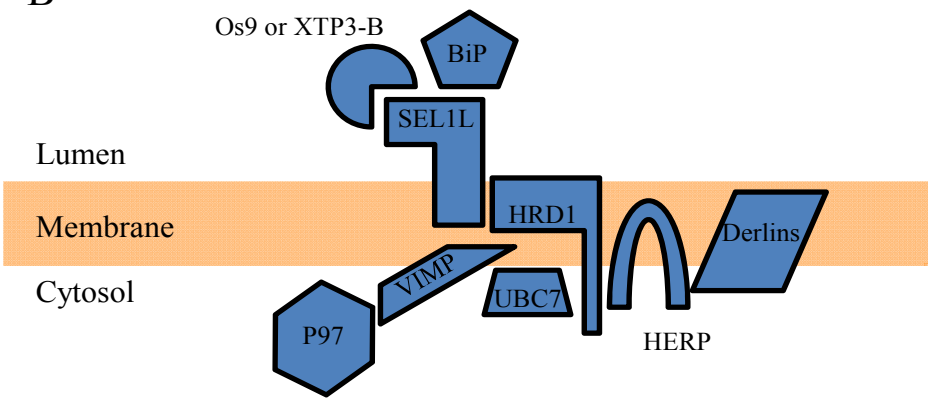
Os9 or XTP3-B
BiP
SEL1L
Lumen
Membrane
Cytosol
HRD1
Derlins
VIMP
UBC7
P97
HERP

C

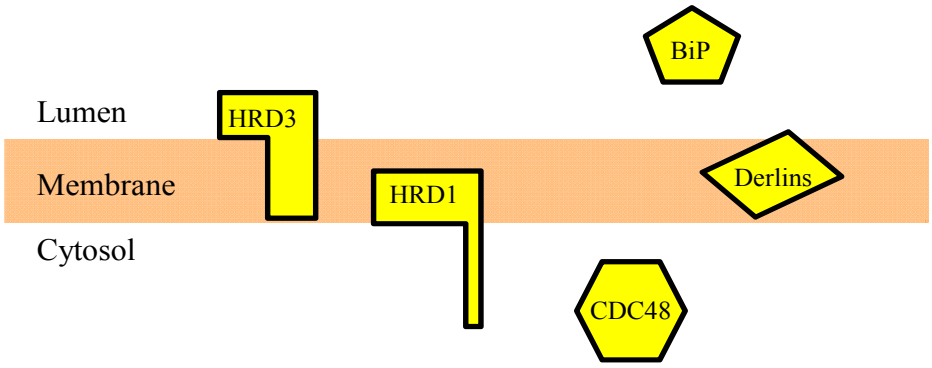
BiP
Lumen
HRD3
Membrane
HRD1
Derlins
Cytosol
CDC48

Chapter 2: Ubiquitination contributes to pleiotropic effects in the *De*-B30* endosperm mutant of maize

Abstract

Protein bodies are endoplasmic reticulum derived organelles that serve as repositories for storage protein accumulation. The storage protein packing process is sophisticated and well organized. The disturbed packing process presumably triggers a series of cellular responses. Here, we report a specific increase in ubiquitin signals associated with malformed *De*-B30* protein bodies and defective 19-kD α-zein synthesis. By using a combination of biochemical tools and proteomic analysis, we have identified ubiquitinated substrates in *De*-B30* protein bodies. These results add the ubiquitination as a new aspect to understand the effects of the *De*-B30* mutation in maize endosperm.

Introduction

Secretory proteins are primarily translocated, folded and modified in the endoplasmic reticulum (ER). Once achieving their native conformations for proper functions, secretory proteins depart from the ER to their final destinations. As a part of its quality control mechanism, the ER is equipped with a series of molecular chaperones as well as folding and modification enzymes to assist nascent peptides for folding and maturation. However, without achieving their proper conformations, misfolded proteins might be dislocated to the cytosol for a ubiquitin dependent degradation through a disposal mechanism designated as ER associated protein degradation (ERAD; Hirsch et al., 2009). A canonical ERAD process

comprises substrate recognition in the ER lumen, retrotranslocation through the ER membrane, initial ubiquitination on the ER membrane, and final ubiquitin-dependent degradation by the 26S proteasome.

A conserved ER quality control mechanism including ERAD has been reported in plants (Vitale and Boston, 2008). However, only a few ERAD substrates have been shown to require 26S proteasome activity for their degradation. Castor bean ricin toxin A chain (RTA), *Ricinus communis* agglutinin A chain (RCA A), mutant barley mildew resistance o (MLO) proteins, and mutant brassinosteroid receptors bri1-9 are four examples (Di Cola et al., 2001; Muller et al., 2005; Marshall et al., 2008; Hong et al., 2009). Although changing the number of lysine residues in RTA affects its degradation, only the mutant MLO-1 protein among these substrates was shown to be ubiquitinated when it was expressed in Arabidopsis protoplasts. Not all ER misfolded proteins in plants require the 26S proteasome activity. A mutant BR receptor bri1-5 has been reported to be degraded through a proteasome independent process (Hong et al., 2008). The different degradation routes of various substrates imply ERAD is as complex in plants as it is in yeast and mammals.

Maize endosperm is a terminal tissue that contains protein bodies for storage protein accumulation (Larkins and Hurkman, 1978). An efficient mechanism has evolved to facilitate the storage protein packing into protein bodies. An early model suggested that β- and γ-zeins are first synthesized by membrane bound ribosomes and transported into the endoplasmic reticulum (ER) lumen to initiate protein body formation (Lending and Larkins, 1989).

Subsequently, α- and δ-zeins are synthesized and accumulate in the center of a protein body. A mature protein body finally consists of a central core of α- and δ-zeins with a continuous peripheral layer of β- and γ-zeins. Holding et al. (2007) showed that the 22-kD and 19-kD α-zeins are differentially localized in the core region of a protein body. In the presence of membrane protein Floury1 (FL1), the 22-kD α-zein is discretely localized beneath the β- and γ-zein layer in the core region, whereas the 19-kD α-zein is more evenly distributed throughout the central region. Studies in heterologous systems showed that β- or γ-zeins were important for protein body formation, as the coexpression of β- or γ-zeins stabilized the α-zein accumulation in transgenic tobacco endosperm (Coleman et al., 1996; Coleman et al., 2004). However, an RNAi study in maize endosperm demonstrated that eliminating both β- and γ-zeins only affected protein body morphology, but did not disturb the accumulation of α-zeins (Wu and Messing, 2010). The authors suggested that a sophisticated packing mechanism beyond the expression of β- or γ-zeins is critical for the α-zein accumulation and protein body formation in maize endosperm.

Protein trafficking to protein bodies is typically believed to be unidirectional. However, studies on three opaque endosperm mutants, *defective endosperm B30* (*De*-B30*), *floury-2* (*fl2*), and *Mucronate* (*Mc*), have shed light on the dynamics of protein bodies. The molecular mechanisms of these three maize opaque endosperm mutants have been unraveled recently. The *De*-B30* and *fl2* mutants both produce defective α-zeins. The signal sequence of a defective 22-kD α-zein encoded by the *fl2* mutant allele is not able to be processed by signal peptidase (Gillikin et al., 1997). The signal sequence of a defective 19-kD α-zein encoded by

the *De*-B30* mutant allele is inefficiently processed (Kim et al., 2004). In the *Mc* mutant, a 38 bp deletion in the 16-kD γ-zein transcript creates a frameshift mutant in which the 16-kD γ-zein accumulates to a lesser degree (Kim et al., 2006). Previous studies showed that the deposition of mutant storage proteins disrupts protein body homeostasis, and results in the induction of the unfolded protein response (UPR) with the accumulation of a series of ER molecular chaperones including BiP, PDI, calnexin and calreticulin, and the ERAD related ZmDerlin proteins (Boston et al., 1991; Zhang and Boston, 1992; Houston et al., 2005; Kirst et al., 2005). The induction of ER chaperones and ERAD related proteins raises the possibility that proteins are removed in order to maintain the homeostasis of *De*-B30* and *fl2* protein bodies.

Herein, we report increased ubiquitin signals that were specifically partitioned into the protein body fraction of *De*-B30* endosperm. By combining biochemical tools and mass spectrometry, we identified ubiquitinated proteins that suggest a broad impact of the *De*-B30* mutant allele in endosperm development.

Materials and Methods

Plant materials

The normal maize inbred W64A and its near isogenic mutants, *De*-B30*, *fl2*, *Mc*, *o2*, and *fl1*, were grown at the Central Crops Research Station, Clayton, North Carolina. At indicated days after pollination (DAP), ears were harvested and directly frozen in liquid nitrogen. Frozen kernels were shelled on dry ice and stored at -80°C until use.

Endosperm protein extraction

Endosperm from normal and mutant inbred lines was dissected from frozen kernels. Equal fresh weights of endosperm were homogenized with a Pro 200 homogenizer (PRO Scientific, Oxford, CT) in buffer B (10 mM Tris-HCl, pH 8.5 at 25°C, 10 mM KCl, 5 mM $MgCl_2$) containing 7.2% (w/v) sucrose and protease inhibitor cocktail for plant cell and tissue extracts [1:1,000 (v/v); Sigma, St Louis, MO] at a 1:4 (w/v) grinding ratio. When ATP depletion was required, 10 mM glucose and 5 U/ml hexokinase were included in the grinding buffer as reported (Kim et al., 2006). When excess ATP was required, ATP was added to the grinding buffer to give a final concentration of 5 mM. All steps were carried out at 4°C, unless otherwise noted. The homogenate was filtered through 2 layers of Miracloth (Calbiochem, San Diego, CA) and subjected to a centrifugation at 300 g for 5 min to remove cellular debris and starch. The supernatant was denoted as the unfractionated aqueous extract.

Protein body isolation and subcellular fractionation

Protein bodies from endosperm at stages from 8 DAP to 18 DAP were isolated by discontinuous sucrose gradient centrifugation as described by Larkins and Hurkman (1978). The unfractionated aqueous extract was overlaid on the top of 1.5 M and 2 M sucrose pads containing buffer B. The step gradients were subjected to a centrifugation at 100,000 g for 30 min. Protein bodies were recovered from the interface between the 1.5 M and 2 M sucrose pads, and diluted with buffer B at a 1:3 (v/v) ratio. Diluted protein bodies were subsequently subjected to a centrifugation at 100,000 g for 30 min to generate a protein body pellet. Except

for the subcellular fractionation experiment, all protein bodies were isolated through sucrose gradients.

A differential centrifugation was performed in the subcellular fractionation experiment. The unfractionated aqueous extract was subjected to a centrifugation at 5,000 g for 10 min. Protein bodies were obtained from the pellet. The remaining membranes were collected as the pellet after a centrifugation at 100,000 g for 30 min. The supernatant remaining after the 100,000 g centrifugation was denoted as S100. Each fraction was resuspended back to the volume of the original homogenate.

Chemical treatments of protein bodies

The unfractionated aqueous extract was overlaid on the top of 1.5 M and 2 M sucrose pads in buffer B. The step gradients were subjected to a centrifugation at 100,000 g for 30 min. Protein bodies were collected from the interface between the 1.5 M sucrose and 2 M sucrose pads, and diluted with buffer B at a 1:3 (v/v) ratio. Diluted protein bodies from equal fresh weight equivalents (5 mg) were subjected to a centrifugation at 100,000 g for 30 min, and subsequently resuspended in 200 µl of buffer (50 mM Tris, pH 7.5 at 25°C) in the presence of 1 M NaCl, 1% (v/v) Triton X-100, 1 M NaCl and 1% (v/v) Triton X-100, or 1% (w/v) SDS. Samples were agitated on a Nutator (Clay Adams, Parsippany, NJ) for 30 min at room temperature, and then subjected to a centrifugation at 100,000 g for 30 min. Equal fresh weight equivalents (1 mg) of supernatants (SP) and pellets (P) were resolved by SDS-PAGE and visualized by immunoblotting.

Zein and non-zein protein separation

Normal and *De*-B30* protein bodies were resuspended in 70% (v/v) ethanol in the presence or absence of 2% (v/v) β-mercaptoethanol (β-ME**)** as previously described (Kim et al., 2006). Insoluble non-zein proteins were recovered from the pellet after a centrifugation at 14,000 g for 15 min. Zein proteins were recovered from the supernatant and dried by vacuum centrifugation. Non-zein and zein proteins were separated by SDS-PAGE and visualized by immunoblotting.

Identification of ubiquitinated species

Normal and *De*-B30* protein bodies were resuspended in buffer B containing 1 M NaCl and 1% (v/v) Triton X-100 by agitation on a nutator for 30 min at room temperature. After a centrifugation at 14,000 g for 10 min, pellets were resuspended into a solubilization buffer [0.0125 M $Na_2B_4O_7$, pH 10.0 at 25°C; 1% (w/v) SDS; and 2% (v/v) β-ME] as reported (Wallace et al., 1990). Absolute ethanol was subsequently added to a final concentration of 70% (v/v). Non-zein proteins were precipitated and collected by a centrifugation at 14,000 g for 10 min.

Proteins were dissolved in 1% (w/v) SDS. Protein concentration was measured with a BCA protein assay kit and bovine serum albumin standard (Pierce, Rockford, IL). Twenty micrograms of proteins in the non-zein fraction from normal and *De*-B30* endosperm were loaded on a 4-12% NuPAGE® Bis-Tris gel (Invitrogen, Carlsbad, CA). Proteins were stained with a Colloidal Blue Staining Kit according to the manufacturer's instructions (Invitrogen,

Carlsbad, CA). After the gel region below the 50-kD marker was discarded along with dominant bands above the 50-kD marker, the remaining gel region was cut into 1mm^3 blocks. In-gel digestion with trypsin was conducted using a published protocol (Wang et al., 2008). All samples were analyzed by LC/MS^E using a NanoAcquity UPLC with a 75 μm i.d. x 25 cm BEH column coupled to a Q-TOF Premier mass spectrometer (Waters Corporation, Milford, MA). All data were processed using a ProteinLynx Global Server 2.3 (PLGS2.3) and database searching against the B73 filtered translation database (version 4a.53; http://www.maizesequence.org) using ion accounting (IDENTITY^E) and a 5% false discovery rate (Geromanos et al., 2009; Li et al., 2009).

Immunoblot analysis

Equal amounts of sample proteins were adjusted with 2x SDS sample loading buffer to the same volume and heated to 95°C for 5 min (Laemmli, 1970). Sample proteins were separated through SDS polyacrylamide gels and transferred to Immobilon-FL membranes (Millipore, Billerica, MA) as previously reported (Houston et al., 2005). Membranes were then blocked for 1 h with 0.2x phosphate-buffered saline containing 0.1% (w/v) casein. Primary antibodies against ubiquitin (Santa Cruz Biotech, Santa Cruz, CA), BiP (StressGen Biotechnologies, Victoria, British Columbia, Canada), BRITTLE-1 (BT1; a gift from Dr. Thomas D. Sullivan, University of Wisconsin, Madison), SHRUNKEN2 (SH2) and BRITTLE-2 (BT2; gifts from Dr. L. C. Hannah; University of Florida, Gainesville),and zeins were used at a 1:10,000 dilution in 0.2x phosphate-buffered saline containing 0.1% (w/v) casein and 0.05% (v/v) Tween-20 for an overnight incubation (Hunter et al., 2002). After incubation with primary

antibody, membranes were then incubated with appropriate goat anti-rabbit or anti-mouse IgG conjugated to DyLight® 680 or DyLight® 800 (1:10,000; Thermo Scientific, Waltham, MA). Immunoblot images were acquired with an Odyssey® infrared imaging system (Li-COR Biosciences, Lincoln, NE).

Results

Increased ubiquitin signals in protein body fractions

Opaque mutants including *De*B-30*, *fl2*, and *Mc* produce mutant zeins and trigger the UPR including inductions of ER molecular chaperones and ERAD related ZmDerlin proteins (Boston et al., 1991; Coleman et al., 1995; Kim et al., 2004; Kirst et al., 2005; Kim et al., 2006). The opaque mutant *opaque-2* (*o2*) does not produce mutant zeins, but mainly down-regulates the expression of 22-kD α-zeins (Schmidt et al., 1990). The opaque mutant *floury-1* (*fl1*) neither produces mutant zeins, nor affects zein synthesis, although *fl1* perturbs the deposition of 22-kD α-zeins (Holding et al., 2007). Because neither *o2* nor *fl1* shows an induced UPR, both opaque mutants were used as UPR negative controls (Boston et al., 1991; Holding et al., 2007). To understand the linkage between inductions of ER molecular chaperones and ERAD, and to investigate the functional role of induced ERAD, we compared ubiquitin signals between normal and mutant protein body fractions. Equal amounts of total protein from isolated protein body fractions were fractionated by SDS-PAGE, immunoblotted, and probed for ubiquitin (Figure 1). Ubiquitin signals were more abundant in *De*-B30* and *fl2* protein body fractions when compared to the normal protein body fraction. However, few ubiquitin signals were observed in protein body fractions of

mutants *Mc*, *o2* and *fl1*. The control ribosomal protein S6 representing the membrane bound ribosomes showed similar protein loading (Williams et al., 2003). These results indicate a connection between mutant storage protein synthesis and protein ubiquitination in protein body fractions. However, few ubiquitin signals in the *Mc* mutant were unexpected because *Mc* produces a frameshift 16-kD mutant γ-zein.

The induction of ER molecular chaperones and ERAD related ZmDerlin proteins is endosperm specific in *De*-B30* and *fl2* mutants (Kirst et al., 2005). To test whether the increased ubiquitin signals were also endosperm specific, we isolated embryos from normal maize and endosperm mutants including *De*-B30*, *fl2*, *Mc*, *o2*, and *fl1*. Total protein extracts (Supplementary Figure 1A) and protein body equivalent fractions (Supplementary Figure 1B) were immunoblotted with anti-ubiquitin antibody. There was no increase in ubiquitin signals in any of the embryos from endosperm mutants when compared to embryos from normal maize.

Mutant α-zeins encoded by *De*-B30* and *fl2* mutant alleles are deposited into protein bodies along with normal zeins. To test whether the increased ubiquitin signals were preferentially localized in the protein body fraction, we extracted proteins from equal fresh weights of normal and *De*-B30* endosperm in aqueous buffer, and subsequently separated the supernatant after a 300 g centrifugation into cytosol (S100), non-protein body membrane (M), and protein body (PB) fractions by using differential centrifugation (Figure 2). There was a dramatic increase in the amount of ubiquitin signals in the *De*-B30* protein body fraction

when compared to the normal protein body fraction, whereas there were only slight increases in the cytosolic and non-protein body membrane fractions from *De*-B30*. A cytosolic ribosome-inactivating protein (RIP), an ER membrane protein calnexin, and a protein body storage protein α-zein were used as reference proteins of cytosol, non-protein body membrane, and protein body fractions, respectively. These results suggest a co-localization of ubiquitin signals with mutant zeins in the protein body fraction.

In the ERAD process, a Cdc48p complex uses the energy from ATP hydrolysis to export ubiquitinated species from the ER. The 26S proteasome requires the energy from ATP hydrolysis to degrade proteins as well. A lack of ATP can retard the export of ubiquitinated species from the ER membrane and the subsequent degradation of these proteins by the 26S proteasome. To test whether the increased ubiquitin signals in the *De*-B30* protein body fraction were due simply to a lack of ATP, we added ATP to the extraction buffer (Supplementary Figure 2). For a negative control, hexokinase and glucose were added in the extraction buffer to deplete the ATP. The partitioning of the ubiquitin signals across all fractions was similar in the absence or presence of ATP, and the ubiquitin signals were not released from the protein body fraction by either treatment. These results were suggestive that the increased ubiquitin signals in the *De*-B30* protein body fraction were not due to a lack of ATP. In addition, the ubiquitinated species were efficiently extracted from maize endosperm regardless of the availability of ATP. Therefore, none of the buffers used for other experiments reported in this manuscript contained ATP.

Increased ubiquitin signals correlate with *De*-B30* and *fl2* gene dosages

Increased ubiquitin signals were observed in *De*-B30* and *fl2* protein bodies. To investigate whether the increase in ubiquitin signals is proportional to the deposition of defective storage proteins in *De*-B30* and *fl2* protein bodies, we monitored the ubiquitin signals in protein bodies with different *De*-B30* and *fl2* gene dosages. Because of the triploid nature of endosperm, we were able to generate a series of zero, one, two and three gene doses of *De*-B30* and *fl2* mutant alleles in the endosperm. The effects of *De*-B30* and *fl2* gene dosage on ubiquitination are shown in Figure 3. One dose of the *De*-B30* mutant allele resulted in strong ubiquitin signals in the protein body fraction when compared to the normal protein body fraction, and the signal level was increased slightly more when two and three doses of the *De*-B30* mutant allele were present. A similar but less intense staining pattern was observed in protein body fractions with zero to three *fl2* gene doses. A different trend was observed in the non-protein body membrane fractions (Supplementary Figure 3B). There, one to three doses of the *De*-B30* mutant allele gave similar signals, whereas two doses of the *fl2* mutant allele were required for elevated ubiquitin signals. The *De*-B30* and *fl2* gene dosages had much less effect on the ubiquitin signals in cytosolic fractions (Supplementary Figure 3A). Increased ubiquitin signals were seen only in the cytosolic fraction of samples representing three doses of the *De*-B30* mutant allele.

Association of ubiquitinated species with protein bodies

ERAD substrates need to be retrotranslocated from the ER lumen through the membrane to the cytosol for degradation. Once an ERAD substrate emerges from the ER membrane, a

transmembrane E3 ligase modifies its lysines exposed to the cytosolic side of the ER with ubiquitin molecules. Subsequently, the polyubiquitinated substrate is exported from the ER membrane to the 26S proteasome for degradation. Insoluble ubiquitinated proteins might limit themselves from being efficiently exported out of the ER. To investigate the solubility of ubiquitinated species in the *De*-B30* protein body fraction, we resuspended *De*-B30* protein body fractions under conditions that release peripheral and integral membrane proteins. However, neither 1 M NaCl (Figure 4, lanes 2, 3) nor 1% (v/v) Triton X-100 (Figure 4, lanes 4, 5) was effective in dissociating ubiquitinated species from the protein body pellet. A small portion of ubiquitinated species was released into the supernatant, however, when protein bodies were treated by a combination of 1 M NaCl and 1% (v/v) Triton X-100 (Figure 4, lanes 6, 7). Most ubiquitinated species were solubilized into the supernatant in the presence of 1% (w/v) SDS (Figure 4, lane 8, 9). These results suggest a tight but noncovalent association between ubiquitinated species and other protein body proteins.

Partitioning of ubiquitinated species into non-zein fractions

As the major storage proteins, zeins are a group of prolamins that are alcohol soluble, but not soluble in high salt and/or nonionic detergent alone (Wallace et al., 1990). Since ubiquitinated species were not soluble in the presence of high salt and nonionic detergent, we were interested to determine whether they might co-fractionate with zeins. Zeins from normal and *De*-B30* protein body fractions were separated from non-zein proteins by solubilization in 70% (v/v) ethanol in the presence or absence of β-ME. Figure 5A shows that

most ubiquitinated species partitioned into the non-zein fraction and very little of the ubiquitinated species were present in the zein fraction. The α-zein immunoblot showed that most α-zeins were extracted into the zein fraction. A Coomassie Brilliant Blue-stained gel of zeins and non-zein proteins from the *De*-B30* protein body fraction (Figure 5B) further demonstrated that most zeins were efficiently extracted in ethanol.

Finding zein and ubiquitin signals in different fractions raised the possibility that either ubiquitination changes the solubility of the mutant zeins or other proteins instead of mutant zeins were ubiquitinated in the protein body fraction. To address the first option, we separated zein and non-zein fractions and probed with antibody that recognizes both normal and defective *De*-B30* α-zeins (Kim et al., 2004). The blot showed that α-zeins in the *De*-B30* protein body fraction form high molecular weight complexes that were reducing agent sensitive. However, no high molecular weight forms of α-zeins in the normal protein body fraction were found regardless of the presence or absence of reducing agents (Figure 5C). Since disulfide bonds but not the ubiquitin modification are sensitive to reducing agents (Figure 5D), the results together suggested that the defective 19-kD α-zeins form high molecular weight complexes through intermolecular disulfide bonds.

Increased ubiquitin signals during *De*-B30* endosperm development

Maize endosperm development includes several overlapping phases (Clore et al., 1996; Sabelli and Larkins, 2009). Shortly after pollination to around 12 DAP, the endosperm undergoes syncytium formation, cellularization, and mitotic division. Around 10 DAP, starch,

zeins and other storage compounds start to accumulate rapidly within endosperm cells. To determine when ubiquitin signals start to increase during *De*-B30* endosperm development and understand the connection between ubiquitinated species and mutant storage protein synthesis, we probed for the ubiquitination level in a developmental series of normal and *De*-B30* protein bodies by using immunoblotting. Figure 6 shows that there was slightly stronger ubiquitin signal in the *De*-B30* protein body fraction than in the normal protein body fraction at 8 DAP. The ubiquitin signal in *De*-B30* protein body fractions increased at 10 DAP and reached a plateau at 12 DAP. However, the ubiquitin signal in normal protein body fractions stayed at a very low level from 8 DAP to 18 DAP. The expression of α-zeins in both *De*-B30* and normal protein body fractions was first detected on the immunoblot at 10 DAP, increased at 12 DAP and was persistent to 18 DAP. The ER molecular chaperone BiP in *De*-B30* protein body fractions showed little induction at 8 DAP and 10 DAP, and much stronger induction from 12 DAP and later when compared to BiP in normal protein body fractions. The induction pattern of BiP in *De*-B30* protein body fractions is similar to what was described in *fl2* protein body fractions by Houston et al. (2005).

The *De*-B30* mutant has been reported to have decreased α-zein protein synthesis (Soave et al., 1979; Kim et al., 2004). To determine whether this effect extends to other storage proteins in the *De*-B30* protein body fraction, we probed immunoblots for several storage proteins (Figure 6). Corn legumin 1 (CL-1) showed similar protein levels in *De*-B30* protein body fractions when compared with normal protein bodies at 8 and 10 DAP, whereas slightly less intense signals were seen in *De*-B30* protein bodies when compared with normal protein

bodies at 12 DAP and later stages. Maize 50-kD γ-zein showed a lower protein level in the *De*-B30* protein body fraction than in the normal protein body fraction at same developmental stages. Protein levels of corn legumin 2 (CL-2) were very similar at each of the developmental stages when normal and *De*-B30* protein body fractions were compared. Porin, a mitochondrial outer membrane protein, was used as a protein loading control. A Coomassie-stained gel showed a similar loading between normal and *De*-B30* protein body fractions at the same developmental stage (Supplementary Figure 5).

Identification of ubiquitinated species in *De*-B30* protein bodies

To investigate which proteins were ubiquitinated in the *De*-B30* protein body fraction, we enriched ubiquitinated species in the non-zein pellet by using 1M NaCl and 1% (v/v) Triton X-100 to wash off peripheral and membrane proteins, and using 70% (v/v) ethanol and 2% (v/v) β-ME to solubilize and remove major zeins (Figure 7A). The successful separation was shown by the ubiquitin immunoblot and Coomassie Brilliant Blue-stained gel of selected fractions (I, II, III, and IV) in Supplementary Figure 4. To determine whether the ubiquitinated species vary during *De*-B30* endosperm development, we enriched ubiquitinated species (fraction IV in figure 7A) from *De*-B30* protein body fractions at 12 DAP and 18 DAP (Figure 7B). The non-zein pellets (fraction IV in figure 7A) from the normal protein body fraction at the same developmental stage were used as a control for common ubiquitinated species. After peripheral and integral membrane proteins, and zeins were removed, there were more distinct bands from protein bodies at 18 DAP when compared to protein bodies at 12 DAP.

After dominant bands were removed, the gel region above 50-kD was subjected to in-gel digestion and and the extracted peptides were subjected to LC/MS^{E} analysis. Peptides were assigned to potential protein candidates when searched against a B73 filtered translation database. Several identified proteins, including ubiquitin, in the *De*-B30* sample were related to the ubiquitin dependent protein degradation process. This finding is consistent with a successful enrichment of ubiquitinated species. It is worth noting that SEL1L protein, the maize homolog of yeast HRD3 protein was identified in the *De*-B30* protein body fraction but not in the normal protein body fraction at 12 DAP. In addition, the transcript level of SEL-l like protein in *De*-B30* endosperm is induced at 18 DAP (data not shown). The increased transcript level might suggest that maize SEL1L protein participates in the induced UPR in *De*-B30* protein bodies at 12 DAP, since Arabidopsis SEL1L protein was shown to be induced in the UPR (Kamauchi et al., 2005). A canonical ubiquitinated peptide contains two unique features facilitating its identification, including an internal uncleaved lysine (K) when it was modified with ubiquitin and an additional 114.1 Da left by trypsin digested ubiquitin on the modified lysine. In addition, non-canonical ubiquitinated peptides with trypsin cleavage at the ubiquitin modified lysine have also been reported (Denis et al., 2007; Saracco et al., 2009). Tables 1 and 2 include both identified canonical and non-canonical ubiquitinated peptides and their assigned protein entities from 12 DAP and 18 DAP protein body fractions, respectively. All other identified peptides assigned to these putative ubiquitinated substrates are listed in Supplementary Tables 1 and 2. The full list of identified proteins in the non-zein fractions of normal and *De*-B30* protein bodies at 12 DAP and 18 DAP are listed in Supplementary Tables 3 and 4, respectively. Among the ubiquitin

peptides, we identified two K48 linked polyubiquitin peptides in the *De*-B30* protein body fractions at 12 DAP and 18 DAP, and one K63 linked polyubiquitin peptide in the *De*-B30* protein body fraction at 12 DAP. Surprisingly, three enzymes involved in starch synthesis [ADP-glucose pyrophosphorylase large subunit SHRUNKEN-2 (SH2), adenylate translocator BRITTLE-1 (BT1), and starch synthase DULL1 (DU1)] were ubiquitinated in the *De*-B30* protein body fraction at 18 DAP. Two isoforms of the N-linked glycosylation enzyme oligosaccharyl transferase STT3 were ubiquitinated in *De*-B30* protein body fractions at 12 DAP and 18 DAP, respectively. In addition, α-glucosidase like protein was ubiquitinated in the *De*-B30* protein body fraction at 12 DAP. We also found that several proteins functioning in protein quality control processes were ubiquitinated, including two cytosolic and one luminal Hsp70 protein, and the ubiquitin E3 ubiquitin-protein ligase 1 (UPL1). We identified two ubiquitin substrates related to the cytoskeletal network around protein bodies. A ubiquitinated peptide of elongation factor-1α (EF-1α) was identified in the *De*-B30* protein body fraction at 12 DAP. Different ubiquitinated peptides of the cytoskeletal protein myosin were found in both normal and *De*-B30* protein body fractions. Common ubiquitination substrates, translational activator GCN1 and heat shock cognate 70 kD proteins, were identified in normal and *De*-B30* protein body fractions (Saracco et al., 2009).

Discussion

Misfolded proteins in the ER are primarily recognized and folded with the assistance of ER molecular chaperones; however, misfolded proteins can be also removed by the ubiquitin-

dependent ERAD process (Vembar and Brodsky, 2008). Previous studies have shown the induction of ER chaperones and ERAD related ZmDerlin proteins in *De*-B30*, *fl2*, and *Mc* protein bodies in response to the synthesis of mutant zein proteins (Boston et al., 1991; Coleman et al., 1995; Kim et al., 2004; Houston et al., 2005; Kirst et al., 2005; Kim et al., 2006). In line with the induction of these ER quality control components, we investigated whether or not an increased ubiquitination was associated with these maize mutants.

Earlier studies revealed that the *De*-B30* and *fl2* mutants have endosperm specific phenotypes, because the mutations are embedded in signal peptides of α-zeins that are exclusively expressed in the maize endosperm. The lack of elevated ubiquitin signals in *De*-B30* and *fl2* embryo extracts is in agreement with *De*-B30* and *fl2* being endosperm mutants (Supplementary Figure 2). Furthermore, subcellular fractionation demonstrated that the ubiquitin signals were particularly enriched in the *De*-B30* protein body fraction when compared to the cytosolic and non-protein body membrane fractions (Figure 2). The pattern of ubiquitin signals correlates well with our previous finding of an induction of ERAD related ZmDerlin proteins in protein body fractions but little in non-protein body membrane fractions of the *fl2* mutant (Kirst et al., 2005). Furthermore, the ubiquitin signals in protein body fractions were shown to increase incrementally with *De*-B30* and *fl2* gene dosages (Figure 3). The results are in agreement with previous findings that the morphological changes, along with the induction of BiP and choline-phosphate cytidylyltransferase (CCT) activity, gradually increased with *fl2* gene dosage (Boston et al., 1991; Shank et al., 2001). CCT is the rate limiting enzyme of membrane phospholipid biosynthesis, and has been

reported to be induced during the UPR in *fl2* endosperm. In line with the gene dosage effects of *De*-B30* and *fl2*, the ubiquitin signals concomitantly increased with mutant α-zein deposition during endosperm development. Together, the evidence suggests a positive correlation between the mutant α-zein accumulation and the increased ubiquitin signals in the *De*-B30* and *fl2* protein body fractions. Surprisingly, although *De*-B30* has been reported as a dominant mutant and *fl2* as a semi-dominant mutant, the increased ubiquitin signals from one to two doses of the *De*-B30* mutant allele suggested that *De*-B30* is a semi-dominant mutant as well. Previous reports of the dominance of *De*-B30* might be due to its pronounced mutant effect that one dose of the *De*-B30* mutant allele changes the kernel to an opaque phenotype (Soave et al., 1979).

We observed the increased ubiquitin signals specifically in protein body fractions of *De*-B30* and *fl2* mutants, but little in *Mc*, *o2* and *fl1* mutants (Figure 1A). The elevated ubiquitination level fits well with the deposition of mutant α-zeins and strong UPR in the *De*-B30* and *fl2* mutants (Coleman et al., 1995; Kim et al., 2004). In the *Mc* mutant, little accumulation of the mutant 16-kD γ-zein leads to a weaker UPR induction than in the *De*-B30* and *fl2* mutants (Kim et al., 2004; Kirst et al., 2005). In the *o2* and *fl1* mutants, neither the mutant zein accumulation nor the UPR was observed (Boston et al., 1991; Holding et al., 2007). One possible explanation for stronger ubiquitin signals in the *De*-B30* and *fl2* mutants, but little in the *Mc*, *o2* and *fl1* mutants is the spatial redistribution of α-zeins. The *fl2* mutant allele encodes a mutant α-zein that is tethered to the protein body membranes because of its unprocessed signal peptide (Gillikin et al., 1997). We hypothesize that the α-zein

encoded by the *De*-B30* mutant allele is also tethered to the membrane because of its inefficiently processed signal peptide (Kim et al., 2004). In the spherical normal protein bodies, the core of α-zeins is surrounded by a continuous peripheral layer of β- and γ-zeins, whereas in the misshapen *De*-B30* and *fl2* protein bodies, α-zeins are directly exposed to the protein body membranes with a highly discontinuous peripheral region of β- and γ-zeins (Zhang and Boston, 1992; Gillikin et al., 1997). *Mc*, *o2* and *fl1* do not show such distinct location changes of α-zeins. The protein bodies in *Mc* are angular but contain an almost continuous peripheral layer of β- and γ-zeins (Zhang and Boston, 1992). The down-regulation of the 22-kD α-zeins in the *o2* mutant causes smaller spherical protein bodies with little disruption of the continuous peripheral layer of β- and γ-zeins (Schmidt et al., 1990). In spherical *fl1* protein bodies, the 22-kD α-zein localization is altered in the central region but the continuous peripheral layer of β- and γ-zeins is still intact. Taken together, the exposed α-zeins might lead to a strong UPR including ERAD related ZmDerlin proteins, and increased ubiquitin signals in the *De*-B30* and *fl2* protein body fractions.

Although mutant α-zeins in the *De*-B30* and *fl2* protein bodies are both tethered to the protein body membranes, the ubiquitin signals were more intense in protein body fractions of *De*-B30* than *fl2*. Two interpretations were developed by Kim et al. (2004) to explain the dominant *De*-B30* and the semi-dominant *fl2* mutant alleles. First, the 22-kD α-zein and the 19-kD α-zein localize differently and interact differently with other classes of zeins. The 22-kD α-zein discretely localizes to the border of the protein body central region, whereas the 19-kD α-zein is uniformly distributed in the protein body central region (Holding et al.,

2007). The 22-kD α-zein was shown to interact strongly with the 16-kD γ-zein, 15-kD β-zein, and 10-kD δ-zein in yeast two-hybrid experiments, whereas the 19-kD α-zein was shown to interact weakly with other classes of zeins including the 22-kD α-zein (Kim et al., 2002). Therefore, the membrane tethered 19-kD α-zein in *De*-B30* protein bodies is expected to have stronger effects on the protein body organization than the corresponding 22-kD α-zein in the *fl2* protein bodies. The second reason for the stronger ubiquitin signals in the *De*-B30* protein body fraction might be that the prolonged binding of the signal peptidase complex to the inefficiently processed *De*-B30* signal peptides results in large protein complexes or aggregates that lead to a stronger disruption effect than the unrecognized *fl2* signal peptide. Thus, the more severely disrupted protein body formation might result in stronger ubiquitin signals in the *De*-B30* than in the *fl2* protein body fraction.

A logical hypothesis is that mutant α-zeins in *De*-B30* and *fl2* protein bodies are recognized by the ER quality control mechanism and subsequently processed by ERAD. Indeed in the *Mc* mutant, mutant 16-kD γ-zein is recognized and bound by BiP in an ATP-sensitive manner (Kim et al., 2006). BiP has also been shown to bind to *fl2* protein bodies in an ATP-sensitive manner (Gillikin et al., 1995). However, evidence provided here does not support the hypothesis that mutant α-zeins are processed by ERAD. First, ubiquitinated species partitioning into the non-zein fraction indicated that mutant zeins might not be the substrates resulting in the strong ubiquitin signals. Within the non-zein fraction, the lack of high molecular weight forms of *De*-B30* α-zeins in the presence of a reducing agent further supported that De*-B30 α-zeins might not be the ubiquitinated species, or at least not the

major ubiquitinated species. Second, the mass spectrometry data showed no identification of ubiquitinated peptides of the *De*-B30* α-zein, although we cannot completely rule out the possibility that the amount of the α-zein moiety was below the detection limits of our instruments. In addition, having only one lysine and three arginines in the protein sequence of a *De*-B30* α-zein adds to the difficulty of identifying large ubiquitinated peptides remaining after trypsin digestion. Third, the *De*-B30* α-zein is extremely hydrophobic and one entire protein sequence contains only one lysine in its signal peptide. It might be a very low chance that the *De*-B30* α-zein gets ubiquitinated and exported to the cytosol. Taken together, these results implied that the *De*-B30* α-zein might indirectly cause the ubiquitination of other proteins. The reason of this indirect effect might be the redistributed *De*-B30* α-zein at the protein body membrane disrupts normal protein packing within the protein body, that has been discussed in comparison with *fl2*, *Mc*, *o2* and *fl1* mutants in a previous paragraph. In addition to the redistribution, the inefficiently processed signal peptide contains one extra cysteine. This might allow the *De*-B30* α-zein to form multi-protein complexes through intermolecular disulfide bonds which could disrupt the deposition of other storage proteins. Indeed, the *De*-B30* α-zein was observed in high molecular weight forms that were sensitive to a reducing agent and exclusively partitioned into non-zein fractions. We hypothesize that the solubility of the *De*-B30* α-zein was changed through its disulfide bond interaction with other proteins. The induction of PDI in *De*-B30* indirectly supported an increased need of PDI for extra disulfide bond formation (Houston et al., 2005). Because of the membrane tether and novel interaction with other proteins, the *De*-B30* α-

zein could affect the protein packing within the protein body, induce the UPR and related protein degradation through ubiquitination in order to maintain protein body homeostasis.

Among the ubiquitinated species, ubiquitin with K48 linked and K63 linked polyubiquitination were identified. Ubiquitin is a highly conserved molecule among eukaryotes (Hershko et al., 2000). There are seven lysine residues that can form different polyubiquitin chains for distinct functions. The K48 linked polyubiquitination has been well documented as the signal for protein degradation by the 26S proteasome (Pickart and Fushman, 2004). This is consistent with our hypothesis that ubiquitination is induced to degrade misfolded proteins and sustain homeostasis in the *De*-B30* protein bodies. The K63 linked polyubiquitination has been reported in nonproteolytic processes, including clathrin-dependent protein trafficking (Mukhopadhyay and Riezman, 2007). This fits with the detection of clathrin in *De*-B30* but not in normal protein bodies at 18 DAP (Supplementary Table 3 and 4). However, due to the lack of quantitative data, we were unable to determine if the vesicle trafficking is increased in *De*-B30* compared to normal endosperm cells, and whether the vesicle trafficking to lytic vacuoles is involved in maize protein body quality control as reported elsewhere (Yang et al., 2005; Pimpl et al., 2006). In addition, we have identified two putative maize oligosaccharyl transferase (OST) isoforms, that play an essential role in *N*-linked glycosylation by attaching the polysaccharide moiety, *N*-acetylglucosamine$_2$-mannose$_9$-glucose$_3$ (GlcNAc$_2$-Man$_9$-Glc$_3$), to the asparagine residue in conserved Asn-X-Ser/Thr motifs (Dempski and Imperiali, 2002). These identified maize OST isoforms show strong homology with two Arabidopsis STT3 isoforms that have been

reported to play important roles in salt and osmotic stress responses (Koiwa et al., 2003). Furthermore, we identified a ubiquitinated peptide of α-glucosidase like protein in the *De*-B30* protein body fraction at 12 DAP. The detected ubiquitination of maize STT3 isoforms and the α-glucosidase like protein in *De*-B30* protein body fractions implied a disrupted *N*-linked glycosylation in *De*-B30* protein bodies. This hypothesis is partially supported by the observations of unglycosylated calreticulin in *fl2* (Pagny et al., 2000) and *De*-B30* but not in normal protein bodies (Figure 6). We also identified ubiquitinated peptides of EF-1α and myosin XI in *De*-B30* protein body fractions at 12 DAP and 18 DAP, respectively. EF-1α has been shown to form a matrix with cytoskeleton proteins for the organization of protein bodies and starch granules in maize endosperm (Clore et al., 1996). Myosin XI has been reported to be associated with subcellular organelles in maize tissues (Wang and Pesacreta, 2004). Together, the ubiquitination of EF-1α and myosin XI might contribute to the clustered distribution of protein bodies in *De*-B30* endosperm compared to the even distribution of protein bodies in normal endosperm (Zhang and Boston, 1992). A ubiquitinated peptide of myosin XI detected in the normal protein body fraction at 18 DAP raises another possibility that the ubiquitination of myosin XI might just represent normal protein turnover.

During starch biosynthesis, ADP-glucose pyrophosphorylases, starch synthases, and starch branching and debranching enzymes are required for substrate synthesis, chain elongation, branch formation and trimming, respectively (Yu et al., 1998). Surprisingly, three identified ubiquitinated substrates are involved in starch synthesis, including ADP-glucose pyrophosphorylase large subunit SH2, starch synthase DU1, and adenylate translocator BT1

(Sullivan and Kaneko, 1995; Gao et al., 1998; Greene and Hannah, 1998; Shannon et al., 1998). The protein level of SH2 and BT1 slightly decreased in *De*- B30* endosperm at 18 DAP (Supplementary Figure 6). The lower amount of BT1 and SH2 fits well with the observation that there was less starch but increased sucrose in *De*- B30* compared to normal endosperm, and is consistent with the BT1 mutant endosperm phenotype (Salamini et al., 1979), although it is not clear how the mutant α-zein expression might affect the BT1 ubiquitination. On the contrary, the protein level of BT2 was similar between normal and *De*-B30* endosperm at 18 DAP (Supplementary Figure 6). Other mechanisms can also contribute to the reduction of starch content in *De*-B30* endosperm. In *o2* endosperm, starch accumulation was reported to be higher during early development, but lower during later development because of earlier termination of starch synthesis-related enzyme activities (Mehta et al., 1979; Joshi et al., 1980). Accordingly, we detected a little increase of BT1 and SH2 in *o2* endosperm at 18 DAP. In addition, a reduction of starch accumulation has been reported in *o2* endosperm (Tsai et al., 1978). The increased ubiquitination might contribute to the decreased BT1 and SH2 protein levels and reduced starch content in *De*-B30* endosperm.

In order to maintain maize ER homeostasis, the UPR increases protein folding capacity, and enhances protein degradation through ERAD. It has been shown in human embryonic kidney cells that the UPR further activates programmed cell death during a prolonged ER stress (Rao et al., 2004). A general connection between the UPR and programmed cell death has been demonstrated by pharmacologically treated plants or cell cultures (Iwata and Koizumi, 2005; Wang et al., 2007; Watanabe and Lam, 2008; Williams et al., 2010). These studies raise an

interesting question of whether the prolonged ER stress in the *De*-B30* and *fl2* mutants will lead to a programmed cell death. Notably, promotion of programmed cell death is developmentally controlled in maize endosperm, and starts in the center of normal endosperm at 16 DAP (Young and Gallie, 2000). With the disturbance of its carbohydrate metabolism, the starch deficient mutant *shrunken2* (*sh2*) showed an elicited programmed cell death at 16 DAP (Young et al., 1997). UPR induced programmed cell death might provide an alternative explanation for the broad ubiquitination in the *De*-B30* and *fl2* mutants. We think this is unlikely because the induced ubiquitination starts at 12 DAP in the *De*-B30* mutant.

We discovered that the increased ubiquitination coordinates with the induced UPR to maintain protein body homeostasis in the *De*-B30* and *fl2* mutants. These findings can be incorporated with the microarray data of opaque mutants together to provide a more comprehensive view to explain the pleiotropic effects of these two mutants (Hunter et al., 2002).

References

Boston RS, Fontes EB, Shank BB, Wrobel RL (1991) Increased expression of the maize immunoglobulin binding protein homolog b-70 in three zein regulatory mutants. Plant Cell **3:** 497-505

Clore AM, Dannenhoffer JM, Larkins BA (1996) EF-1α is associated with a cytoskeletal network surrounding protein bodies in maize endosperm cells. Plant Cell **8:** 2003-2014

Coleman CE, Herman EM, Takasaki K, Larkins BA (1996) The maize γ-zein sequesters α-zein and stabilizes its accumulation in protein bodies of transgenic tobacco endosperm. Plant Cell **8:** 2335-2345

Coleman CE, Lopes MA, Gillikin JW, Boston RS, Larkins BA (1995) A defective signal peptide in the maize high-lysine mutant floury 2. Proc Natl Acad Sci USA **92:** 6828-6831

Coleman CE, Yoho PR, Escobar S, Ogawa M (2004) The accumulation of α-zein in transgenic tobacco endosperm is stabilized by co-expression of β-zein. Plant Cell Physiol **45:** 864-871

Dempski RE, Jr., Imperiali B (2002) Oligosaccharyl transferase: gatekeeper to the secretory pathway. Curr Opin Chem Biol **6:** 844-850

Denis NJ, Vasilescu J, Lambert JP, Smith JC, Figeys D (2007) Tryptic digestion of ubiquitin standards reveals an improved strategy for identifying ubiquitinated proteins by mass spectrometry. Proteomics **7:** 868-874

Di Cola A, Frigerio L, Lord JM, Ceriotti A, Roberts LM (2001) Ricin A chain without its partner B chain is degraded after retrotranslocation from the endoplasmic reticulum to the cytosol in plant cells. Proc Natl Acad Sci USA **98:** 14726-14731

Gao M, Wanat J, Stinard PS, James MG, Myers AM (1998) Characterization of *dull1*, a maize gene coding for a novel starch synthase. Plant Cell **10:** 399-412

Geromanos SJ, Vissers JP, Silva JC, Dorschel CA, Li GZ, Gorenstein MV, Bateman RH, Langridge JI (2009) The detection, correlation, and comparison of peptide precursor and product ions from data independent LC-MS with data dependant LC-MS/MS. Proteomics **9:** 1683-1695

Gillikin JW, Fontes EP, Boston RS (1995) Protein-protein interactions within the endoplasmic reticulum. Methods Cell Biol **50:** 309-323

Gillikin JW, Zhang F, Coleman CE, Bass HW, Larkins BA, Boston RS (1997) A defective signal peptide tethers the *floury-2* zein to the endoplasmic reticulum membrane. Plant Physiol **114:** 345-352

Greene TW, Hannah LC (1998) Maize endosperm ADP-glucose pyrophosphorylase SHRUNKEN2 and BRITTLE2 subunit interactions. Plant Cell **10:** 1295-1306

Hershko A, Ciechanover A, Varshavsky A (2000) Basic Medical Research Award. The ubiquitin system. Nat Med **6:** 1073-1081

Hirsch C, Gauss R, Horn SC, Neuber O, Sommer T (2009) The ubiquitylation machinery of the endoplasmic reticulum. Nature **458:** 453-460

Holding DR, Otegui MS, Li B, Meeley RB, Dam T, Hunter BG, Jung R, Larkins BA (2007) The maize *floury1* gene encodes a novel endoplasmic reticulum protein involved in zein protein body formation. Plant Cell **19:** 2569-2582

Hong Z, Jin H, Fitchette AC, Xia Y, Monk AM, Faye L, Li J (2009) Mutations of an α1,6 mannosyltransferase inhibit endoplasmic reticulum-associated degradation of defective brassinosteroid receptors in *Arabidopsis*. Plant Cell **21:** 3792-3802

Hong Z, Jin H, Tzfira T, Li J (2008) Multiple mechanism-mediated retention of a defective brassinosteroid receptor in the endoplasmic reticulum of *Arabidopsis*. Plant Cell **20:** 3418-3429

Houston NL, Fan C, Xiang JQ, Schulze JM, Jung R, Boston RS (2005) Phylogenetic analyses identify 10 classes of the protein disulfide isomerase family in plants, including single-domain protein disulfide isomerase-related proteins. Plant Physiol **137:** 762-778

Hunter BG, Beatty MK, Singletary GW, Hamaker BR, Dilkes BP, Larkins BA, Jung R (2002) Maize opaque endosperm mutations create extensive changes in patterns of gene expression. Plant Cell **14:** 2591-2612

Iwata Y, Koizumi N (2005) Unfolded protein response followed by induction of cell death in cultured tobacco cells treated with tunicamycin. Planta **220:** 804-807

Joshi S, Lodha ML, Mehta SL (1980) Regulation of starch biosynthesis in normal and opaque-2 maize during endosperm development. Phytochemistry **19:** 2305-2309

Kamauchi S, Nakatani H, Nakano C, Urade R (2005) Gene expression in response to endoplasmic reticulum stress in *Arabidopsis thaliana*. FEBS J **272:** 3461-3476

Kim CS, Gibbon BC, Gillikin JW, Larkins BA, Boston RS, Jung R (2006) The maize *Mucronate* mutation is a deletion in the 16-kDa γ-zein gene that induces the unfolded protein response. The Plant Journal **48:** 440-451

Kim CS, Hunter BG, Kraft J, Boston RS, Yans S, Jung R, Larkins BA (2004) A defective signal peptide in a 19-kD α-zein protein causes the unfolded protein response and an opaque endosperm phenotype in the maize *De*-B30* mutant. Plant Physiol **134:** 380-387

Kim CS, Woo Ym YM, Clore AM, Burnett RJ, Carneiro NP, Larkins BA (2002) Zein protein interactions, rather than the asymmetric distribution of zein mRNAs on endoplasmic reticulum membranes, influence protein body formation in maize endosperm. Plant Cell **14:** 655-672

Kirst ME, Meyer DJ, Gibbon BC, Jung R, Boston RS (2005) Identification and characterization of endoplasmic reticulum-associated degradation proteins differentially affected by endoplasmic reticulum stress. Plant Physiol **138:** 218-231

Koiwa H, Li F, McCully MG, Mendoza I, Koizumi N, Manabe Y, Nakagawa Y, Zhu J, Rus A, Pardo JM, Bressan RA, Hasegawa PM (2003) The STT3a subunit isoform of the Arabidopsis oligosaccharyltransferase controls adaptive responses to salt/osmotic stress. Plant Cell **15:** 2273-2284

Larkins BA, Hurkman WJ (1978) Synthesis and deposition of zein in protein bodies of maize endosperm. Plant Physiol **62:** 256-263

Lending CR, Larkins BA (1989) Changes in the zein composition of protein bodies during maize endosperm development. Plant Cell **1:** 1011-1023

Li GZ, Vissers JP, Silva JC, Golick D, Gorenstein MV, Geromanos SJ (2009) Database searching and accounting of multiplexed precursor and product ion spectra from the data independent analysis of simple and complex peptide mixtures. Proteomics **9:** 1696-1719

Marshall RS, Jolliffe NA, Ceriotti A, Snowden CJ, Lord JM, Frigerio L, Roberts LM (2008) The role of CDC48 in the retro-translocation of non-ubiquitinated toxin substrates in plant cells. J Biol Chem **283:** 15869-15877

Mehta SL, Dongre AB, Johari RP, Lodha ML, Naik MS (1979) Biochemical constraints that determine protein quality and grain yield in cereals. *In* Seed Protein Improvement in Cereals and Grain Legumes, Vol 1. International Atomic Energy Agency, Vienna, Austria, pp 241-257

Mukhopadhyay D, Riezman H (2007) Proteasome-independent functions of ubiquitin in endocytosis and signaling. Science **315:** 201-205

Muller J, Piffanelli P, Devoto A, Miklis M, Elliott C, Ortmann B, Schulze-Lefert P, Panstruga R (2005) Conserved ERAD-like quality control of a plant polytopic membrane protein. Plant Cell **17:** 149-163

Pagny S, Cabanes-Macheteau M, Gillikin JW, Leborgne-Castel N, Lerouge P, Boston RS, Faye L, Gomord V (2000) Protein recycling from the Golgi apparatus to the endoplasmic reticulum in plants and its minor contribution to calreticulin retention. Plant Cell **12:** 739-756

Pickart CM, Fushman D (2004) Polyubiquitin chains: polymeric protein signals. Curr Opin Chem Biol **8:** 610-616

Pimpl P, Taylor JP, Snowden C, Hillmer S, Robinson DG, Denecke J (2006) Golgi-mediated vacuolar sorting of the endoplasmic reticulum chaperone BiP may play an active role in quality control within the secretory pathway. Plant Cell **18:** 198-211

Rao RV, Ellerby HM, Bredesen DE (2004) Coupling endoplasmic reticulum stress to the cell death program. Cell Death Differ **11:** 372-380

Sabelli PA, Larkins BA (2009) The development of endosperm in grasses. Plant Physiol **149:** 14-26

Salamini F, Fonzo N, Gentinetta E, Soave C (1979) A dominant mutation interfering with protein accumulation in maize seeds. *In* Seed Protein Improvement in Cereals and Grain Legumes, Vol 1. International Atomic Energy Agency, Vienna, Austria, pp 97-108

Saracco SA, Hansson M, Scalf M, Walker JM, Smith LM, Vierstra RD (2009) Tandem affinity purification and mass spectrometric analysis of ubiquitylated proteins in Arabidopsis. Plant J **59:** 344-358

Schmidt RJ, Burr FA, Aukerman MJ, Burr B (1990) Maize regulatory gene opaque-2 encodes a protein with a "leucine-zipper" motif that binds to zein DNA. Proc Natl Acad Sci USA **87:** 46-50

Shank KJ, Su P, Brglez I, Boss WF, Dewey RE, Boston RS (2001) Induction of lipid metabolic enzymes during the endoplasmic reticulum stress response in plants. Plant Physiol **126:** 267-277

Shannon JC, Pien FM, Cao H, Liu KC (1998) Brittle-1, an adenylate translocator, facilitates transfer of extraplastidial synthesized ADP-glucose into amyloplasts of maize endosperms. Plant Physiol **117:** 1235-1252

Soave C, Viotti A, DiFonzo N, Salamini F (1979) Maize prolamine: synthesis and genetic regulation. *In* Seed Protein Improvement in Cereals and Grain Legumes, Vol 1. International Atomic Energy Agency, Vienna, Austria, pp 165-174

Sullivan TD, Kaneko Y (1995) The maize *brittle1* gene encodes amyloplast membrane polypeptides. Planta **196:** 477-484

Tsai CY, Larkins BA, Glover DV (1978) Interaction of the *opaque-2* gene with starch-forming mutant genes on the synthesis of zein in maize endosperm. Biochem Genet **16:** 883-896

Vembar SS, Brodsky JL (2008) One step at a time: endoplasmic reticulum-associated degradation. Nat Rev Mol Cell Biol **9:** 944-957

Vitale A, Boston RS (2008) Endoplasmic reticulum quality control and the unfolded protein response: insights from plants. Traffic **9:** 1581-1588

Wallace JC, Lopes MA, Paiva E, Larkins BA (1990) New methods for extraction and quantitation of zeins reveal a high content of γ-zein in modified *opaque-2* maize. Plant Physiol **92:** 191-196

Wang S, Narendra S, Fedoroff N (2007) Heterotrimeric G protein signaling in the Arabidopsis unfolded protein response. Proc Natl Acad Sci USA **104:** 3817-3822

Wang X, Kota U, He K, Blackburn K, Li J, Goshe MB, Huber SC, Clouse SD (2008) Sequential transphosphorylation of the BRI1/BAK1 receptor kinase complex impacts early events in brassinosteroid signaling. Dev Cell **15:** 220-235

Wang Z, Pesacreta TC (2004) A subclass of myosin XI is associated with mitochondria, plastids, and the molecular chaperone subunit TCP-1α in maize. Cell Motil Cytoskeleton **57:** 218-232

Watanabe N, Lam E (2008) BAX inhibitor-1 modulates endoplasmic reticulum stress-mediated programmed cell death in Arabidopsis. J Biol Chem **283:** 3200-3210

Williams AJ, Werner-Fraczek J, Chang IF, Bailey-Serres J (2003) Regulated phosphorylation of 40S ribosomal protein S6 in root tips of maize. Plant Physiol **132:** 2086-2097

Williams B, Kabbage M, Britt R, Dickman MB (2010) AtBAG7, an Arabidopsis Bcl-2-associated athanogene, resides in the endoplasmic reticulum and is involved in the unfolded protein response. Proc Natl Acad Sci USA **107:** 6088-6093

Wu Y, Messing J (2010) RNA interference-mediated change in protein body morphology and seed opacity through loss of different zein proteins. Plant Physiol **153:** 337-347

Yang YD, Elamawi R, Bubeck J, Pepperkok R, Ritzenthaler C, Robinson DG (2005) Dynamics of COPII vesicles and the Golgi apparatus in cultured *Nicotiana tabacum* BY-2 cells provides evidence for transient association of Golgi stacks with endoplasmic reticulum exit sites. Plant Cell **17:** 1513-1531

Young TE, Gallie DR (2000) Programmed cell death during endosperm development. Plant Mol Biol **44:** 283-301

Young TE, Gallie DR, DeMason DA (1997) Ethylene-mediated programmed cell death during maize endosperm development of wild-type and *shrunken2* genotypes. Plant Physiol **115:** 737-751

Yu Y, Mu HH, Mu-Forster C, Wasserman BP (1998) Polypeptides of the maize amyloplast stroma. Stromal localization of starch-biosynthetic enzymes and identification of an 81-kilodalton amyloplast stromal heat-shock cognate. Plant Physiol **116:** 1451-1460

Zhang F, Boston RS (1992) Increases in binding protein (BiP) accompany changes in protein body morphology in three high-lysine mutants of maize. Protoplasma **171:** 142-152

Table 1. Identified ubiquitinated peptides from normal and *De*-B30* at 12 DAP

Description	Accession number[a]	Ubiquitinated peptide[b]	Number of identified peptide[c]
De*-B30			
canonical Ub footprint[d]			
Ubiquitin	GRMZM2G047727_P01	LIFAGK*QLEDGR	24
	GRMZM2G118637_P01	TLADYNIQK*ESTLHLVLR	24
	GRMZM2G116689_P01		24
	GRMZM2G409726_P01		24
	GRMZM2G419891_P01		24
	GRMZM2G431821_P01		24
	GRMZM2G357296_P01		24
	GRMZM2G006293_P01		24
	GRMZM2G047732_P01		24
Heat shock cognate 70 kD protein 2	GRMZM2G428391_P01	KVNAK*NTLENYAYNMRNTIR	3
non-canonical Ub footprint[e]			
Oligosaccharyl transferase, similar to STT3	GRMZM2G044096_P01	SKSPQTTGK*	9
WD-40 repeat protein	GRMZM2G029186_P01	GLGDKLFNQLEK*	4
Luminal-binding protein 3 precursor	AC211651.4_FGP001	IINEPTATAIAYGLDK*	21
α-glucosidase like protein	GRMZM2G034575_P01	NGSPYKGSVTHK*	15
Elongation factor-1α	GRMZM2G151193_P01	DIK*RGYVASNSK*	7

[a]B73 filtered translation database (version 4a.53; http://www.maizesequence.org) was used.
Ubiquitinated peptide was assigned to one or multiple protein entities.
[b]Lysine marked with asterisk indicates the ubiquitin modification site.
[c]Number of identified peptides assigned to the protein.
[d]Canonical Ub footprint is designated to a peptide containing an uncleaved internal lysine which is ubiquitinated.
[e]Non-canonical Ub footprint is designated to a peptide containing a terminal lysine which is ubiquitinated.

Table 2. Identified ubiquitinated peptides from normal and *De*-B30* at 18 DAP

Description	Accession number[a]	Ubiquitinated peptide[b]	Number of identified peptide[c]
De*-B30			
canonical Ub footprint[d]			
Ubiquitin	GRMZM2G118637_P01	LIFAGK*QLEDGR	9
	GRMZM2G047732_P01		9
	GRMZM2G409726_P01		9
	GRMZM2G006293_P01		9
	GRMZM2G431821_P01		9
	GRMZM2G419891_P01		9
	GRMZM2G116689_P01		9
	GRMZM2G047727_P01		9
	GRMZM2G357296_P01		9
ADP-glucose pyrophosphorylase endosperm large subunit SHRUNKEN2 (SH2)	GRMZM2G429899_P01	LSIGGRKQEK*ALRNR	9
Putative translational activator GCN1	GRMZM2G139341_P01	GVIK*HAGK*SVSSAIRSR	7
Heat shock cognate 70 kD protein	GRMZM2G056039_P01	QATK*DAGVIAGLNVLR	7
	GRMZM2G340251_P01		5
Ubiquitin ligase UPL1	GRMZM2G411536_P01	SPQDLK*GR	26
	GRMZM2G331368_P01		19
non-canonical Ub footprint[e]			
Protein BRITTLE-1 (BT1)	GRMZM2G144081_P01	KQKGGGSKK*	9
Starch synthase DULL1 (DU1)	GRMZM2G141399_P01	VEIGIDKAK*	11
Oligosaccharyl transferase, similar to STT3	GRMZM2G154165_P02	VAWEIFNSLDVK*	4
Myosin XI SC	AC155377.1_FGP001	RLRTDLEEAK*	9
Normal			
canonical Ub footprint			
Translational activator GCN1	GRMZM2G477879_P01	K*YGIAATLQK	5
Myosin XI SC	AC155377.1_FGP001	KQFAELK*R	8

Table 2. Continued

[a]B73 filtered translation database (version 4a.53; http://www.maizesequence.org) was used.
Ubiquitinated peptide was assigned to one or multiple protein entities.
[b]Lysine marked with asterisk indicates the ubiquitin modification site.
[c]Number of identified peptides assigned to the protein.
[d]Canonical Ub footprint is designated to a peptide containing an uncleaved internal lysine which is ubiquitinated.
[e]Non-canonical Ub footprint is designated to a peptide containing a terminal lysine which is ubiquitinated.

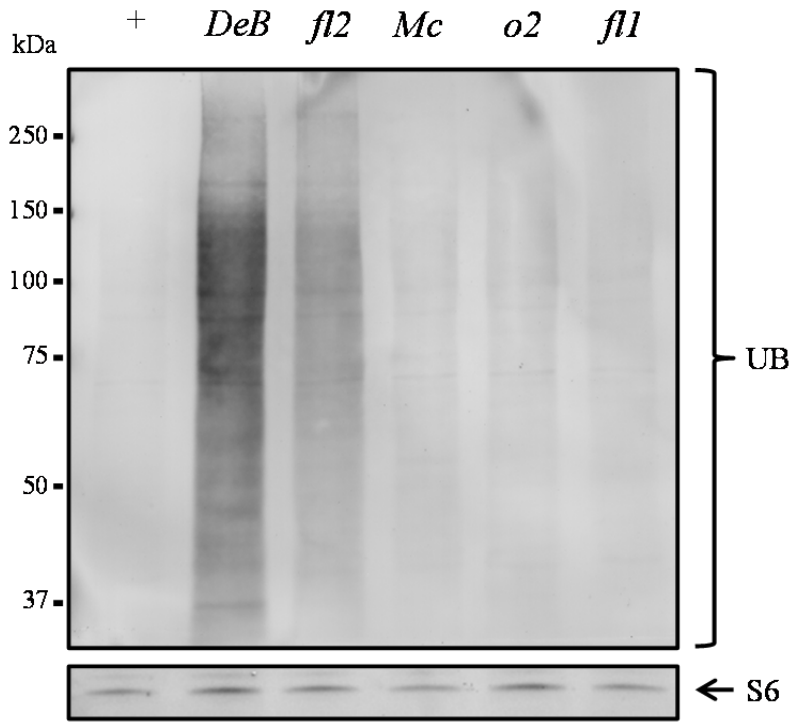

Figure 1. Comparison of ubiquitinated species in protein body fractions. Equal amounts of total protein (20 µg) from normal (+) and mutant protein body fractions were resolved by SDS-PAGE and subjected to anti-ubiquitin immunoblotting (UB). A duplicate blot probed for S6 was used as a loading control.

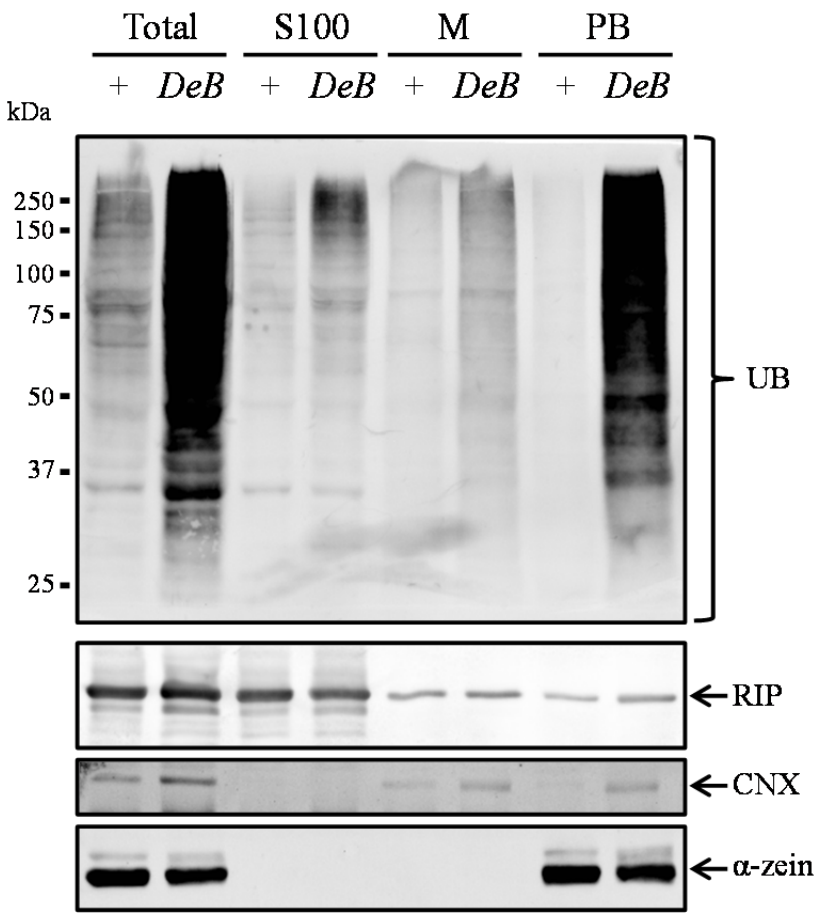

Figure 2. Comparison of ubiquitinated species in an unfractionated aqueous extract and subcellular fractions of normal (+) and *De*-B30* (*DeB*) endosperm. The unfractionated aqueous extract (Total), S100, non-protein body membrane (M) and protein body (PB) fractions from equal fresh weight equivalents of endosperm tissues (5 mg) were separated by differential centrifugation. Proteins were separated by SDS-PAGE and visualized by immunoblotting with anti-ubiquitin antibody (UB). Duplicate blots were probed for ribosome-inactivating protein (RIP), calnexin (CNX), and 19 kD α-zein as cytosol, membrane (non-protein body membrane and protein body membrane), and protein body controls, respectively.

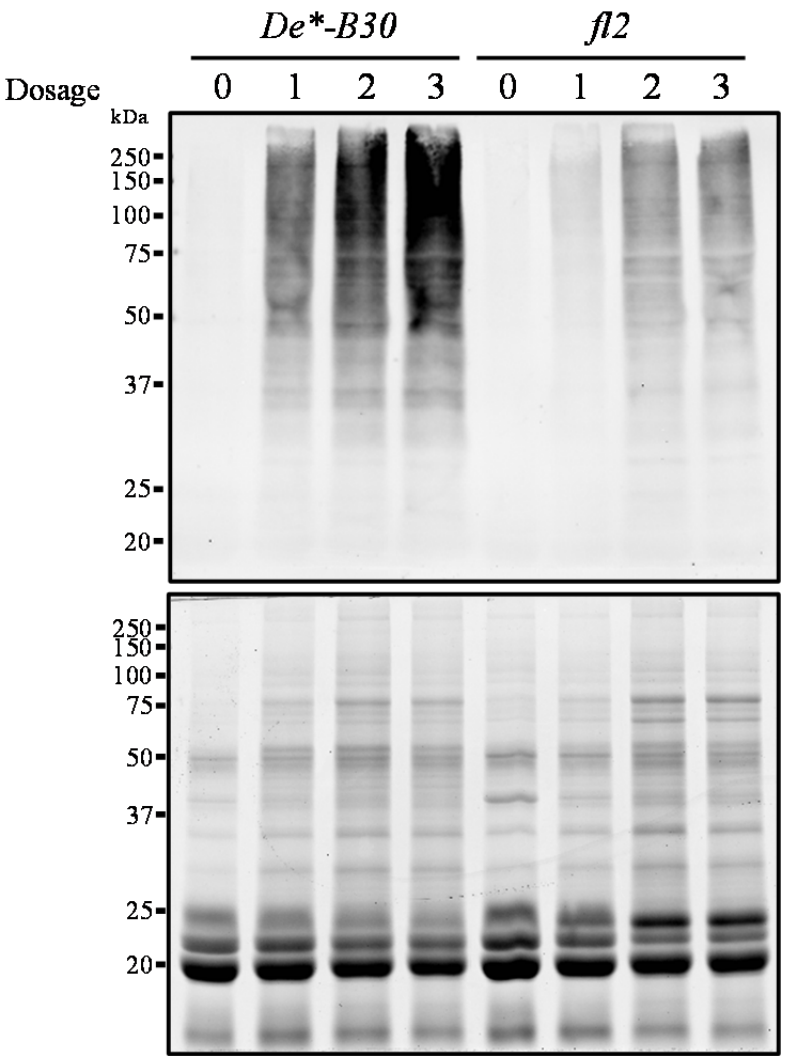

Figure 3. Comparison of ubiquitinated species in protein body fractions from *De*-B30* and *fl2* gene dosage endosperm. Equal amounts of total protein (20 μg) isolated from normal and mutant protein body fractions were separated through SDS-polyacrylamide gels and analyzed by immunoblotting with anti-ubiquitin antibody (upper panel). A duplicate gel stained with Coomassie Brilliant Blue (lower panel) was used to show total protein loading.

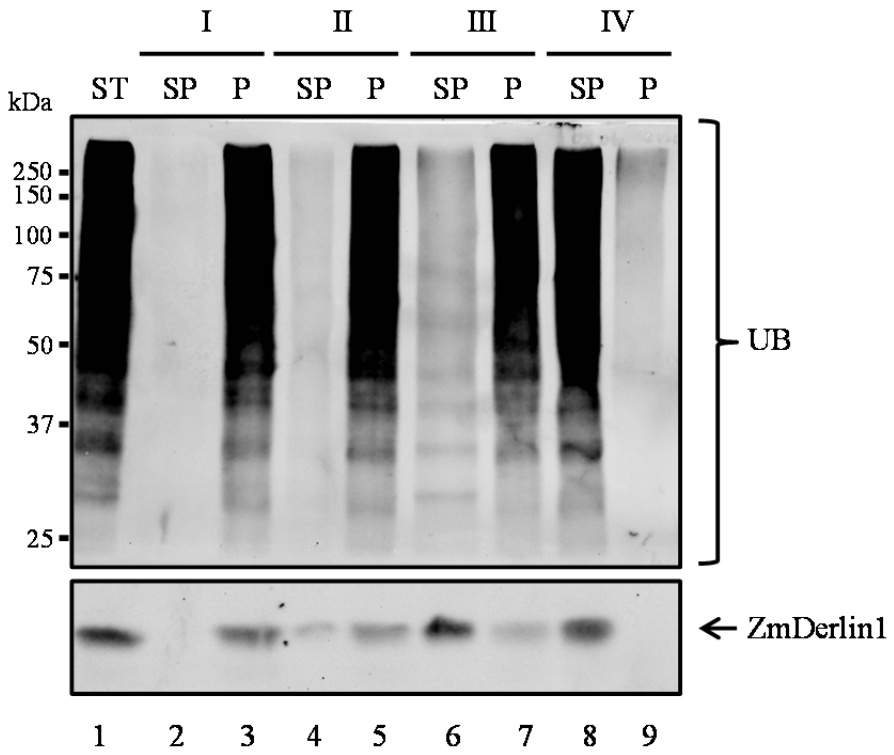

Figure 4. Analysis of ubiquitinated species in *De*-B30* protein body fractions. Protein bodies from equal fresh weight equivalents of *De*-B30* endosperm tissues (5 mg) were treated with buffer (50 mM Tris, pH 7.5 at 25°C) containing 1 M NaCl (I), 1% (v/v) Triton X-100 (II), 1 M NaCl and 1% (v/v) Triton X-100 (III), or 1% (w/v) SDS (IV). Treated samples were separated into supernatants (SP) and pellets (P) by centrifugation. An untreated protein body fraction was used as the starting material (ST, lane 1). Proteins were separated by SDS-PAGE and visualized by probing the immunoblot with an anti-ubiquitin antibody. A duplicate blot was probed for a transmembrane protein, ZmDerlin1.

Figure 5. Protein seperation in zein and nonzein fractions from normal (+) and *De*-B30* (*DeB*) protein bodies. A. Immunoblot analysis of ubiquitinated species in zein and nonzein fractions. Equal amounts of proteins (20 μg) from total protein body (total), zein and nonzein fractions were resolved by SDS-PAGE and subjected to immunoblotting with anti-ubiquitin antibody. A duplicate α-zein immunoblot shows the separation between zein and nonzein fractions (lower panel). B. Coomassie Brilliant Blue stained gel of total, zein and nonzein proteins of *De*-B30* protein bodies. Equal amounts of protein (20 μg) from separated *De*-B30* protein body fractions were resolved by SDS-PAGE and stained with Coomassie Brilliant Blue (lane 1. total protein body; lane 2. zein; lane 3. non zein). C. Immunoblot analysis of *De*-B30* α-zeins separated in the presence or absence of β-ME. Equal amounts of protein (20 μg) in nonzein fractions separated in the presence or absence of β-ME from normal and *De*-B30* protein body fractions were resolved by SDS-PAGE and immunoblotted with anti-19kD α-zein antibody. D. Duplicate samples were immunoblotted with anti-ubiquitin antibody.

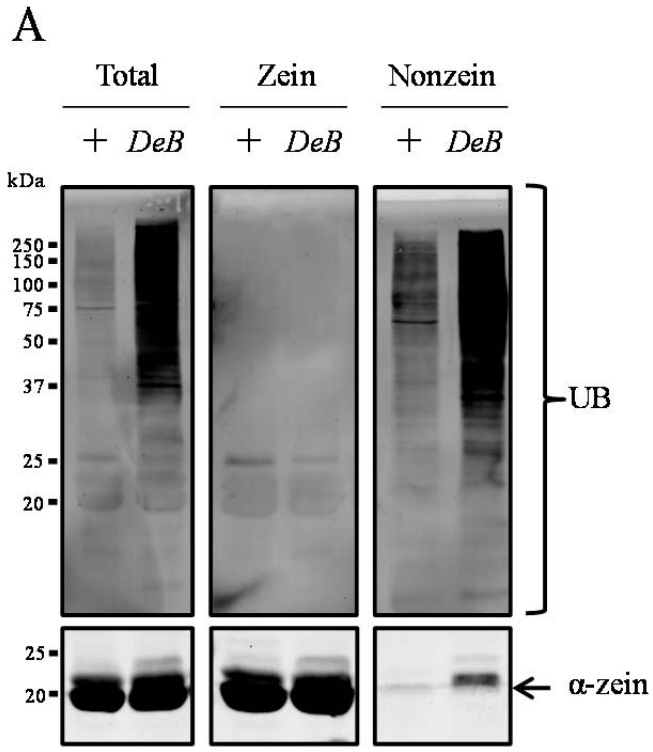
A
Total
Zein
Nonzein
+ DeB
+ DeB
+ DeB
kDa
250
150
100
75
50
37
25
20
UB
25
20
α-zein

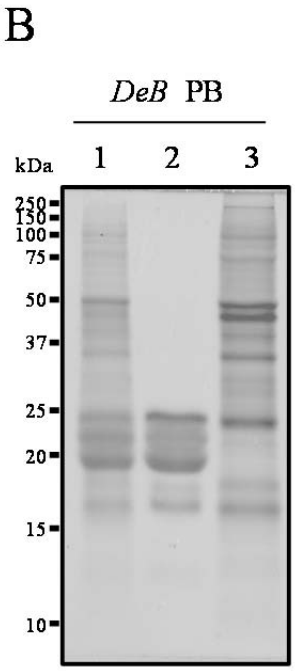
B
DeB PB
kDa
1
2
3
250
150
100
75
50
37
25
20
15
10

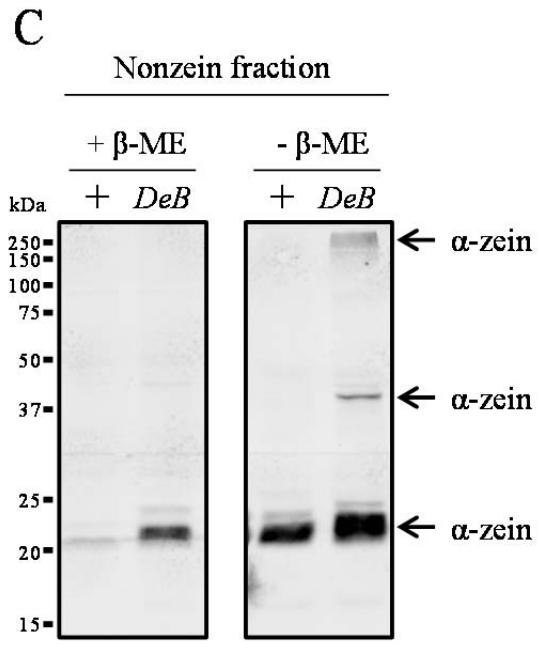
C
Nonzein fraction
+ β-ME
- β-ME
kDa
+ DeB
+ DeB
250
150
100
75
50
37
25
20
15
α-zein
α-zein
α-zein

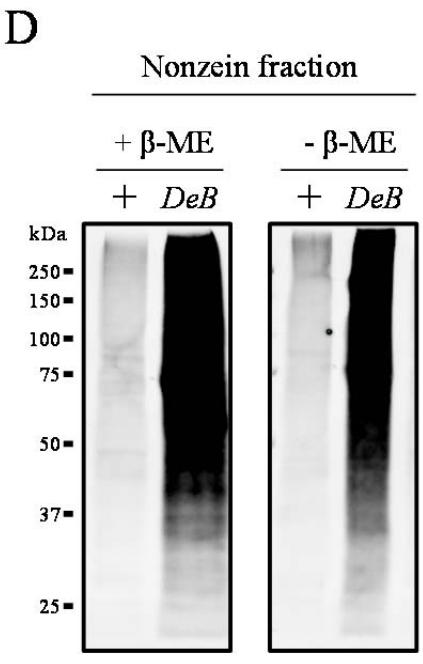
D
Nonzein fraction
+ β-ME
- β-ME
kDa
+ DeB
+ DeB
250
150
100
75
50
37
25

Figure 6. Comparison between normal (+) and *De*-B30* (*D*) protein bodies during endosperm development. Total proteins in protein body fractions from equal fresh weight equivalents of normal and *De*-B30* endosperm (15 mg) were separated through a SDS-polyacrylamide gel and subjected to immunoblot analysis using anti-ubiquitin antibody. Duplicate blots were probed with several storage protein antibodies, 19-kD α-zein (cross-reacts with 22-kD α-zein), 50-kD γ-zein, legumin 1 (CL-1), legumin 2 (CL-2). Calnexin (CNX), calreticulin (CRT), and BiP were probed on duplicate blots as ER stress controls. An asterisk indicates the unglycosylated form of CRT. A duplicate blot was probed for porin as a loading control.

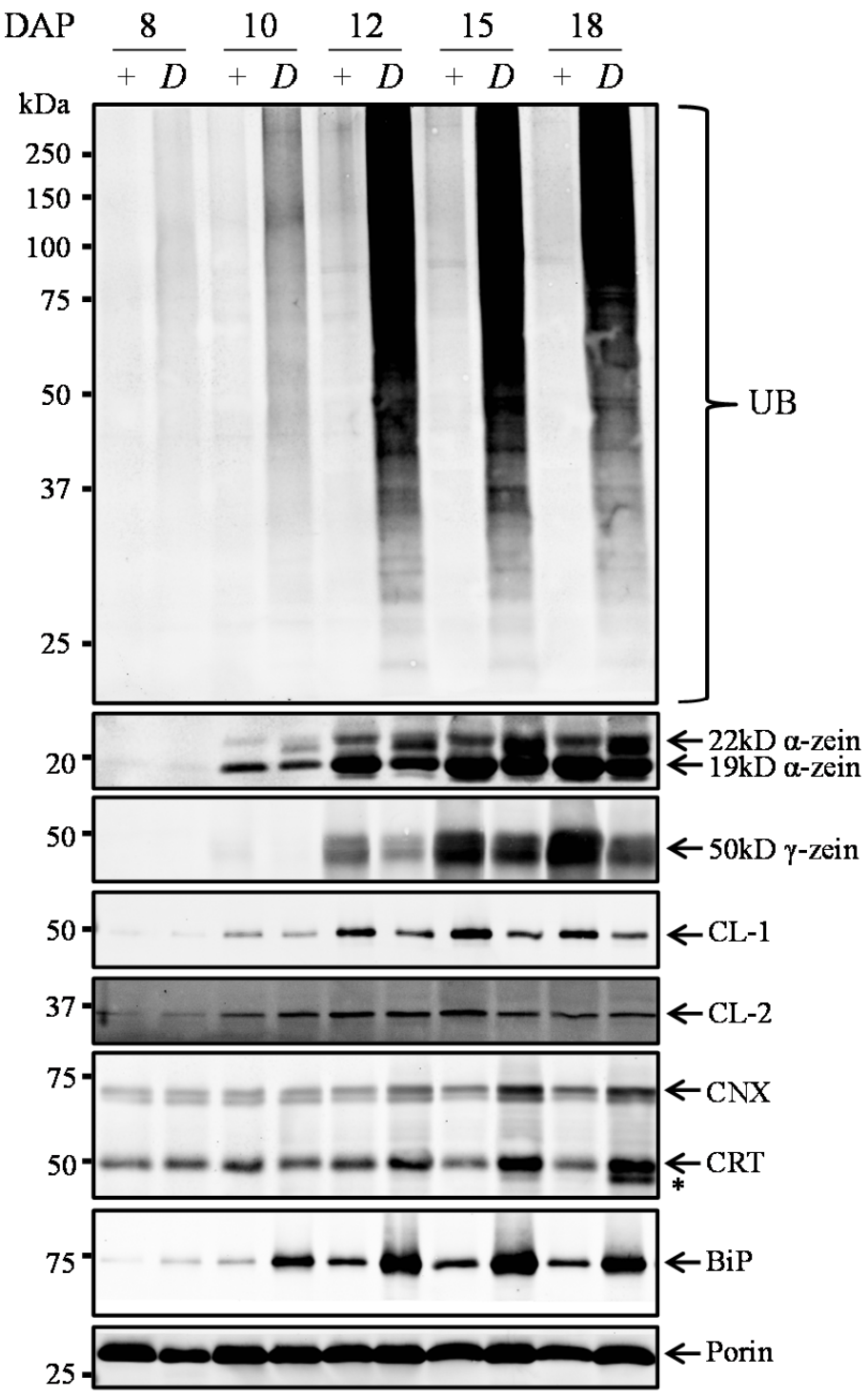
DAP
8
10
12
15
18
+ D
kDa
250
150
100
75
50
37
25
UB
20
22kD α-zein
19kD α-zein
50
50kD γ-zein
50
CL-1
37
CL-2
75
CNX
50
CRT
*
75
BiP
25
Porin

Figure 7. Enrichment of ubiquitinated species from normal (+) and *De*-B30* (*DeB*) protein bodies. A. Flowchart for enriching ubiquitinated species. The ubiquitin immunoblot and Coomassie Brilliant Blue stained gel of fractions (I. II, III, IV) are presented in Supplementary Figure 4. B. Equal amounts of nonzein protein (fraction IV, 10 μg) from normal and *De*-B30* protein bodies harvested at 12 DAP and 18 DAP were resolved by SDS-PAGE and stained with the Colloidal Blue Staining Kit. The regions from normal and *De*-B30* samples at 12 DAP and18 DAP used for mass spectrometry are indicated as (1) and (2), respectively.

A

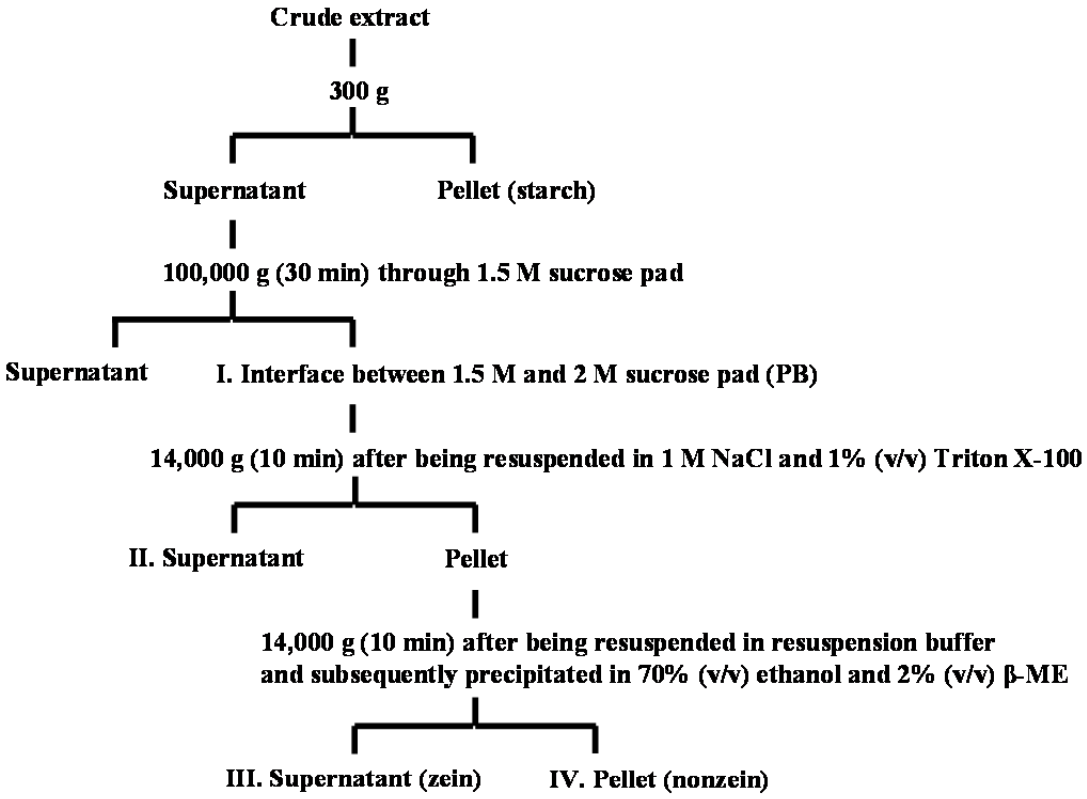
Crude extract
300 g
Supernatant
Pellet (starch)
100,000 g (30 min) through 1.5 M sucrose pad
Supernatant
I. Interface between 1.5 M and 2 M sucrose pad (PB)
14,000 g (10 min) after being resuspended in 1 M NaCl and 1% (v/v) Triton X-100
II. Supernatant
Pellet
14,000 g (10 min) after being resuspended in resuspension buffer
and subsequently precipitated in 70% (v/v) ethanol and 2% (v/v) β-ME
III. Supernatant (zein)
IV. Pellet (nonzein)

B

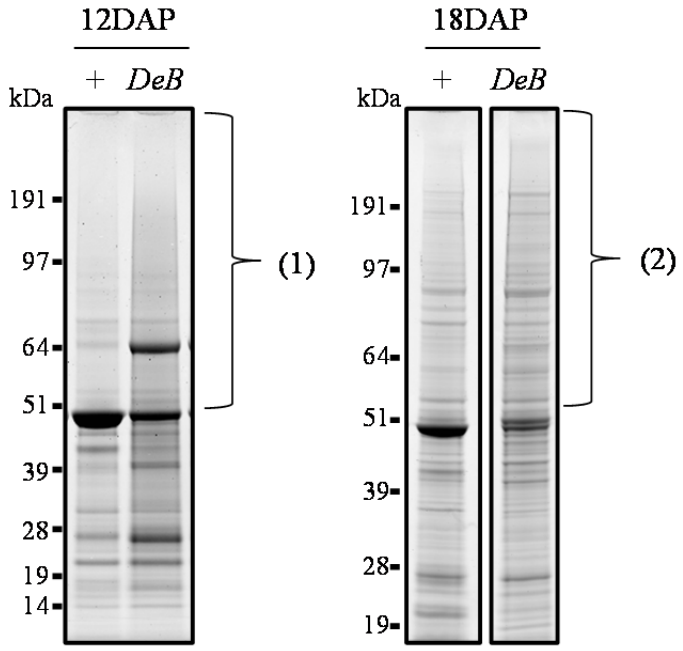
12DAP
18DAP
+ DeB
+ DeB
kDa
kDa
191
97
64
51
39
28
19
14
191
97
64
51
39
28
19
(1)
(2)

Supplementary Table 1. Identified peptide list of putative ubiquitinated substrates at 12 DAP

Description	Accession number[a]	Ubiquitinated peptide[b]	Identified peptides[c]
De*-B30 canonical Ub footprint[d]			
Ubiquitin	GRMZM2G047727_P01	LIFAGK*QLEDGR	TLADYNIQK
	GRMZM2G118637_P01	TLADYNIQK*ESTLHLVLR	ESTLHLVLR
	GRMZM2G116689_P01		IQDKEGIPPDQQR
	GRMZM2G409726_P01		QIFVK
	GRMZM2G419891_P01		MQIFVK
	GRMZM2G431821_P01		LIFAGK*QLEDGR
	GRMZM2G357296_P01		FAGK*QLEDGR
	GRMZM2G006293_P01		IFVK
	GRMZM2G047732_P01		IQDKEGI
			PPDQQR
			LIFAGK
			TLADYNIQK*ESTLHLVLR
			FAGK
			IFAGK
			ADYNIQK
			IQDK
			STLHLVLR
			TLHLVLR
			EGIPPDQQR
			DYNIQK
			PDQQR
			LHLVLR
			FVK
			DKEGIPPDQQR
Heat shock cognate 70 kD protein 2	GRMZM2G428391_P01	KVNAK*NTLENYAYNMRNTIR	IINEPTAAAIAYGLDKK
			IINEPTAAAIAYGLDK
			KVNAK*NTLENYAYNMRNTIR
Oligosaccharyl transferase, similar to STT3	GRMZM2G044096_P01	SKSPQTTGK*	APPALDSLPAPLR
			FYSLLDPTYAK
			IGGGVFPVIK
			EAYYWLR
			FGELTTEYGKPPGYDR
			SKSPQTTGK*
			FYSLLDPTYAK
			IGGGVFPVIK
			EAYYWLR
WD-40 repeat protein	GRMZM2G029186_P01	GLGDKLFNQLEK*	VLNINTALR
			YTSDPGLVLGR
			EISSLGPVVAR
			GLGDKLFNQLEK*
Luminal-binding protein 3 precursor	AC211651.4_FGP001	IINEPTATAIAYGLDK*	SQIHEIVLVGGSTR
			INDAVVTVPAYFNDAQR

Supplementary Table 1. Continued

Description	Accession number[a]	Ubiquitinated peptide[b]	Identified peptides[c]
			IMEYFIK
			FEELNNDLFR
			ARFEELNNDLFR
			KINDAVVTVPAYFNDAQR
			ARFEELNNDLFRK
			IMEYFIK
			DYFNGKEPNK
			IINEPTATAIAYGLDK*
			SQIHEIVLV
			SQIHEIVL
			GGSTR
			VGGSTR
			SQIHEIV
			SQIHEIVLVG
			EYFIK
			GSTR
			LVGGSTR
			ARFEE
			ARFEELNNDLFR
α-glucosidase like protein	GRMZM2G034575_P01	NGSPYKGSVTHK*	GPGVEESEPYR
			LQIDEDYSTATPPHR
			LQVLEDSIPSFQR
			AFFAGSQR
			SGSSPVVPTIR
			FVFADNK
			LQIDEDYSTATPPHRR
			SVSVYLPGK
			RREPWLFGER
			RFVFADNK
			KFTSGCVIER
			KMVTIVDPHIKR
			NGSPYKGSVTHK*
			FAGSQR
			SVYLPGK
Elongation factor-1α	GRMZM2G151193_P01	DIK*RGYVASNSK*	IGGIGTVPVGR
			STTTGHLIYK
			QTVAVGVIK
			LPLQDVYK
			GYVASNSKDDPAK
			FLKNGDAGMVK
			DIK*RGYVASNSK*

Supplementary Table 1. Continued

[a]B73 filtered translation database (version 4a.53; http://www.maizesequence.org) was used. Ubiquitinated peptide was assigned to one or multiple protein entities.
[b]Lysine marked with an asterisk indicates the ubiquitin modification site.
[c]Number of identified peptides assigned to the protein.

Supplementary Table 2. Identified peptide list of putative ubiquitinated substrates at 18 DAP

Description	Accession number[a]	Ubiquitinated peptide[b]	Identified peptides[c]
De*-B30 canonical Ub footprint[d]			
Ubiquitin	GRMZM2G118637_P01	LIFAGK*QLEDGR	TLADYNIQK
	GRMZM2G047732_P01		ESTLHLVLR
	GRMZM2G409726_P01		LIFAGK
	GRMZM2G006293_P01		MQIFVK
	GRMZM2G431821_P01		LIFAGKQLEDGR
	GRMZM2G419891_P01		FAGK
	GRMZM2G116689_P01		IFAGK
	GRMZM2G047727_P01		FAGKQLEDGR
	GRMZM2G357296_P01		QIFVK
ADP-glucose pyrophosphorylase endosperm large subunit SH2	GRMZM2G429899_P01	LSIGGRKQEK*ALRNR	VSAIILGGGTGSQLFPLTSTR
		GRKQEK*ALRNR	TPFFTAPR
			SIDNIVILSGDQLYR
			SGIVVILK
			ATPAVPVGGCYR
			IFVMSQFNSTSLNR
			VLQFFEKPK
			LSIGGRKQEKALRNR
			GRKQEKALRNR
Putative translational activator GCN1	GRMZM2G139341_P01	GVIK*HAGK*SVSSAIRSR	ALEDDDTSATALDGLK
			ESAGLAFSTLYK
			SAGLQAIDEIVPTLLR
			TLKEVVVPITGPLIR
			GSLKDDKFPVR
			GVIKHAGKSVSSAIRSR
			GVIKHA
Heat shock cognate 70 kD protein	GRMZM2G056039_P01	QATK*DAGVIAGLNVLR	ATAGDTHLGGEDFDNR
			NAVVTVPAYFNDSQR
			SSVHDVVLVGGSTR
			VQQLLQDFFNGK
			ITITNDKGR
			QATKDAGVIAGLNVLR
			SSVHDVVL
	GRMZM2G340251_P01	QATK*DAGVIAGLNVLR	ATAGDTHLGGEDFDNR
			NAVVTVPAYFNDSQR
			VQQLLQDFFNGK
			ITITNDKGR
			QATKDAGVIAGLNVLR

Supplementary Table 2. Continued

Description	Accession number[a]	Ubiquitinated peptide[b]	Identified peptides[c]
Ubiquitin ligase ZmUPL1	GRMZM2G331368_P01	SPQDLK*GR	ANQFLVASSIR
			STSIYNLLGR
			ILSGSSIISAGGNR
			LQQILAGSR
			ALGSATYSPGNPAR
			HAIQESTASLAK
			HSLVTAANR
			ALFDGQLLDAHFTR
			VVQPLYK
			TSLVIDDSKR
			EALAFSVR
			NGSAAPAVPEGIEELLISHLR
			FLQFVTGTSK
			VVQALSSLVNTLQER
			VVEFVDGMLLDR
			EDDLSILKQCVDK
			DNSNIKTSLVIDDSK
			SPQDLKGR
			LTVQFQGEEGIDAGGLT**R
	GRMZM2G411536_P01		ALGSSTYSPGIPAR
			ANQFLVASSIR
			VVSGDTAAGSPANAQGK
			STSIYNLLGR
			ILSGSSIISAGGNR
			LQQILAGSR
			HAIQESTASLAK
			HSLVTAANR
			VPLEGFSALQGISGPQR
			FLVYTFTSR
			ALFDGQLLDAHFTR
			VVQPLYK
			VVSNASIEHATEMQYER
			DIGSAASDSQR
			SEDSVPGPIR
			FLQFVTGTSK
			AVLEDGEERK
			EVLEDIGR
			VESEPPANVK
			SKEDHLYSQK
			EDDLSILKQCVDK
			STSKPIEIEGAPLVDEDGLK
			VGSDRYSSLGLPSSSQDQSSSSSDANVSTR
			LEASSEKPSENAVK
			SPQDLKGR

Supplementary Table 2. Continued

Description	Accession number[a]	Ubiquitinated peptide[b]	Identified peptides[c]
			AAAAAAHR
non-canonical Ub footprint[e]			
Protein brittle-1	GRMZM2G144081_P01	KQKGGGSKK*	ILRDEGPSELYR
			TFVAPLETIR
			LVSGAIAGAVSR
			QQQLGDLSLR
			GNAVNVLR
			AIEHFTYDTAK
			AIEHFTYDTAKK
			KQQQLGDLSLRK
			KQKGGGSKK
Starch synthase ZmDULL1	GRMZM2G141399_P01	VEIGIDKAK*	VGGLGDVVTSLSR
			ADSTIDLYFNR
			STTGLHEQDQSVVSSHGQDK
			DLSAVANEPDVLIK
			SIVGVPQQIQYNDQSIAGSHR
			ELENLANEEAER
			QRELENLANEEAER
			ENYAKSSLANAR
			AEMKEKTMRMFLVSQK
			IQSIVHYTKPNQS**IVGLPK
			VEIGIDKAK
Oligosaccharyl transferase, similar to STT3	GRMZM2G154165_P02	VAWEIFNSLDVK*	SLSLLDPTYASK
			VTQFLSK
			FVETDGKGFDR
			VAWEIFNSLDVK
Myosin XI SC	AC155377.1_FGP001	RLRTDLEEAK*	TLDPASAVASR
			FVEIQFDK
			QQAVAISPTSK
			TPENGNALNGEVK
			LFDWIVEK
			TGRISGAAIR
			RLRTDLEEAK
			TGRISGA
			TGRISGAAIR
Normal canonical Ub footprint[d]			
Putative translational activator GCN1	GRMZM2G477879_P01	K*YGIAATLQK	ALADPNVDVR
			LLDVLNTPSEAVQR
			EGVVIFTGALAK
			ASDEETYDLVR
			KYGIAATLQK

Supplementary Table 2. Continued

Description	Accession number[a]	Ubiquitinated peptide[b]	Identified peptides[c]
Myosin XI SC	AC155377.1_FGP001	KQFAELK*R	TLDPASAVASR SSPDITPILPNPK FVEIQFDK INVSIGQDPNSK ISGAAIRTYLLERSR AEVLGRAARIIQR LIGGLGDLRQVEAK KQFAELKR

[a]B73 filtered translation database (version 4a.53; http://www.maizesequence.org) was used.
Ubiquitinated peptide was assigned to one or multiple proteins.
[b]Lysine marked with an asterisk indicates the ubiquitin modification site.
[c]Identified peptides assigned to the protein.
[d]Canonical Ub footprint is designated to a peptide containing uncleaved internal lysine which is ubiquitinated.
[e]Non-canonical Ub footprint is designated to a peptide containing terminal lysine which is ubiquitinated.

Supplementary Table 3. Identified proteins at 12 DAP

Accession number	Description
Normal	
GRMZM2G174883_P01	uncleaved legumin 1
GRMZM2G109677_P01	ribosomal protein L3
GRMZM2G163277_P01	hypothetical protein, similar to protein transport protein Sec16B
GRMZM2G032628_P01	starch branching enzyme Iib
GRMZM2G097457_P01	pyruvate,orthophosphate dikinase
GRMZM2G152768_P01	hypothetical protein LOC100382099
GRMZM2G033130_P01	unknown
GRMZM2G133943_P01	phospholipase D
GRMZM2G089713_P01	sucrose synthase 1
GRMZM2G415007_P01	luminal-binding protein 3 precursor
GRMZM2G352129_P01	polyadenylate-binding protein 2
GRMZM2G013619_P01	unknown, similar to polyadenylate-binding protein
GRMZM2G056039_P01	heat shock cognate 70 kD protein
AC211651.4_FGP001	luminal-binding protein 3 precursor
GRMZM2G102829_P01	unknown, similar to poly(A)-binding protein
GRMZM2G469380_P02	unknown, similar to r40c1 protein
GRMZM2G042008_P01	unknown
GRMZM2G032766_P01	SRC2
GRMZM2G164088_P01	unknown
GRMZM2G145308_P01	40S ribosomal protein SA
GRMZM2G027451_P01	60S ribosomal protein L10-3
GRMZM2G072315_P01	60S ribosomal protein L13a
GRMZM2G037327_P01	aquaporin TIP3.1
GRMZM2G445169_P01	α-expansin 6
De*-B30	
GRMZM2G047727_P01	ubiquitin
GRMZM2G047727_P01	ubiquitin-60S ribosomal L40 fusion protein
GRMZM2G060611_P01	oligosaccharyl transferase, similar to STT3
GRMZM2G174883_P01	legumin 1
GRMZM2G037327_P02	aquaporin TIP3.1
GRMZM2G130987_P04	Sec61α subunit
GRMZM2G415007_P01	luminal-binding protein 3 precursor
GRMZM2G428391_P01	heat shock cognate 70 kD protein 2
GRMZM2G109677_P01	ribosomal protein L3
GRMZM2G343543_P01	elongation factor-1α
GRMZM2G144081_P01	protein brittle-1, chloroplastic/amyloplastic precursor
GRMZM2G029186_P01	WD-40 repeat protein ; similar to VCS (VARICOSE-RELATED)
GRMZM2G372398_P01	SEL1L protein
GRMZM2G163129_T01	α-glucosidase like protein; RSW3 (RADIAL SWELLING 3)
GRMZM2G032628_P01	starch branching enzyme Iib
GRMZM2G135968_P01	unknown
AC233949.1_FGP004	Cell division cycle protein 48

Supplementary Table 3. Continued

Accession number	Description
GRMZM2G127308_P01	alliin lyase 2
GRMZM2G174619_P02	unknown
GRMZM2G004736_P01	unknown
AC196426.3_FGP007	unknown, similar to root hair defective 3 GTP-binding (RHD3) family protein
GRMZM2G089713_P01	sucrose synthase 1
GRMZM2G097457_P02	pyruvate,orthophosphate dikinase
GRMZM2G092447_T01	ubiquitin-associated protein; zinc ion binding protein
GRMZM2G058910_P01	unknown, similar to VHA-A3 (VACUOLAR PROTON ATPASE A3)
GRMZM2G365688_P01	TOC1b
GRMZM2G133943_P01	phospholipase D
GRMZM2G103884_P01	unknown
GRMZM2G113163_P01	unknown
GRMZM2G349462_P01	putative Cucumisin precursor
GRMZM2G470438_P02	unknown, similar to DNA topoisomerase III α
GRMZM2G150681_P01	similar to E3 ubiquitin-protein ligase BRE1-like 1
GRMZM2G104958_P01	unknown
GRMZM2G118403_P01	unknown
GRMZM2G439339_P05	unknown, similar to NUA (NUCLEAR PORE ANCHOR)
GRMZM2G102829_P02	unknown, similar to poly(A)-binding protein
AC212859.3_FGP007	unknown, similar to DCAF1 (DDB1-CUL4 ASSOCIATED FACTOR 1)
GRMZM2G469380_P02	unknown

Supplementary Table 4. Identified protein at 18 DAP

Accession number	Description
Normal	
GRMZM2G174883_P01	uncleaved legumin 1
GRMZM2G037327_P02	aquaporin TIP3.1
GRMZM2G144081_P02	protein brittle-1
GRMZM2G343543_P01	elongation factor-1α
GRMZM2G097457_P02	pyruvate,orthophosphate dikinase
GRMZM2G477879_P01	Translational activator GCN1
GRMZM2G429899_P01	ADP-glucose pyrophosphorylase endosperm large subunit SH2
GRMZM2G011507_P01	pyruvate,orthophosphate dikinase
GRMZM2G138727_P01	27-kD γ-zein
GRMZM2G141399_P01	starch synthase DULL1
GRMZM2G057576_P01	Clathrin heavy chain
GRMZM2G429899_P02	ADP-glucose pyrophosphorylase endosperm large subunit
GRMZM2G139341_P01	putative Translational activator GCN1
GRMZM2G409726_P03	ubiquitin
AC155377.1_FGP001	myosin XI SC
De*-B30	
GRMZM2G477879_P01	putative translational activator GCN1
GRMZM2G461586_P01	E3 ubiquitin-protein ligase, similar to UBR4
GRMZM2G312110_P01	WD40 repeat protein
GRMZM2G411536_P01	E3 ubiquitin protein ligase, similar to UPL1
GRMZM2G553687_P01	ubiquitin-protein ligase
GRMZM2G162184_P01	E3 ubiquitin-protein ligase BRE1-like 1
GRMZM2G110509_P01	translational elongation EF1a
GRMZM2G116689_P01	ubiquitin
GRMZM2G057576_P01	Clathrin heavy chain
GRMZM2G037327_P01	aquaporin TIP3.1
GRMZM2G144081_P02	protein brittle-1
GRMZM2G429899_P01	ADP-glucose pyrophosphorylase endosperm large subunit SH2
GRMZM2G071599_P01	proline-rich family protein
GRMZM2G104017_P01	actin
GRMZM2G130987_P03	Sec61α subunit
GRMZM2G097457_P02	pyruvate,orthophosphate dikinase
AC209784.3_FGP007	heat shock cognate 70 kD protein
AC203173.3_FGP004	elongation factor EF-2
GRMZM2G347319_P01	coatmer β subunit
GRMZM2G141399_P01	starch synthase DULL1
GRMZM2G154165_P03	oligosaccharyl transferase, similar to STT3
GRMZM2G088064_P02	alanine aminotransferase
GRMZM2G174785_P01	unknown
GRMZM2G144645_P01	unknown

Supplementary Table 4. Continued

Accession number	Description
GRMZM2G356805_P01	β-glucosidase
GRMZM2G001895_P01	DnaJ (Hsp40) homolog
AC155377.1_FGP001	myosin XI SC
GRMZM2G029186_P03	WD-40 repeat protein, similar to VCS (VARICOSE)
AC149633.4_FGP002	unkown, transcriptional regulator-related

Supplementary Figure 1. Comparison of ubiquitination in embryos from normal (+) and maize endosperm mutants. Equal amounts of total protein (20 μg) from an unfractionated aqueous extract (panel A) or a pellet after a centrifugation at 5,000 g for 10 min (panel B) were resolved by SDS-PAGE and subjected to anti-ubiquitin immunoblotting.

A

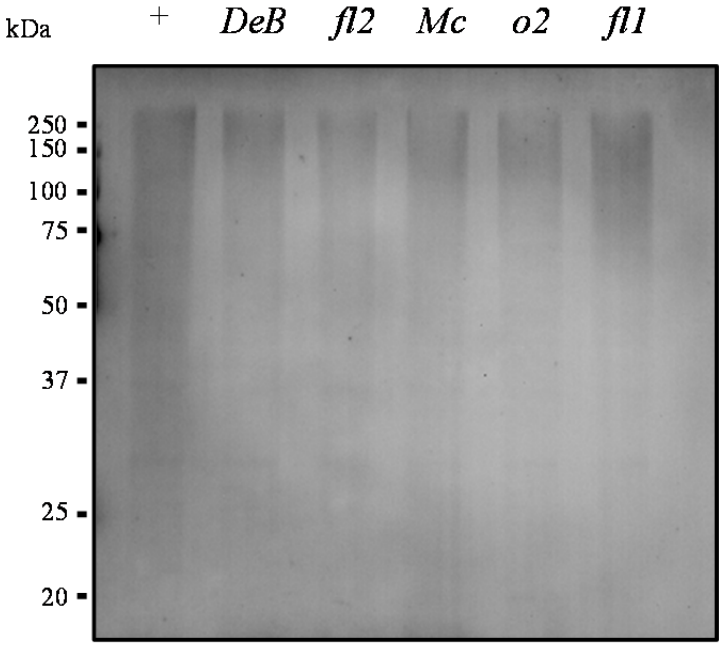
kDa
+
DeB
fl2
Mc
o2
fl1
250
150
100
75
50
37
25
20

B

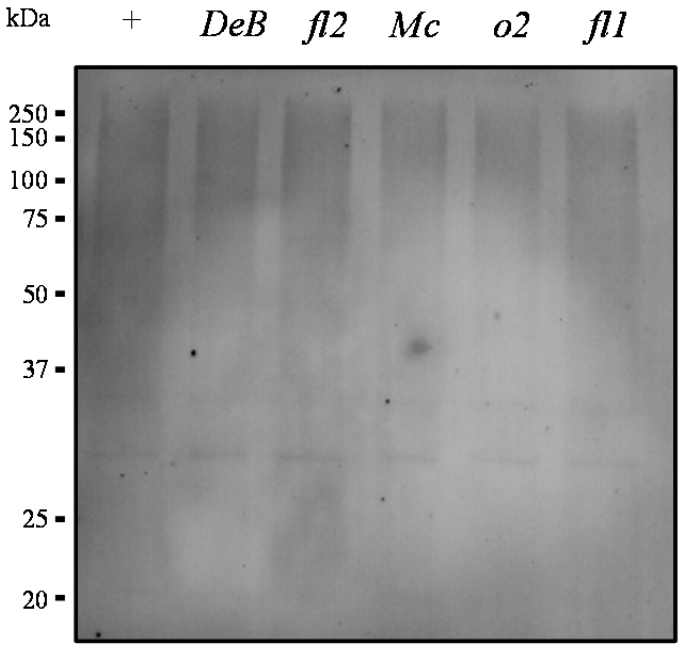
kDa
+
DeB
fl2
Mc
o2
fl1
250
150
100
75
50
37
25
20

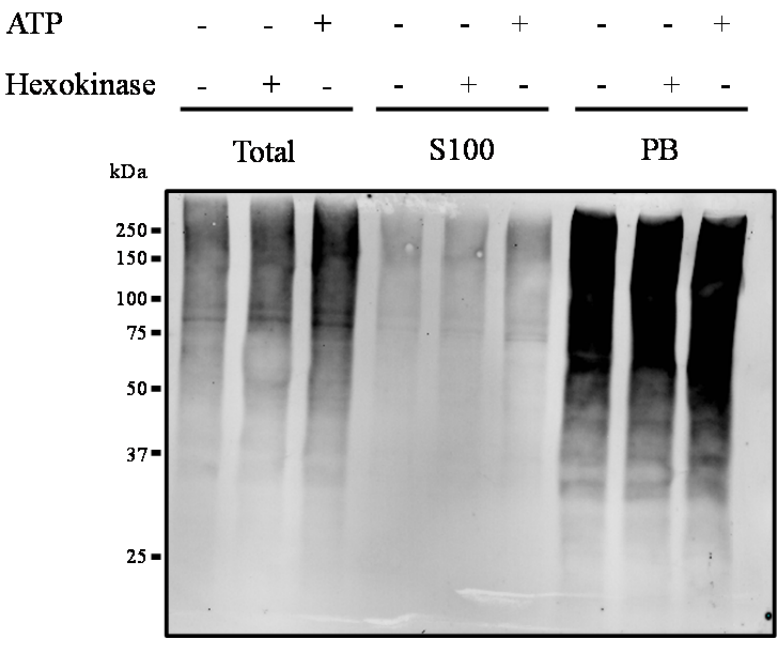

Supplementary Figure 2. Immunoblot analysis of proteins extracted from *De*-B30* endosperm in the presence or absence of ATP. A total aqueous extract was separated into S100 and protein bodies by differential centrifugation. Equal amounts of protein (20 μg) from each fraction were resolved by SDS-PAGE and subjected to anti-ubiquitin immunoblotting.

Supplementary Figure 3. Accumulation of ubiquitinated species in S100 and non-protein body membrane fractions with *De*-B30* and *fl2* gene dosages. Total aqueous extract from *De*-B30* and *fl2* mutant endosperm were separated into S100, total membranes after removal of protein body membranes, and protein bodies by differential centrifugation. Equal amounts of protein (20 μg) from S100 (panel A) and non-protein body membrane (panel B) fractions were separated through SDS-polyacrylamide gels and analyzed by immunoblotting with anti-ubiquitin antibody.

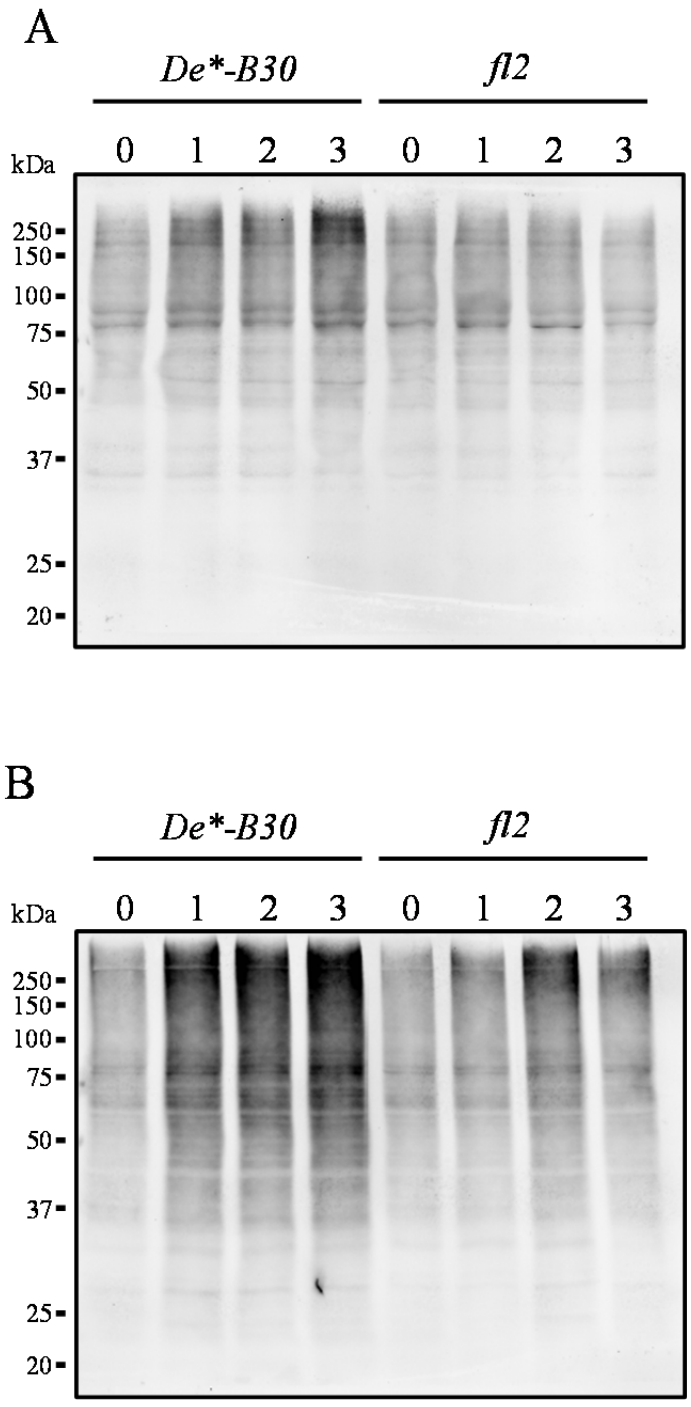
A
De*-B30
fl2
0 1 2 3 0 1 2 3
kDa
250
150
100
75
50
37
25
20
B
De*-B30
fl2
0 1 2 3 0 1 2 3
kDa
250
150
100
75
50
37
25
20

Supplementary Figure 4. Immunoblot and Coomassie Brilliant Blue stained SDS-polyacrylamide gel of normal (+) and *De*-B30* (*DeB*) protein body fractions during the enrichment of ubiquitinated species. Fractions from equal fresh weight equivalents (2.5 mg) of normal and *De*-B30* endosperm harvested at 12 DAP were separated by SDS-PAGE and visualized by immunoblotting with anti-ubiquitin antibody (upper panel), or stained with Coomassie Brilliant Blue (lower panel).

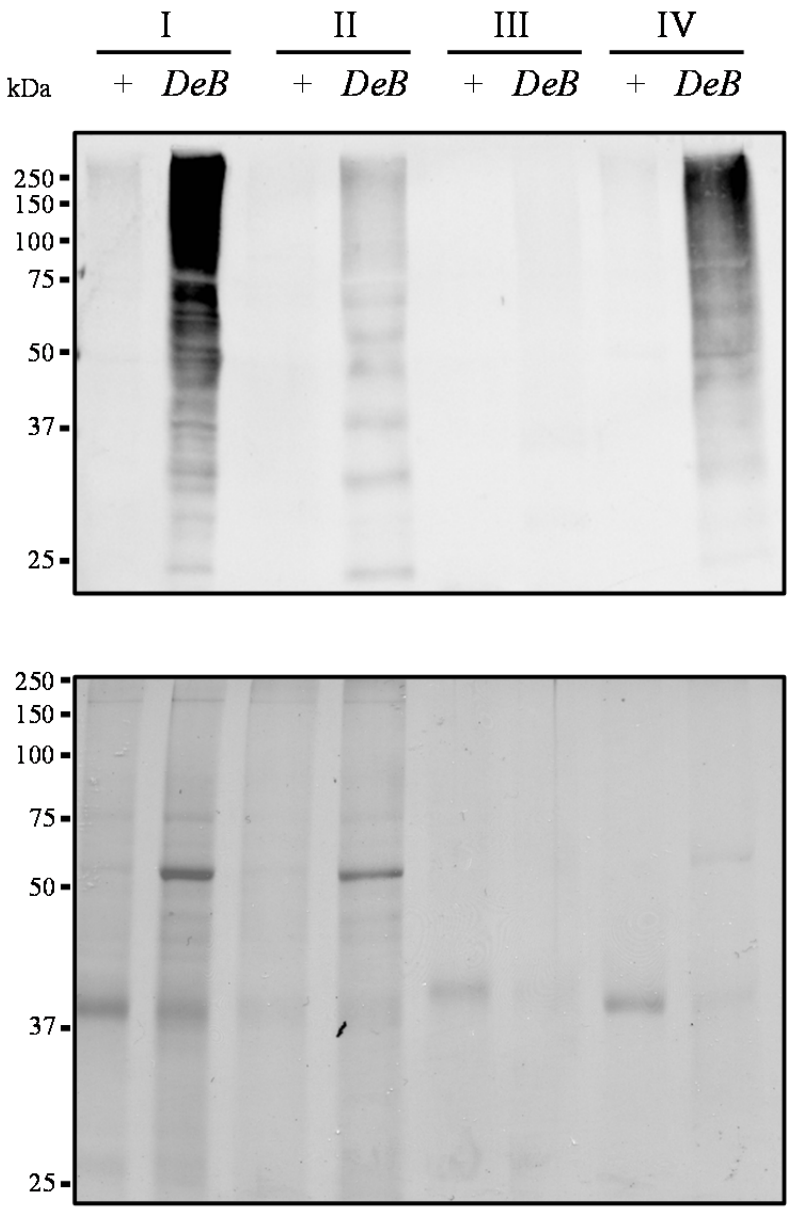
I
II
III
IV
kDa
+ DeB
+ DeB
+ DeB
+ DeB
250
150
100
75
50
37
25
250
150
100
75
50
37
25

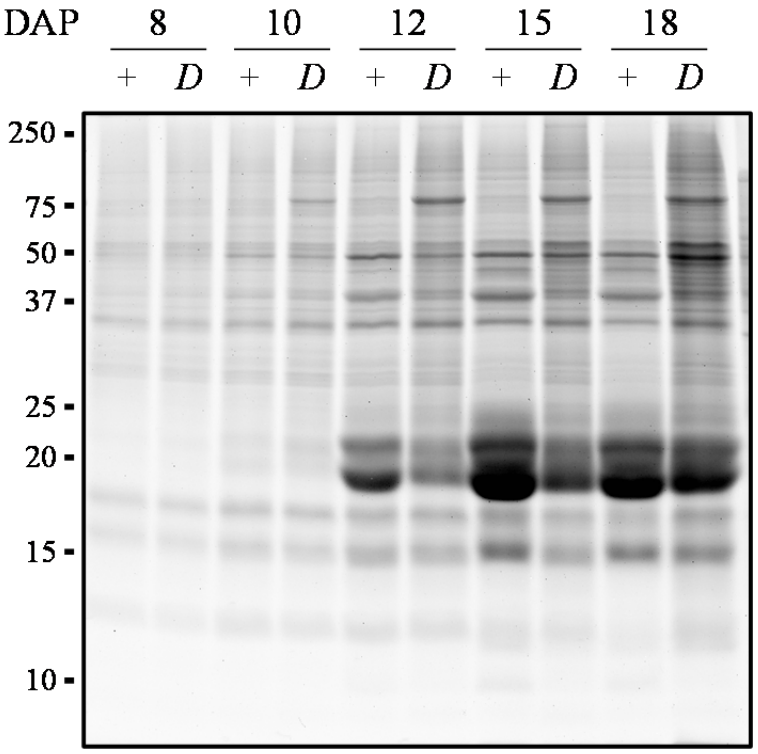

Supplementary Figure 5. Coomassie Brilliant Blue stained SDS-polyacrylamide gel of normal (+) and *De*-B30* (*D*) protein bodies during endosperm development. Total protein body proteins from equal fresh weight equivalents of normal and *De*-B30* endosperm (15 mg) were separated by SDS-PAGE and stained with Coomassie Brilliant Blue.

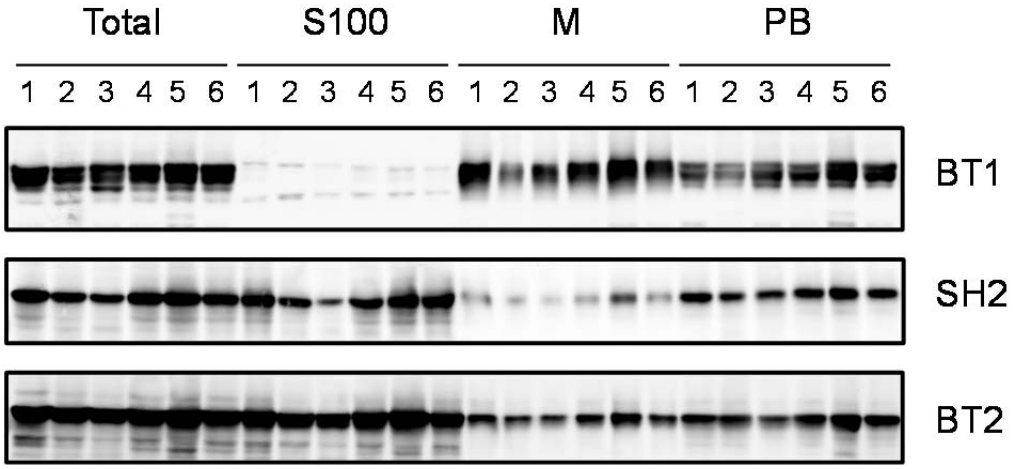

Supplementary Figure 6. Comparison of starch biosynthesis related enzymes in an unfractionated aqueous extract and subcellular fractions of normal and mutant endosperm tissue. The unfractionated aqueous extract (Total), S100, non-protein body membrane (M) and protein body (PB) fractions from equal fresh weight equivalents of endosperm tissues (750 µg for SH2 and BT-2, 375 µg for BT1) were separated by differential centrifugation. Proteins were separated by SDS-PAGE and visualized by immunoblotting with anti-BT1, anti-SH2, and anti-BT2 antibodies. Numbers 1, 2, 3, 4, 5, and 6 were assigned as normal, *De*-B30*, *fl2*, *Mc*, *o2*, and *fl1*, respectively.

Chapter 3: Identification and characterization of endoplasmic reticulum associated degradation (ERAD) related proteins in maize endosperm mutants

Abstract

The accumulation of misfolded proteins in the ER results in a perturbation of ER homeostasis. Conserved ER quality control machinery in plants is involved to maintain ER homeostasis. In addition to the folding assistance from ER molecular chaperones, misfolded proteins can be removed by an ER specific protein degradation process, termed ERAD. Three maize homologs of ERAD related proteins, ZmCDC48, ZmHRD1, and ZmUFD1, were identified and characterized in maize endosperm. An increased association of ZmCDC48 and ZmHRD1 with *De*-30* and *fl2* protein bodies correlated well with accumulation of mutant zeins. The interactions between ZmCDC48 and ZmHRD1, and ZmCDC48 and ZmUFD1 were characterized in immunoprecipitation assays. A direct interaction between recombinant ZmCDC48 and ZmUFD1 was demonstrated in binding assays *in vitro*. These results are suggestive that ZmCDC48, ZmHRD1, and ZmUFD1 play conserved roles in the ERAD process in response to mutant zein accumulation.

Introduction

The ER is the primary compartment for processing secretory proteins to achieve their proper conformations. Errors are inherent from DNA synthesis to protein maturation, due to mutations, transcriptional or translational mistakes, folding defects or inappropriate

*Nomenclature differs between species. Yeast gene names are shown in upper case and italicized. Yeast protein names are shown in lower case followed by a lower case p except for the first letter in upper case. Plant and mammalian gene names are shown in upper case and italicized. Plant and mammalian protein name are shown in upper case and not italicize.

modifications (Hirsch et al., 2009). Adverse environmental stresses could further disturb the protein folding environment, and result in the accumulation of misfolded proteins. Increased deposition of misfolded proteins in turn disrupts ER homeostasis and the secretory pathway, and even compromises cell viability. An efficient ER quality control mechanism has been involved to ensure that proteins attain their proper conformations. Misfolded proteins can be eliminated through the ERAD process, a part of the ER quality control system. The current working model suggests that a misfolded protein is recognized by ER molecular chaperones, and subsequently dislocated from the ER to the cytosol. After being tagged with polyubiquitin chains, the misfolded protein is transported to the 26S proteasome for its final degradation.

Various ERAD pathways and their required ERAD components have been identified through genetic and biochemical studies in yeast and mammalian systems (Vembar and Brodsky, 2008). Yeast Hrd1p* (its mammalian homolog is known as SEL1L) is one key ER transmembrane E3 ubiquitin ligase that not only plays the central role of ubiquitinating a set of substrates with misfolded ER-luminal or intra-membrane domains, but also recruits protein cofactors for different functions throughout the ERAD process. On the ER luminal side, Hrd1p and its cofactor Hrd3p interact with a number of ER molecular chaperones and lectins that recognize and deliver misfolded proteins to the retrotranslocon (Carvalho et al., 2006). In the ER membrane, Hrd1p interacts with the membrane protein Der1p, a putative retrotranslocon component, through a membrane protein Usa1p (Carvalho et al., 2006; Carroll and Hampton, 2009; Horn et al., 2009). On the cytosolic side, Hrd1p utilizes a

membrane protein Ubx2p to recruit a conserved Cdc48p-Npl4p-Ufd1p complex for exporting ubiquitinated substrates (Neuber et al., 2005; Schuberth and Buchberger, 2005).

As members of the AAA-ATPases, yeast Cdc48p and its mammalian homolog p97 were reported to be involved in various cellular processes, including cell division, membrane fusion, and ERAD (Moir et al., 1982; Hetzer et al., 2001; Ye et al., 2001; Uchiyama and Kondo, 2005). Two models of how Cdc48p functions in the ERAD process have been proposed. One model suggested that Cdc48p/p97 is capable of binding directly to the ubiquitin moiety of substrates (Dai and Li, 2001; Rape et al., 2001). A more prevailing model suggested that Cdc48p/p97 recruits its cofactors, Npl4p and Ufd1p, to recognize and bind to ubiquitinated substrates (Ye et al., 2001; Neuber et al., 2005).

Emerging evidence implicates conserved ERAD machinery in plants (Kirst, 2006). However, only a few ERAD components have been identified. One is AtCDC48, the Arabidopsis homolog of yeast Cdc48p, which was initially shown to complement a yeast temperature sensitive *cdc48* mutant (Feiler et al., 1995). It was reported that AtCDC48 was involved in the degradation of mutant barley mildew resistance o (MLO) proteins (Muller et al., 2005). The expression of a mutant AtCDC48 with defective ATP hydrolysis stabilized the mutant forms of MLO protein in Arabidopsis protoplasts. Another study demonstrated that a functional AtCDC48 was essential in retrotranslocation of castor bean ricin toxins, ricin A chain (RTA) and *Ricinus communis* agglutinin A chain (RCA; Marshall et al., 2008). The same defective form of AtCDC48 has been shown to stabilize the dislocated RTA and RCA

A in the ER membrane fraction in tobacco leaf protoplasts. Notably, this retrotranslocation process of AtCDC48 was independent from ubiquitination, since AtCDC48 was able to dislocate the non-lysine form of RTA into cytosol. Similar observations that CDC48p is able to recognize ERAD substrates without ubiquitination were reported in other systems (Thoms, 2002; Ye et al., 2003).

Other identified ERAD components in plants are Arabidopsis homologs of yeast Hrd1p and Hrd3p. Arabidopsis encodes two *HRD3* genes (At1g18260, *At1g73570*) and two *HRD1* genes (At1g65040, At3g16090). Expressing of *HRD3* and *HRD1* genes has been reported to be induced in Arabidopsis seedlings under ER stress (Kamauchi et al., 2005). Su et al. (2011) recently indicated that these two components were involved in the ERAD of mutant brassinosteroid receptors in genetic studies. In an Arabidopsis *HRD3* (At1g18260) or double *HRD1* (At1g65040 and At3g16090) knockout background, the degradation of mutant receptors bri1-5 or bri1-9 was retarded. Furthermore, the transformation of Arabidopsis HRD3 (At1g18260) can functionally complement the degradation defect of carboxypeptidase Y (CPY*) in a *Δhrd3* yeast mutant.

The other identified ERAD components in plants are ZmDerlin proteins, maize homologs of yeast Der1p (Kirst et al., 2005). Maize contains four Derlins that can be divided into two groups based on their sequence similarity. In the presence of mutant zein proteins, *ZmDerlin1-1* but not *ZmDerlin2-1* mRNA was dramatically induced in the endosperm mutants, *defective endosperm B30* (*De*-B30*), *floury-2* (*fl2*), and *Mucronate* (*Mc*).

Nevertheless, both ZmDerlin1-1 and ZmDerlin2-1 proteins were shown to functionally complement the growth of a *Δire1/Δder* yeast strain at the nonpermissive temperature of 37°C. In addition, the induction of ZmDerlin1 proteins was mainly restricted to the protein body fractions in which mutant zeins accumulate. Along with the induction of ZmDerlin1 proteins, a series of ER molecular chaperones, including BiP, protein disulfide isomerase (PDI), and calreticulin (CRT), were induced in the endosperm mutants as well (Boston et al., 1991; Houston et al., 2005). Based on the induced ER molecular chaperones, ERAD protein ZmDerlin, and the accumulation of ubiquitinated species, we hypothesized that conserved ERAD machinery is involved in maintaining protein body homeostasis in *De*-B30* and *fl2* endosperm. By using sequence homology analysis, we identified three maize homologs of yeast ERAD components, including ZmCDC48, ZmHRD1 and ZmUFD1. We generated specific antibodies and investigated these three homologs in maize endosperm mutants.

Materials and methods

Plant materials

The normal maize inbred W64A and its near isogenic mutants, *De*-B30*, *fl2*, *Mc*, *opaque2* (*o2*), and *floury1* (*fl1*), were grown and pollinated at the Central Crops Research Station, Clayton, North Carolina. Whole ears were harvested at 8, 10, 12, 15, and 18 days after pollination (DAP) and immediately frozen in liquid nitrogen. Kernels were removed and stored at -80°C until use.

RNA extraction, cDNA synthesis

The extraction of maize endosperm RNA was adapted from an SDS/Trizol protocol with modifications (Holding et al., 2007). Briefly, 1.5 g of endosperm dissected from kernels harvested at 18 DAP was ground in a mortar and pestle in 3 ml of NTES [20 mM Tris-HCl, pH 8.0 at 25°C, 100 mM NaCl, 10 mM EDTA, and 1% (w/v) SDS]. The extracts were ground in 3 ml of Tris-buffered phenol/chloroform (1:1; pH 8.0 at 25°C) before a centrifugation at 2,600 g in a Sorval HB-4 rotor at 4°C for 15 min. The top aqueous phase was re-extracted with phenol/chloroform before being mixed with 2.5 volumes of absolute ethanol and 0.1 volume of 3 M sodium acetate, pH 5.3 at 25°C to precipitate nucleic acids. After being resuspended in 1 ml of RNase free deionized water, RNA was precipitated with 3 volumes of 4 M LiCl at -20°C for at least 1 h. The RNA was resuspended in 500 μl of Rnase free deionized water, mixed with extraction buffer using an RNeasy Mini Kit (Qiagen, Valencia, CA), and further purified according to the manufacturer's instructions, with an additional DNase treatment to remove genomic DNA contamination. Subsequently, cDNA was synthesized using Omniscript reverse transcriptase according to the manufacturer's instructions (Qiagen, Valencia, CA).

Semi-quantitative RT-PCR

One microliter of each cDNA reaction was used for PCR amplification with GO Taq polymerase (Promega, Madison, WI). Primers are listed in Table 1. PCR was performed by using a program of 95°C for 5 min, followed with 27 cycles of 95°C for 30 sec, 60°C for 30 sec, and 72°C for 1 min. PCR products were separated by DNA electrophoresis through

1% (w/v) agarose gels in Tris-acetate-EDTA (TAE) buffer containing 0.04 M Tris-acetate, 0.001 M EDTA. Images were taken with a Gel Logic 100 Imaging System (Kodak, Rochester, NY). All genes were amplified with 27 cycles, except *BiP* and 18s rRNA which were amplified with 25 cycles.

Recombinant protein and antibody production

The coding regions of full-length and truncated *ZmCDC48*, *ZmUFD1*, and *ZmHRD1* genes were amplified using primer sets described in Table 1. For the 6x histidine (His)-tagged ZmUFD1-N construct, PCR was carried out with GoTaq DNA polymerase and the amplified product was cloned into the pGEM-T Easy vector according to the manufacturer's protocol (Promega, Madison, WI). After being verified by sequencing, the truncated *ZmUFD1* sequence was cleaved from the pGEM-T Easy vector with BamHI and HindIII and subcloned into a pRSET A expression vector (Promega, Madison, WI). The expression construct was subsequently transformed into the *E. coli* strain BL21(DE3)pLysS (Invitrogen, Carlsbad, CA) for expression. The other PCRs were carried out using Platinum® Pfx DNA polymerase according to the manufacturer's instructions (Invitrogen, Carlsbad, CA). PCR products were cloned into the pENTR/SD/D-TOPO vector (Invitrogen, Carlsbad, CA) according to the manufacturer's protocol, and verified by sequencing. The entry clones were recombined with pDEST15 or pDEST17 (Invitrogen, Carlsbad, CA) to generate N-terminal glutathione S-transferase (GST)-tagged or His-tagged fusion proteins in *E. coli* strain BL21(DE3)pLysS (Invitrogen, Carlsbad, CA). On a Biologic Dual-Flow System (Bio-Rad, Hercules, CA), recombinant proteins were purified using Bio-Scale Mini Profinity GST cartridges (Bio-Rad,

Hercules, CA) or His-select cartridges (Sigma, St Louis, MO) according to their manufacturers' instructions. The concentration of water soluble protein was determined with the Coomassie Plus assay (Pierce, Rockford, IL) with bovine serum albumin (BSA) as a standard. Water insoluble proteins were dissolved in 1% (w/v) SDS and quantified with a BCA protein assay (Pierce, Rockford, IL) with BSA as a standard. C-terminal truncated ZmCDC48 and ZmHRD1 proteins were used as antigens for raising antibodies (Covance, Denver, PA).

Binding assays *in vitro*

Purified recombinant proteins were used in binding assays *in vitro*. GST-tagged full length ZmCDC48 and GST-tagged full length ZmUFD1 were immobilized on Glutathione Sepharose™ 4B beads (GE Healthcare, Piscataway, NJ) according to the manufacturer's protocol. Immobilized GST-tagged recombinant proteins were incubated with soluble His-tagged recombinant proteins as follows: I. GST-ZmCDC48 with His-ZmUFD1; II. GST-ZmUFD1 with His-ZmCDC48. Excess GST protein incubated with His-ZmUFD1 or His-ZmCDC48 was used as negative binding controls. Binding was performed in buffer [50 mM Tris-HCl, pH 7.4 at 25°C; 150 mM NaCl; 5 mM $MgCl_2$; 1 mM DTT; 0.1% (v/v) Triton X-100; 5% (v/v) glycerol] on a Nutator (Clay Adams, Parsippany, NJ) for 1 h at 4°C. Beads were washed with binding buffer, and bound proteins were eluted with 2x SDS sample loading buffer and heated to 95°C for 5 min (Laemmli, 1970). Eluted proteins were subject to SDS–PAGE followed by Coomassie Brilliant Blue staining.

Endosperm protein extraction

Endosperm from normal and mutant inbred lines was dissected from frozen kernels. Equal fresh weights of endosperm were homogenized with a Pro 200 homogenizer (PRO Scientific, Oxford, CT) in buffer B (10 mM Tris-HCl, pH 8.5 at 25°C, 10 mM KCl, 5 mM $MgCl_2$) containing 7.2% (w/v) sucrose and protease inhibitor cocktail for plant cell and tissue extracts [1:1,000 (v/v); Sigma, St Louis, MO] at a 1:4 (w/v) grinding ratio. All steps were carried out at 4°C, unless otherwise noted. The homogenate was filtered through 2 layers of Miracloth (Calbiochem, San Diego, CA) and subjected to a centrifugation at 300 g for 5 min to remove cellular debris and starch. The supernatant was denoted as the unfractionated aqueous extract.

Protein body isolation and subcellular fractionation

Protein bodies from endosperm harvested at stages from 8 DAP to 18 DAP were isolated by discontinuous sucrose gradient centrifugation, as described by Larkins and Hurkman (1978). The unfractionated aqueous extract was overlaid on the top of 1.5 M and 2 M sucrose pads containing buffer B. The step gradients were subjected to a centrifugation at 100,000 g for 30 min at 4°C. Protein bodies were recovered from the interface between the 1.5 M and 2 M sucrose pads, and diluted with buffer B at a 1:3 (v/v) ratio. Diluted protein bodies were subsequently subjected to a centrifugation at 100,000 g for 30 min to generate a protein body pellet. Except for the subcellular fractionation experiment, all protein bodies were isolated through sucrose gradients.

For the subcellular fractionation experiment, the unfractionated aqueous extract was subjected to a centrifugation at 5,000 g for 10 min. Protein bodies were obtained from the pellet. The remaining membranes were collected as the pellet after centrifugation in a TLA55 rotor (Beckman Coulter Inc., Fullerton, CA) at 100,000 g for 30 min. The supernatant remaining after the 100,000 g centrifugation was denoted as S100. Each fraction was resuspended back to the volume of the original homogenate.

Chemical treatments of protein bodies

The unfractionated aqueous extract was overlaid on top of 1.5 M and 2 M sucrose pads containing buffer B. The step gradients were subjected to a centrifugation at 100,000 g for 30 min at 4°C. After collection from the interface between the 1.5 M sucrose and 2 M sucrose pads, protein bodies were diluted with buffer B at a 1:3 (v/v) ratio. Diluted protein bodies from equal fresh weight equivalents (5 mg) were subjected to a centrifugation at 100,000 g for 30 min, and subsequently resuspended in 200 μl of buffer (50 mM Tris, pH 7.5 at 25°C) in the presence of 1 M NaCl, 1% (v/v) Triton X-100, 1 M NaCl and 1% (v/v) Triton X-100, or 1% (w/v) SDS. Samples were agitated on a Nutator (Clay Adams, Parsippany, NJ) for 30 min at room temperature, and then subjected to 100,000 g centrifugation for 30 min. Equal fresh weight equivalents (1 mg) of supernatant (SP) and pellet (P) were resolved by SDS-PAGE and visualized by immunoblotting.

Proteinase K digestion

Protein body pellets from equal fresh weight equivalents of *De*-B30* endosperm tissue (20 mg) were resuspended in buffer B containing 7.5 μg of proteinase K in the absence or presence of 0.5% (v/v) SDS, and incubated at 4°C for 30 min. Digestion was stopped by adding PMSF to 5 mM final concentration. After treatments, samples from equal fresh weight equivalents of *De*-B30* endosperm tissue (5 mg) were subjected to SDS-PAGE and analyzed by immunoblotting with anti-ZmCDC48 and anti-ZmHRD1 antibodies. A duplicate blot probed for BiP was used as a luminal protein control.

Antibody crosslinking and immunoprecipitation

Antibodies against ZmCDC48, ZmHRD1, and ZmUFD1 were cross-linked to Protein A-Agarose Fast Flow (Sigma, St Louis, MO) as described by Harlow and Lane (1988). For subsequent immunoprecipitation, membrane proteins were solubilized in immunoprecipitation buffer [50 mM Tris-HCl, pH 8.0 at 25°C; 150 mM NaCl; 1% (v/v) IGEPAL CA 630 and 0.5% (w/v) sodium deoxycholate] for 30 min on a Nutator. The supernatant was clarified by centrifugation at 100,000 g for 30 min, and precleaned by Protein A-Agarose Fast Flow (Sigma, St Louis, MO). The precleaned supernatant was quantified with a BCA protein assay kit and BSA standard (Pierce, Rockford, IL), and then incubated with cross-linked antibodies overnight on a Nutator. After five extensive washes, the bound species were eluted as described by Cristea et al. (2005). Eluted proteins were subject to SDS–PAGE and immunoblotting with anti-CDC48, anti-HRD1, and anti-UFD1 antibodies, respectively.

Immunoblot analysis

Equal amounts of sample proteins were adjusted with 2x SDS sample loading buffer to the same volume and heated to 95°C for 5 min (Laemmli, 1970). Sample proteins were separated through SDS polyacrylamide gels and transferred to Immobilon-FL membranes (Millipore, Billerica, MA) as previously reported (Houston et al., 2005). Membranes were then blocked for 1 h with 0.2x phosphate-buffered saline containing 0.1% (w/v) casein. Primary antibodies against BiP (StressGen Biotechnologies, Victoria, British Columbia, Canada), 22-kD α-zein, or 16-kD γ-zein (Hunter et al., 2002) were used at a 1:10,000 dilution with 0.2x phosphate-buffered saline containing 0.1% (w/v) casein and 0.05% (v/v) Tween-20 and incubated overnight. After incubation with primary antibody, membranes were incubated with appropriate anti-rabbit or anti-mouse IgG conjugated Dylight® 680 or Dylight® 800 (1:10,000; Thermo Scientific, Waltham, MA). Immunoblot images were acquired with an Odyssey® infrared imaging system (Li-COR Biosciences, Lincoln, NE).

Results

Antibody production and characterization

To dissect the ERAD machinery in maize, we identified putative ERAD components including ZmUFD1, ZmCDC48, and ZmHRD1 by using previously identified plant protein sequences for homology searches against the B73 filtered translation database (Kirst, 2006; version 4a.53; http://www.maizesequence.org). The maize genome encodes two *ZmUFD1* genes: Zm*UFD1A* (GRMZM2G037185) and Zm*UFD1B* (GRMZM2G114220); three *ZmCDC48* genes: *ZmCDC48A* (GRMZM2G063060), *ZmCDC48B* (GRMZM2G036765),

and *ZmCDC48C* (AC233949.1_FGT004); and two *ZmHRD1* genes: *ZmHRD1A* (GRMZM2G028183) and *ZmHRD1B* (GRMZM2G055643). Antibodies for ZmUFD1, ZmCDC48, and ZmHRD1 were raised against recombinant proteins of truncated His-ZmUFD1A-N (amino acids 1 to 228), His-ZmCDC48A-C (amino acids 635 to 811), and His-ZmHRD1A-C (amino acids 248-508), respectively. These three purified recombinant proteins were resolved by SDS-PAGE and stained with Coomassie Brilliant Blue (Figure 1A).

An aqueous extract from normal endosperm harvested at 18 DAP was separated by SDS-PAGE and immunoblotted with pre-immune or immune sera of anti-ZmCDC48, anti-ZmHRD1, and anti-ZmUFD1 antibodies, respectively. The ZmUFD1 antibody recognized two bands with similar molecular weights in the endosperm extract (Figure 1B). The subsequent ZmUFD1 immunoprecipitation and LC/MS^{E} analysis showed that these two immunoreactive bands were maize ZmUFD1A and maize ZmUFD1B (Supplementary Table 1). The ZmCDC48 antibody recognized a single dominant band in the extract (Figure 1B). Because of high sequence similarities, ZmCDC48 antibody recognizes all three isoforms (Supplementary Table 1). A similar cross reactivity has been reported for Arabidopsis CDC48 antibody (Rancour et al., 2002). ZmHRD1 antibody also recognized two bands. There are peptides that can be definitively assigned to ZmHRD1A and conserved peptides that can be assigned to both ZmHRD1A and ZmHRD1B (Supplementary Table 1; Figure 1B).

Association of ZmCDC48 and ZmHRD1 with *De*-B30* and *fl2* protein bodies

Yeast Cdc48p is a cytosolic protein, and has been reported to be recruited to the ER transmembrane Hrd1p complex for exporting ubiquitinated species (Neuber et al., 2005; Schuberth and Buchberger, 2005). We showed increased ubiquitin signals in *De*-B30* and *fl2* protein body fractions (Chapter 2). To investigate whether ZmCDC48 is associated with protein body fractions, we isolated protein bodies from endosperm of normal maize and *De*-B30*, *fl2*, *Mc*, *o2*, and *fl1* mutants. Total protein body proteins were separated by SDS-PAGE and immunoblotted with anti-ZmCDC48 and anti-ZmHRD1 antibodies (Figure 2). There were increased amounts of ZmCDC48 in *De*-B30* and *fl2* protein body fractions relative to equivalent fractions from the normal counterpart. Little or no increase of ZmCDC48 was observed in protein body fractions from *Mc*, *o2*, and *fl1*. We observed a similar increase of ZmHRD1 in *De*-B30* and *fl2*, but not in *Mc*, and *fl1* protein body fractions (Figure 2). Surprisingly, we found an increase of ZmHRD1 in *o2*. The ER molecular chaperone BiP increased in *De*-B30* and *fl2* protein body fractions as has been reported (Boston et al., 1991). A duplicate blot probed for the ribosome-associated membrane protein RAMP4 was used for a protein loading comparison (Gorlich et al., 1992).

Yeast Der1p and its mammalian homologs Derlins have been shown to facilitate the membrane extraction of ERAD substrates (Knop et al., 1996; Lilley and Ploegh, 2004; Ye et al., 2004). ZmDerlin proteins were reported to be induced at the transcript level in *De*-B30*, *fl2*, *Mc* and *o2* (Kirst et al., 2005). To determine whether *ZmCDC48*, *ZmHRD1*, and other putative maize ERAD component genes were induced at the transcript level as well, we

performed semi-quantitative RT-PCR on cDNA from normal and mutant endosperm at 18 DAP (Figure 2B). There were little gene expression differences among these samples, except for the *ZmHRD1A* and *ZmHRD3* genes being induced in *De*-B30* and *fl2* mutants. We also observed a little induction of *ZmHRD3* in *Mc* mutant. The induction of *ZmHRD1A* and *ZmHRD3* genes was similar to that of the *BiP1* gene control in *De*-B30* and *fl2* mutants, and in agreement with the tunicamycin induced Arabidopsis *HRD1* and *SEL1L* gene (a homolog of the yeast *HRD3* gene; Kamauchi et al., 2005). *SEC61α* which encodes a translocon subunit and 18S rRNA were used as amplification controls. These results together are suggestive that ZmCDC48 is recruited from the cytosol and ZmHRD1 is induced in *De*-B30* and *fl2* protein body fractions for maintaining protein body homeostasis.

Association of ZmCDC48 and ZmHRD1 correlates with *De*-B30* and *fl2* gene dosages

As we observed the increased recruitment of ZmCDC48 and induction of ZmHRD1 in *De*-B30* and *fl2* protein body fractions, we wanted to determine whether the association of ZmCDC48 and ZmHRD1 in protein body fractions proportionally increases with the gene dosage of *De*-B30* and *fl2* mutant alleles. We analyzed normal and mutant protein body fractions with varying *De*-B30* and *fl2* gene dosages. Because of the triploid nature of maize endosperm, we were able to generate endosperm with zero (normal) up to three doses of a mutant allele. The immunoblot in Figure 3A shows that the recruitment of ZmCDC48 increased with *De*-B30* and *fl2* mutant alleles, and so did the induction of ZmHRD1. Even one dose of a *De*-B30* or *fl2* mutant allele led to an increase of ZmCDC48 and ZmHRD1 association with protein bodies. These results were consistent with a small induction of

ubiquitinated species in protein body fractions with one dose of the *De*-B30* or *fl2* mutant allele (Figure 3 in Chapter 2). The ER molecular chaperones BiP, PDI, and CRT had similar induction patterns in response to the increase of *De*-B30* and *fl2* gene dosages. It is worth noting that an unglycosylated form of CRT was observed in the protein body fraction with one dose of the *De*-B30* mutant allele, but it appeared in the protein body fraction only when there were at least two doses of the *fl2* mutant allele. This result is consistent with results from Chapter 2 that oligosaccharyl transferases were identified as ubiquitinated substrates and a stronger ubiquitination correlated with the *De*-B30* mutant allele than with the *fl2* mutant allele. A duplicate blot probed for 22-kD and 19-kD α-zein was used as a protein loading control.

Maize Derlin proteins have been reported to be predominantly induced in the protein body fraction compared to the microsome fraction (Kirst et al., 2005). To determine whether ZmCDC48 recruitment and ZmHRD1 induction are protein body specific as well, we separated protein bodies from the total membrane fraction. The immunoblot in Figure 3B shows similar protein levels of ZmCDC48, but slightly decreased amounts of ZmHRD1 in these non-protein body membrane fractions of endosperm aqueous extract from maize plants with *De*-B30* and *fl2* mutant alleles. The increase in protein body fractions and decrease in non-protein body membrane fractions of ZmHRD1 may suggest its redistribution between these two fractions. The ER molecular chaperones BiP, PDI, and CRT showed little induction.

Characterization of protein body associated ZmCDC48 and ZmHRD1

We observed that more ZmCDC48 proteins were recruited to *De*-B30* and *fl2* protein body fractions, whereas the RNA levels of the *ZmCDC48* genes are similar between those mutants and normal endosperm (Figure 2). We hypothesized that this inconsistency is due to most ZmCDC48 protein being localized in the cytosolic fraction. To determine the subcellular localization of ZmCDC48 and ZmHRD1, we separated normal and *De*-B30* cellular extracts into an S100 fraction containing mostly cytosol, non-protein body membranes, and protein bodies by differential centrifugation. The immunoblot in Figure 4 shows that most ZmCDC48 was localized in the cytosol and only a small portion was localized in protein bodies and other membranes. Most ZmHRD1 was localized in the two membrane fractions. Most ZmUFD1 was localized in the cytosol, and only very small amounts of ZmUFD1 were localized to membrane fractions. Duplicate blots probed for ZmDerlin1 and 16-kD γ-zein were used as membrane and protein body controls, respectively.

To determine the nature of the membrane association of ZmCDC48, we applied various chemical treatments that release peripheral or transmembrane membrane proteins from membranes. The immunoblot in Figure 5A shows that ZmCDC48 was partially released by 1 M NaCl or 1% (w/v) Triton X-100. These results suggest that ZmCDC48 is a peripheral protein, a portion of which was tightly associated with the protein body fraction, or embedded in the protein bodies. In contrast, ZmHRD1 was released by 1% (w/v) Triton X-100 but not 1 M NaCl. This result is consistent with the prediction that ZmHRD1 is a

transmembrane protein. ZmRAMP4 was used as a single transmembrane protein control (Gorlich et al., 1992).

In the absence of detergent, luminal proteins are protected by the membrane from proteinase digestion. However, peripheral membrane proteins or membrane proteins containing cytosolic domains are accessible to proteinase digestion. To further confirm the peripheral localization of ZmCDC48 and the orientation of ZmHRD1, we performed a proteinase K digestion on isolated *De*-B30* protein bodies. The immunoblots in Figure 5B show that both ZmCDC48 and ZmHRD1 are sensitive to proteinase K in the absence of detergent. The ER molecular chaperone BiP was used as a luminal protein control that was heavily digested only when detergent was added. Since the ZmHRD1 antibody was made against the carboxyl-terminal region that contains a conserved RING-H2 motif, the result suggested that the carboxyl-terminal region in maize ZmHRD1 was localized to the cytosolic face of the protein body membranes as reported for yeast Hrd1p (Gardner et al., 2000).

ZmCDC48, ZmHRD1 and ZmUFD1 interactions

Yeast Ufd1p has been shown to form a conserved protein complex with Cdc48p and Npl4p in the cytosol (Meyer et al., 2000). To identify the ZmUFD1 protein complex in the cytosol, we immunoprecipitated ZmUFD1 from a *De*-B30* S100 fraction by using a ZmUFD1 antibody (Figure 6). Proteins in distinct bands from ZmUFD1 immunoprecipitates were identified with LC/MS^{E} analysis as potential interacting partners, including ZmCDC48, maize heat shock protein 70, chaperonin CPN60, and starch synthase DULL1. To test

whether maize ZmCDC48 and ZmHRD1 antibodies were also suitable for immunoprecipitation, we performed immunoprecipitation and LC/MS^E analysis (Figure 6). Identified peptides are listed in supplementary Table 1. The data are suggestive that these antibodies could successfully recognize native forms of ZmUFD1, ZmCDC48, and ZmHRD1, respectively. In addition, ZmUFD1 and ZmCDC48 form a protein complex in the cytosol.

The yeast Cdc48p-Ufd1p-Npl4p complex has been reported to be recruited to the Hrd1p complex on the ER membrane to extract ubiquitinated substrates (Ye et al., 2001). We observed an increased recruitment of ZmCDC48 and induction of ZmHRD1 in *De*-B30* protein body fractions. To determine whether ZmCDC48, ZmUFD1, and ZmHRD1 form complexes on the membrane, we isolated total membranes including protein body membranes from *De*-B30* endosperm for immunoprecipitation. Co-immunoprecipitated proteins were assayed with immunoblotting. In Figure 7, ZmCDC48 and ZmUFD1 interaction is shown in both ZmCDC48 and ZmUFD1 immunoprecipitations. ZmCDC48 and ZmHRD1 interaction was observed in ZmHRD1 immunoprecipitation but not detected in the reciprocal ZmCDC48 immunoprecipitation. These data are suggestive that ZmCDC48 interacts with ZmUFD1 and ZmHRD1 on the membrane.

To further test whether ZmCDC48, ZmUFD1, and ZmHRD1 interact directly, we purified recombinant proteins of ZmCDC48 and ZmUFD1 from *E. coli*. Because of the insolubility of full length and C-terminal truncated ZmHRD1, we were able to perform only recombinant ZmCDC48 and ZmUFD1 interaction assays *in vitro*. As shown in Figure 8A, His-ZmUFD1

was bound by immobilized GST-ZmCDC48, but not immobilized GST. Figure 8B showed that His-ZmCDC48 was specifically pulled down by immobilized GST-ZmUFD1, but not immobilized GST. The reciprocal binding assays suggested a direct binding *in vitro* between ZmUFD1 and ZmCDC48.

Association of ZmCDC48 and ZmHRD1 during endosperm development

ER chaperones have been shown to be induced along with mutant α-zein expression during *fl2* endosperm development (Boston et al., 1991; Fontes et al., 1991; Houston et al., 2005). To understand whether the recruitment of ZmCDC48 and the induction of ZmHRD1 correlates with mutant zein accumulation and the induction of the ER quality control machinery, we investigated membrane bound ZmCDC48 and ZmHRD1 in protein body fractions of normal and *De*-B30* endosperm during developmental stages from 8 DAP to 18 DAP. Figure 9 demonstrates that there were similar amounts of protein body membrane bound ZmCDC48 between normal and *De*-B30* endosperm at early developmental stages (8 and 10 DAP). From 12 DAP and later, a dramatic increase of membrane bound ZmCDC48 was observed in *De*-30* protein body fractions. The induction of ZmHRD1 was shown to follow a similar pattern. The ER quality control machinery including the molecular chaperones BiP, calnexin (CNX), calreticulin (CRT), PDI, and the ERAD component ZmDerlin1 were shown to be induced starting from 12 DAP. Ribosome-inactivating protein (RIP) was used for protein loading comparisons (Bass et al., 1992).

Discussion

The synthesis and deposition of mutant zeins in protein bodies leads to a series of unfolded protein responses in the maize endosperm mutants *De*-B30*, *fl2*, and *Mc*. Along with the induction of ER molecular chaperones BiP, PDI, and CRT, the expression of the ERAD related ZmDerlin proteins is also induced (Boston et al., 1991; Houston et al., 2005; Kirst et al., 2005). Besides ZmDerlin proteins, the maize genome encodes several conserved ERAD related proteins (Kirst, 2006). Three conserved ERAD related proteins, ZmCDC48, ZmHRD1, and ZmUFD1 were investigated.

We found increased recruitment of ZmCDC48 to protein body fractions of *De*-B30* and *fl2* endosperm, but not of *Mc*, *o2*, and *fl1* endosperm when compared to normal endosperm (Figure 1A). This result is consistent with induced ZmDerlin proteins and increased ubiquitin signals in *De*-B30* and *fl2* protein body fractions (Chapter 2; Kirst et al., 2005). Together, these results are suggestive that the ERAD process is induced in *De*-B30* and *fl2* protein body fractions. The mutant and endosperm developmental studies further supported the positive correlation between the increased recruitment of ZmCDC48, increased ubiquitin signals and mutant α-zein expression in *De*-B30* and *fl2* protein body fractions (Figure 3A; Figure 9). In addition, the increased accumulation of ZmCDC48 protein in *De*-B30* and *fl2* protein body fractions did not correlate with *ZmCDC48* transcript level which was similar among normal, *De*-B30* and *fl2* endosperm (Figure 1B). This similar transcript level is supported by the total pool of ZmCDC48 not changing among normal, *De*-B30*, and *fl2* endosperm (Figure 4). Taken together, these results demonstrate that the increased

recruitment of ZmCDC48 to mutant protein body membranes is positively correlated with increased ubiquitin signals and mutant α-zein expression in *De*-B30* and *fl2* protein body fractions.

Our finding of membrane bound ZmCDC48 is consistent with a previous study showing that a portion of AtCDC48 was localized to the periphery of membranes (Rancour et al., 2002). In agreement with AtCDC48 being a peripheral membrane protein, ZmCDC48 was proteinase K-sensitive in the absence of detergent (Figure 5B), which suggested that it was localized to the cytosolic side of the protein body membrane. In addition, we found that ZmCDC48 in *De*-B30* protein body fractions was sensitive to high salt (1 M NaCl) and detergent [1% (v/v) Triton X-100], suggesting its ionic interactions with membrane proteins. However, the result here is somewhat different from a previous report, in which microsomal membrane bound AtCDC48 was not salt sensitive but was able to be fully solubilized by 1% (v/v) Triton X-100 (Rancour et al., 2002). The difference could be due to membrane bound AtCDC48 interacting with different membrane protein recruiters compared to protein body membrane bound ZmCDC48. It is well documented that CDC48 acts together with various cofactors for its versatile functions (Woodman, 2003; Park et al., 2008). Indeed, Rancour et al. (2002) showed that AtCDC48 interacts with SPY31, the plant homolog of syntaxin 5, which facilitates cytokinesis. The membrane bound ZmCDC48 in the normal protein body fraction may represent a similar or other membrane related function.

In addition, CDC48 plays a crucial role in the ERAD process. In the yeast model, Cdc48p forms a heterogeneous complex with its cofactor Ufd1p-Npl4p to recognize and bind to ubiquitinated ERAD substrates for their retrotranslocation (Meyer et al., 2000; Ye et al., 2001). We hypothesize that increased amounts of ZmCDC48 recruited to *De*-B30* and *fl2* protein body membranes play a similar function to export ubiquitinated proteins. In Chapter 2, we showed that ubiquitinated proteins in *De*-B30* protein body fractions were insoluble in the presence of high salt and nonionic detergent. It raises the possibility that these proteins may be accessible to ubiquitination, but cannot be completely exported from protein bodies and degraded by the 26S proteasome. As a result, ubiquitin signals increased in *De*-B30* protein body fractions. The accumulation of ubiquitinated proteins requires an increased recruitment of ZmCDC48 to the protein body membrane. Another piece of supporting evidence is that CDC48 has been shown to bind to poly-ubiquitin (Dai and Li, 2001), although we were not able to test the interaction between ZmCDC48 and ubiquitinated proteins by using immunoprecipitation because of the insolubility of ubiquitinated proteins associated with protein bodies. Another simple and but unlikely explanation is that there is no direct functional linkage between the increased recruitment of ZmCDC48 and increased ubiquitin signals.

In yeast, Hrd1p forms a multi-transmembrane protein complex in the degradation of proteins with misfolded ER-luminal or intra-membrane domains (Carvalho et al., 2006; Denic et al., 2006). Three pieces of evidence here support ZmHRD1 being a transmembrane protein. First, ZmHRD1 was exclusively localized to the membrane fractions in the subcellular

fractionation experiment (Figure 4). Second, ZmHRD1 was solubilized in the presence of detergent but not by high salt alone (Figure 5A). Third, the carboxyl terminal region of ZmHRD1 that was used for raising its antibody was completely digested by proteinase K, whereas only a small portion of the luminal protein BiP was digested in the absence of detergent (Figure 5B). We observed a slight induction of ZmHRD1 in *De*-B30* and *fl2* protein body fractions, and this induction was correlated with the slightly increased transcript level (Figure 2). The increased transcript level is in agreement with previous studies of the *HRD1* gene expression being induced (Travers et al., 2000; Martinez and Chrispeels, 2003; Kamauchi et al., 2005). In addition to the transcript induction, we observed the interaction between ZmHRD1 and ZmCDC48 by using ZmHRD1 antibody in an immunoprecipitation experiment. This result is in agreement with a previous report in yeast that Cdc48p interacts with Hrd1p on the ER membranes (Gauss et al., 2006). However, we did not detect the interaction by using ZmCDC48 antibody. It is possible that membrane bound ZmCDC48 is recruited through another membrane protein. In yeast, Ubx2p has been shown to be the membrane anchor to recruit Cdc48p to the ER membrane (Neuber et al., 2005; Schuberth and Buchberger, 2005). However, we did not find any maize homologs of Ubx2p. Another possibility is that ubiquitin signals alone might be enough to recruit ZmCDC48 to the protein body membrane.

In yeast, Ufd1p and Npl4p are cytosolic cofactors recruited by Cdc48p to function in the ERAD process (Ye et al., 2001). We generated a specific antibody against ZmUFD1, the maize homolog of yeast Ufd1p. However, we did not identify any maize homologs of Npl4p

by sequence similarity. A subcellular fractionation study showed that most ZmUFD1 was localized in the cytosol fractions as is yeast Ufd1p (Meyer et al., 2000). Immunoprecipitation and binding assays *in vitro* demonstrated the directed interaction between ZmCDC48 and ZmUFD1. We observed a low efficiency of ZmUFD1co-immunoprecipitation by using ZmCDC48 antibody. Part of the reason for such a low efficiency could be due to a similar situation as is found in the stoichiometry of p97 (mammalian homolog to yeast Cdc48p) protein complexes where one p97 hexamer interacts with one heterodimer of UFD1 and NPL4 (Pye et al., 2007). In addition to the stoichiometry of the CDC48 protein complex, another possibility for the less efficient pulldown of ZmUFD1 could be that besides interacting with ZmUFD1, ZmCDC48 interacts with various cofactors for its versatile functions as I previously discussed. With all of these cofactors competing for interaction sites in CDC48, it would not be surprising to see a low binding efficiency of ZmUFD1 by using ZmCDC48 antibody. We did not detect any protein functioning as Npl4p in maize endosperm extract by doing a ZmCDC48 binding assay (data not shown). It is possible that the ZmCDC48 complex contains cofactors with distinct protein sequences or ZmCDC48 itself is enough for its ERAD functions in maize endosperm.

In conclusion, we identified and characterized three maize homologs of ERAD components, including ZmCDC48, ZmHRD1, and ZmUFD1. The increased recruitment of ZmCDC48 and induction of ZmHRD1 are strongly correlated with mutant α-zein expression in *De*-B30* and *fl2* protein bodies. In addition, we demonstrated that these three proteins form protein complexes on the membrane and they might have conserved functions in the maize

endosperm ERAD process. Combined with the induction of ER molecular chaperones and the result in Chapter 2 of increased ubiquitin signals in *De*-B30* and *fl2* protein bodies, this study implies an induced ERAD process associated with *De*-B30* and *fl2* protein bodies in response to the mutant zein accumulation.

References

Bass HW, Webster C, GR OB, Roberts JK, Boston RS (1992) A maize ribosome-inactivating protein is controlled by the transcriptional activator *Opaque-2*. Plant Cell **4:** 225-234

Boston RS, Fontes EB, Shank BB, Wrobel RL (1991) Increased expression of the maize immunoglobulin binding protein homolog b-70 in three zein regulatory mutants. Plant Cell **3:** 497-505

Carroll SM, Hampton RY (2009) Usa1p is required for optimal function and regulation of the Hrd1p endoplasmic reticulum-associated degradation ubiquitin ligase. J Biol Chem **285:** 5146-5156

Carvalho P, Goder V, Rapoport TA (2006) Distinct ubiquitin-ligase complexes define convergent pathways for the degradation of ER proteins. Cell **126:** 361-373

Cristea IM, Williams R, Chait BT, Rout MP (2005) Fluorescent proteins as proteomic probes. Mol Cell Proteomics **4:** 1933-1941

Dai RM, Li CC (2001) Valosin-containing protein is a multi-ubiquitin chain-targeting factor required in ubiquitin-proteasome degradation. Nat Cell Biol **3:** 740-744

Denic V, Quan EM, Weissman JS (2006) A luminal surveillance complex that selects misfolded glycoproteins for ER-associated degradation. Cell **126:** 349-359

Feiler HS, Desprez T, Santoni V, Kronenberger J, Caboche M, Traas J (1995) The higher plant *Arabidopsis thaliana* encodes a functional CDC48 homologue which is highly expressed in dividing and expanding cells. EMBO J **14:** 5626-5637

Fontes EB, Shank BB, Wrobel RL, Moose SP, GR OB, Wurtzel ET, Boston RS (1991) Characterization of an immunoglobulin binding protein homolog in the maize *floury-2* endosperm mutant. Plant Cell **3:** 483-496

Gardner RG, Swarbrick GM, Bays NW, Cronin SR, Wilhovsky S, Seelig L, Kim C, Hampton RY (2000) Endoplasmic reticulum degradation requires lumen to cytosol signaling. Transmembrane control of Hrd1p by Hrd3p. J Cell Biol **151:** 69-82

Gauss R, Sommer T, Jarosch E (2006) The Hrd1p ligase complex forms a linchpin between ER-lumenal substrate selection and Cdc48p recruitment. EMBO J **25:** 1827-1835

Gorlich D, Prehn S, Hartmann E, Kalies KU, Rapoport TA (1992) A mammalian homolog of SEC61p and SECYp is associated with ribosomes and nascent polypeptides during translocation. Cell **71:** 489-503

Harlow E, Lane D (1988) Antibodies: a laboratory manual. Cold Spring Harbor Laboratory Press, Cold Spring Harbor, NY

Hetzer M, Meyer HH, Walther TC, Bilbao-Cortes D, Warren G, Mattaj IW (2001) Distinct AAA-ATPase p97 complexes function in discrete steps of nuclear assembly. Nat Cell Biol **3:** 1086-1091

Hirsch C, Gauss R, Horn SC, Neuber O, Sommer T (2009) The ubiquitylation machinery of the endoplasmic reticulum. Nature **458:** 453-460

Holding DR, Otegui MS, Li B, Meeley RB, Dam T, Hunter BG, Jung R, Larkins BA (2007) The maize *floury1* gene encodes a novel endoplasmic reticulum protein involved in zein protein body formation. Plant Cell **19:** 2569-2582

Horn SC, Hanna J, Hirsch C, Volkwein C, Schutz A, Heinemann U, Sommer T, Jarosch E (2009) Usa1 functions as a scaffold of the HRD-ubiquitin ligase. Mol Cell **36:** 782-793

Houston NL, Fan C, Xiang JQ, Schulze JM, Jung R, Boston RS (2005) Phylogenetic analyses identify 10 classes of the protein disulfide isomerase family in plants, including single-domain protein disulfide isomerase-related proteins. Plant Physiol **137:** 762-778

Hunter BG, Beatty MK, Singletary GW, Hamaker BR, Dilkes BP, Larkins BA, Jung R (2002) Maize opaque endosperm mutations create extensive changes in patterns of gene expression. Plant Cell **14:** 2591-2612

Kamauchi S, Nakatani H, Nakano C, Urade R (2005) Gene expression in response to endoplasmic reticulum stress in *Arabidopsis thaliana*. FEBS J **272:** 3461-3476

Kirst ME "Identification and characterization of maize Derlins in response to endoplasmic reticulum stress." Ph.D. diss., North Carolina State University, 2006. http://www.lib.ncsu.edu/resolver/1840.16/4954

Kirst ME, Meyer DJ, Gibbon BC, Jung R, Boston RS (2005) Identification and characterization of endoplasmic reticulum-associated degradation proteins differentially affected by endoplasmic reticulum stress. Plant Physiol **138:** 218-231

Knop M, Finger A, Braun T, Hellmuth K, Wolf DH (1996) Der1, a novel protein specifically required for endoplasmic reticulum degradation in yeast. EMBO J **15:** 753-763

Laemmli UK (1970) Cleavage of structural proteins during the assembly of the head of bacteriophage T4. Nature **227:** 680-685

Lilley BN, Ploegh HL (2004) A membrane protein required for dislocation of misfolded proteins from the ER. Nature **429:** 834-840

Marshall RS, Jolliffe NA, Ceriotti A, Snowden CJ, Lord JM, Frigerio L, Roberts LM (2008) The role of CDC48 in the retro-translocation of non-ubiquitinated toxin substrates in plant cells. J Biol Chem **283:** 15869-15877

Martinez IM, Chrispeels MJ (2003) Genomic analysis of the unfolded protein response in Arabidopsis shows its connection to important cellular processes. Plant Cell **15:** 561-576

Meyer HH, Shorter JG, Seemann J, Pappin D, Warren G (2000) A complex of mammalian ufd1 and npl4 links the AAA-ATPase, p97, to ubiquitin and nuclear transport pathways. EMBO J **19:** 2181-2192

Moir D, Stewart SE, Osmond BC, Botstein D (1982) Cold-sensitive cell-division-cycle mutants of yeast: isolation, properties, and pseudoreversion studies. Genetics **100:** 547-563

Muller J, Piffanelli P, Devoto A, Miklis M, Elliott C, Ortmann B, Schulze-Lefert P, Panstruga R (2005) Conserved ERAD-like quality control of a plant polytopic membrane protein. Plant Cell **17:** 149-163

Neuber O, Jarosch E, Volkwein C, Walter J, Sommer T (2005) Ubx2 links the Cdc48 complex to ER-associated protein degradation. Nat Cell Biol **7:** 993-998

Park S, Rancour DM, Bednarek SY (2008) In planta analysis of the cell cycle-dependent localization of AtCDC48A and its critical roles in cell division, expansion, and differentiation. Plant Physiol **148:** 246-258

Pye VE, Beuron F, Keetch CA, McKeown C, Robinson CV, Meyer HH, Zhang X, Freemont PS (2007) Structural insights into the p97-Ufd1-Npl4 complex. Proc Natl Acad Sci USA **104:** 467-472

Rancour DM, Dickey CE, Park S, Bednarek SY (2002) Characterization of AtCDC48. Evidence for multiple membrane fusion mechanisms at the plane of cell division in plants. Plant Physiol **130:** 1241-1253

Rape M, Hoppe T, Gorr I, Kalocay M, Richly H, Jentsch S (2001) Mobilization of processed, membrane-tethered SPT23 transcription factor by CDC48(UFD1/NPL4), a ubiquitin-selective chaperone. Cell **107:** 667-677

Schuberth C, Buchberger A (2005) Membrane-bound Ubx2 recruits Cdc48 to ubiquitin ligases and their substrates to ensure efficient ER-associated protein degradation. Nat Cell Biol **7:** 999-1006

Su W, Liu Y, Xia Y, Hong Z, Li J (2011) Conserved endoplasmic reticulum-associated degradation system to eliminate mutated receptor-like kinases in *Arabidopsis*. Proc Natl Acad Sci USA **108:** 870-875

Thoms S (2002) Cdc48 can distinguish between native and non-native proteins in the absence of cofactors. FEBS Lett **520:** 107-110

Travers KJ, Patil CK, Wodicka L, Lockhart DJ, Weissman JS, Walter P (2000) Functional and genomic analyses reveal an essential coordination between the unfolded protein response and ER-associated degradation. Cell **101:** 249-258

Uchiyama K, Kondo H (2005) p97/p47-Mediated biogenesis of Golgi and ER. J Biochem **137:** 115-119

Vembar SS, Brodsky JL (2008) One step at a time: endoplasmic reticulum-associated degradation. Nat Rev Mol Cell Biol **9:** 944-957

Woodman PG (2003) p97, a protein coping with multiple identities. J Cell Sci **116:** 4283-4290

Ye Y, Meyer HH, Rapoport TA (2001) The AAA ATPase Cdc48/p97 and its partners transport proteins from the ER into the cytosol. Nature **414:** 652-656

Ye Y, Meyer HH, Rapoport TA (2003) Function of the p97-Ufd1-Npl4 complex in retrotranslocation from the ER to the cytosol: dual recognition of nonubiquitinated polypeptide segments and polyubiquitin chains. J Cell Biol **162:** 71-84

Ye Y, Shibata Y, Yun C, Ron D, Rapoport TA (2004) A membrane protein complex mediates retro-translocation from the ER lumen into the cytosol. Nature **429:** 841-847

Table 1. Oligonucleotides used in this study

Name	Sequence (5'-3')[a]	Target gene	Accession number[b]	Purpose
ZmHRD1A_RT_F	gggcatctgttccatgtgcattgt	*ZmHRD1A*	GRMZM2G028183	semi-quantitative RT-PCR
ZmHRD1A_RT_R	atggagtggcagtaccaggttgaa	*ZmHRD1A*	GRMZM2G028183	semi-quantitative RT-PCR
ZmCDC48_RT_F	tggagctacaaacaggcctgacat	*ZmCDC48A, ZmCDC48B, ZmCDC48C*	AC233949.1_FGT004; GRMZM2G036765; GRMZM2G063060	semi-quantitative RT-PCR
ZmCDC48_RT_R	agactgctcatcaggcagtggaat	*ZmCDC48A, ZmCDC48B, ZmCDC48C*	AC233949.1_FGT004; GRMZM2G036765; GRMZM2G063060	semi-quantitative RT-PCR
ZmUFD1A_RT_F	accgacgttccagctgaagaagaa	*ZmUFD1A*	GRMZM2G037185	semi-quantitative RT-PCR
ZmUFD1A_RT_R	tcgcattagcttgtcgctttgcag	*ZmUFD1A*	GRMZM2G037185	semi-quantitative RT-PCR
ZmUFD1B_RT_F	aaatcagcaaatctcagcacccgc	*ZmUFD1B*	GRMZM2G114220	semi-quantitative RT-PCR
ZmUFD1B_RT_R	aacctcagctcgtcgtccttcttt	*ZmUFD1B*	GRMZM2G114220	semi-quantitative RT-PCR
ZmSEC61α_RT_F	gctgatttcatgggtgcgattggt	*ZmSEC61α*	GRMZM2G130987	semi-quantitative RT-PCR
ZmSEC61α_RT_R	agtcgccctttccttctcaaaggt	*ZmSEC61α*	GRMZM2G130987	semi-quantitative RT-PCR
Zm18srRNA_RT_F	cgcgcaaattacccaatcctgaca	Zm18srRNA	AF168884[c]	semi-quantitative RT-PCR
Zm18srRNA_RT_R	ttgccctccaatggatcctcgtta	Zm18srRNA	AF168884[c]	semi-quantitative RT-PCR
ZmBiP1_RT_F	aaccaaggatgctggtgtcattgc	*ZmBiP1*	GRMZM2G415007_T01; AC199439.4_FGT005; GRMZM2G056039 (Hsp70); GRMZM2G340251 (HsP70)	semi-quantitative RT-PCR
ZmBiP1_RT_R	aaagtgccaccaccaaggtcaaag	*ZmBiP1*	GRMZM2G415007_T01; AC199439.4_FGT005; GRMZM2G056039 (Hsp70); GRMZM2G340251 (HsP70)	semi-quantitative RT-PCR
ZmHRD3_RT_F	agacatcttcgtgcgcatgctttg	*ZmHRD3*	GRMZM2G372398	semi-quantitative RT-PCR
ZmHRD3_RT_R	tctgctgcacgttcatagtccctt	*ZmHRD3*	GRMZM2G372399	semi-quantitative RT-PCR
ZmCDC48A_C_F	CACCATGatcattgaccctgctctgct	*ZmCDC48A*	AC233949.1_FGT004; GRMZM2G036765	antibody production
ZmCDC48A_C_R	aacagatgagtgacgggactg	*ZmCDC48A*	AC233949.1_FGT004; GRMZM2G036765	antibody production
ZmHRD1A_C_F	CACCATGctgcacttgattcgtgagcta	*ZmHRD1A*	GRMZM2G028183	antibody production
ZmHRD1A_C_R	gatgcaggagtgcctgttta	*ZmHRD1A*	GRMZM2G028183	antibody production
ZmUFD1A_C_F	CGGGATCCgaaacgatgtacttc	*ZmHRD1A*	GRMZM2G037185	antibody production
ZmUFD1A_C_R	CCCAAGCTTggttctttgtagtca	*ZmHRD1A*	GRMZM2G037185	antibody production
ZmCDC48A_full_F	CACCatggcgagccaagggga	*ZmCDC48A*	GRMZM2G036765	recombinant protein production
ZmCDC48A_full_R	ctagctgtatagatcgtcatcatca	*ZmCDC48A*	GRMZM2G036765	recombinant protein production
ZmUFD1A_full_F	CACCatgtacttcgaaggctatgg	*ZmUFD1A*	GRMZM2G037185	recombinant protein production
ZmUFD1A_full_R	cgcttctccctgagaatgtc	*ZmUFD1A*	GRMZM2G037185	recombinant protein production

[a]Sequences in lower case indicate the homologous regions of oligonucleotides to target genes. Sequences in capitals indicate artificial extensions for cloning. Start condons and restriction enzyme sites are underlined.
[b]B73 filtered translation database (version 4a.53; http://www.maizesequence.org) was used.
[c]GenBank was used.

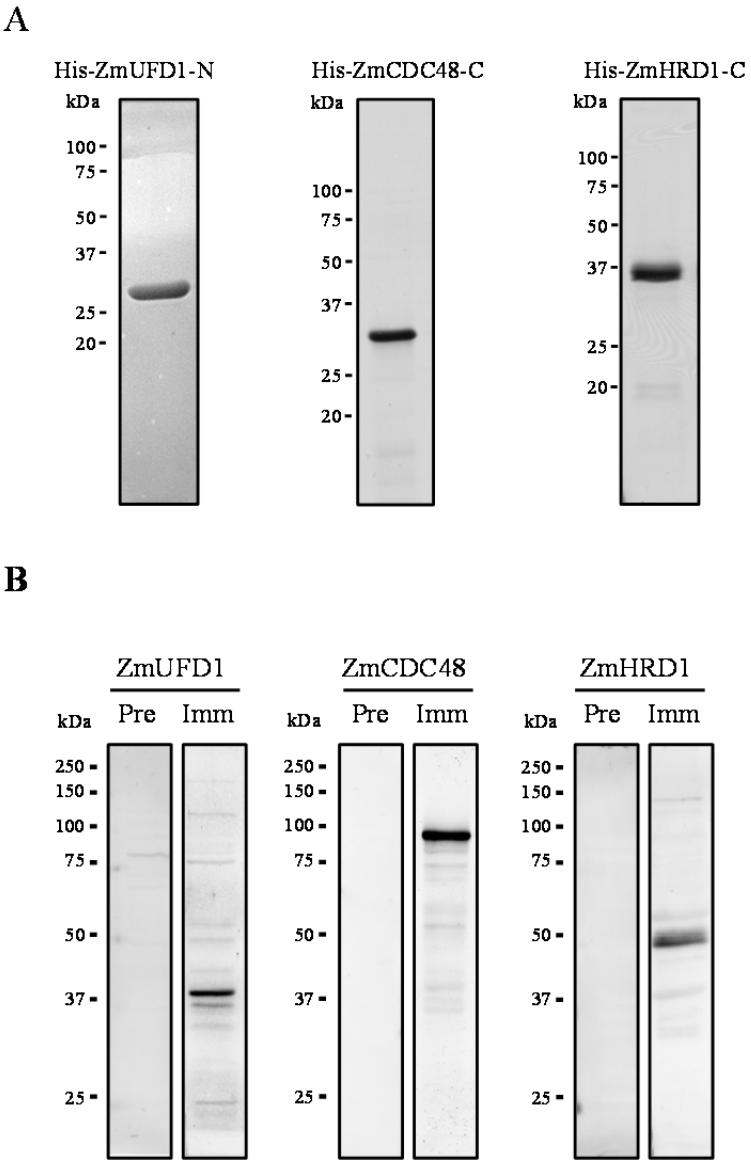

Figure 1. Analysis of recombinant proteins and antibodies. **A**. Coomassie Brilliant Blue stained SDS-polyacrylamide gels of purified His-ZmUFD1-N, His-ZmCDC48-C, and His-ZmHRD1-C. **B**. Total proteins from equal fresh weight equivalents of normal endosperm (0.625 mg for ZmCDC48, 1.25 mg for ZmUFD1, and 2.5 mg for ZmHRD1) were separated by SDS-PAGE and immunoblotted with pre-immune (Pre) and immune (Imm) sera of anti-ZmUFD1, anti-ZmCDC48, or anti-ZmHRD1 antibodies. Full length endogenous proteins migrated at different molecular weight positions when compared to truncated recombinant proteins.

Figure 2. Analysis of ZmCDC48 and ZmHRD1. **A**. Comparison of ZmCDC48 and ZmHRD1 in protein body fractions of normal (+) and mutant endosperm. Equal amounts of total protein (20 μg) from isolated protein body fractions of normal and mutant endosperms were resolved by SDS-PAGE and subjected to immunoblotting with anti-ZmCDC48 and anti-ZmHRD antibodies. A duplicate blot probed for BiP was used as an ER stress control. A duplicate blot probed for ZmRAMP4 was used as a protein loading comparison. **B**. Semi-quantitative RT-PCR analysis of several putative ERAD components in maize endosperm. Complementary DNA (cDNA) was synthesized from total RNA of normal and mutant endosperm harvested at 18 DAP. The 18S rRNA (18S) was used as an amplification control. PCR samples were analyzed with DNA gel electrophoresis and visualized on a 1% (w/v) agarose gel stained with ethidium bromide.

A

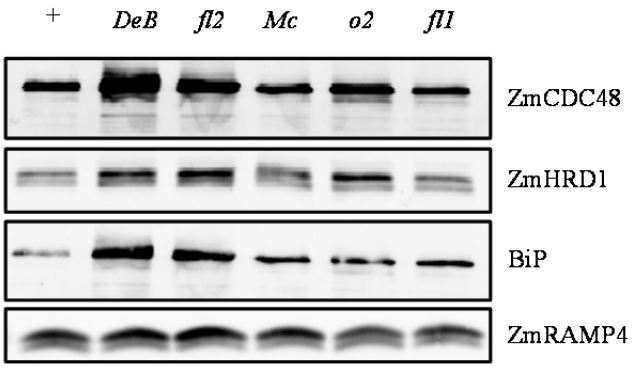
+
DeB
fl2
Mc
o2
fl1
ZmCDC48
ZmHRD1
BiP
ZmRAMP4

B

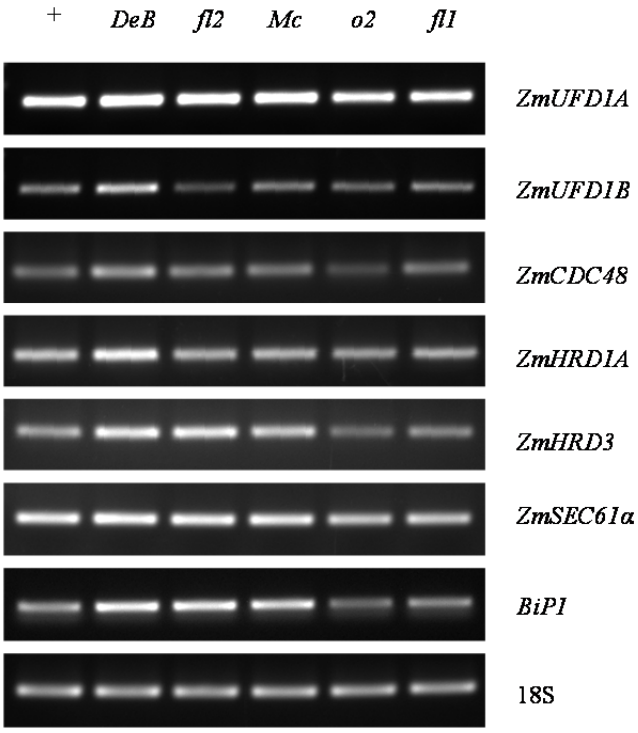
+
DeB
fl2
Mc
o2
fl1
ZmUFD1A
ZmUFD1B
ZmCDC48
ZmHRD1A
ZmHRD3
ZmSEC61α
BiP1
18S

Figure 3. Comparison of membrane bound ZmCDC48 and ZmHRD1 in protein body fractions from *De*-B30* and *fl2* gene dosage endosperm. A. Equal amounts of protein (20 μg) from isolated protein body fractions in normal and mutant endosperm were analyzed by SDS-PAGE and immunoblotting with anti-ZmCDC48 and anti-ZmHRD1 antibodies. B. Equal amounts of protein (20 μg) from non-protein body membranes were separated by SDS-PAGE and analyzed by immunoblotting with anti-ZmCDC48 and anti-ZmHRD1 antibodies. Duplicate blots probed for BiP, PDI, calnexin (CNX) and calreticulin (CRT) were used as ER stress controls, and a duplicate blot probed for 22-kD α-zein was used as a loading control. An asterisk indicates the unglycosylated form of CRT.

A

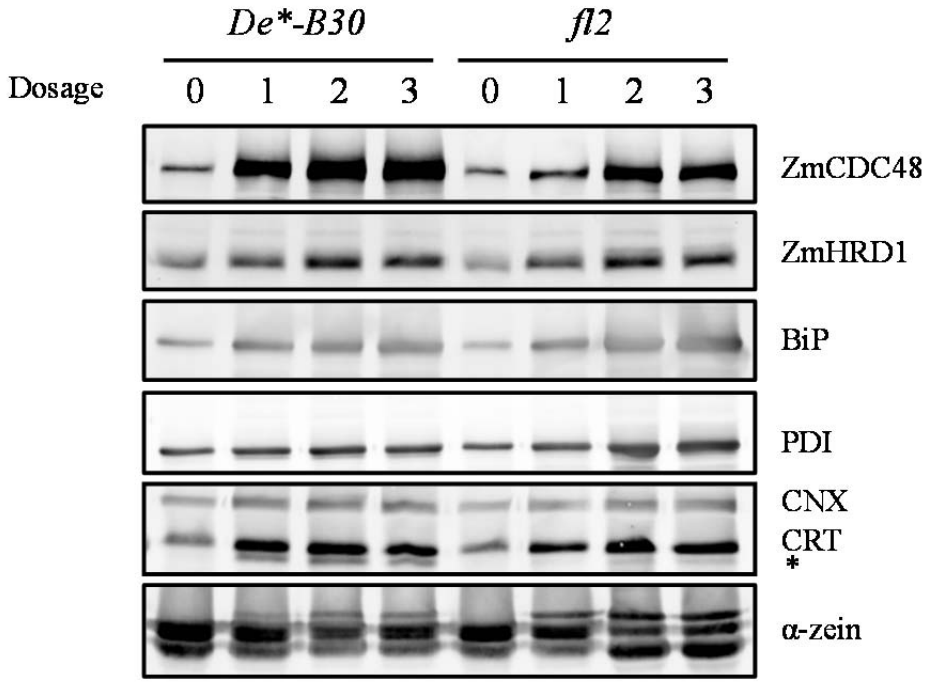
De*-B30
fl2
Dosage
0 1 2 3 0 1 2 3
ZmCDC48
ZmHRD1
BiP
PDI
CNX
CRT
*
α-zein

B

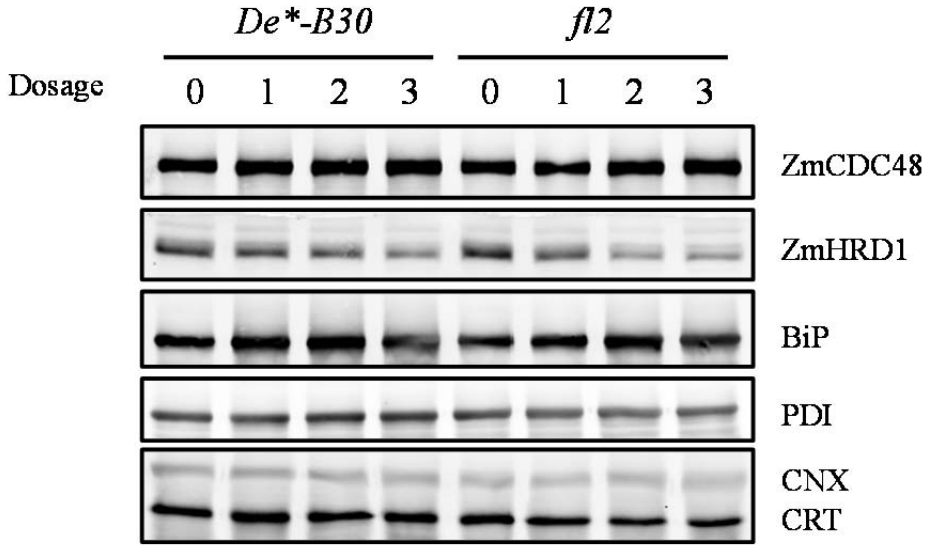
De*-B30
fl2
Dosage
0 1 2 3 0 1 2 3
ZmCDC48
ZmHRD1
BiP
PDI
CNX
CRT

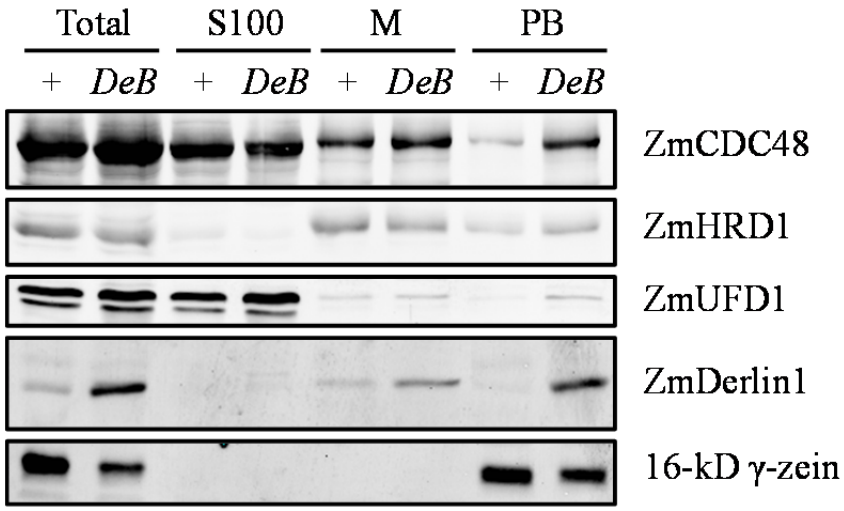

Figure 4. Comparison of ZmCDC48, ZmHRD1, and ZmUFD1 in an unfractionated aqueous extract (total) and the subcellular fractions of normal and *De*-B30* endosperm tissue. S100, non-protein body membranes (M) and protein bodies (PB) from equal fresh weight equivalents of endosperm tissue (5 mg) were separated by differential centrifugation. Proteins were separated by SDS-PAGE and subjected to immunoblotting with anti-ZmCDC48, anti-ZmHRD1, or anti-ZmUFD1 antibodies. Duplicate blots probed for ZmDerlin1 and 16-kD γ-zein were used as membrane and protein body controls, respectively.

Figure 5. Analysis of ZmCDC48 and ZmHRD1 in *De*-B30* protein body fractions. Protein bodies from equal fresh weight equivalents of *De*-B30* endosperm tissue (5 mg) were subjected to buffer (50 mM Tris, pH 7.5 at 25°C) containing 1 M NaCl (I), 1% (v/v) Triton X-100 (II), 1 M NaCl and 1% (v/v) Triton X-100 (III), or 1% (w/v) SDS (IV). An untreated protein body fraction was used as the starting material (ST, lane 1). Treated samples were separated into supernatant (SP) and pellet (P) fractions by centrifugation. Proteins were resolved by SDS-PAGE and visualized by immunoblotting with anti-ZmCDC48 and anti-ZmHRD1 antibodies. A duplicate blot probed for ZmRAMP4 was used as a membrane protein control. B. Immunoblot of a proteinase K digest of protein bodies from *De*-B30* endosperm. Protein bodies (PB) from equal fresh weight equivalents of fresh *De*-B30* endosperm tissue (2 mg) were incubated with 0.75 μg proteinase K (PK) in the absence and presence of 0.5% (w/v) SDS. Digested samples (lane 3, 4) were separated by SDS-PAGE and subjected to immunoblotting with anti-ZmCDC48 and anti-ZmHRD1 antibodies. Proteinase K only (lane 1) or untreated protein bodies (lane 2) were used as negative controls. A duplicate blot was probed for BiP as an ER luminal protein control.

A

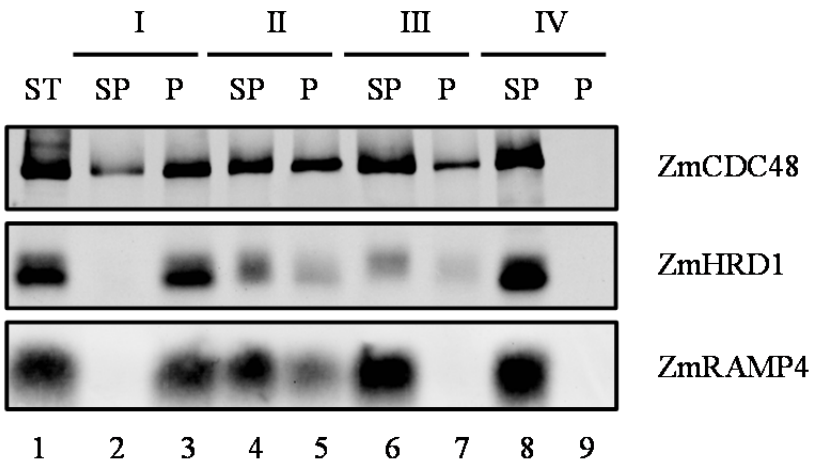
I
II
III
IV
ST
SP
P
SP
P
SP
P
SP
P
ZmCDC48
ZmHRD1
ZmRAMP4
1
2
3
4
5
6
7
8
9

B

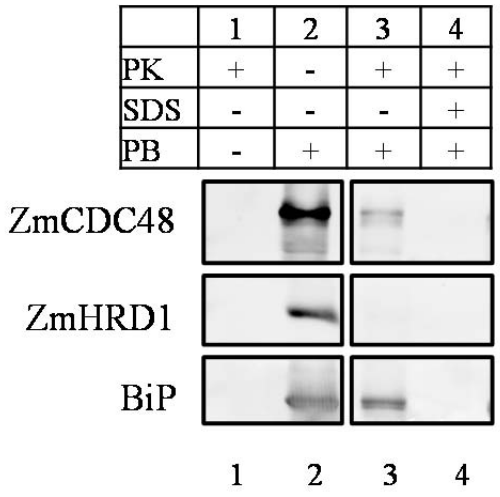
1
2
3
4
PK
+
-
+
+
SDS
-
-
-
+
PB
-
+
+
+
ZmCDC48
ZmHRD1
BiP
1
2
3
4

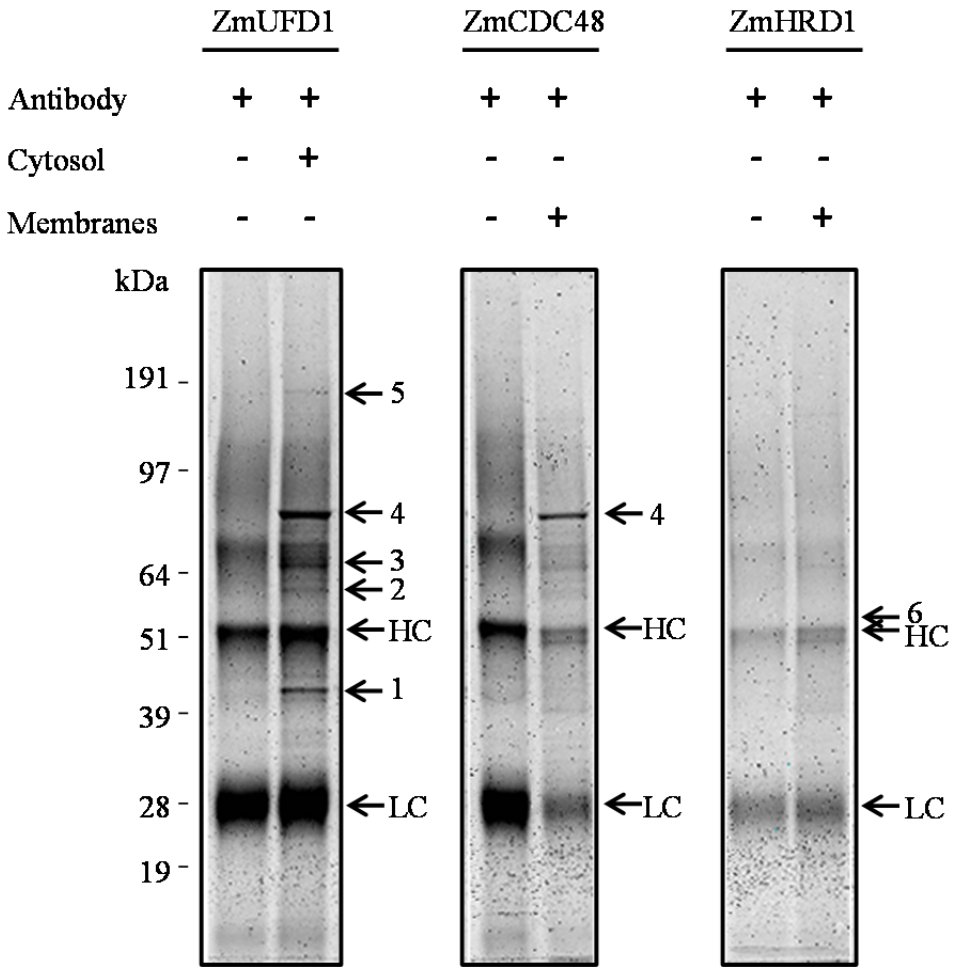

Figure 6. Colloidal Blue stained gels of immunoprecipitates. The cytosolic fraction (S100) of *De*-B30* endosperm was subjected to immunoprecipitation with anti-ZmUFD1 antibody. The solubilized total membrane fraction of *De*-B30* endosperm was subjected to immunoprecipitation with anti-ZmCDC48 or anti-ZmHRD1 antibody. Immunoprecipitates were resolved by SDS-PAGE and followed by Colloidal Blue staining. Arrows indicate the bands in which proteins were identified by mass spectrometry (Bands 1, 2, 3, 4, 5, and 6 were assigned as ZmUFD1, Chaperonin CPN60, heat shock protein 70, ZmCDC48, starch synthase DULL1, and ZmHRD1, respectively). HC and LC were assigned as heavy chains and light chains of IgG, respectively.

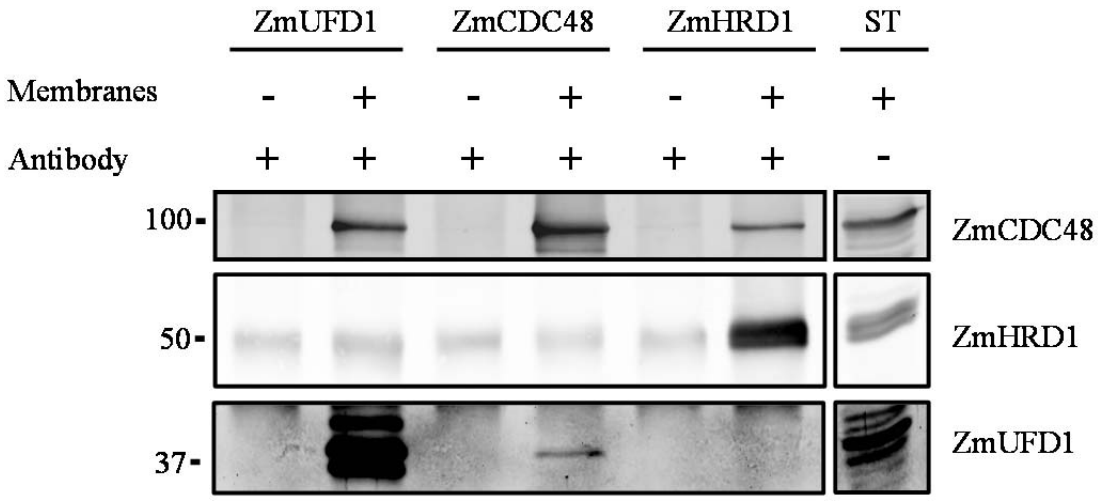

Figure 7. Immunoprecipitation of ZmUFD1, ZmCDC48 and ZmHRD1. Detergent solubilized total membranes including protein bodies from *De*-B30* endosperm were incubated with anti-ZmUFD1, anti-ZmCDC48, or anti-ZmHRD1 antibodies as noted above lanes. The starting material (ST) and immunoprecipitates were analyzed by SDS-PAGE and subject to immunoblotting with anti-ZmCDC48, anti-ZmHRD1, or anti-ZmUFD1 antibodies as noted as right.

Figure 8. Pull down assays of recombinant ZmUFD1 and ZmCDC48. GST-ZmCDC48 (A) or GST-ZmUFD1 (B) was immobilized on glutathione-Sepharose beads and incubated with His-ZmUFD1 (A) or His-ZmCDC48 (B). Excess immobilized GST was incubated with His-ZmUFD1 (A) or His-ZmCDC48 (B) and used as negative binding controls. Proteins were analyzed by SDS-PAGE followed by Coomassie Brilliant Blue staining.

A

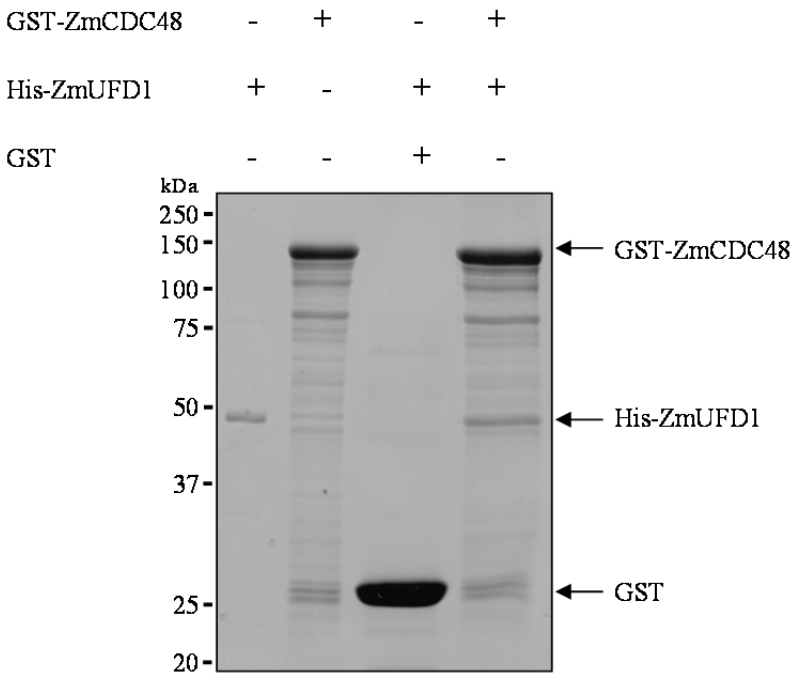
GST-ZmCDC48 - + - +
His-ZmUFD1 + - + +
GST - - + -
kDa
250
150
100
75
50
37
25
20
GST-ZmCDC48
His-ZmUFD1
GST

B

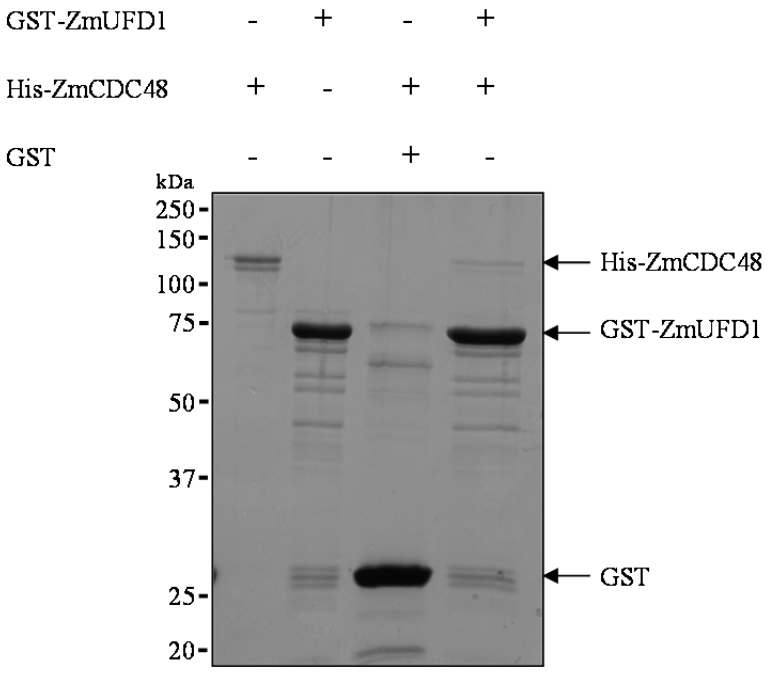
GST-ZmUFD1 - + - +
His-ZmCDC48 + - + +
GST - - + -
kDa
250
150
100
75
50
37
25
20
His-ZmCDC48
GST-ZmUFD1
GST

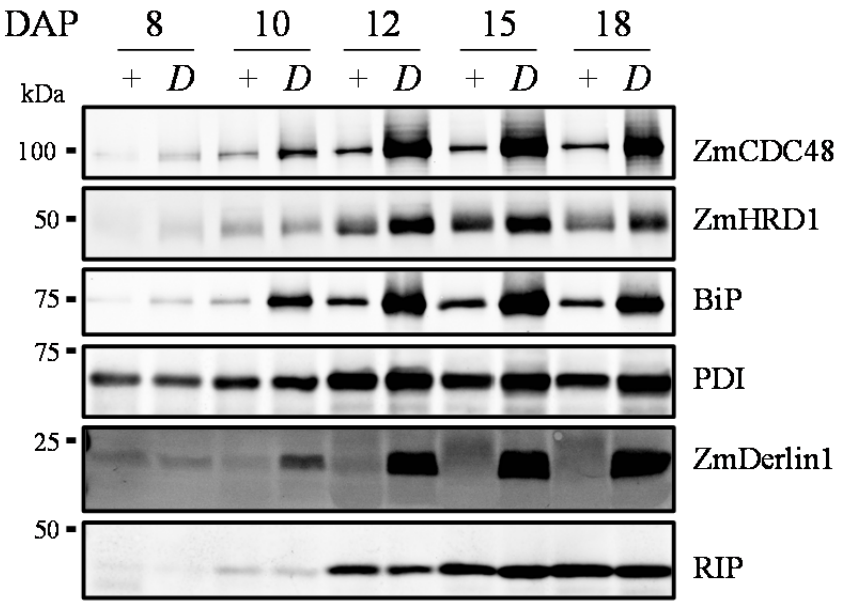

Figure 9. Analysis of ZmCDC48 and ZmHRD1 in protein body fractions during normal (+) and *De*-B30* (*D*) endosperm development. Total proteins in protein body fractions from equal fresh weight equivalents of endosperm tissue (15 mg) were analyzed by SDS-PAGE and immunoblotting with anti-ZmCDC48 and anti-ZmHRD1 antibodies. Duplicate blots probed for BiP, PDI, and ZmDerlin1 were used as ER stress controls. A duplicate blot probed for RIP was used as loading comparisons.

Supplementary Table 1. Identified peptides of ZmCDC48, ZmHRD1, and ZmUFD1

Identified peptides[a]	Accession number[b]
ZmCDC48	
ELVELPLR	AC233949.1_FGT004; GRMZM2G036765; GRMZM2G063060
AIANECQANFISVK	AC233949.1_FGT004; GRMZM2G036765; GRMZM2G063060
DTHGYVGADLAALCTEAALQCIR	AC233949.1_FGT004; GRMZM2G036765; GRMZM2G063060
EIDIGVPDEVGR	AC233949.1_FGT004; GRMZM2G036765; GRMZM2G063060
ELVELPLR	AC233949.1_FGT004; GRMZM2G036765; GRMZM2G063060
GVLFYGPPGCGK	AC233949.1_FGT004; GRMZM2G036765; GRMZM2G063060
LAGESESNLR	AC233949.1_FGT004; GRMZM2G036765; GRMZM2G063060
LDEVGYDDVGGVR	AC233949.1_FGT004; GRMZM2G036765; GRMZM2G063060
LDQLIYIPLPDEQSR	AC233949.1_FGT004; GRMZM2G036765; GRMZM2G063060
LVVDEATNDDNSVVALHPDTMER	AC233949.1_FGT004; GRMZM2G036765; GRMZM2G063060
NAPSIIFIDEIDSIAPK	AC233949.1_FGT004; GRMZM2G036765; GRMZM2G063060
PYFLEAYR	AC233949.1_FGT004; GRMZM2G036765; GRMZM2G063060
TALGTSNPSALR	AC233949.1_FGT004; GRMZM2G036765; GRMZM2G063060
VLNQLLTEMDGMNAK	AC233949.1_FGT004; GRMZM2G036765; GRMZM2G063060
YQAFAQTLQQSR	AC233949.1_FGT004; GRMZM2G036765; GRMZM2G063060
YTQGFSGADITEICQR	AC233949.1_FGT004; GRMZM2G036765; GRMZM2G063060
EDEERLDEVGYDDVGGVR	AC233949.1_FGT004; GRMZM2G036765; GRMZM2G063060
KGDLFLVR	AC233949.1_FGT004; GRMZM2G036765; GRMZM2G063060
KYQAFAQTLQQSR	AC233949.1_FGT004; GRMZM2G036765; GRMZM2G063060
TVFIIGATNRPDIIDPALLR	AC233949.1_FGT004; GRMZM2G036765; GRMZM2G063060
MKDNPEAMEEDEVDEIAEIK	GRMZM2G036765
KDYSTAILER	GRMZM2G036765; GRMZM2G063060
DYSTAILER	GRMZM2G036765; GRMZM2G063060
KDFSTAILER	AC233949.1_FGT004;
DFSTAILER	AC233949.1_FGT004;
DNPEAMEEDEVDEIAEIK	GRMZM2G036765
DNPEAMEEDEVDEIAEIR	AC233949.1_FGT004;
GILLFGPPGSGK	GRMZM2G063060
GILLYGPPGSGK	AC233949.1_FGT004; GRMZM2G036765
LGDVVSVHQCPDVK	GRMZM2G063060
LGDVVSVHQCQDVK	AC233949.1_FGT004; GRMZM2G036765
DVDLHALAK	GRMZM2G063060
DVDLNALAK	AC233949.1_FGT004; GRMZM2G036765
AHVIVMGATNRPNSIDPALR	GRMZM2G063060
SHVIVMGATNRPNSIDPALR	AC233949.1_FGT004; GRMZM2G036765
ELQETVQYPVEHPDKFEK	GRMZM2G063060
ELQETVQYPVEHPDK	GRMZM2G063060
ELQETVQYPVEHPEK	AC233949.1_FGT004; GRMZM2G036765
GFGSEFR	GRMZM2G036765; GRMZM2G063060
LAEDVNLELISK	AC233949.1_FGT004; GRMZM2G036765

Supplementary Table 1. Continued

Identified peptides[a]	Accession number[b]
ZmHRD1	
LEAAAAAASLYGR	GRMZM2G028183; GRMZM2G055643
DLENSLQK	GRMZM2G028183; GRMZM2G055643
AQENFIK	GRMZM2G028183; GRMZM2G055643
ELYETFR	GRMZM2G028183; GRMZM2G055643
VEYIETTPSVPLLSHIR	GRMZM2G028183
LNEQSWR	GRMZM2G028183
ALHWLAQK	GRMZM2G028183
APIVPADNGR	GRMZM2G028183
LNEQSWR	GRMZM2G028183
ZmUFD1	
LQPHTTDFLDISNPK	GRMZM2G037185; GRMZM2G114220
YYIDIVETK	GRMZM2G037185; GRMZM2G114220
GSTFEQTYR	GRMZM2G037185
DKDVLASSPAK	GRMZM2G037185
FIPFTGSGR	GRMZM2G037185
IIMPPSALDR	GRMZM2G037185
LVFGSGGNR	GRMZM2G037185
MYFEGYGFR	GRMZM2G037185
EPEPVKPAVPASTEPGTDVPAEEEPK	GRMZM2G037185
CYPASFIDKPQLEAGDK	GRMZM2G037185
QANATNGVQPSTATTSQGSSSR	GRMZM2G037185
CYPASFIDKPQLEAGDK	GRMZM2G037185
LASLHIEYPMLFEVHNAAAER	GRMZM2G037185
FAAFTGK	GRMZM2G037185
ANQQISAPAASGASNYSR	GRMZM2G114220
FKPFTGFGK	GRMZM2G114220
LQASEVPSTALSAPSDSNK	GRMZM2G114220
TGKLVFGSSASNNK	GRMZM2G114220
LVFGSSASNNKEPQK	GRMZM2G114220
FQAFSGK	GRMZM2G114220
APAEDGNTAVEDEPK	GRMZM2G114220

[a]Identified peptides from multiple runs.
[b]B73 filtered translation database (version 4a.53; http://www.maizesequence.org) was used. Identified peptides were assigned to one or multiple protein entities.

APPENDICES

Appendix 1: Immunolocalization of ZmCDC48 and ZmHRD1 in normal and *De*-B30* protein bodies

Abstract

Increases in ubiquitin, ZmCDC48 and ZmHRD1 were detected in *De*-B30* protein body fractions with immunoblotting. To better understand their localizations, we performed immunolocalization studies on normal and *De*-B30* protein bodies. The results showed protein body localization of ZmCDC48 and ZmHRD1. However, we were unable to localize ubiquitinated species.

Introduction

Maize major storage proteins, zeins, accumulate in endoplasmic reticulum (ER) derived organelles termed protein bodies (Larkins and Hurkman, 1978). In the presence of mutant α-zeins, the morphology of protein bodies in *De*-B30* endosperm changes from a spherical to an irregular shape (Zhang and Boston, 1992). Along with the altered structure of protein bodies, a series of ER molecular chaperones has been induced in response to the synthesis of mutant α-zeins (Boston et al., 1991; Kim et al., 2004; Houston et al., 2005). Zhang and Boston (1992) have shown that BiP was localized to the peripheral region of protein bodies and endoplasmic reticulum. We have shown an increase in ubiquitin signals associated with *De*-B30* protein body fractions by using immunoblotting (Chapter 2). In addition, we observed the increased recruitment of ZmCDC48 and induction of ZmHRD1. However, the distribution of ubiquitin signals, membrane bound ZmCDC48 and ZmHRD1 was still unclear.

In order to determine a more precise localization and better understand the function of protein body associated ERAD proteins, we performed immunolocalization studies on normal and *De*-B30* protein bodies with confocal laser scanning microscopy (CLSM) and transmission electron microscopy (TEM).

Materials and methods

Endosperm and isolated protein body fixation

Normal and *De*-B30* maize kernels were harvested at 18 days after pollination (DAP) and sectioned into 1mm thick longitudinal sections under ice-cold fixative containing 4% (w/v) paraformaldehyde and 1% (v/v) glutaraldehyde in phosphate buffer (50 mM KH_2PO_4/Na_2HPO_4, pH 7.1 at 25°C). For tissue, 1 mm^3 endosperm blocks including pericarp from the middle section opposite to the embryo were prepared as described (Zhang and Boston, 1992). For protein bodies, material was collected at the interface between 1.5 M and 2 M sucrose pads as described in Chapter 2. Endosperm blocks and isolated protein bodies were fixed in 4% (w/v) paraformaldehyde and 0.2% (v/v) glutaraldehyde in 20 mM sodium cacodylate buffer (pH 7.2 at 25°C). Both endosperm and isolated protein bodies were embedded in LR White resin according to the microwave-assisted protocol reported by Avci et al. (2008). Samples were polymerized at 60°C for 24 h in gelatin capsules.

Immunocytochemical staining

Semi-thin sections for CLSM and ultrathin sections for TEM were immunolabeled as previously described (Lending et al., 1988). After incubation in TBS-T blocking buffer

[20 mM Tris-HCl, pH 8.2 at 25°C; 500 mM NaCl and 0.3% (v/v) Tween-20] containing 1% (w/v) BSA for 1 h, sections were further incubated with antibody against 22-kD α-zein (1:50), 16-kD γ-zein (1:50), ubiquitin (1:50; FK2, Millipore, Billerica, MA), ZmCDC48 (1:50), or ZmHRD1 (1:50) in TBS-T for 2 h. For TEM, sections were incubated for 1 h in goat anti-rabbit IgG conjugated with 6 nm gold or goat anti-mouse IgG conjugated with 18 nm gold (EMS, Fort Washington, PA) at a 1:25 dilution. Grids were gently washed with TBS-T for 5 min. Sections were post-stained in 5% (w/v) uranyl acetate for 10 min and in Reynold's lead citrate for 3 min (Reynolds, 1963). Sections were examined on a JEOL 1200EX transmission electron microscope (JEOL U.S.A., Peabody, MA). For CLSM, sections were incubated for 1 h in Alexa Fluor® 568 goat anti-rabbit IgG antibody or Alexa Fluor® 488 goat anti-mouse IgG antibody (Invitrogen, Carlsbad, CA) at a 1:200 dilution. After a 5 min gentle wash in TBS-T, slides were mounted with Prolong Gold anti-fade reagent (Invitrogen, Carlsbad, CA). Images were obtained on a Zeiss LSM 710 microscope (Carl Zeiss NTS, Peabody, MA).

Results and discussion

To test whether antibodies against ubiquitin, ZmCDC48, and ZmHRD1 were suitable for immunolocalization studies, we fixed protein bodies isolated from normal and *De*-B30* endosperm harvested at 18 days after pollination (DAP) and embedded them in LR White resin. Semi-thin sections were incubated individually with these three antibodies followed by secondary antibodies labeled with fluorescent dye, and examined with CLSM. Sections incubated with antibody against 22-kD α-zein, or 16-kD γ-zein were used as positive controls.

Figure 1 shows CLSM images of immunolabeled normal and *De*-B30* protein bodies. Normal protein bodies (Figure 1, Panels A and C) had a distinct individual spherical structure. Most 22-kD α-zeins (Figure 1, Panel A) were localized to central regions of the protein bodies, and most 16-kD γ-zeins (Figure 1, Panel C) were localized to peripheral regions of the protein bodies. In contrast, *De*-B30* protein bodies (Figure 1, Panels B and D) were clumped together. ZmCDC48 (Figure 1, Panel E, normal; Figure 1, Panel F, *De*-B30*) and ZmHRD1 (Figure 1, Panel G, normal; Figure 1, Panel H, *De*-B30*) were both stained as dots that were smaller than normal or *De*-B30* protein bodies. Sections incubated with secondary antibodies only were used as negative controls. There was no visible fluorescence in the negative controls or in sections immunolabeled with antibody against ubiquitin (data not shown). These CLSM results show that antibodies against 22-kD α-zein, 16-kD γ-zein, ZmCDC48, and ZmHRD1 are suitable for immunolocalization. In addition, Figure 1, Panels E, F, G, and H show that ZmCDC48 and ZmHRD1 might be localized within protein bodies but this cannot be determined without a counterstain to allow visualization of protein bodies.

To obtain detailed subcellular localization information for ZmCDC48 and ZmHRD1, we embedded normal and *De*-B30* endosperm harvested at 18 DAP or isolated protein bodies in LR White resin. Ultra-thin sections of endosperm and isolated protein bodies were incubated with primary antibodies followed by gold conjugated secondary antibodies, and examined with TEM. Figure 2 shows micrographs of immunolabeled endosperm (Panels A-J), or isolated protein bodies (Panels K-R). Panels ending with Arabic numbers are enlarged views of box-enclosed regions in the corresponding panels. A normal protein body had a typical

light-staining central region containing α-zeins and a continuous dark-staining peripheral region containing β- and γ-zeins (Figure 2, Panel A; Lending and Larkins, 1989). However, *De*-B30* protein bodies had lobed structures with discontinuous dark-staining peripheral regions (Figure 2, Panel B; Zhang and Boston, 1992). We could not detect immunolabeled ubiquitinated species at an ultrastructural level (Figure 2, Panels A and B). In Chapter 2, we reported that starch synthesis-related enzymes were ubiquitinated in *De*-B30* endosperm at 18 DAP. Figure 2, Panel B shows that *De*-B30* protein body membranes appear to attach to amyloplast membranes. It might be possible that starch synthesis related enzymes were ubiquitinated because of the physical contact between these membranes. However, the membrane contact, while intriguing, could also be independent from the ubiquitination of starch synthesis-related enzymes.

In normal (Figure 2, Panels E, E-1, and E-2) and *De*-B30* (Figure 2, Panels F, F-1, and F-2) endosperm sections labeled with anti-22-kD α-zein antibody, 22-kD α-zeins were localized to central regions of protein bodies. In contrast, very few randomly localized gold particles were observed in normal (Figure 2, Panel C) and *De*-B30* (Figure 2, Panel D) endosperm sections that were labeled with gold conjugated secondary antibody only. In normal (Figure 2, Panels G, G-1, and G-2) and *De*-B30* (Figure 2, Panels H, H-1, and H-2) endosperm sections labeled with anti-ZmCDC48 antibody, gold particles were localized within and outside of protein bodies, as well as at membranes. Gold particles residing in protein bodies were consistent with a portion of ZmCDC48 being insensitive to detergent, salt, and proteinase K digestion in the absence of detergent (Figure 5 in Chapter 3). The portion of

ZmCDC48 localized inside protein bodies was also supported by CLSM images of normal and *De*-B30* protein bodies immunolabeled with ZmCDC48 (Figure 1, Panels E and F).

In normal (Figure 2, Panels I, I-1, and I-2) and *De*-B30* (Figure 2, Panels J, J-1, and J-2) endosperm sections labeled with anti-ZmHRD1 antibody, ZmHRD1 was localized primarily to peripheral regions and some to central regions of protein bodies. We also detected ZmHRD1 at the endoplasmic reticulum (ER; Figure 2, Panel I-1). However, we did not observe increased amounts of ZmCDC48 and ZmHRD1 associated with *De*-B30* protein bodies when compared to normal protein bodies. One explanation could be that ZmCDC48 and ZmHRD1 were forming high molecular weight oligomers as foci on protein body membranes. Since the average diameter of a mature protein body is 1 μm and the TEM section thickness is around 60-70 nm, it is not feasible to reveal their localization using TEM. Using CLSM, Aragon et al. (2009) reported that the unfolded protein response (UPR) sensor Ire1p formed high molecular weight oligomers on ER membranes as discrete foci under ER stress in yeast. In addition, we observed that increased amounts of ZmCDC48 and ZmHRD1 were present in the higher molecular weight fractions using size exclusion chromatography (J. Wu and J. Gillikin, unpublished data). However, the detection of ZmHRD1 in the protein bodies was intriguing since it is a transmembrane protein. It is possible that anti-ZmHRD1 antibody might have a low efficiency to react with ZmHRD1 and can cross react with other protein body proteins. Indeed, in the ZmHRD1 immunoprecipitation we could detect ZmHRD1 protein only by using immunoblotting (Figure 7 in Chapter 3), but not by using

Colloidal blue stain (Figure 6 in Chapter 3), although the low immunoprecipitation efficiency may be due in part to the hydrophobicity of ZmHRD1.

Isolated normal and *De*-B30* protein bodies were also immunolabeled for zeins, ZmCDC48, and ZmHRD1. Micrographs of these sections immunolabeled with ZmCDC48 (Figure 2, Panels O, O-1, and O-2, normal; Figure 2, Panels P, P-1, and P-2, *De*-B30*), and ZmHRD1 (Figure 2, Panels Q, Q-1, and Q-2, normal; Figure 2, Panels R, R-1, and R-2, *De*-B30*) show similar localization patterns as were observed with endosperm sections, except that there were more gold particles dispersed in the open spaces between protein bodies. We also observed increased amounts of clustered gold particles in open spaces between protein bodies that were immunolabeled with 22-kD α-zeins and 16-kD γ-zeins (Figure 2, Panels M, M-1, and M-2, normal; Figure 2, Panels N, N-1, and N-2, *De*-B30*). On the contrary, there were few gold particles in the background of control samples (Figure 2, Panel K, normal; Figure 2, Panel L, *De*-B30*). These clustered gold particles in the open area might be associated with protein body membranes that are dissociated from protein bodies during protein body isolation.

These results together showed protein body localization of ZmCDC48 and ZmHRD1. However, we did not detect the increased amounts of ZmCDC48 and ZmHRD1 associated with *De*-B30* protein bodies that we detected with immunoblotting. A potential explanation could be that ZmCDC48 and ZmHRD1 form higher order assemblies that have an uneven distribution around protein bodies. Membrane localization of ZmCDC48 and ZmHRD1

would be suggestive of a function in ERAD. However, we detected some gold particles within protein bodies that were labeled with anti-ZmCDC48 or anti-ZmHRD1 antibodies. These gold particles might be due to ZmCDC48 and ZmHRD1 being enclosed within protein bodies, or the cross reactivity of antibodies to storage proteins in protein bodies.

References

Avci U, Petzold HE, Ismail IO, Beers EP, Haigler CH (2008) Cysteine proteases XCP1 and XCP2 aid micro-autolysis within the intact central vacuole during xylogenesis in Arabidopsis roots. Plant J **56:** 303-315

Boston RS, Fontes EB, Shank BB, Wrobel RL (1991) Increased expression of the maize immunoglobulin binding protein homolog b-70 in three zein regulatory mutants. Plant Cell **3:** 497-505

Houston NL, Fan C, Xiang JQ, Schulze JM, Jung R, Boston RS (2005) Phylogenetic analyses identify 10 classes of the protein disulfide isomerase family in plants, including single-domain protein disulfide isomerase-related proteins. Plant Physiol **137:** 762-778

Kim CS, Hunter BG, Kraft J, Boston RS, Yans S, Jung R, Larkins BA (2004) A defective signal peptide in a 19-kD α-zein protein causes the unfolded protein response and an opaque endosperm phenotype in the maize *De*-B30* mutant. Plant Physiol **134:** 380-387

Larkins BA, Hurkman WJ (1978) Synthesis and deposition of zein in protein bodies of maize endosperm. Plant Physiol **62:** 256-263

Lending CR, Kriz AL, Larkins BA, Bracker CE (1988) Structure of maize protein bodies and immunocytochemical localization of zeins. Protoplasma **143:** 51-62

Lending CR, Larkins BA (1989) Changes in the zein composition of protein bodies during maize endosperm development. Plant Cell **1:** 1011-1023

Reynolds ES (1963) The use of lead citrate at high pH as an electron-opaque stain in electron microscopy. J Cell Biol **17:** 208-212

Zhang F, Boston RS (1992) Increases in binding protein (BiP) accompany changes in protein body morphology in three high-lysine mutants of maize. Protoplasma **171:** 142-152

Figure 1. CLSM images of immunolocalized α-zeins, γ-zeins, ZmCDC48, and ZmHRD1. Isolated normal protein bodies (Panels A, C, E, and G) or *De*-B30* protein body (Panels B, D, F, and H) at 18DAP were fixed and sectioned. Sections were incubated with anti-22-kD α-zein (Panels A and B), anti-16-kD γ-zein (Panels C and D), anti-ZmCDC48 (Panels E and F), and anti-ZmHRD1 (Panels G and H). Sections were subsequently incubated with Alexa Fluor® 568 goat anti-rabbit IgG antibody. Bar: 5 μm.

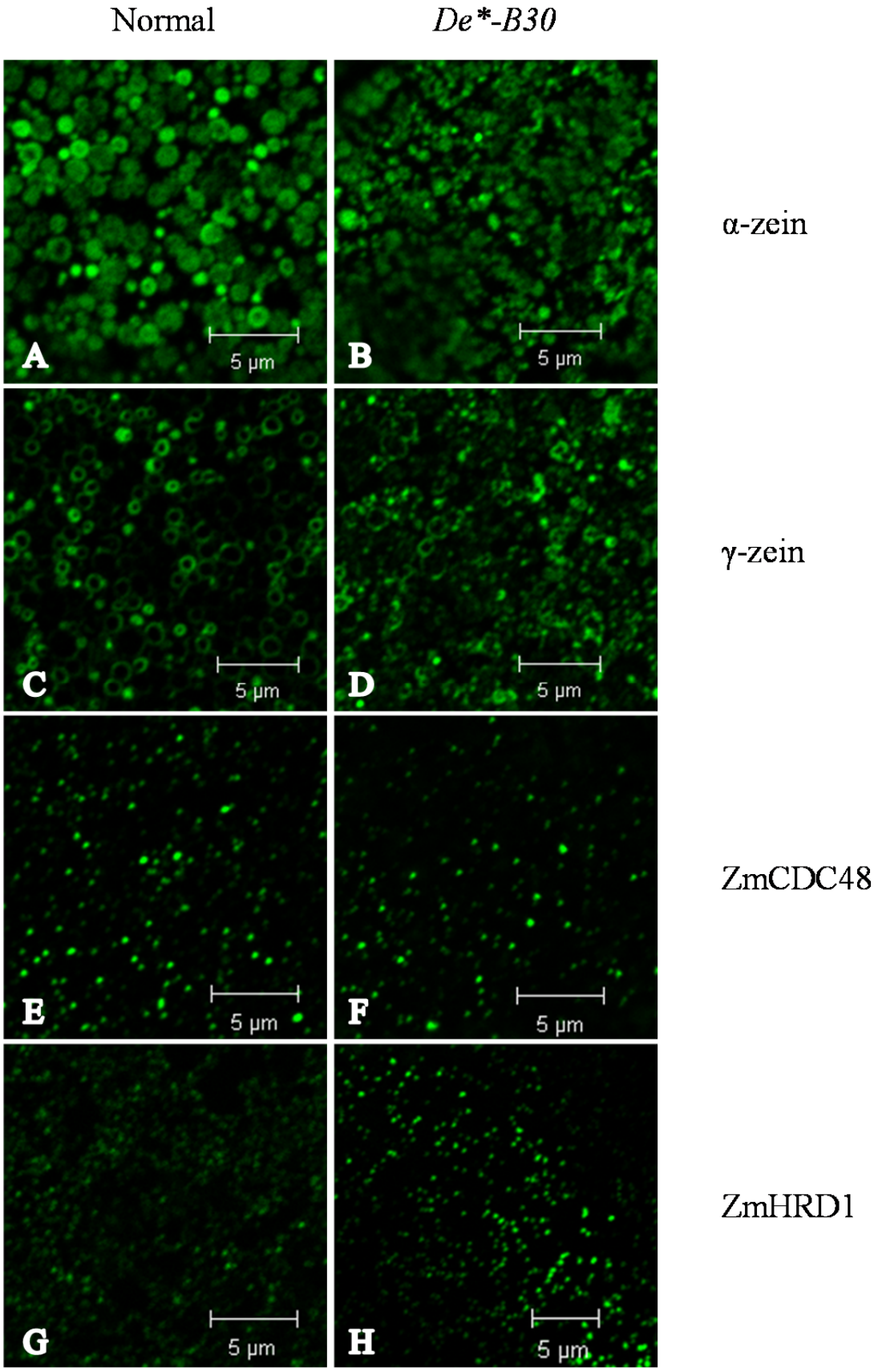
Normal
De*-B30
A
B
C
D
E
F
G
H
5 μm
α-zein
γ-zein
ZmCDC48
ZmHRD1

Figure 2. Electron micrographs of immunolocalized ubiquitinated species, zeins, ZmCDC48, and ZmHRD1. Normal endosperm (Panels A, C, E, G, and I), *De*-B30* endosperm (Panels B, D, F, H, and J), isolated normal protein bodies (Panels K, M, O, and Q), or isolated *De*-B30* protein body (Panels L, N, P, and R) at 18DAP were fixed and sectioned. Sections were incubated with anti-ubiquitin (Panels A and B), anti-22-kD α-zein (Panels E and F), a mix of anti-22-kD α-zein and anti-16-kD-γ-zein (Panels M and N), anti-ZmCDC48 (Panels G, H, O, and P), and anti-ZmHRD1 (Panels I, J, Q, and R) antibodies. Sections were subsequently incubated with goat anti-rabbit IgG conjugated with 6nm gold or goat anti-mouse IgG conjugated with 18nm gold. Sections incubated with secondary antibody alone (Panels C, D, K, and L) were used as negative controls. PB, protein body; ST, starch granule. Bar: 200 nm. Panels ending with 1 and 2 are enlarged TEM images of regions indicated by upper and lower boxes in the corresponding Panels, respectively (Bar: 50 nm). Solid arrows indicate gold particles. Open arrows indicate junctions between amyloplast and protein body membranes. Solid arrowheads indicate protein body membrane bound ribosomes.

Normal endosperm

De-B30* endosperm

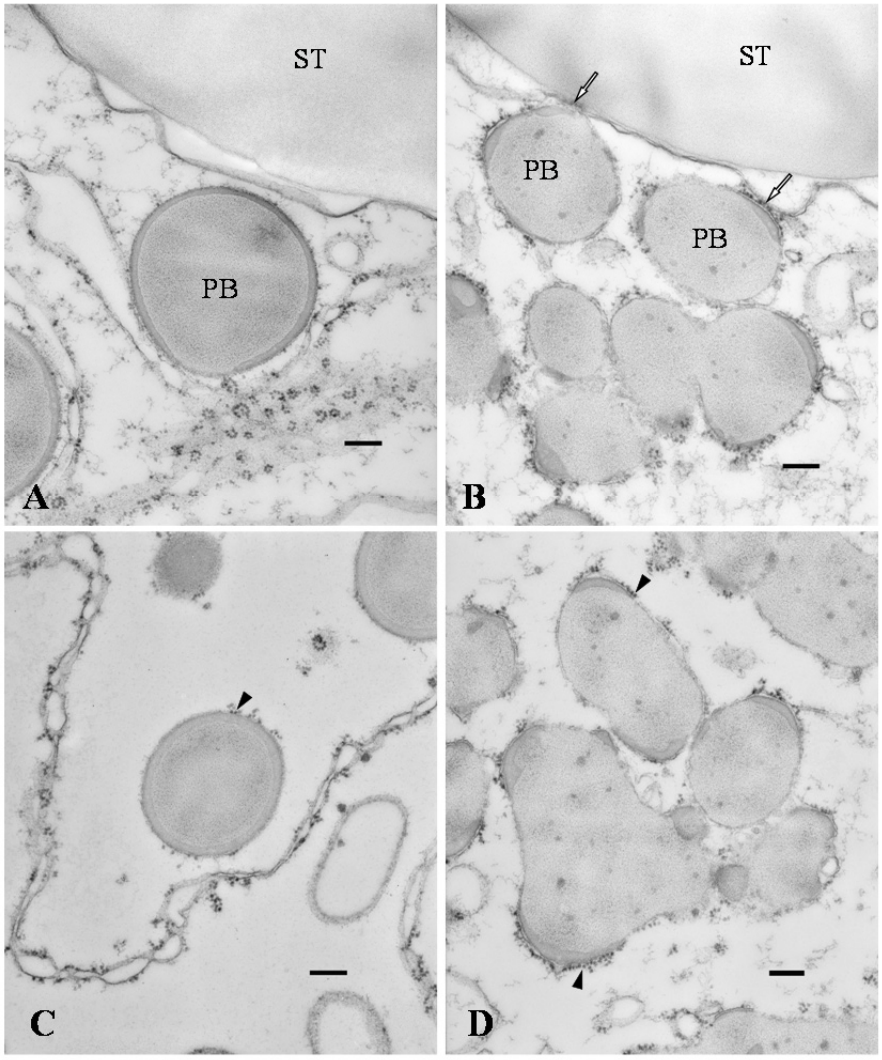

Ubiquitin

Secondary antibody only

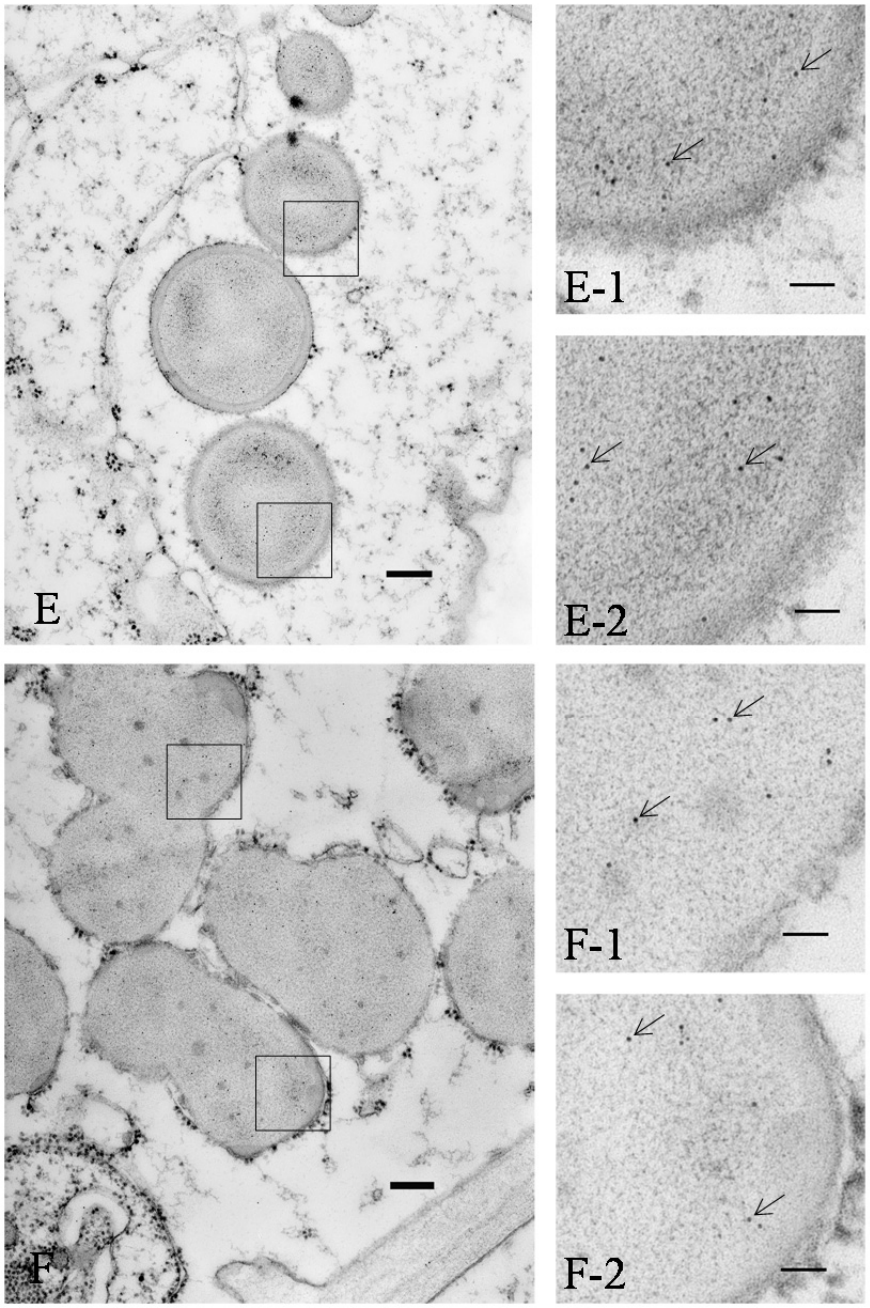
E
E-1
E-2
F
F-1
F-2
Normal endosperm
De-B30* endosperm
22-kD α-zein

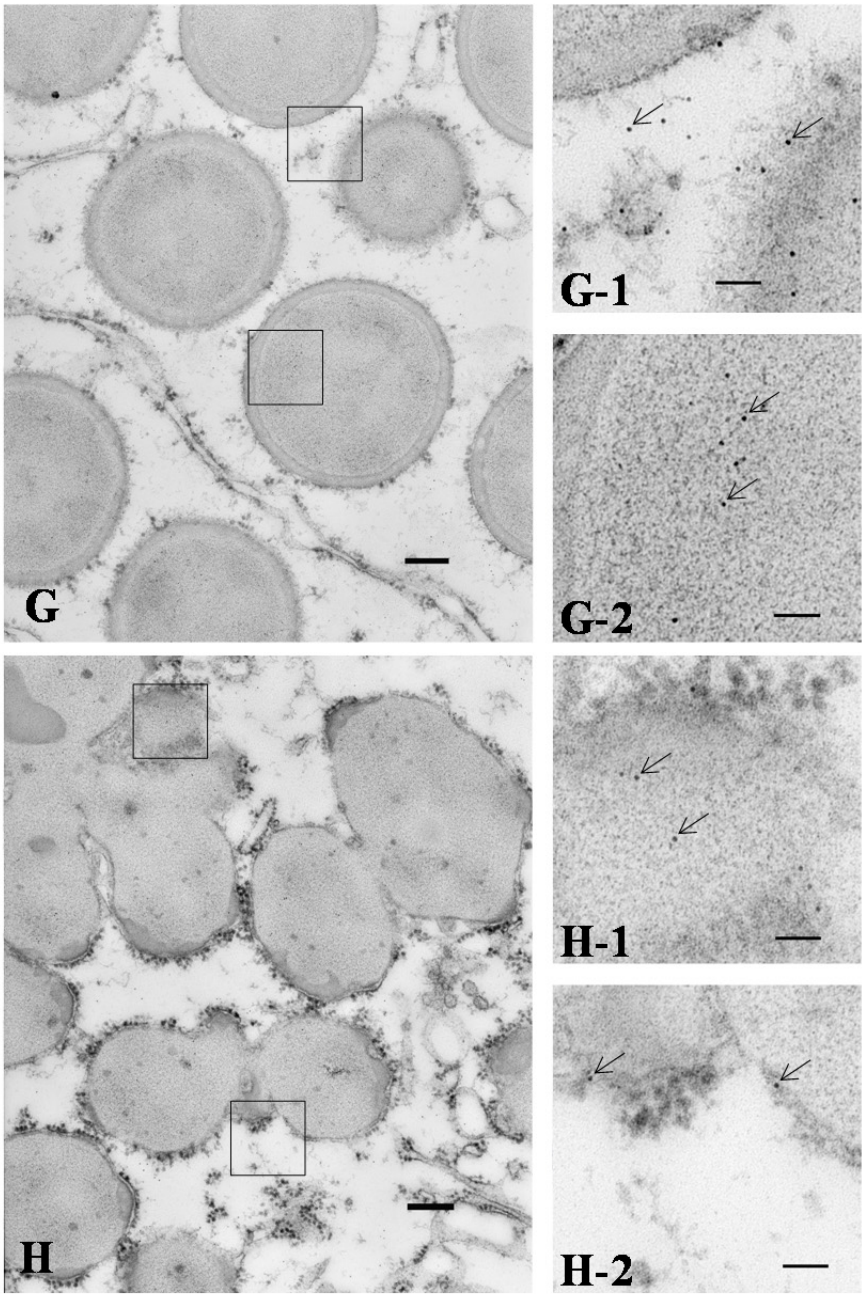

Normal endosperm

De-B30* endosperm

ZmCDC48

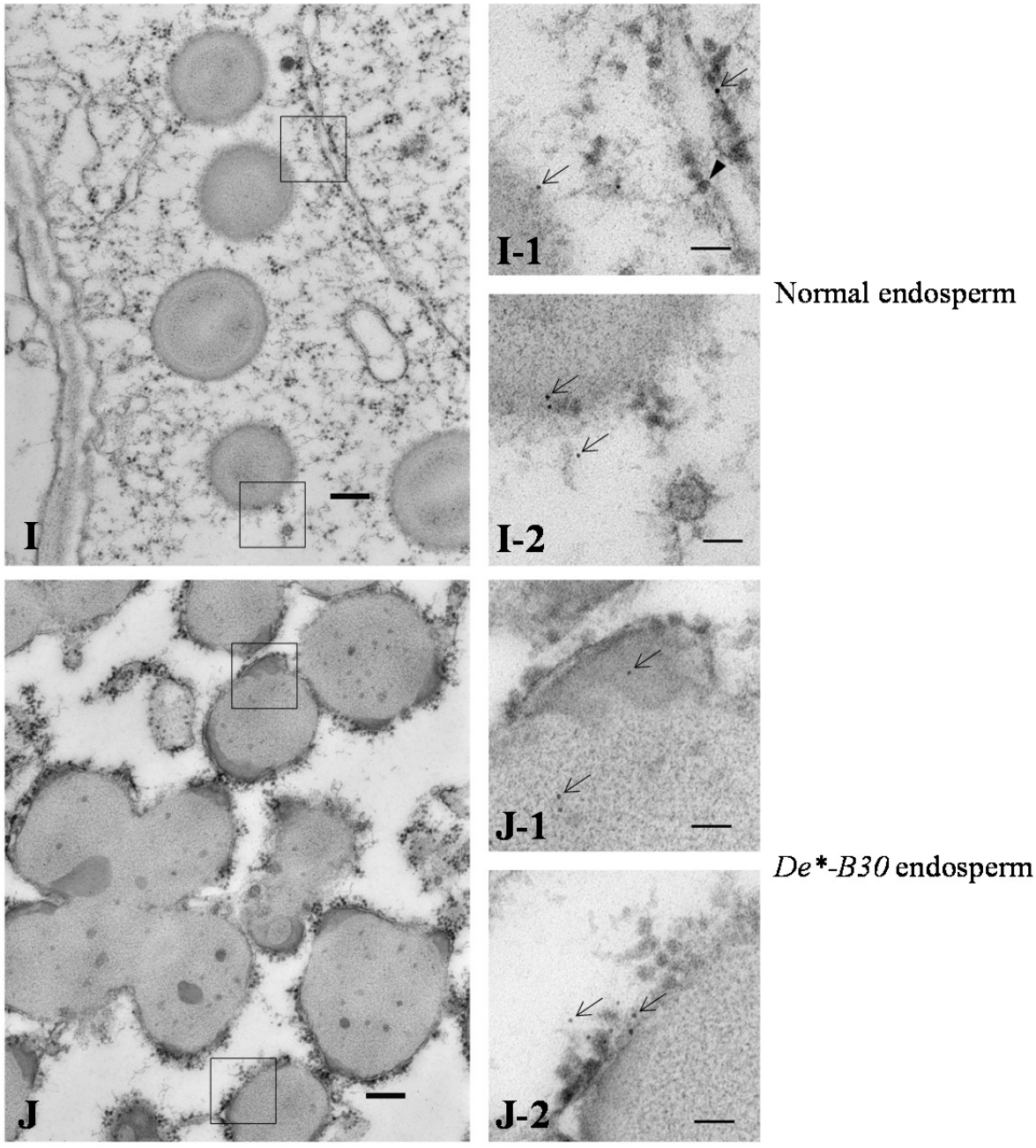
I
I-1
I-2
Normal endosperm
J
J-1
J-2
De*-B30 endosperm
ZmHRD1

Isolated Normal protein bodies

Isolated *De*-B30* protein bodies

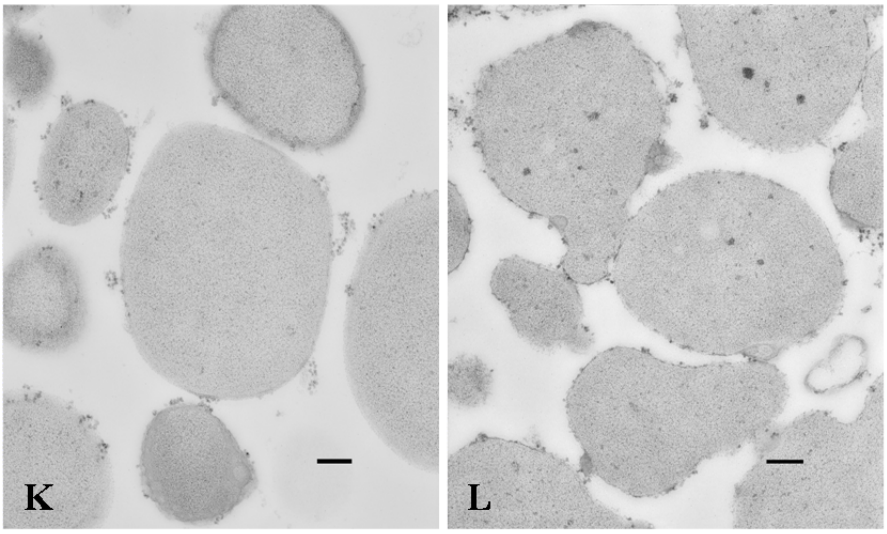

Secondary antibody only

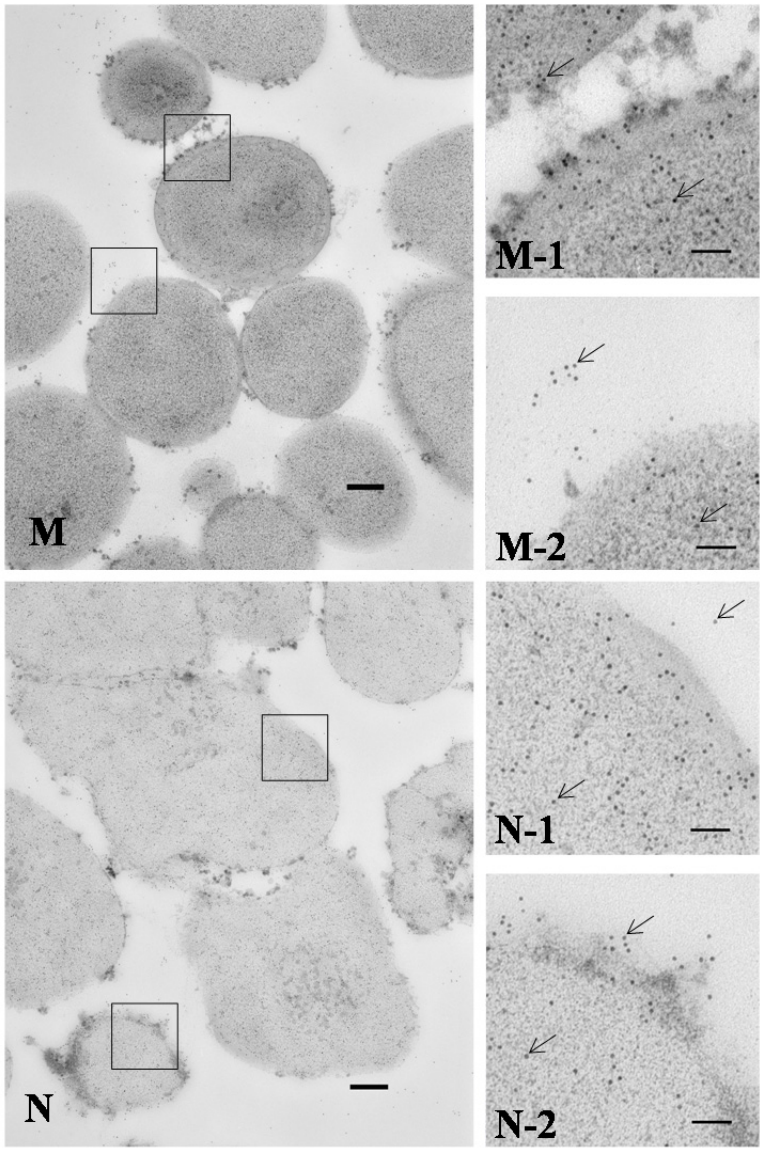

Isolated Normal protein bodies

Isolated *De*-B30* protein bodies

22-kD α-zein and 16-kD γ-zein

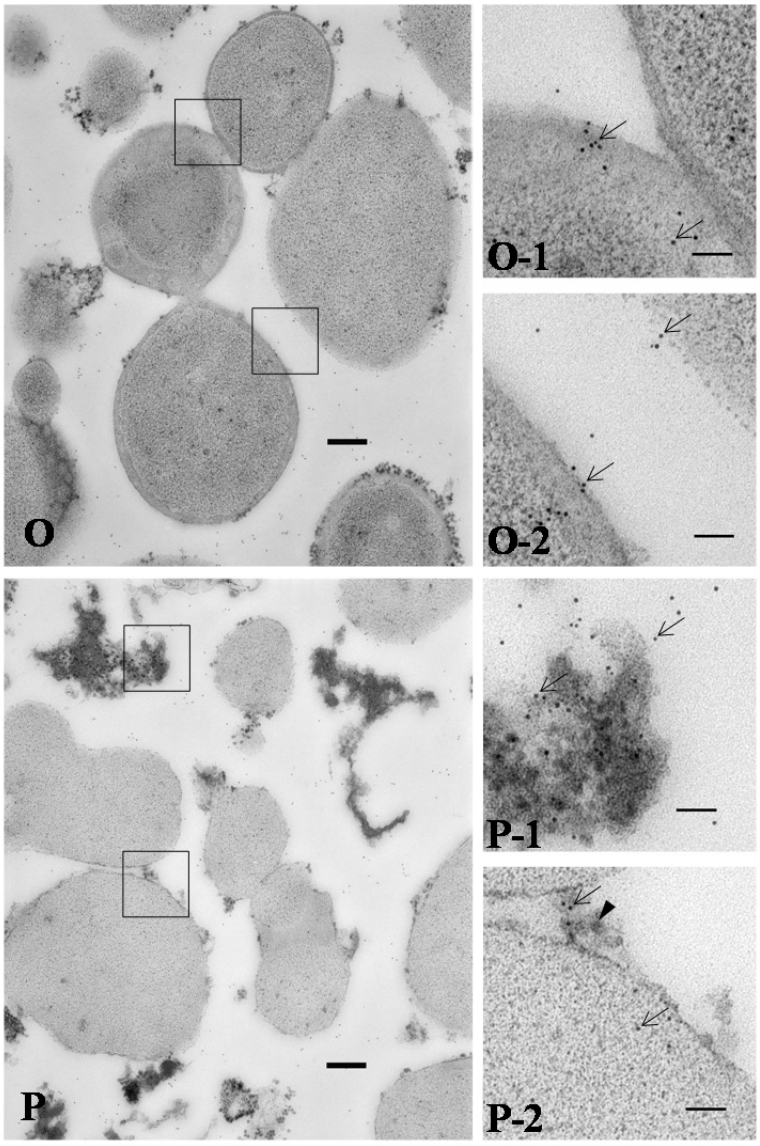

Isolated Normal protein bodies

Isolated *De*-B30* protein bodies

ZmCDC48

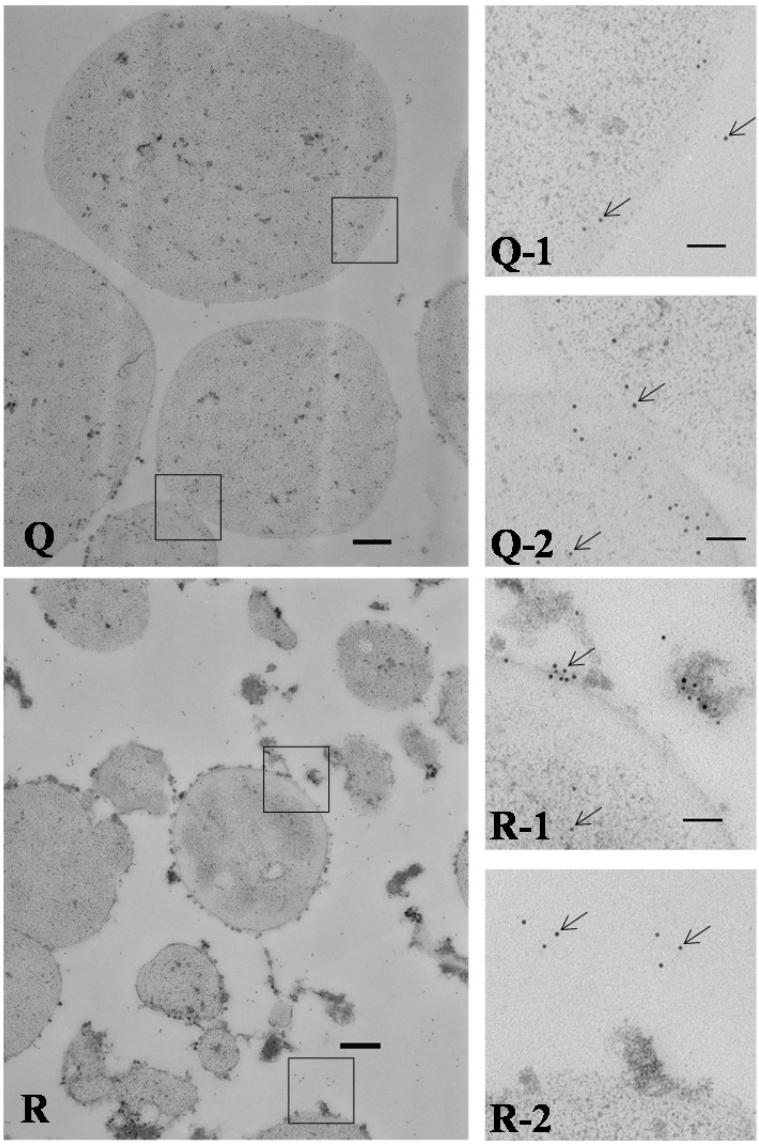

Isolated Normal protein bodies

Isolated *De*-B30* protein bodies

ZmHRD1

Appendix 2: Investigation of maize ribosome associated membrane protein 4 (RAMP4)

Abstract

Synthesis and folding of functional secretory proteins require the coordinated interaction of several multi-subunit protein complexes: ribosomes that associate with the endoplasmic reticulum (ER), the membrane translocation apparatus (also termed the translocon, or Sec61 complex), and molecular chaperones for protein folding and assembly. We have identified a group of maize homologs of RAMP4 that have been reported to interact with both membrane bound ribosomes and the translocation apparatus. Maize RAMP4 proteins (ZmRAMP4) are encoded by a small gene family with 5 different loci. We show that ZmRAMP4 proteins are tightly associated with membranes but not protein bodies. The *ZmRAMP4-2* gene was slightly induced in the *fl2* mutant. However, a similar level of ZmRAMP4 was detected between normal and *fl2* mutant maize lines. In addition, little difference in the amounts of ZmRAMP4 was observed between DMSO treated and tunicamycin treated BMS suspension cultured cells.

Introduction

Accumulation of misfolded proteins in the ER perturbs the secretory pathway and induces a cellular response called the unfolded protein response (UPR). The UPR is characterized in part by induction of molecular chaperones and reversal of protein translocation for ER associated degradation. The coordination of these cellular processes in response to ER stress requires intracellular communication. The signaling pathway varies in different organisms. In

yeast, inositol requiring enzyme 1 (Ire1p) acts alone to sense ER stress and activate the UPR when released from the ER molecular chaperone BiP (Sidrauski and Walter, 1997). In animal cells, three ER stress sensors, IRE1, activating transcription factor 6 (ATF6), and protein kinase-like endoplasmic reticulum kinase (PERK) are primarily bound to BiP under normal conditions (Bertolotti et al., 2000). Upon an increase of misfolded proteins in the ER, these three sensors are released from BiP and initiate a signal transduction cascade. Through a splicing mechanism on the transcript, IRE1 activates the expression of X box binding protein 1 (XBP1), which binds to the promoter region of ER stress response genes and induces their expression (Shen et al., 2001). ATF6 moves to the nucleus to induce ER stress related gene expression after it is proteolytically activated in the Golgi apparatus (Yoshida et al., 2001). PERK phosphorylates eukaryotic initiation factor 2α (eIF2α) that reduces general protein synthesis (Harding et al., 1999).

Plant homologs of IRE1 have been identified in Arabidopsis and rice (Koizumi et al., 2001; Noh et al., 2002; Okushima et al., 2002). In addition, the sensor domains of AtIre1-1 and AtIre1-2 can functionally substitute for the counterpart of yeast Ire1p. However, no *xbp1* mRNA, the substrate of IRE1, has been identified in plants. Two bZIP transmembrane transcription factors (At-bZIP60, At-bZIP28) in Arabidopsis have been identified as putative ER stress sensors (Iwata and Koizumi, 2005; Liu et al., 2007). Similar to ATF6 during ER stress, both At-bZIP60 and At-bZIP28 are translocated from the ER membrane to the nucleus to activate stress response gene expression, but details of their translocation are still not clear. Since there is no PERK homolog that has been identified in plants, we wanted to investigate

whether other proteins can act like PERK to regulate the protein loading into the ER during ER stress.

RAMP4 was initially reported as a transmembrane protein that associates with ribosomal proteins and the Sec61p complex (Gölich and Rapoport, 1993). Its overexpression stabilizes newly synthesized membrane proteins under ER stress by interacting with calnexin and the Sec61p complex (Yamaguchi et al., 1999), and its deletion induces ER stress and causes a noticeable phenotype in mice (Hori et al., 2006). A study from Pool (2009) further showed that RAMP4 interacts with the ribosomal protein Rpl17 and Sec61β when a transmembrane segment is synthesized. However, deletion of the *ysy6* gene, the yeast homolog of the *ramp4* gene, did not show any apparent phenotype in yeast (Hori et al., 2006), although YSY6 suppresses the protein export defect of a *secY* mutant in *E. coli* (Sakaguchi et al., 1991). The details of RAMP4 function still remain poorly understood. Two Arabidopsis RAMP4 homologs were induced when seedlings were treated with pharmacological reagents inducing ER stress (Kamauchi et al., 2005). The induction of Brassica and Arabidopsis *RAMP4* genes has also been related to cellular responses to cadmium exposure and drought stress, respectively (Minglin et al., 2005; Torres et al., 2006).

In the maize endosperm mutant *floury-2* (*fl2*), deposition of mutant storage proteins triggers the UPR to maintain protein body homeostasis. We observed a decrease of storage protein accumulation but an increase of ER chaperone accumulation in *fl2* endosperm. To understand whether maize homologs of RAMP4 respond to the mutant storage protein accumulation, we

investigated the transcript and protein levels of maize RAMP4 in normal and *fl2* mutant endosperm.

Materials and methods

Plant materials

The normal maize inbred W64A and its near isogenic mutant *fl2* were grown and pollinated at the Central Crops Research Station, Clayton, North Carolina. Whole ears harvested at 18 days after pollination (DAP) were immediately frozen in liquid nitrogen. Kernels were stored at -80°C until use.

Peptide competition assay

Peptide "PKTAKFQKNITRRGSVPETTVKKGND" was synthesized from the amino acid sequence of GRMZM2G022403_P01 (designated as ZmRAMP4-1; Table 3). Anti-ZmRAMP4 antibody (0.5 μM) was incubated with 100x (5 μM), 500x (25 μM), or 2500x (125 μM) excess of peptide "PKTAKFQKNITRRGSVPETTVKKGND" in 100μl of phosphate-buffered saline (PBS) at room temperature for 2 h. Antibody incubated with PBS only was used as a control. Non-protein body membranes (5 μg) from normal endosperm harvested at 18 DAP were separated by SDS-PAGE. Proteins were then transferred to Immobilon-FL membranes (Millipore, Billerica, MA) as previously reported (Houston et al., 2005). Membranes were immunoblotted using the mixture of anti-ZmRAMP4 antibody with or without its peptide. After extensive washes, membranes were subsequently incubated with goat anti-Rabbit IgG conjugated to DyLight® 680 (1:10,000; Thermo Scientific, Waltham,

MA). Immunoblot images were acquired with an Odyssey® infrared imaging system (Li-COR Biosciences, Lincoln, NE).

Subcellular fractionation

Subcellular fractionation was performed as described in previous chapters. Endosperm from normal and *fl2* inbred lines was dissected from frozen kernels. Equal fresh weights of endosperm were homogenized with a Pro 200 polytron (PRO Scientific, Oxford, CT) in buffer B [10 mM Tris-HCl, pH 8.5 at 25°C, 10 mM KCl, 5 mM $MgCl_2$, 7.2% (w/v) sucrose] containing protease inhibitor cocktail for plant cell and tissue extracts [1:1,000 (v/v); Sigma, St Louis, MO] at a 1:4 (w/v) grinding ratio. Crude endosperm supernatant after a 300 g centrifugation was subjected to a centrifugation at 5,000 g for 10 min. Protein bodies were obtained from the pellet. The remaining membranes were collected as the pellet after centrifugation in a TLA55 rotor (Beckman Coulter Inc., Fullerton, CA) at 100,000 g for 30 min. The supernatant remaining after the 100,000 g centrifugation was denoted as the S100. Each fraction was resuspended back to the volume of the original homogenate.

Immunoprecipitation of ZmRAMP4

For immunoprecipitation, non-protein body membranes from normal endosperm harvested at 18 DAP were solubilized in immunoprecipitation buffer [50 mM Tris-HCl, pH 8.0 at 25°C; 150 mM NaCl; 1% (v/v) IGEPAL CA 630 and 0.5% (w/v) sodium deoxycholate] for 30 min on a Nutator. The supernatant was clarified by centrifugation at 100,000 g for 30 min, and pre-cleaned by Protein A-Agarose Fast Flow (Sigma, St Louis, MO). Pre-cleaned supernatant

(2 mg) was incubated with 20 ul of anti-ZmRAMP4 antibody overnight on a Nutator at 4°C. Subsequently, Protein A-Agarose Fast Flow was incubated with the mixture for 1 h on a Nutator at 4°C. Bound proteins were eluted by SDS loading buffer. Proteins were separated by a 4-12% NuPAGE® Bis-Tris gel (Invitrogen, Carlsbad, CA). Proteins were stained with Colloidal blue according to the manufacturer's instructions (Invitrogen, Carlsbad, CA).

Semi-quantitative RT-PCR of *ZmRAMP4*

Total RNA was extracted from normal and *fl2* endosperm harvested at 18 DAP as described in Chapter 3. Complementary DNA was synthesized using Omniscript reverse transcriptase according to the manufacturer's instructions (Qiagen, Valencia, CA). One microliter of each cDNA reaction was used for PCR amplification with GO Taq polymerase (Promega, Madison, WI). Primers are listed in Table 1. PCR was performed by using a program of 95°C for 5 min, followed with 25 cycles of 95°C for 30 sec, 60°C for 30 sec, and 72°C for 1 min. PCR products were separated by DNA electrophoresis through 1% (w/v) agarose gels in Tris-acetate-EDTA (TAE) buffer containing 0.04 M Tris-acetate, 0.001 M EDTA. Images were taken with a Gel Logic 100 Imaging System (Kodak, Rochester, NY). All genes were amplified with 25 cycles, except *BiP* and *catalase1* which were amplified with 20 cycles.

Tunicamycin treatment of BMS suspension cultured cells

BMS suspension cultured cells were grown in liquid media containing 1x MS salts, 10 mg/l thiamine-HCl, 100 mg/l myo-inositol, 1.16 g/l L-proline, 1 g/l casein hydrolysate, 3 mg/l 2, 4-D, and 30 g/l sucrose at pH 5.8. Five milliliters of culture were sub-cultured into 45 ml

of fresh liquid media every 10 days. Culture was grown on a horizontal shaker with 150 rpm at 25°C. BMS suspension cultured cells were treated with tunicamycin (10 μg/ml; Calbiochem, San Diego, CA) at 6 days after passage. Cells treated with an equal volume of DMSO were used as negative controls. Equal volumes of culture (10 ml) were harvested at 8, 12, and 24 h after adding tunicamycin or DMSO. Cells were collected on filter paper (Whatman no.1) using a water aspirator. After being immediately frozen in liquid N_2, collected cells were ground in liquid N_2 and stored at -80°C until use. Cells were mixed with 2x SDS loading buffer at a 1:4 (w/v) ratio. After being incubated at 60°C for 1 h, the mixture was centrifuged at 1,000 g for 5 min. Twenty microliters of the supernatant were diluted with 2x SDS loading buffer to a final volume of 100 μl. Subsequently, 5 μl of the diluted sample was separated by SDS-PAGE and probed for BiP, calnexin and calreticulin, S6 ribosomal protein, and ZmRAMP4.

Results and discussion

Antibody production

The oligopeptide "PKTAKFQKNITRRGSVPETTVKKGND" from amino acid sequence GRMZM2G022403_P01 (designated as ZmRAMP4-1; Table 3) was used for anti-ZmRAMP4 antibody production. The anti-ZmRAMP4 antibody recognizes multiple bands on the immunoblot of non-protein body membranes from normal maize endosperm extract. In order to identify which band is specific to the antibody, we immunoblotted duplicated blots with anti-ZmRAMP4 antibody mixed with excess peptides that were used to generate the antibody. Figure 1 shows that a doublet close to 10 kDa gradually disappeared with

increasing amounts of peptides. These results are suggestive that anti-RAMP4 antibody can recognize endogenous ZmRAMP4 proteins in non-protein body membrane fractions.

In addition, we used the antibody to immunoprecipitate ZmRAMP4 from solubilized non-protein body membranes. Figure 2 shows the immunoprecipitated ZmRAMP4 doublet stained with Colloidal blue. The doublet was excised and proteins were digested by trypsin and identified using mass spectrometry analysis. Table 2 shows the identified peptides. The peptide competition assay and identified ZmRAMP4 peptides show that anti-ZmRAMP4 antibody can recognize and immunoprecipitate endogenous ZmRAMP4.

ZmRAMP4 expression and sub-cellular distribution in normal and *fl2* endosperm

RAMP4 contains a single transmembrane domain, and belongs to the group of tail-anchored proteins that are inserted into the membrane after their synthesis (Rabu et al., 2009). To understand how the ZmRAMP4 proteins are distributed in the cells, and whether ZmRAMP4 proteins are induced under ER stress, we separated total endosperm aqueous extracts from normal and *fl2* endosperm into S100, non-protein body membranes, and protein body fractions. Proteins were separated by SDS-PAGE and visualized by immunoblotting with anti-S6 and anti-ZmRAMP4 antibodies. Figure 3 shows that ZmRAMP4 had a similar protein expression level in normal and *fl2* endosperm. In addition, ZmRAMP4 proteins were primarily localized in the membrane fractions, including non-protein body membranes, and protein body fractions. We also detected a small amount of ZmRAMP4 in the S100 fraction

that contains most of the cytosolic proteins. These results are consistent with ZmRAMP4 proteins being predicted as tail-anchored proteins.

ZmRAMP4 gene expression in normal and *fl2* endosperm

To determine how many *ZmRAMP4* genes are present in the maize genome, we performed a homology search against the maize B73 transcript database. Six different transcripts were found and can be mapped to five different loci (Table 3). Two of the six transcripts (GRMZM2G110044_T01 and GRMZM2G110044_T02) were splicing variants from the same locus. To determine whether *ZmRAMP4* genes are induced under ER stress, we performed semi-quantitative RT-PCR assays using synthesized cDNA from normal and *fl2* endosperm harvested at 18 DAP (Figure 4). Maize *BiP1* and *catalase1* (*CAT1*) genes were used as ER stress and amplification controls, respectively. Surprisingly, the transcript levels of the *ZmRAMP4* genes varied a lot, with *ZmRAMP4-1* as the most abundant and *ZmRAMP4-6* transcript being undetectable in the endosperm tissue. All of the detected *ZmRAMP4* genes were expressed at the same level between normal and *fl2* endosperm, except for the *ZmRAMP4-2* gene that was slightly induced in *fl2* endosperm. To understand the different gene expression patterns, we searched 2 kb upstream promoter regions of all *ZmRAMP4* genes for *cis*-acting elements. We identified 2 plant UPR *cis*-acting elements in the promoter region of the *ZmRAMP4-2* gene (CCatgtcagcctggCCACG and cgccagCCACGTCAcccg). These two elements have been reported in the promoter regions of many Arabidopsis UPR genes (Martinez and Chrispeels, 2003). These results are suggestive that only *ZmRAMP4-2* was induced under ER stress. The expression levels of the other four detected *ZmRAMP4*

transcripts were consistent with the observation of no increased ZmRAMP4 accumulation in *fl2* endosperm when compared to that of normal endosperm.

ZmRAMP4 expression in tunicamycin treated BMS suspension cultured cells

Because we observed a similar expression of ZmRAMP4 between normal and *fl2* endosperm, we further tested if ZmRAMP4 can be induced under ER stress with the pharmacological reagent, tunicamycin, that specifically inhibits *N*-linked glycosylation. BMS suspension cultured cells were collected at different time points after tunicamycin treatment. Cells treated with DMSO were used as negative controls. Figure 5 shows total protein extract from BMS suspension cultured cells probed for ER molecular chaperones and ZmRAMP4 with immunoblot analysis. In tunicamycin treated samples, BiP and calnexin were induced from 8 h to 24 h after tunicamycin was added. In addition, an unglycosylated form of calreticulin appeared at 8 h and kept accumulating to 24 h. However, ZmRAMP4 showed similar protein levels from 0 h to 24 h after tunicamycin treatment. In line with unchanged ZmRAMP4 expression in normal and *fl2* endosperm, these results showed that the total protein level of ZmRAMP4 does not change under ER stress.

Conclusion

Previous reports suggested that RAMP4 is involved in the interaction between membrane bound ribosomes and the translocon (Gölich and Rapoport, 1993; Yamaguchi et al., 1999; Pool, 2009). However, only one of five detectable *ZmRAMP4* transcripts was slightly induced in *fl2* endosperm, and the total protein level of ZmRAMP4 was similar between

normal and *fl2* endosperm. It is possible that all six ZmRAMP4 proteins have redundant functions because of their highly conserved sequences.

References

Bertolotti A, Zhang Y, Hendershot LM, Harding HP, Ron D (2000) Dynamic interaction of BiP and ER stress transducers in the unfolded-protein response. Nat Cell Biol **2:** 326-332

Gölich D, Rapoport TA (1993) Protein translocation into proteoliposomes reconstituted from purified components of the endoplasmic reticulum membrane. Cell **75:** 615-630

Harding HP, Zhang Y, Ron D (1999) Protein translation and folding are coupled by an endoplasmic-reticulum-resident kinase. Nature **397:** 271-274

Hori O, Miyazaki M, Tamatani T, Ozawa K, Takano K, Okabe M, Ikawa M, Hartmann E, Mai P, Stern DM, Kitao Y, Ogawa S (2006) Deletion of SERP1/RAMP4, a component of the endoplasmic reticulum (ER) translocation sites, leads to ER stress. Mol Cell Biol **26:** 4257-4267

Houston NL, Fan C, Xiang JQ, Schulze JM, Jung R, Boston RS (2005) Phylogenetic analyses identify 10 classes of the protein disulfide isomerase family in plants, including single-domain protein disulfide isomerase-related proteins. Plant Physiol **137:** 762-778

Iwata Y, Koizumi N (2005) An Arabidopsis transcription factor, AtbZIP60, regulates the endoplasmic reticulum stress response in a manner unique to plants. Proc Natl Acad Sci USA **102:** 5280-5285

Kamauchi S, Nakatani H, Nakano C, Urade R (2005) Gene expression in response to endoplasmic reticulum stress in *Arabidopsis thaliana*. FEBS J **272:** 3461-3476

Koizumi N, Martinez IM, Kimata Y, Kohno K, Sano H, Chrispeels MJ (2001) Molecular characterization of two Arabidopsis Ire1 homologs, endoplasmic reticulum-located transmembrane protein kinases. Plant Physiol **127:** 949-962

Liu JX, Srivastava R, Che P, Howell SH (2007) An endoplasmic reticulum stress response in Arabidopsis is mediated by proteolytic processing and nuclear relocation of a membrane-associated transcription factor, bZIP28. Plant Cell **19:** 4111-4119

Martinez IM, Chrispeels MJ (2003) Genomic analysis of the unfolded protein response in Arabidopsis shows its connection to important cellular processes. Plant Cell **15:** 561-576

Minglin L, Yuxiu Z, Tuanyao C (2005) Identification of genes up-regulated in response to Cd exposure in *Brassica juncea* L. Gene **363:** 151-158

Noh SJ, Kwon CS, Chung WI (2002) Characterization of two homologs of Ire1p, a kinase/endoribonuclease in yeast, in *Arabidopsis thaliana*. Biochim Biophys Acta **1575:** 130-134

Okushima Y, Koizumi N, Yamaguchi Y, Kimata Y, Kohno K, Sano H (2002) Isolation and characterization of a putative transducer of endoplasmic reticulum stress in *Oryza sativa*. Plant Cell Physiol **43:** 532-539

Pool MR (2009) A trans-membrane segment inside the ribosome exit tunnel triggers RAMP4 recruitment to the Sec61p translocase. J Cell Biol **185:** 889-902

Rabu C, Schmid V, Schwappach B, High S (2009) Biogenesis of tail-anchored proteins: the beginning for the end? J Cell Sci **122:** 3605-3612

Sakaguchi M, Ueguchi C, Ito K, Omura T (1991) Yeast gene which suppresses the defect in protein export of a *secY* mutant of *E. coli*. J Biochem **109:** 799-802

Shen X, Ellis RE, Lee K, Liu CY, Yang K, Solomon A, Yoshida H, Morimoto R, Kurnit DM, Mori K (2001) Complementary signaling pathways regulate the unfolded protein response and are required for *C. elegans* development. Cell **107:** 893-903

Sidrauski C, Walter P (1997) The transmembrane kinase Ire1p is a site-specific endonuclease that initiates mRNA splicing in the unfolded protein response. Cell **90:** 1031-1039

Torres GAM, Pflieger S, Corre-Menguy F, Mazubert C, Hartmann C, Lelandais-Briere C (2006) Identification of novel drought-related mRNAs in common bean roots by differential display RT-PCR. Plant Science **171:** 300-307

Yamaguchi A, Hori O, Stern DM, Hartmann E, Ogawa S, Tohyama M (1999) Stress-associated endoplasmic reticulum protein 1 (SERP1)/Ribosome-associated membrane protein 4 (RAMP4) stabilizes membrane proteins during stress and facilitates subsequent glycosylation. J Cell Biol **147:** 1195-1204

Yoshida H, Matsui T, Yamamoto A, Okada T, Mori K (2001) XBP1 mRNA is induced by ATF6 and spliced by IRE1 in response to ER stress to produce a highly active transcription factor. Cell **107:** 881-891

Table 1. Oligonucleotides for semi-quantitative RT-PCR

Name	Sequence (5'-3')	Target gene	Gene ID[a]
CAT1_F	GTCCAGACACCTGTTATTGTCCGT	*CAT-1*	GRMZM2G433801
CAT1_R	GAGGAAGGTGAACATGTGTAGGCT	*CAT-1*	GRMZM2G433801
ZmR4_1_F	TCCGGCGATCTCGCTCA	*ZmRAMP4-1*	GRMZM2G022403
ZmR4_1_R	GGCCCACCAAATGAACG	*ZmRAMP4-1*	GRMZM2G022403
ZmR4_2_F	GCACGCGGATATGACTACT	*ZmRAMP4-2*	GRMZM2G060856
ZmR4_2_R	AGATTAAGGTTTCTCCCATACTC	*ZmRAMP4-2*	GRMZM2G060856
ZmR4_3_F	GCGTCAATCGCCATGACTACC	*ZmRAMP4-3*	GRMZM2G110044
ZmR4_3_R	GTCAACCCTGTTCCTCGACTTTAGAGTG	*ZmRAMP4-3*	GRMZM2G110044
ZmR4_4_F	CCGAGCGCAATCACCGTC	*ZmRAMP4-4*	GRMZM2G156246
ZmR4_4_R	GCGAAAGATTACCAAATTACTCGATAAAT	*ZmRAMP4-4*	GRMZM2G156246
ZmR4_5_F	AAACAAACGGGCCTTAGGGAAAT	*ZmRAMP4-5*	GRMZM2G110044
ZmR4_5_R	CGTATTCCCTGTCAGCTAAGTGACTTAA	*ZmRAMP4-5*	GRMZM2G110044

[a]B73 database (version 4a.53; http://www.maizesequence.org) was used.

Table 2. Identified peptides of ZmRAMP4

Gene	Protein ID[a]	Identified peptide sequence	# of identified peptides	Position on gel
ZmRAMP4-1	GRMZM2G022403_P01	GSVPETTVK	1	lower band
ZmRAMP4-2	GRMZM2G060856_P01	GSVPETTVK	1	lower band
ZmRAMP4-3	GRMZM2G110044_P01	TASNAGLF	1	upper band
ZmRAMP4-4	GRMZM2G156246_P02	TASNAGLF	1	upper band
ZmRAMP4-5	GRMZM2G110044_P02	TASNAGLF	2	upper band
		GSVPETVK		

[a]B73 database (version 4a.53; http://www.maizesequence.org) was used.

Table 3. *ZmRAMP4* gene family

Gene Name	**Transcript ID**[a]	**Protein ID**[a]	**Chromosome**
ZmRAMP4-1	GRMZM2G022403_T01	GRMZM2G022403_P01	II
ZmRAMP4-2	GRMZM2G060856_T01	GRMZM2G060856_P01	VI
ZmRAMP4-3	GRMZM2G110044_T01	GRMZM2G110044_P01	VII
ZmRAMP4-4	GRMZM2G156246_T02	GRMZM2G156246_P02	II
ZmRAMP4-5	GRMZM2G110044_T02	GRMZM2G110044_P02	VII
ZmRAMP4-6	GRMZM2G039630_T01	GRMZM2G039630_P01	IV

[a]B73 database (version 4a.53; http://www.maizesequence.org) was used.

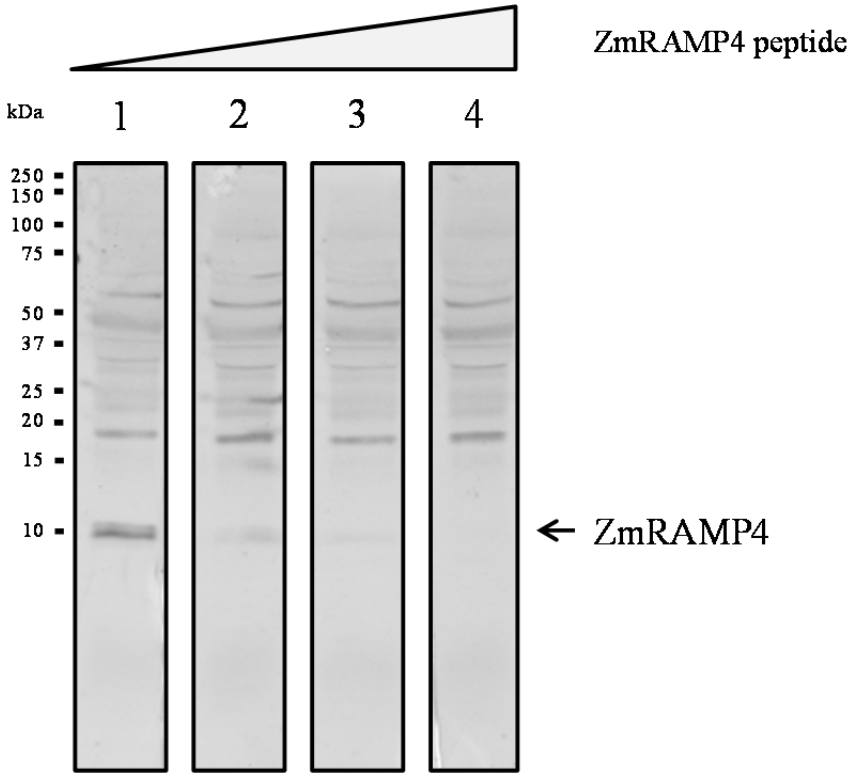

Figure 1. Peptide competition assay of ZmRAMP4. Equal amounts of total protein (5 µg) from non-protein body membranes from normal endosperm harvested at 18 DAP were separated by SDS-PAGE and immunoblotted with anti-RAMP4 antibody (lane 1), anti-RAMP4 antibody with 100x excess of peptide (lane 2), anti-RAMP4 antibody with 500x excess of peptide (lane 3), or anti-RAMP4 antibody with 2,500x excess of peptide (lane 4).

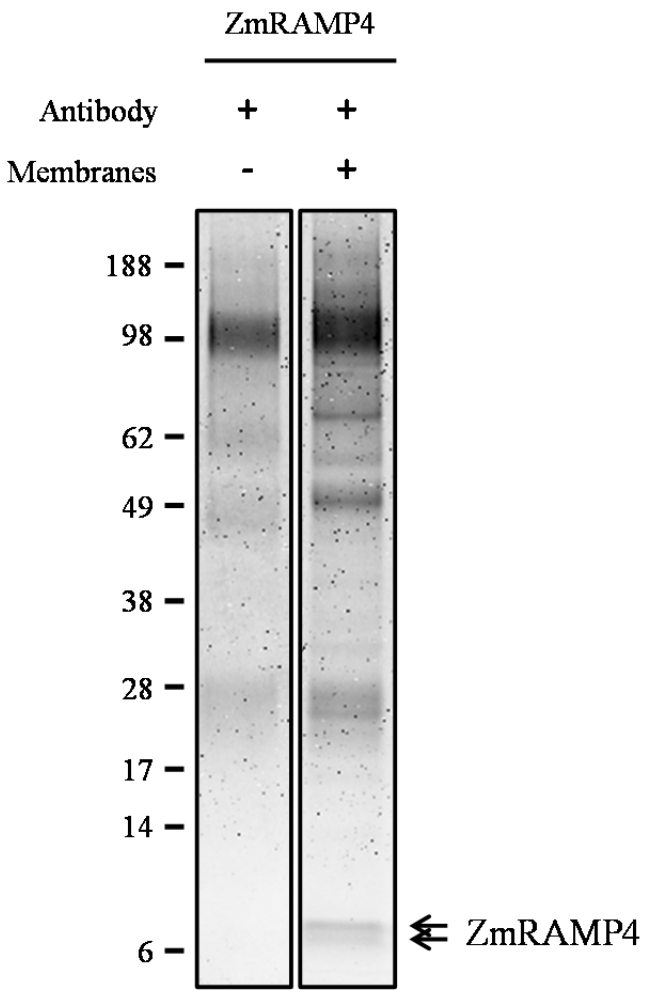

Figure 2. Analysis of ZmRAMP4 immunoprecipitates. Non-protein body membranes from normal endosperm harvested at 18 DAP were subjected to immunoprecipitation with anti-ZmRAMP4 antibody. Immunoprecipitates were separated by SDS-PAGE and visualized by Colloidal blue staining. Arrows indicate the bands in which ZmRAMP4 proteins were identified with mass spectrometry.

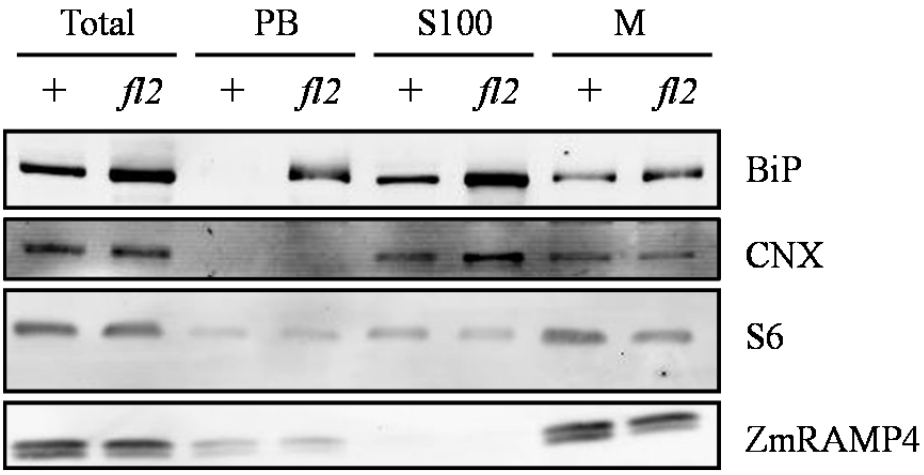

Figure 3. Comparison of ZmRAMP4 in an unfractionated aqueous extract and subcellular fractions of normal and *fl2* endosperm. An unfractionated aqueous extract (Total), S100, non-protein body membrane (M) and protein body (PB) fractions from equal fresh weight equivalents of endosperm tissues (5 mg) were separated by differential centrifugation. Proteins were separated by SDS-PAGE and probed for ZmRAMP4. Duplicate blots were probed for BiP, calnexin (CNX), and ribosomal protein S6, as ER stress, membrane, and total protein loading controls, respectively.

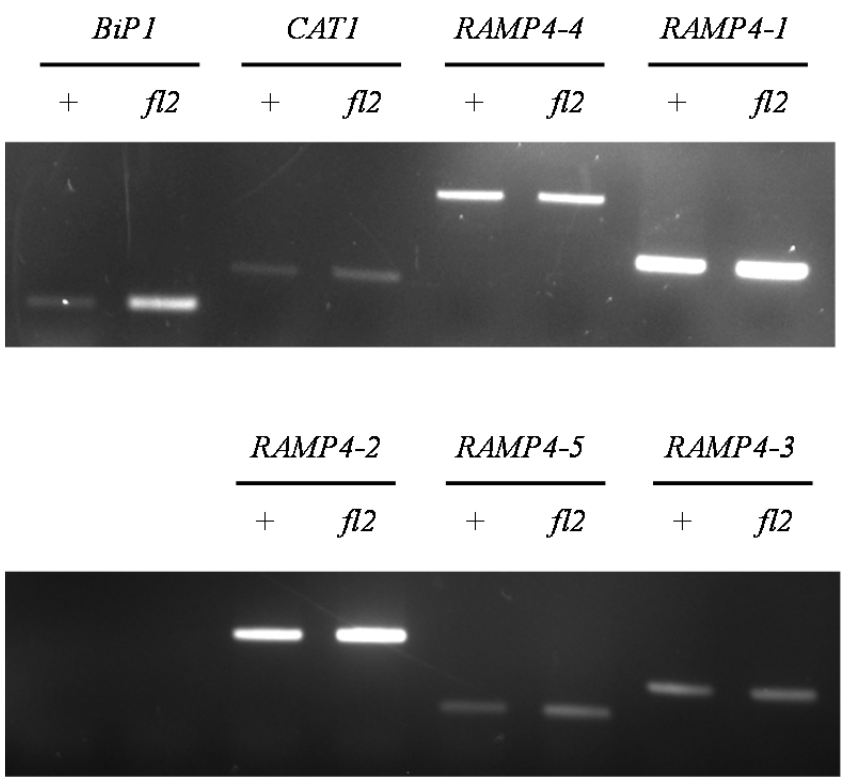

Figure 4. Semi-quantitative RT-PCR analysis of *ZmRAMP4* genes. Complementary DNA (cDNA) was synthesized from total RNA of normal and *fl2* endosperm harvested at 18 DAP. The *catalase1* (*CAT1*) gene was used as an amplification control. PCR samples were analyzed by DNA gel electrophoresis and visualized on a 1% agarose gel stained with ethidium bromide.

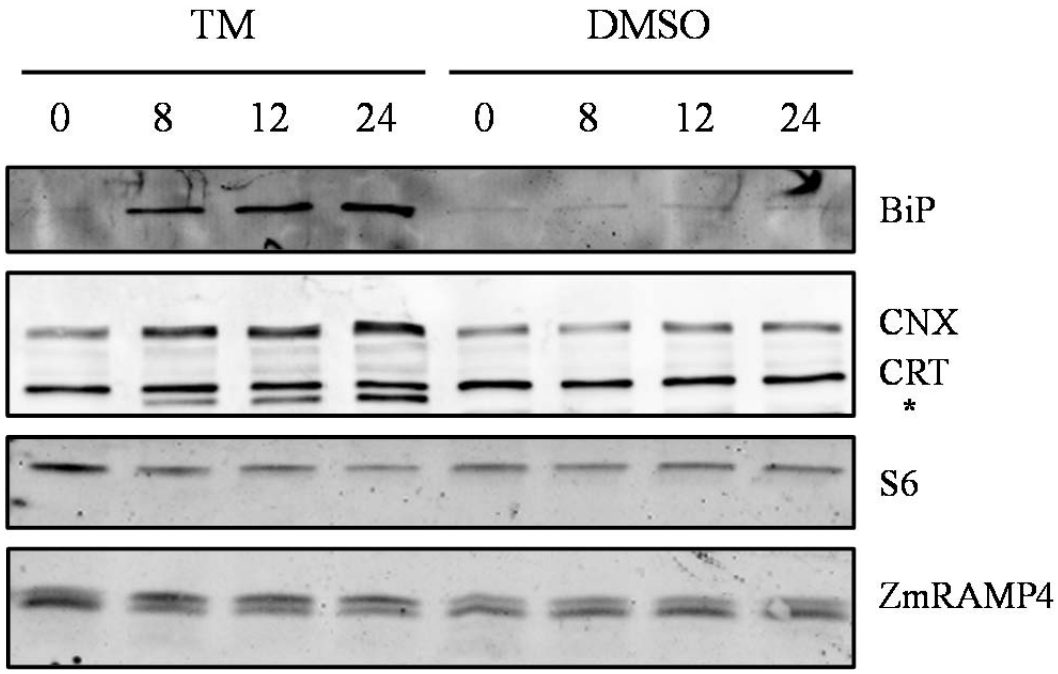

Figure 5. Analysis of ZmRAMP4 under tunicamycin stress. BMS suspension cultured cells at 6 days after passage were treated with DMSO or DMSO with 10 μg/ml of tunicamycin (Tm) for 8 h, 12 h, and 24 h. Total proteins from equal fresh weight equivalents of BMS cells (250 mg) were separated by SDS-PAGE and visualized by immunoblotting with antibodies against BiP, calnexin (CNX) and calreticulin (CRT), ribosomal protein S6, and ZmRAMP4. An asterisk indicates unglycosylated calreticulin. Three biological replicates showed similar results.

Appendix 3: Genotyping and characterization of UPR deficient Arabidopsis mutants

Abstract

Accumulation of misfolded proteins leads to a series of unfolded protein responses (UPR) to maintain ER homeostasis. Arabidopsis genes encoding HRD1 and ribosome associated membrane protein (RAMP4) are among the up-regulated genes when Arabidopsis seedlings were treated with tunicamycin that induces the UPR (Kamauchi et al., 2005). In order to understand functions of AtHRD1 and AtRAMP4 during the UPR, we investigated their T-DNA insertion lines under various stress conditions. However, we did not observe any pronounced phenotypic difference between wild type and T-DNA insertion lines.

Introduction

When unfolded or misfolded proteins accumulate in the ER due to adverse environmental conditions, a series of ER stress responses designated as unfolded protein responses (UPR) is triggered to increase protein folding and degradation (Ron and Walter, 2007). Misfolded proteins in the ER have to be recognized and dislocated into the cytosol for ubiquitin dependent degradation, and this process is referred to as ER associated degradation (ERAD; Hirsch et al., 2009). In yeast, Hrd1p is a multi-transmembrane RING type E3 ligase (Bays et al., 2001). By recruiting various protein partners on both sides of the ER membrane, Hrd1p plays a central role in the degradation of ER proteins with misfolded luminal domains or misfolded transmembrane domains (Carvalho et al., 2006; Denic et al., 2006). Based on sequence homology search, the Arabidopsis genome encodes three *AtHRD1* genes isoforms

At1g65040, At3g16090, and At5g01960, termed *AtHRD1a*, *AtHRD1b*, and *AtHRD1c*, respectively. The *AtHRD1a* gene has been reported to be induced in a microarray study of Arabidopsis seedlings with an induced UPR (Kamauchi et al., 2005). However, the authors did not detect the E3 ligase activity of its protein in a ubiquitination assay in *vitro*. To understand the function of AtHRD1 during the UPR, we tested AtHRD1 T-DNA knockout lines under ER stress and various other stress conditions.

Ribosome associated membrane protein (RAMP4) has been shown to interact with ribosomal proteins and the Sec61p complex (Gölich and Rapoport, 1993; Pool, 2009). Its overexpression stabilizes membrane protein accumulation and facilitates protein glycosylation under ER stress, whereas its deletion induces ER stress and causes a noticeable phenotype in mice (Hori et al., 2006). In plants, two Arabidopsis RAMP4 homologs (At1g27330, At1g27350) were induced when Arabidopsis seedlings were treated with pharmacological reagents inducing ER stress (Kamauchi et al., 2005). Other plant RAMP4 genes have been shown to be induced in response to cadmium exposure and drought stress (Minglin et al., 2005; Torres et al., 2006). Furthermore, overexpressing an Arabidopsis RAMP4 homolog (At1g27330) led to an increased tolerance of oxidative stress (Luhua et al., 2008). To understand the function of Arabidopsis RAMP4 (AtRAMP4), we investigated its T-DNA knockout lines under oxidative stress.

Materials and methods

T-DNA knockout lines of *AtHRD1* and *AtRAMP4* genes were acquired from the Arabidopsis Biological Resource Center. T-DNA insertion lines SALK_061776C (At1g65040), SALK_013258C (At3g16090), SALK_032914 (At3g16090), SALK_23968 (At5g01960), and SALK_104947 (At5g01960) were designated here as *hrd1a*, *hrd1b_2*, *hrd1b*, *hrd1c_1*, and *hrd1c_2*, respectively. T-DNA insertion lines SALK_012050 (At1g27350), SALK_014897 (At1g27350), SALK_ 152878 (At1g27350), and CS340111 (At1g27330) were designated as *r4_1*, *r4_2*, *r4_3*, and *r4_4*, respectively. Seeds were planted and screened for homozygous T-DNA knockout lines. Double knockout lines (*hrd1b_2/hrd1a*, *hrd1c_1/hrd1a*, and *hrd1c_1/hrd1b_2*) were created by crossing, and homozygous double knockout lines were selected from the F2 generation for seed propagation. Seeds from the F3 generation were tested. Primers (listed in Table 1) for screening homozygous T-DNA insertion lines were designed with the SALK T-DNA verification primer design program (http://signal.salk.edu/tdnaprimers.2.html).

The chronic ER stress assay was performed according to Wang et al. (2007) with modifications. Seeds from Arabidopsis wild type (Col-0) and homozygous T-DNA insertion lines were surface-sterilized and sown on solid MS medium [1× MS salts, 1% (w/v) sucrose, MES buffer, pH 5. 7 at 25°C, 0.8% (w/v) agar] containing tunicamycin (0.1 μg/ml; Calbiochem, San Diego, CA). Solid MS medium containing paraquat (0.1 μM; Sigma, St Louis, MO), NaCl (100 mM), or abscisic acid (15 μM; Sigma, St Louis, MO) was used as previously reported (Luhua et al., 2008). Plates were maintained in a vertical position in a

growth chamber under a short day cycle (8 h light and 16 h dark). Plates were photographed at indicated days after germination (DAG), and root growth was measured and analyzed with Adobe Photoshop (Adobe Systems, Mountain View, CA) and Excel (Microsoft, Seattle, Washington).

The Y axis in every table represents the relative average root growth of a treated sample as a percentage in comparison to the mean value of total root growth of the wild type control group. Mean values of total root growth with the same letter are not significantly different ($p<0.05$). All statistical analyses were performed with the SAS statistical software package (version 9.1; SAS Inc., Cary, NC).

Results and discussion

Yeast Hrd1p has been reported to play a crucial role during ERAD. In plants, the Arabidopsis *HRD1a* gene was induced under ER stress (Kamauchi et al., 2005). We hypothesized that T-DNA insertion lines containing disrupted Arabidopsis *HRD1* genes would exhibit to a hyper-sensitive phenotype under stress conditions, if Arabidopsis *HRD1* genes play an important role in ERAD. Seeds from wild type and homozygous T-DNA insertion lines were stressed on MS medium containing tunicamycin (Figure 1, 2, and 7), paraquat (Figure 3 and 6), sodium chloride (Figure 4), or abscisic acid (ABA, Figure 5). Root growth was used to represent how plants respond to the stress. We observed the inhibition of root growth of the Arabidopsis seedlings under all tested stress conditions as expected. However, there was no significant difference ($p<0.05$) in root length between wild type and different Arabidopsis

HRD1 knockout lines under the same stress condition. In addition, we did not observe obvious phenotypic differences between wild type and Arabidopsis *RAMP4* knockout lines under oxidative stress.

There are several explanations for the small amount of variation between the wild type and T-DNA insertion lines under various stress conditions. One possibility is that the stress assay was not optimized. In Figure 5, there was no significant difference of total root growth between ABA treated and untreated samples, except for *hrd1a* (H1a). However, we might be able to detect the phenotypical difference under different ABA concentrations or using different stress durations. Another possibility is that there are three *HRD1* genes and two *RAMP4* genes in Arabidopsis. It is possible that these genes have redundant functions under stress conditions, and an obvious phenotype could appear only after all genes are knocked out. A last but not least possibility is that up-regulation of other genes might complement the function of the knockout gene and result in no obvious phenotype.

A plant steroid hormone brassinosteriod receptor mutant, bri1-9, contains a proper functionality but defective structure. Su et al. (2011) recently showed that the degradation of bri1-9 through ERAD was blocked in a *hrd1a/hrd1b* double knockout background. However, the degradation of bri 1-9 was not affected in either a *hrd1a* or *hrd1b* single knockout background. These results suggested redundant functions of Arabidopsis *HRD1a* and *HRD1b* genes. My sequencing results showed that the T-DNA insertion site in SALK_014897 (*designated as hrd1b_2*) was localized in the 5' untranslated region of the *HRD1b* transcript.

In contrast, the T-DNA insertion site in SALK_032914 (*designated as hrd1b*) was localized in the second exon region. It is possible that the *HRD1b* gene was not completely inhibited in the *hrd1b_2/hrd1a* line. This might lead to no obvious phenotype of the *hrd1a*/*hrd1b_2* double knockout under tunicamycin stress. Since one *HRD1a* or *HRD1b* gene is still present in *hrd1c_1/hrd1b_2* and *hrd1c_1/hrd1a* double knockout lines, respectively, these two genes might functionally complement each other and lead to no obvious phenotype under tunicamycin stress.

References

Bays NW, Gardner RG, Seelig LP, Joazeiro CA, Hampton RY (2001) Hrd1p/Der3p is a membrane-anchored ubiquitin ligase required for ER-associated degradation. Nat Cell Biol **3:** 24-29

Carvalho P, Goder V, Rapoport TA (2006) Distinct ubiquitin-ligase complexes define convergent pathways for the degradation of ER proteins. Cell **126:** 361-373

Denic V, Quan EM, Weissman JS (2006) A luminal surveillance complex that selects misfolded glycoproteins for ER-associated degradation. Cell **126:** 349-359

Gölich D, Rapoport TA (1993) Protein translocation into proteoliposomes reconstituted from purified components of the endoplasmic reticulum membrane. Cell **75:** 615-630

Hirsch C, Gauss R, Horn SC, Neuber O, Sommer T (2009) The ubiquitylation machinery of the endoplasmic reticulum. Nature **458:** 453-460

Hori O, Miyazaki M, Tamatani T, Ozawa K, Takano K, Okabe M, Ikawa M, Hartmann E, Mai P, Stern DM, Kitao Y, Ogawa S (2006) Deletion of SERP1/RAMP4, a component of the endoplasmic reticulum (ER) translocation sites, leads to ER stress. Mol Cell Biol **26:** 4257-4267

Kamauchi S, Nakatani H, Nakano C, Urade R (2005) Gene expression in response to endoplasmic reticulum stress in *Arabidopsis thaliana*. FEBS J **272:** 3461-3476

Luhua S, Ciftci-Yilmaz S, Harper J, Cushman J, Mittler R (2008) Enhanced tolerance to oxidative stress in transgenic Arabidopsis plants expressing proteins of unknown function. Plant Physiol **148:** 280-292

Minglin L, Yuxiu Z, Tuanyao C (2005) Identification of genes up-regulated in response to Cd exposure in *Brassica juncea* L. Gene **363:** 151-158

Pool MR (2009) A trans-membrane segment inside the ribosome exit tunnel triggers RAMP4 recruitment to the Sec61p translocase. J Cell Biol **185:** 889-902

Ron D, Walter P (2007) Signal integration in the endoplasmic reticulum unfolded protein response. Nat Rev Mol Cell Biol **8:** 519-529

Su W, Liu Y, Xia Y, Hong Z, Li J (2011) Conserved endoplasmic reticulum-associated degradation system to eliminate mutated receptor-like kinases in *Arabidopsis*. Proc Natl Acad Sci USA **108:** 870-875

Torres GAM, Pflieger S, Corre-Menguy F, Mazubert C, Hartmann C, Lelandais-Briere C (2006) Identification of novel drought-related mRNAs in common bean roots by differential display RT-PCR. Plant Science **171:** 300-307

Wang S, Narendra S, Fedoroff N (2007) Heterotrimeric G protein signaling in the Arabidopsis unfolded protein response. Proc Natl Acad Sci USA **104:** 3817-3822

Table 1. Oligonucleotides used for genotyping

Name	Sequence (5'-3')	Target gene	Gene locus	Mutant line
AtH1a_F	AGTGGCATCATTTCTGCAAAC	*AtHRD1a*	At1g65040	SALK_061776C
AtH1a_R	GGAAGGGCTCAGGTGATTAAG	*AtHRD1a*	At1g65040	SALK_061776C
AtH1b_2_F	GTCGAAATGTGGTTTTGATGG	*AtHRD1b*	At3g16090	SALK_013258C
AtH1b_2_R	ACAAATTTGACCAAATGCCAG	*AtHRD1b*	At3g16090	SALK_013258C
AtH1b_F	CTTGAGCTTATCCGTGACCTG	*AtHRD1b*	At3g16090	SALK_032914
AtH1b_R	TGCTACTGTGTTTGCAGATGG	*AtHRD1b*	At3g16090	SALK_032914
AtH1c_1_F	CCTAGTCATGAGGCTGAGACG	*AtHRD1c*	At5g01960	SALK_023968
AtH1c_1_R	ACGGTACCATACAGGGGTAGG	*AtHRD1c*	At5g01960	SALK_023968
AtH1c_2_F	AAGAGAAAGCTTCTGGGATGG	*AtHRD1c*	At5g01960	SALK_104947
AtH1c_2_R	CGTCTCAGCCTCATGACTAGG	*AtHRD1c*	At5g01960	SALK_104947
LBb1.3	ATTTTGCCGATTTCGGAAC	T-DNA sequence		
AtR4_1_F	ATTACTAATGCGCAGAGGCAG	*AtRAMP4-1*	At1g27350	SALK_012050
AtR4_1_R	GGAGGAAAAGACTTTGGATCG	*AtRAMP4-1*	At1g27350	SALK_012050
AtR4_2_F	CGGATTAGCTTTACGTTATGCC	*AtRAMP4-1*	At1g27350	SALK_014897
AtR4_2_R	CGGTTTTGATTTTCGAGACTG	*AtRAMP4-1*	At1g27350	SALK_014897
AtR4_3_F	ATTTTAGAGTGTCCATCCCCG	*AtRAMP4-1*	At1g27350	SALK_152878
AtR4_3_R	ATTCATACCATGATTACGCCG	*AtRAMP4-1*	At1g27350	SALK_152878
AtR4_4_F	ATATTGACCATCATACTCATTGC	T-DNA sequence		
AtR4_4_R	GTCGAATTTCTCAATCTTCCTGTC	*AtRAMP4-2*	At1g27330	CS340111

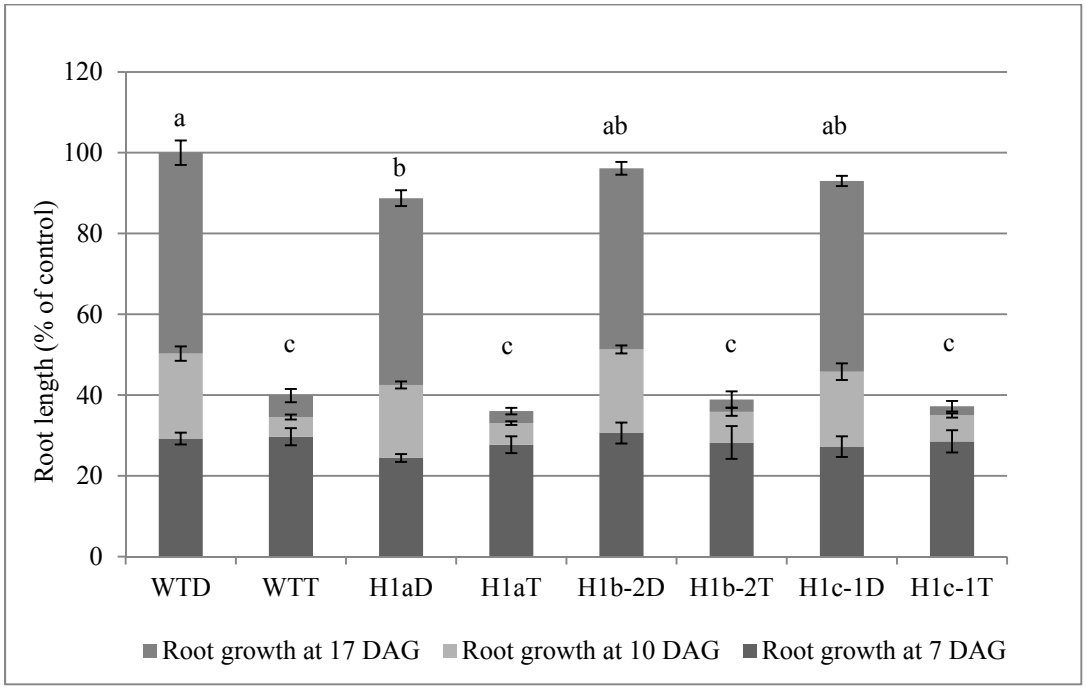

Figure 1. Tunicamycin stress of Arabidopsis seedlings (I). Arabidopsis wild type (WT), *hrd1a* (H1a), *hrd1b_2* (H1b-2), and *hrd1c_1* (H1c-1) were germinated on solid MS media for 7 days. At 7 days after germination (DAG), seedlings were transferred to solid MS media containing DMSO (D) or 0.1 μg/ml tunicamycin (T) for 3 days. Subsequently, seedlings were transferred to solid MS media for 7 days. Root growth was measured at 7 DAG, 10 DAG, and 17 DAG. On every figure, each column represents the average root length, and each error bar represents the standard deviation (n=78).

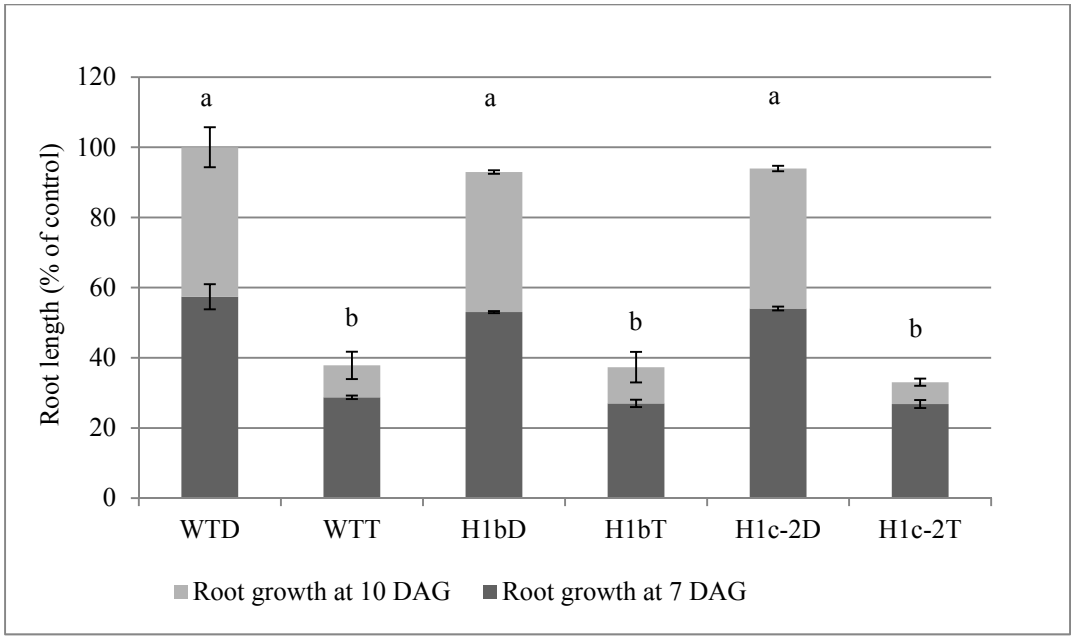

Figure 2. Tunicamycin stress of Arabidopsis seedlings (II). Arabidopsis wild type (WT), *hrd1b* (H1b), and *hrd1c_2* (H1c-2) seeds were germinated on solid MS media containing DMSO (D) or 0.1 μg/ml tunicamycin (T) for 7 days. At 7 DAG, seedlings were transferred to solid MS media for 3 days. Root growth was measured at 7 DAG and 10 DAG.

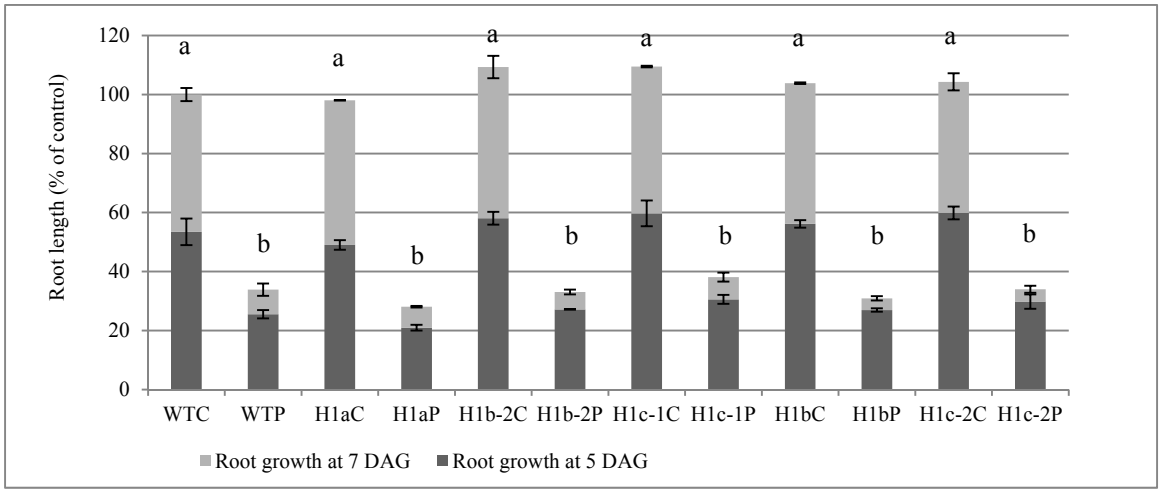

Figure 3. Paraquat stress of Arabidopsis seedlings (I). Arabidopsis wild type (WT), *hrd1a* (H1a), *hrd1b_2* (H1b-2), *hrd1c_1* (H1c-1), *hrd1b* (H1b), and *hrd1c_2* (H1c-2) were germinated on solid MS media (C) or solid MS media containing 0.1 μM paraquat (P). Root growth was measured at 5 DAG and 7 DAG.

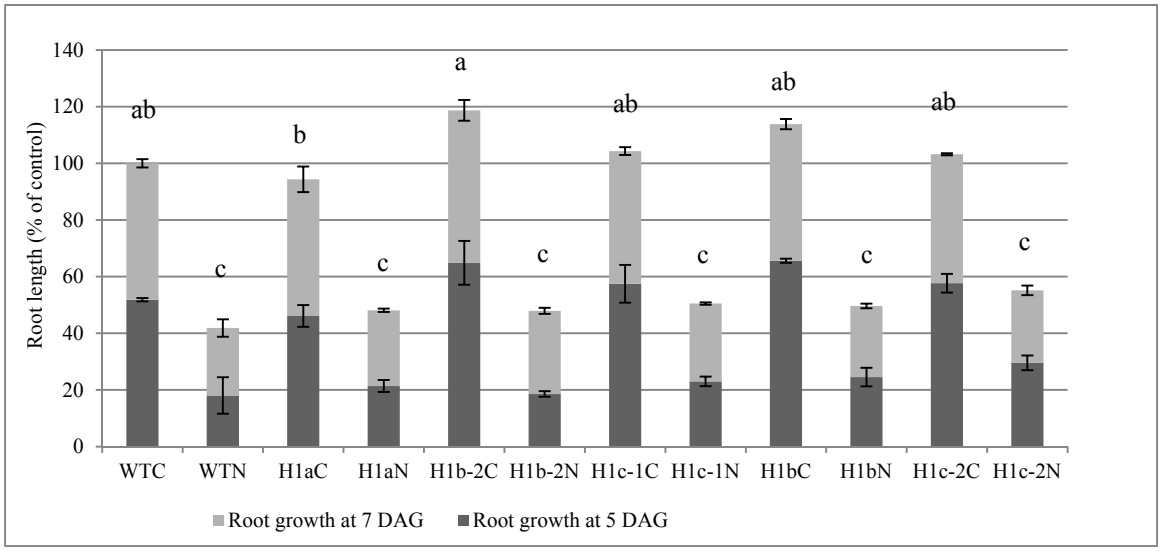

Figure 4. NaCl stress of Arabidopsis seedlings. Arabidopsis wild type (WT), *hrd1a* (H1a), *hrd1b_2* (H1b-2), *hrd1c_1* (H1c-1), *hrd1b* (H1b), and *hrd1c_2* (H1c-2) were germinated on solid MS media (C) or solid MS media containing 100 mM NaCl (N). Root growth was measured at 5 DAG and 7 DAG.

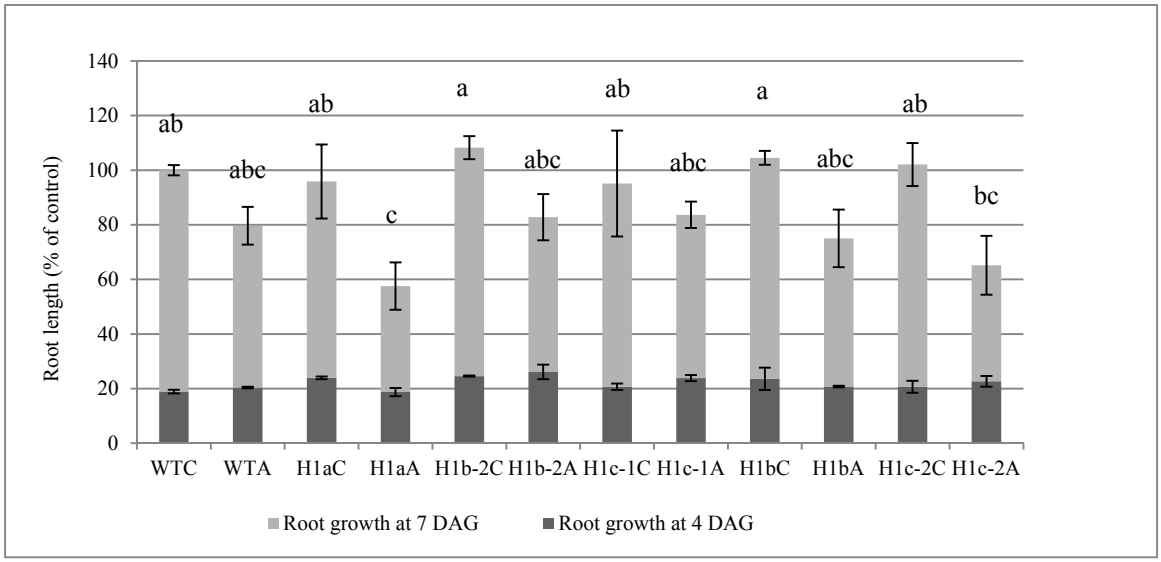

Figure 5. ABA stress of Arabidopsis seedlings. Arabidopsis wild type (WT), *hrd1a* (H1a), *hrd1b_2* (H1b-2), *hrd1c_1* (H1c-1), *hrd1b* (H1b), and *hrd1c_2* (H1c-2) were germinated on solid MS media for 4 days, and then transferred on solid MS media (C) or solid MS media containing 15 μM ABA (A) for 3 days. Root growth was measured at 4 DAG and 7 DAG.

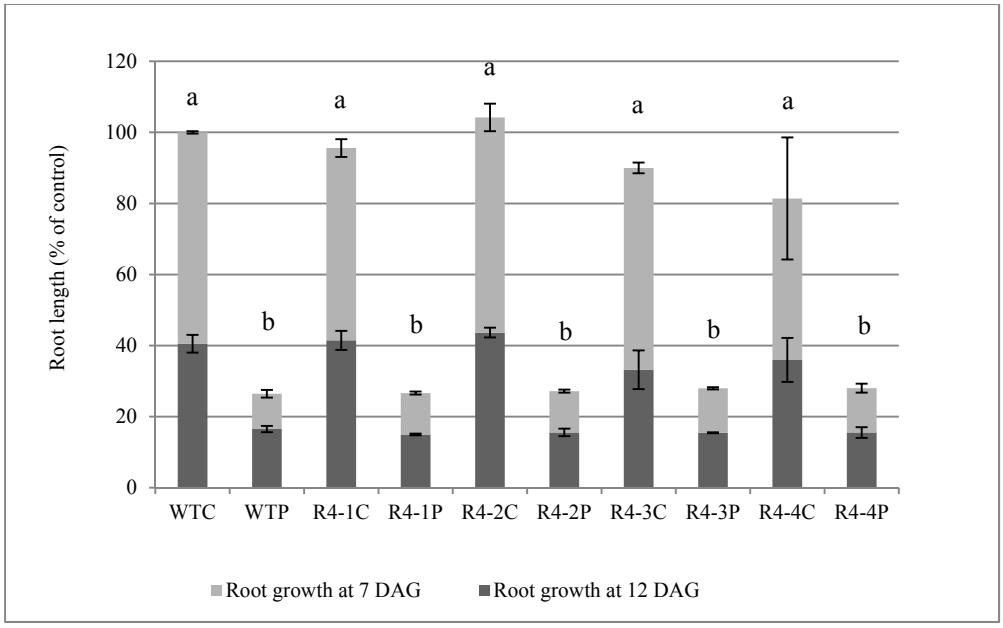

Figure 6. Paraquat stress of Arabidopsis seedlings (II). Arabidopsis wild type (WT), *r4_1* (R4-1), *r4_2* (R4-2), *r4_3* (R4-3), and *r4_4* (R4-4) were germinated on solid MS media (C) or solid MS media containing 0.1 μM Paraquat (P) for 7 days, and then transferred to solid MS media for 5 days. Root growth was measured at 7 DAG and 12 DAG.

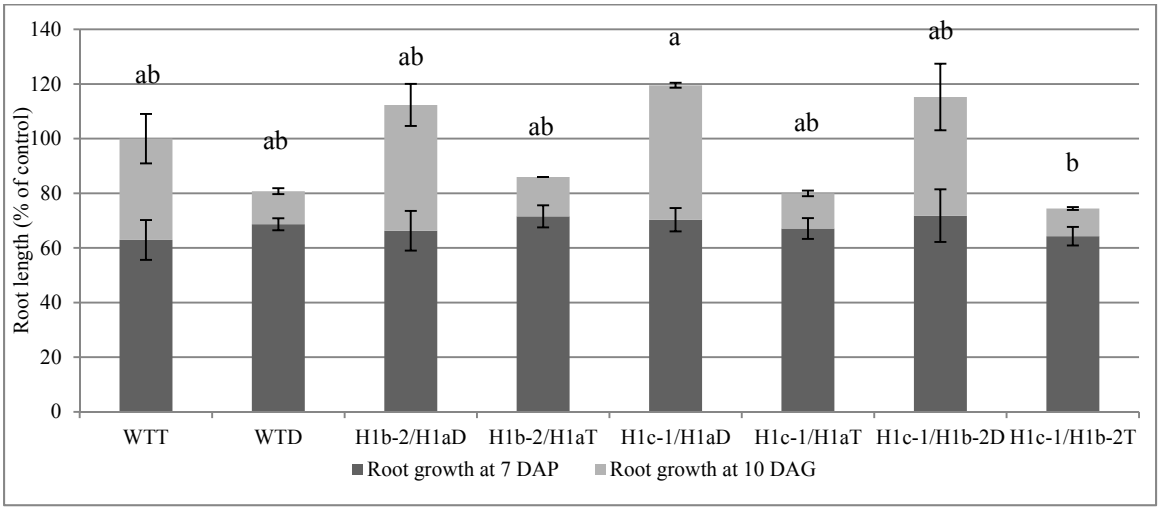

Figure 7. Tunicamycin stress of wild type and Arabidopsis *HRD1* double mutant lines. Arabidopsis wild type (WT), *hrd1b_2*/*hrd1a* (H1b-2/H1a), *hrd1c_1*/*hrd1a* (H1c-1/H1a), and *hrd1c_1*/*hrd1b_2* (H1c-1/H1b-2) were germinated on solid MS media for 7 days. At 7 DAG, seedlings were transferred to solid MS media containing DMSO or 0.1 μg/ml tunicamycin (Tm) for 3 days. Root growth was marked at 7 DAG and 10 DAG.

Conclusions and perspectives

In my previous chapters, I have summarized current knowledge of ERAD in yeast, animals, and plants. In addition, my studies provide an important link between increased ubiquitination, induced ERAD components and ER molecular chaperones, and defective α-zein accumulation in *De*-B30* and *fl2* protein bodies. Here, I will discuss that how my work contributes to the field and pose some remaining questions.

In plants, castor bean ricin toxin A chain (RTA), *Ricinus communis* agglutinin A chain (RCA A), mutant barley mildew resistance o (MLO) proteins, and mutant brassinosteroid receptors bri1-5 and bri1-9 were characterized as ERAD substrates (Muller et al., 2005; Hong et al., 2008; Marshall et al., 2008; Hong et al., 2009). Interestingly, the retrotranslocation of RTA does not require ubiquitination and the degradation of bri1-5 is 26S proteasome-independent. In an attempt to understand how mutant α-zeins are handled in *De*-B30* and *fl2* protein bodies, I demonstrated in Chapter 2 that specific increases in ubiquitin signals were associated with mutant α-zein accumulation in *De*-B30* and *fl2* protein bodies. By using mass spectrometry, I identified a variety of ubiquitinated substrates. One particularly interesting substrate is the maize homolog of oligosaccharyl transferase. How is it recognized? Does the disturbed protein packing within protein bodies lead to its defective conformation or is its ubiquitination under a developmental regulation? It will be interesting to further investigate its protein abundance and its interaction partners within mutant protein bodies to answer why it is degraded. Another interesting question is whether all ubiquitinated substrates contribute equally to the increased ubiquitin signals or particular substrates

contribute more than others. A quantitative mass spectrometry study might provide valuable answers.

One more interesting finding is the connection between starch granules and protein bodies. Starch granules have been proposed to be surrounded by a proteinaceous matrix of protein bodies (Gibbon et al., 2003; Wu et al., 2010; Wu and Messing, 2010). In addition, changed protein body content could affect starch composition. In endosperm of a maize *opaque-2* modifier that contains higher amounts of 27 kD γ-zeins, Gibbon et al. (2003) showed that the extractable granule-bound starch synthase I increased and the amylopectin contained more short-length α-1,4 linked branches than in normal endosperm. In chapter 2, I identified several starch synthesis related enzymes as ubiquitin substrates in *De*-B30* protein body fractions, although it is not still clear that whether any protein exchange between protein body membranes and amyloplast membranes, or even between the amyloplast stroma and protein body lumen in *De*-B30* endosperm cells leads to their ubiquitination. Nevertheless, my finding suggested ubiquitination as one of the possible mechanisms to explain the lower starch content in *De*-B30* endosperm.

Recent studies indicated that the presence of ERAD machinery is conserved in plants as in yeast and animals (Kirst et al., 2005; Muller et al., 2005; Marshall et al., 2008; Su et al., 2011). One conserved ERAD component is ZmDerlin that can partially complement the function of its yeast homolog. Transformations of ZmDerlin1-1 or ZmDerlin2-1 recovered the growth of a *Δire1/Δder* temperature sensitive yeast mutant at the nonpermissive

temperature of 37°C (Kirst et al., 2005). The second conserved ERAD component is CDC48. A mutant AtCDC48A with defective ATP hydrolysis (AtCDC48A QQ) prevented the degradation of MLO-1 protein in Arabidopsis protoplasts, and retarded the dislocation of RTA from the ER lumen to the cytosol in tobacco leaf protoplasts (Muller et al., 2005; Marshall et al., 2008). My studies in Chapter 3 added a new perspective that increased amounts of ZmCDC48 were recruited to *De*-B30* and *fl2* protein bodies in which high levels of ubiquitin signals accumulated. A third conserved ERAD component is HRD1. Its transcript was initially shown to be induced in Arabidopsis seedlings treated with tunicamycin (Kamauchi et al., 2005). In addition, Su et al. (2011) recently showed that ERAD of mutant brassinosteroid receptor bri1-9 was inhibited in an *AtHRD1* gene double knockout line. My studies in Chapter 3 showed the induction of ZmHRD1 and its transcript in response to mutant α-zein accumulation in *De*-B30* and *fl2* protein bodies. In addition, I demonstrated the interaction between ZmCDC48 and ZmHRD1 at the membrane by using immunoprecipitation. A fourth conserved ERAD component is HRD3 (homolog to yeast Hrd3p or mammalian SEL1L). Su et al. (2011) showed that an AtHRD3 (At1g18260) mutation resulted in retarded degradation of both mutant brassinosteroid receptors bri1-5 and bri1-9. AtHRD3 was also shown to interact with bri1-5 and bri1-9. Furthermore, transformation of AtHRD3 recovered the degradation of carboxypeptidase Y (CPY*) in a *Δhrd3* yeast mutant. In agreement with HRD3 as one ERAD component, I showed that the transcript of *ZmHRD3* was induced in *De*-B30* and *fl2* endosperm. It will be interesting to investigate its protein level and interaction with ZmHRD1 and ERAD luminal components.

However, some interesting questions remain in the field. For example, how misfolded glycoproteins were delivered from ER molecular chaperones to HRD3 is still unknown in plants. In yeast, Yos9p interacts with Hrd3p together to recognize an *N*-glycan with a terminal α-1,6 linked mannose that is generated by Htm1p (Quan et al., 2008; Clerc et al., 2009). Hrd3p can also recognize hydrophobic patches of misfolded regions independently of Yos9p (Denic et al., 2006; Gauss et al., 2006). Nevertheless, no plant homologs of Yos9p and Htm1p have been identified yet. So, are there any plant homologs of Htm1p and Yos9p to generate and recognize the same α-1,6 linked mannose signal, is a different glycan signal used as an ERAD signal, or is HRD3 itself adequate to recognize misfolded glycoproteins in plants? Addressing these questions will improve our understanding about the plant ERAD machinery, and provide valuable information for efficiently expressing novel proteins in plants.

References

Clerc S, Hirsch C, Oggier DM, Deprez P, Jakob C, Sommer T, Aebi M (2009) Htm1 protein generates the N-glycan signal for glycoprotein degradation in the endoplasmic reticulum. J Cell Biol **184:** 159-172

Denic V, Quan EM, Weissman JS (2006) A luminal surveillance complex that selects misfolded glycoproteins for ER-associated degradation. Cell **126:** 349-359

Gauss R, Jarosch E, Sommer T, Hirsch C (2006) A complex of Yos9p and the HRD ligase integrates endoplasmic reticulum quality control into the degradation machinery. Nat Cell Biol **8:** 849-854

Gibbon BC, Wang X, Larkins BA (2003) Altered starch structure is associated with endosperm modification in Quality Protein Maize. Proc Natl Acad Sci USA **100:** 15329-15334

Hong Z, Jin H, Fitchette AC, Xia Y, Monk AM, Faye L, Li J (2009) Mutations of an α1,6 mannosyltransferase inhibit endoplasmic reticulum-associated degradation of defective brassinosteroid receptors in *Arabidopsis*. Plant Cell **21:** 3792-3802

Hong Z, Jin H, Tzfira T, Li J (2008) Multiple mechanism-mediated retention of a defective brassinosteroid receptor in the endoplasmic reticulum of *Arabidopsis*. Plant Cell **20:** 3418-3429

Kamauchi S, Nakatani H, Nakano C, Urade R (2005) Gene expression in response to endoplasmic reticulum stress in *Arabidopsis thaliana*. FEBS J **272:** 3461-3476

Kirst ME, Meyer DJ, Gibbon BC, Jung R, Boston RS (2005) Identification and characterization of endoplasmic reticulum-associated degradation proteins differentially affected by endoplasmic reticulum stress. Plant Physiol **138:** 218-231

Marshall RS, Jolliffe NA, Ceriotti A, Snowden CJ, Lord JM, Frigerio L, Roberts LM (2008) The role of CDC48 in the retro-translocation of non-ubiquitinated toxin substrates in plant cells. J Biol Chem **283:** 15869-15877

Muller J, Piffanelli P, Devoto A, Miklis M, Elliott C, Ortmann B, Schulze-Lefert P, Panstruga R (2005) Conserved ERAD-like quality control of a plant polytopic membrane protein. Plant Cell **17:** 149-163

Quan EM, Kamiya Y, Kamiya D, Denic V, Weibezahn J, Kato K, Weissman JS (2008) Defining the glycan destruction signal for endoplasmic reticulum-associated degradation. Mol Cell **32:** 870-877

Su W, Liu Y, Xia Y, Hong Z, Li J (2011) Conserved endoplasmic reticulum-associated degradation system to eliminate mutated receptor-like kinases in *Arabidopsis*. Proc Natl Acad Sci USA **108:** 870-875

Wu Y, Holding DR, Messing J (2010) γ-zeins are essential for endosperm modification in quality protein maize. Proc Natl Acad Sci USA **107:** 12810-12815

Wu Y, Messing J (2010) RNA interference-mediated change in protein body morphology and seed opacity through loss of different zein proteins. Plant Physiol **153:** 337-347